uOttawa

L'Université canadienne
Canada's university

FACULTÉ DES ÉTUDES SUPÉRIEURES ET POSTOCTORALES

uOttawa

L'Université canadienne
Canada's university

FACULTY OF GRADUATE AND POSDOCTORAL STUDIES

Miram Kenk

AUTEUR DE LA THÈSE / AUTHOR OF THESIS

Ph.D. (Cellular and Molecular Medicine)

GRADE / DEGREE

Department of Cellular and Molecular Medicine

FACULTÉ, ÉCOLE, DÉPARTEMENT / FACULTY, SCHOOL, DEPARTMENT

In Vivo Evaluation of R-and (S)-[$^{11}$C]Rolipram for Imaging Cardiac Phosphodiesterase-4 Enzymes: Characterization and Applications in Rat Models of Heart Failure

TITRE DE LA THÈSE / TITLE OF THESIS

Jean Da Silva

DIRECTEUR (DIRECTRICE) DE LA THÈSE / THESIS SUPERVISOR

CO-DIRECTEUR (CO-DIRECTRICE) DE LA THÈSE / THESIS CO-SUPERVISOR

Marc Ruel

Patrick G. Burgon

Johnny K. Ngsee

James H. Caldwell

Gary W. Slater

Le Doyen de la Faculte des etudes superieures et postdoctorales / Dean of the Faculty of Graduate and Postdoctoral Studies

# IN VIVO EVALUATION OF (*R*)- AND (*S*)-[$^{11}$C]ROLIPRAM FOR IMAGING CARDIAC PHOSPHODIESTERASE-4 ENZYMES: CHARACTERIZATION AND APPLICATIONS IN RAT MODELS OF HEART FAILURE

by

Miran Kenk

**Department of Cellular and Molecular Medicine**
**Faculty of Graduate and Postdoctoral Studies**
**University of Ottawa**

Thesis submitted as a partial fulfillment of the Ph.D. program in Cellular Molecular Medicine.

Submitted Sep 1st, 2010, Ottawa, Ontario.

*Your file Votre référence*
*ISBN:* 978-0-494-73929-7
*Our file Notre référence*
*ISBN:* 978-0-494-73929-7

**ABSTRACT**

Heart failure is associated with alterations in noradrenergic 3',5'-cyclic adenosine monophosphate (cAMP)-mediated phosphodiesterase 4 (PDE4) signaling. Comprehensive study of the intracellular mechanism involved in the progression of heart failure is hindered by the limitations of in vitro techniques. Intracellular cAMP levels regulate PDE4 expression and activity. Positron emission tomography (PET) imaging with the carbon-11 labeled PDE4-specific inhibitor (*R*)-rolipram provides an in vivo index of PDE4 enzymes, and therefore an indirect index of cAMP signaling. The aim of this research was to characterize (*R*)-[$^{11}$C]rolipram for use in cardiac PET imaging and to evaluate post-receptor changes in animal models of adriamycin-induced cardiotoxicity and post-infarct heart failure. (*R*)-[$^{11}$C]Rolipram exhibits PDE4-specific binding, selectivity for the PDE4 isozyme over other cardiac PDE enzymes, and responsiveness to treatments affecting cAMP levels, as established using biodistribution and autoradiography techniques in rats. Reduced PDE4 intracellular adrenergic response to acute increase in noradrenaline levels suggested a diminished post-receptor signal transduction in adriamycin-treated rats correlated with decreased retention of the β-adrenergic antagonist [$^{3}$H]CGP12177. Small-animal cardiac PET imaging with (*R*)-[$^{11}$C]rolipram detected increased PDE4 in the non-infarcted left ventricle 8 weeks following myocardial infarction with decreased β-adrenergic receptor expression and normal myocardial blood flow. (*R*)-[$^{11}$C]Rolipram sensitivity to altered noradrenergic signaling in animal models of cardiac dysfunction suggests potential application for this radiotracer in non-invasive imaging of alterations in post-receptor cAMP-mediated PDE4 signal transduction in humans.

## ACKNOWLEDGMENTS

First and foremost, I would like to acknowledge a debt of gratitude and love owed to my wife, Ana-Maria Constantin, for years of infinite patience, understanding and love. Her support is the sine qua non of all that I have done in the past years, and thus a foundation for all my efforts. I would like to also thank my family for their unconditional support and for encouraging me to pursue my academic interests.

I am grateful to my supervisor, Dr. Jean DaSilva for the encouragement and guidance which have been instrumental in my academic development, from the summer student position at the CAMH, all the way to the thesis submission. I am thankful to Dr. Rob S. Beanlands for the clinical perspective and leadership contributed to this project.

I would like to thank Stephanie Thorn for the hours invested into the countless sanity checks on the methods and results, as well as for the friendship and unwavering enthusiasm that supported this project through the more difficult stages. I am grateful also to James Thackeray for all the help and camaraderie through the years, as well as for his endless, self-sacrificing willingness to help.

None of the described experiments would be possible without the efforts of the radiochemistry laboratory, for which I thank Samantha Mason, Jeffrey Collins and Paul Colletta. I would also like to thank Drs. Rob deKemp, Ran Klein, Ben Chow, Marc Ruel, Kathy Ascah and Mario Tiberi for their input. The dedication of the UOHI Animal Care staff is acknowledged for supporting the experiments.

Finally, I would like to acknowledge the funding from Heart and Stroke Foundation of Canada, Canadian Institutes of Health Research and a Heart and Stroke Foundation Program grant in Molecular Function and Imaging.

## TABLE OF CONTENTS

## LIST OF TABLES

## LIST OF FIGURES

**Chapter 5: Manuscript #4**



**Chapter 6: Manuscript #5**



**Chapter 7: Manuscript #6**

**Chapter 8: General discussion**

## LIST OF ABBREVIATIONS

| | |
|---|---|
| $^{11}$C | carbon-11 |
| $^{18}$F | fluorine-18 |
| $^{13}$N | nitrogen-13 |
| 5HT | serotonin |
| α-AR | α-adrenergic receptor |
| AC | adenylyl cyclase |
| ADR | adriamycin |
| ANOVA | analysis of variance |
| ANS | autonomic nervous system |
| ATP | adenosine triphosphate |
| β-AR | β-adrenergic receptors |
| β-ARK | β-adrenergic receptor kinase |
| BAT | brown adipose tissue |
| BDNF | brain-derived neurotrophic factor |
| BGO | bismuth germanium orthosilicate |
| BW | body weight |
| cAMP | cyclic adenosine-monophosphate |
| cGMP | cyclic guanosine-monophosphate |
| CRE | cyclic adenosine-monophosphate response element |
| CREB | cyclic adenosine-monophosphate response element binding protein |
| DA | dopamine |
| DAG | diacetylglycerol |
| DMI | desipramine |
| DPBB | 12-deoxyphorbol 13-isobutyrate-20-butyrate |
| DV | distribution volume |
| $ED_{50}$ | effective dose eliciting 50% of maximal response |
| EF | ejection fraction |
| ERK | extracellular signal-regulated kinase |
| [$^{18}$F]FDG | [$^{18}$F]fluorodeoxyglucose |
| FS | fractional shortening |
| GPCR | G protein-coupled receptor |
| HA | histamine |
| HARBS | high-affinity rolipram binding site |
| HF | heart failure |
| HW | heart weight |
| [$^{11}$C]HED | [$^{11}$C]*meta*-hydroxyephedrine |
| HPLC | high-performance liquid chromatography |
| IBMX | 3-isobutyl-1-methylxanthine |
| %ID | percentage of total injected dose |
| IDV | Integrated density value |
| $IP_3$ | inositol trisphosphate |
| IVS | intra-ventricular septum |
| $K_d$ | dissociation constant |
| $K_m$ | metabolic rate constant |

| | |
|---|---|
| $K_i$ | inhibitory constant |
| LA | left atrium |
| LAD | left anterior descending coronary artery |
| LAH | lithium aluminium hydride |
| LARBS | low-affinity rolipram binding site |
| LV | left ventricle |
| LVDV | left ventricle diastolic volume |
| LVDD | left ventricle diastolic dimensions |
| LVSV | left ventricle systolic volume |
| LVSD | left ventricle systolic dimensions |
| LVPW | left ventricle posterior wall |
| mAchR | muscarinic cholinergic receptor |
| MAPK | mitogen-activated protein kinase |
| MAPKK | mitogen-activated protein kinase kinase |
| MBP-C | myosin binding protein C |
| [$^{125}$I]MIBG | [$^{125}$I]metaiodobenzylguanidine |
| MQNB | methylquinuclidinyl benzilate |
| [$^{13}$N]$NH_3$ | [$^{13}$N]ammonia |
| PET | positron emission tomography |
| mRNA | messenger ribonucleic acid |
| MAO | monoamine oxidase |
| MAP | maprotiline |
| MBP-C | myosin-binding protein C |
| MI | myocardial infarction |
| NA | noradrenaline |
| NAT | noradrenaline transporter |
| NYHA | New York Heart Association |
| PDE | phosphodiesterase |
| PET | positron emission tomography |
| $PIP_2$ | phosphatidylinositol 4,5-bisphosphate |
| PKA | protein kinase A |
| PKC | protein kinase C |
| PLB | phospholamban |
| PLC | phospholipase C |
| RA | right atrium |
| $R_t$ | retention time |
| RV | right ventricle |
| RT-PCR | real-time polymerase chain reaction |
| RyR | ryanodine receptor $Ca^{2+}$ channel |
| SD | standard deviation |
| SERCA | sarcoplasmic reticulum $Ca^{2+}$ pump |
| SERT | sertraline |
| SNS | sympathetic nervous system |
| SPECT | single photon emission computed tomography |
| SSRI | selective serotonin reuptake inhibitor |
| SV | stroke volume |

| | |
|---|---|
| TLC | thin layer chromatography |
| TBAOH | tetrabutylammonium hydroxide |
| UCR | upstream conserved region |
| UV | ultra-violet |
| WAT | white adipose tissue |
| GAPDH | glyceraldehydes 3-phosphate dehydrogenase |
| OSEM3D/MAP | ordered-subsets expectation maximization 3D/maximum a posteriori |

# CHAPTER 1: INTRODUCTION

# 1. INTRODUCTION

Heart failure is defined as the inability of the heart to satisfy the metabolic needs of the tissues. It is the final common pathway for a number of different cardiac disorders (Katz, 1989; Parmley, 1989; Lloyd-Jones et al., 2010), and a major cause of morbidity, hospitalization and mortality worldwide (Lloyd-Jones et al., 2010). In a population older than 65 years of age, the incidence of heart failure approaches 1% in the United States, with the associated cost in 2010 estimated at above $39.2 billion (Lloyd-Jones et al., 2010). In Canada, approximately 400 000 people are living with congestive heart failure, with an average mortality rate for one- and five-years following diagnosis of approximately 33 and 50%, respectively (Liu et al., 2001). The increase in the average age in worldwide population will lead to an increased prevalence of cardiovascular disease and heart failure, necessitating more effective therapy and improved early diagnosis.

In the current therapeutic scheme, nuclear imaging is utilized to confirm the presence and assess the scope of the pathological state. Increased availability and affordability of positron emission tomography (PET) imaging with novel tracers further enables nuclear cardiology to evaluate altered molecular mechanisms that underlie heart failure, aiding diagnosis, improving the understanding of the pathology and facilitating evaluation of current and future treatments.

## 1.1. Cardiac innervation by the autonomic nervous system

### *1.1.1. Anatomy of the cardiac nervous system*

Anatomically, the complex of nerves modulating cardiac function is composed of the afferent and efferent neurons which interact at the local cardiac level, the paravertebral ganglia and the brain stem. Afferent sensory outputs from the cardiac ventricles carry the information on blood pressure, flow and chemical milieu from the receptors in the left ventricle, carotid sinus, and the aortic arch to the brainstem. These inputs are integrated in the medulla with efferent neurons, modulating the feedback control onto the heart through the sympathetic and parasympathetic branches of the autonomic nervous system (ANS) (Higuchi and Schwaiger, 2006).

Efferent neuronal bodies are located in the paravertebral ganglia (Hildreth et al., 2009), with the sympathetic efferent cardiac innervation generally proceeding from the paravertebral ganglia (e.g. stellate) through the mediastinal nerves to the heart. The parasympathetic cardiac innervation involves projections from the preganglionic neurons in the medulla through the vagus nerve. The cardiac components of the vagus and sympathetic nerve bundles form the cardiac plexus at the base of the heart, with fibres interacting with the intrinsic cardiac nervous system, or proceeding directly to the cardiac tissues (Armour, 2004).

Postganglionic efferent sympathetic fibers travel along the epicardial vascular structures, enter the myocardium with coronary vessels (Higuchi and Schwaiger, 2006) and branch out, innervating cardiac regions through terminal varicosities (Shepherd and Vanhoutte, 1981). These "swellings" on the nerve fibers are the neuroeffector junctions of the cardiac innervation, the equivalents of neuromuscular junctions in the skeletal muscle fibers (Loffelholz and Pappano, 1985; Crick S.J., 2000).

### *1.1.2. ANS modulation of cardiac function*

Function of the heart is controlled by the sympathetic and parasympathetic branches of the ANS through their neurotransmitters noradrenaline (NA) and acetylcholine. Activation of the sympathetic branch of the ANS in response to physical or psychological stress increases the cardiac output by accelerating the heart rate and strengthening contractility through the post-synaptic adrenergic receptors. Parasympathetic control predominates in periods of low demand, enforcing low heart rate and decreased energy utilization. As exemplified by the behaviour of the transplanted (denervated) heart, the automatic contractions of the myocardium are not dependent on external input. A heart devoid of ANS control exhibits tachycardia and is unable to regulate its function in response to changes in the metabolic demand (e.g. exercise) (Spann et al., 1966; Cotts and Oren, 1997).

## 1.2. Noradrenergic myocardial control

### *1.2.1. Noradrenaline synthesis and release*

Most NA release is from the sympathetic fibers originating from the extrinsic nuclei, even though some intracardiac neuronal cell bodies contain catecholamines (Higuchi and Schwaiger, 2006). The synthesis of NA begins with the rate-limiting step, the conversion of the amino acid L-tyrosine to L-hydroxyphenylalanine by the tyrosine hydroxylase enzyme. L-hydroxyphenylalanine is converted to dopamine by the aromatic L-amino acid decarboxylase enzyme. Final step in the reaction chain is the synthesis by phenylethanolamine-N-methyltransferase of NA, which is stored in vesicles at the sympathetic varicosities (Shepherd and Vanhoutte, 1981; Hildreth et al., 2009). A

stimulatory impulse propagating down the axon opens the voltage-gated N-type $Ca^{2+}$ channels at the varicosities, increasing intracellular $Ca^{2+}$ levels. The NA-containing vesicles migrate to the plasma membrane in response to increased $Ca^{2+}$ levels, fuse with the lipid bilayer and excrete the neurotransmitter (Shepherd and Vanhoutte, 1981; Kurz et al., 1995). NA release is susceptible to autoregulation by presynaptic $\beta_2$ and $\alpha_2$ adrenergic receptors, which affect vesicle docking and exocytosis (Boudreau et al., 1993; Parker et al., 1995; Newton and Parker, 1996). Additionally, parasympathetic system influences NA release through the cholinergic receptor (Azevedo and Parker, 1999). Presence of presynaptic $H_3$ histamine receptors at the adrenergic nerve endings in the heart allows heterologous regulation by inhibiting the NA release (Levi and Smith, 2000; Koyama et al., 2003). Species differences exist in the NA release, with differences in resting cardiac adrenergic tone even reported between different rat strains (Osadchii et al., 2007). Figure 1-1 summarizes the processes involved in the release, reuptake and breakdown of the cardiac NA.

### *1.2.2. NA reuptake and degradation*

Eighty percent of the NA released in the heart is absorbed by the reuptake mechanisms into the presynaptic nerve from the synaptic cleft (Link and Caldwell, 2008). Uptake-1 NA transporter (NAT) proteins carry NA across the lipid bilayer using the energy derived from the $Na^+$ gradient (Bohm et al., 1997; Higuchi and Schwaiger, 2006). The non-energy dependent uptake-2 mechanism present in non-neuronal tissues, transports monoamines into the cardiac myocytes and the vascular endothelial cells (Higuchi and Schwaiger, 2006).

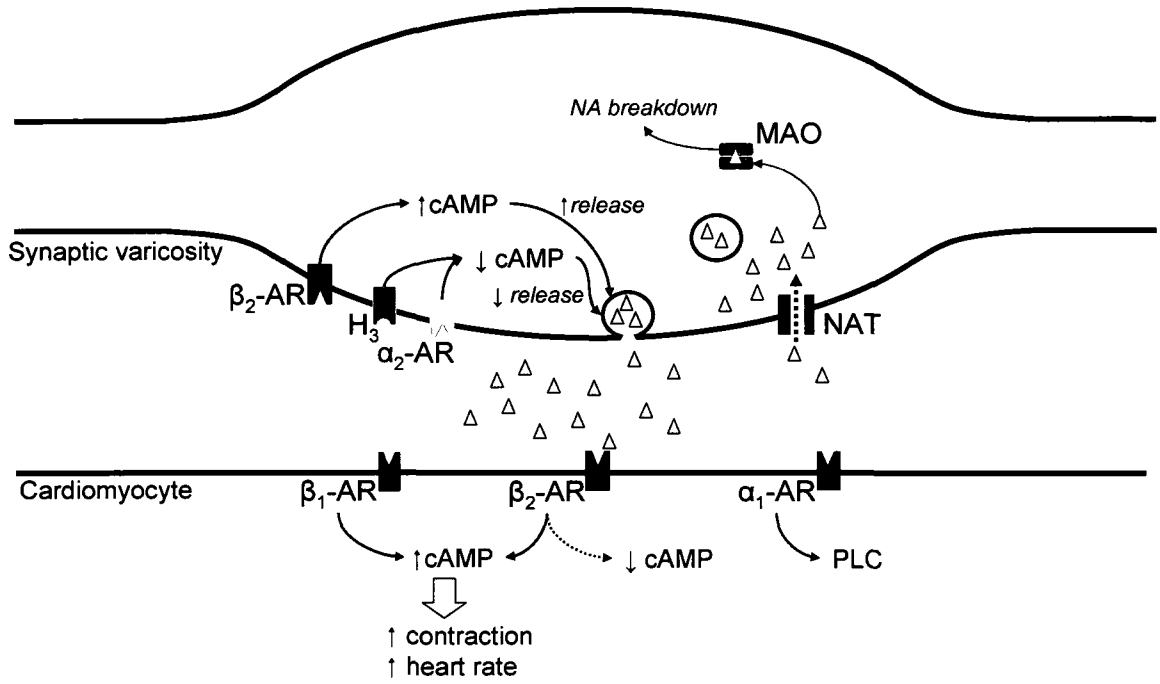


Figure 1-1: Schematic representation of the sympathetic varicosity and the post-synaptic cardiomyocyte. NA (blue triangles) is transported down the axon to the varicosity, where it is released in response to $Ca^{2+}$ influx. Release of NA is inhibited by the activation of $\alpha_2$-AR and $H_3$ histamine receptors on the presynaptic membrane. Stimulation of $\beta_2$-AR potentiates the release of NA. Released NA interacts with the post-synaptic $\alpha_1$-, $\beta_1$- and $\beta_2$-AR to regulate myocardial contractility and heart rate. NA is taken up by the NA transporter (NAT) into the presynaptic varicosity, where it is broken down by the monoamine oxidase (MAO) enzymes.

NA and other monoamines are broken down by the monoamine oxidase (MAO) enzymes. Two distinct subtypes (MAO A and B) are present in cardiac tissue, with MAO A displaying a high affinity for NA and serotonin (5HT). Under normal conditions, the MAO A subtype accounts for approximately 66% of the cardiac monoamine breakdown, as confirmed by the immunohistochemistry experiments showing a higher presence of MAO A protein in the cardiomyocytes than MAO-B (Billett, 2004).

### 1.3. Cardiac α-adrenergic receptors

In 1948, Dr. Ahlquist established that the post-synaptic responses to catecholamines in the heart and other organs can be classified as either α- or β-receptor mediated, initiating decades of inquiry into the expression, regulation and physiological roles of the adrenergic receptors (Ahlquist, 1948; Frishman, 2008). Both α- and β-adrenergic receptors (α-AR and β-AR) are found in the myocardium, where they modulate distinct physiological roles (Bristow, 1993).

$\alpha_1$-AR account for approximately 15% of the total cardiac adrenoceptors (Bristow, 1993), and are localized to the post-synaptic plasma membrane of cardiac myocytes (Brodde et al., 2001). As illustrated in Figure 1-2, agonist stimulation of these receptors activates the phospholipase C (PLC) cleavage of phospholipids in the plasma membrane phosphatidylinositol (4,5)-bisphosphate ($PIP_2$) to cytosolic inositol (1,4,5)-trisphosphate ($IP_3$) and membrane-bound hydrophobic second messenger diacylglycerol (DAG). Ultimately, activation of α-AR regulates the activity of the protein kinase C (PKC), phospholipase A2 and the release of arachidonic acid

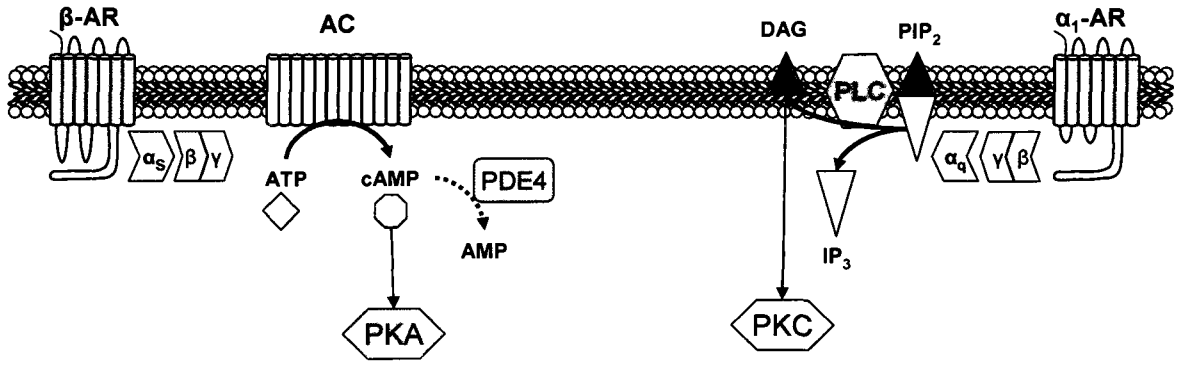


Figure 1-2: Schematic representation of the signaling cascades initiated by a $G_{s\alpha}$- and $G_{\alpha q}$-coupled receptors, represented by β-AR and the muscarinic acetylcholine receptors (mAchR). Agonist stimulation of the β-AR stimulates AC through the $G_{\alpha s}$ subunit to increase production of cAMP, which activates intracellular PKA. Stimulation of the $G_{\alpha q}$-coupled mAchR leads to PLC breaking $PIP_2$ into intracellular $IP_3$ and membrane-bound DAG second messenger, activating PKC.

(Berridge, 1987; Brodde et al., 2001). Stimulation of the $\alpha_1$-AR regulates $Ca^{2+}$ channels through the activation of PKC pathway (Myslivecek and Trojan, 2003), with positive inotropic effects (Brodde et al., 2001; Triposkiadis et al., 2009). $\alpha_2$-ARs are found on the pre- and post-synaptic membrane in the heart and are coupled to the inhibitory $G_{\alpha i}$ subunit (Riemann et al., 2003). Stimulation of pre-synaptic $\alpha_2$-AR decreases the outflow of NA by inhibiting cyclic adenosine 4,5-monophosphate (cAMP) generation in the varicosity, thereby providing negative feedback to excess synaptic NA (Boudreau et al., 1993; Parker et al., 1995).

### 1.4. Cardiac β-adrenergic receptors

Three β-AR subtypes designated $\beta_1$-, $\beta_2$- and $\beta_3$-AR have been cloned so far, with all of the subtypes detected in different concentrations in the mammalian heart (Brodde et al., 2001). Putative $\beta_4$-adrenoceptor is now widely accepted to be an alternate, propranolol-resistant state of the $\beta_1$-AR, with unclear role in signal transduction and cardiac regulation (Kaumann et al., 2001; Myslivecek and Trojan, 2003). $\beta_1$-AR and $\beta_2$-AR subtypes account for approximately 85% of total cardiac adrenoceptors in humans (Bristow, 1993). While $\beta_1$- and $\beta_2$-AR coexist on ventricular myocytes, $\beta_1$-AR is the dominant cardiac subtype (Alexander et al., 1975), outnumbering the $\beta_2$-AR two- to four-fold in the myocardium of humans, pigs and rats (Bristow et al., 1989; Liang and Mills, 2002; Myslivecek and Trojan, 2003; Brouri et al., 2004), while negligible amounts of $\beta_3$-AR are present in the heart (0.25% of all β-AR in left ventricle) (Liang and Mills, 2002; Myslivecek and Trojan, 2003).

Administration of the $\beta_1$- and $\beta_2$-AR agonist isoproterenol increases the strength of cardiac contraction, primarily by its short-term effects through the $\beta_1$-ARs (Bristow et al., 1989; Katano and Endoh, 1990; Katano and Endoh, 1992; Akhter et al., 1997). With prolonged agonist exposure, however, stimulation of $\beta_1$-AR was found to be pro-apoptotic and detrimental to the cardiac functioning (Benjamin et al., 1989; Communal et al., 1998; Communal et al., 1999; Zaugg et al., 2000; Brouri et al., 2004; Hu et al., 2006; Heather et al., 2009), while $\beta_2$-AR has been proposed to be cardioprotective (Communal et al., 1999; Shizukuda and Buttrick, 2002). As noted by Lefkowitz, et al. (Lefkowitz et al., 2000), distinct roles for $\beta_1$- and $\beta_2$-AR subtypes are evident from the fact that even 5-fold overexpression of the $\beta_1$-AR elicits cardiomyopathy in a mouse model (Engelhardt et al., 1999), while 100-fold overexpression of the $\beta_2$-AR elicits increased contractility of cardiomyocytes, with no pathological effects (Liggett et al., 2000).

## 1.5. β-AR signal transduction

### *1.5.1. G protein-coupled receptor*

Agonist binding to the β-AR, as in other G protein-coupled receptors (GPCRs), causes a dissociation of the associated G protein complex, releasing the $G_\alpha$ and $G_{\beta\gamma}$ subunits (Gilman, 1987; Chidiac, 1998; Rockman et al., 2002). Depending on the G protein α subunit associated with the receptor, agonist binding can lead to the stimulation (through the $G_{s\alpha}$ subunit) or inhibition ($G_{i\alpha}$) of adenylyl cyclase (AC), or activation of PLC by the $G_q/G_{11}$ subunit (Gilman, 1987; Rockman et al., 2002). $\beta_1$- and $\beta_2$-ARs are linked through the $G_{\alpha s}$ to AC stimulation (Cleator et al., 1999; Brodde et al., 2001). $\beta_2$-

AR has also been shown to couple with the $G_{i\alpha}$ subunit and inhibit AC (Daaka et al., 1997; Xiao et al., 1999; Rockman et al., 2002).

### *1.5.2. Adenylyl cyclase*

The AC family of proteins is composed of 9 members (I–IX); types V and VI predominate in mammalian cardiac tissues (Katsushika et al., 1992; Krupinski et al., 1992; Tobise et al., 1994; Espinasse et al., 1995; Tang et al., 2010). AC is co-localized at the plasma membrane with β-ARs and G proteins (Dupre et al., 2007). All ACs convert adenosine triphosphate (ATP) to the second messenger cAMP. $G_{s\alpha}$ activation occurs through the interaction of the G protein subunit with two AC cytoplasmic domains C1 and C2, while the inhibition by $G_{i\alpha}$ has been postulated to involve the cytoplasmic domain C1, at a location distinct from the stimulatory site (Sunahara et al., 1996; Dzimiri, 1999).

### *1.5.3. Cyclic adenosine 4,5 monophosphate*

cAMP was first discovered in 1957 by Earl Sutherland as the second messenger to the hormone adrenaline and has since been identified as a key component of the intracellular signal-transduction of dopamine, 5HT and histamine receptors (Bristow et al., 1989; Beavo and Brunton, 2002). Within the cardiac adrenergic signaling, brief exposure of cells to the β-AR agonist isoproterenol results in a rapid elevation in cAMP reaching ~10 μM, persisting less than 5 min (Violin et al., 2008). Intracellular cAMP exerts its functional effects primarily through the regulation of the protein kinase A (PKA).

### *1.5.4. Protein kinase A*

PKA, in its inactive basal state, is a heteromer of two catalytic and two regulatory subunits (Taylor et al., 1990; Bauman and Scott, 2002). Binding of cAMP to the regulatory subunit disassembles the holoenzyme, with the free catalytic subunits detaching and phosphorylating the intracellular target effector proteins (Taylor et al., 1990). The cAMP-binding site on the regulatory subunit of the PKA is susceptible to competitive inhibition by a stereoisomer of cAMP, ($R_p$)-cAMP, which is capable of binding the regulatory-catalytic complex without dissociating the individual subunits (de Wit et al., 1984; Botelho et al., 1988).

### *1.5.5. Cardiac effector proteins*

In the myocardium, activation of PKA following β-AR stimulation phosphorylates the L-type $Ca^{2+}$ channels, ryanodine receptors (RyR), troponin I, sarcoplasmic reticulum $Ca^{2+}$-ATPase (SERCA2a), myosin binding protein C (MBP-C) and phospholamban (PLB), among other effectors, as illustrated in Figure 1-3 (Jurevicius and Fischmeister, 1996; Li et al., 2000; Takahashi et al., 2006; Yamamoto et al., 2008). Ultimately, cAMP-mediated cardiac PKA activation affects $Ca^{2+}$ influx into the cytosol and the sensitivity of the contractile machinery to $Ca^{2+}$, thereby increasing the strength of cardiomyocyte contraction. Physiologically, tissue-dependent modulation of cell function implicates cAMP in the control of processes ranging from thermogenesis to memory formation, with abnormal levels and responsiveness associated with pathological states (Yoshida et al., 2001).

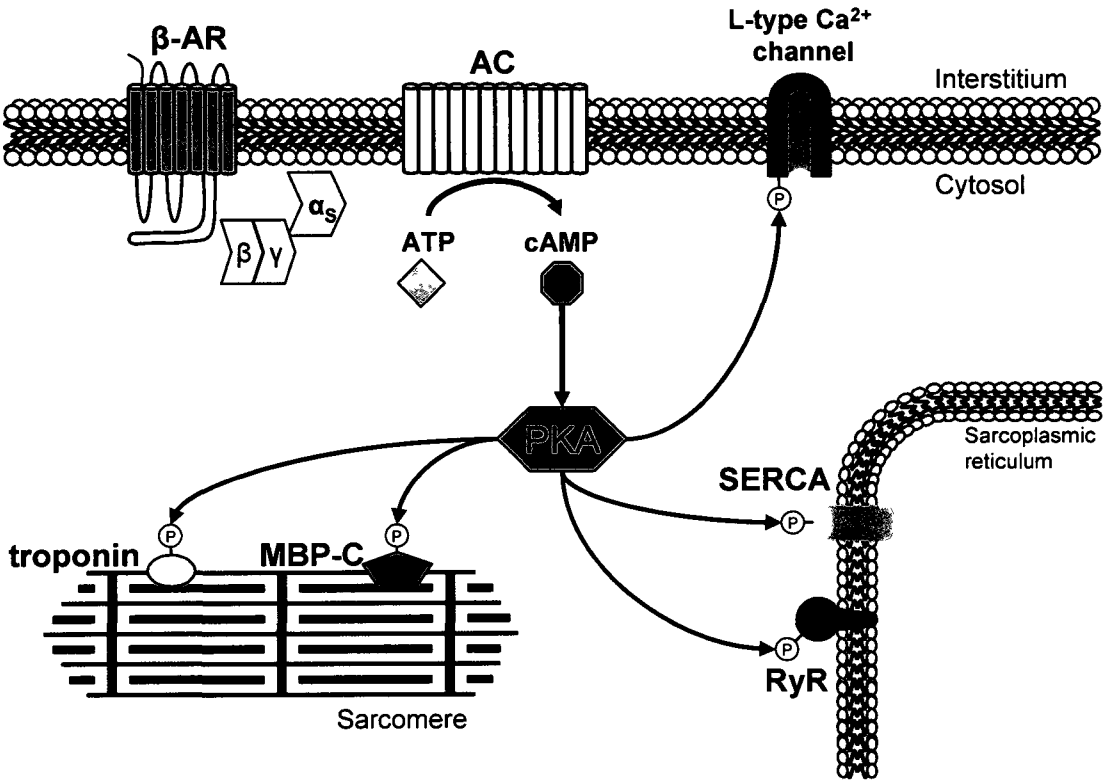


Figure 1-3: Regulation of cardiac $Ca^{2+}$ levels and contractility by the β-AR/AC/cAMP/PKA signal transduction cascade. Agonist stimulation of β-AR activates AC to increase production of cAMP. Elevated intracellular levels of cAMP stimulate PKA to phosphorylate cell surface L-type $Ca^{2+}$ channels, sarcoplasmic reticulum Ca2+-ATPase (SERCA) and ryanodine receptor Ca2+ channels (RyR). Additionally, phosphorylation of the troponin and myosin binding protein C (MBP-C) increases efficiency of the contraction by sensitizing the sarcomere proteins to $Ca^{2+}$.

## 1.6. Regulation of β-AR responsiveness and expression

β-AR function and expression, as with a number of other GPCRs, is modulated by intracellular signaling pathways, including its own cAMP/PKA cascade. At baseline conditions, the β-ARs are distributed almost equally between the sarcolemma and the light vesicle fraction representing the internalized and therefore agonist-insensitive receptor population (Maisel et al., 1985; Maisel et al., 1987). Upon agonist stimulation, desensitization of the β-ARs proceeds through either homologous or heterologous desensitization (Wallukat, 2002).

### *1.6.1. Homologous desensitization of β-AR*

β-AR homologous desensitization, described in Figure 1-4, is dependent on the agonist stimulation of the receptor initializing a downregulation cascade within seconds of receptor stimulation (Wallukat, 2002). GPCR kinases (GRKs), specifically the β-AR kinase (β-ARK1), phosphorylate the agonist-bound $\beta_1$- and $\beta_2$-AR at the cytosolic tail of the receptor protein (Pitcher et al., 1992; Freedman et al., 1995; Koch et al., 1995; Chuang et al., 1996; Wallukat, 2002). Phosphorylation by the GRK of the receptor causes the translocation of the cytosolic protein β-arrestin to the surface receptor and its binding to the third intracellular loop and the C-terminal tail (Bouvier et al., 1988; Barak et al., 1997; Bohm et al., 1997). The membrane-bound $G_{\beta\gamma}$ subunit released on receptor activation plays a role in recruiting the β-ARK1 to the cell membrane (Pitcher et al., 1992; Koch et al., 1993). β-arrestin binding to the β-AR sterically hinders G protein coupling, uncoupling the receptor from the downstream signaling (Lefkowitz, 1998)

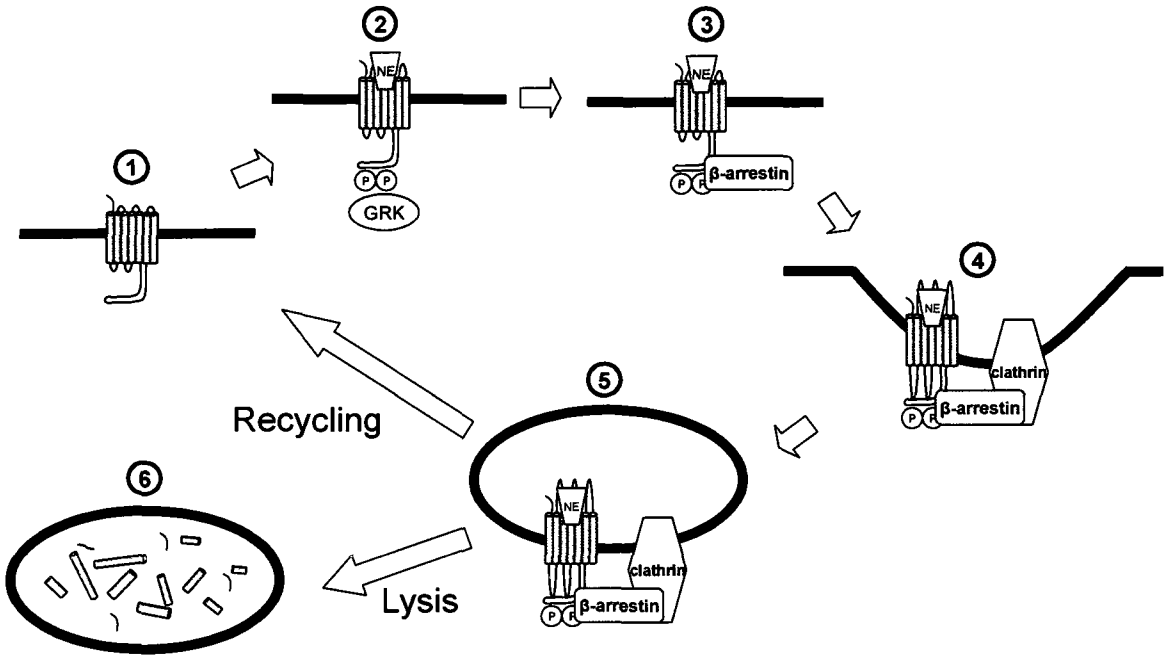


Figure 1-4: Schematic representation of the homologous desensitization of the β-AR. Agonist binding at the cell surface receptor detaches the $G_{s\alpha}$ and $G_{\beta\gamma}$ subunits (1). Agonist-bound receptor is phosphorylated by the G protein-coupled receptor kinase (GRK) (2). Phosphorylated receptor binds to the β-arrestin protein, which is localized to the cell surface through the interaction with the $G_{\beta\gamma}$ subunit (3). β-arrestin serves as an adapter to anchor the entire receptor-β-arrestin complex to the clathrin proteins in the membrane areas (4). Endocytosis of the clathrin-covered pits as an internalized vesicle removes the receptor from the cell surface, and neutralizes its signaling (5). The receptor in the vesicle undergoes degradation in a lysosome (6), or is recycled back to the cell surface (1).

(Violin et al., 2008). The process of $\beta_2$-AR receptor phosphorylation by the GRKs results in receptor deactivation with a half-life of 70s (Violin et al., 2008).

In addition to the decoupling from the G protein, β-arrestin serves to link the GRK-phosphorylated receptors to the clathrin cages (Lin et al., 1997), thus sequestering the receptors into endocytotic vesicles that remove the β-ARs from the cell surface (Pearse and Robinson, 1990; Drake et al., 2006). The internalized vesicles are directed either back to the cell surface, recycling the receptor, or to the lysosomal degradation of the protein (Dzimiri, 1999; Drake et al., 2006). Inhibition of β-arrestin increases cAMP production following agonist stimulation of the β-AR, while receptor internalization is reduced (Ahn et al., 2003).

### *1.6.2. Heterologous desensitization of β-AR*

Heterologous, or agonist-independent desensitization of β-AR proceeds through the phosphorylation of the receptor by the intracellular kinases PKA and PKC, and may be initiated by the activation of other receptors and signaling pathways (Castellano and Bohm, 1997). Receptors phosphorylated in this process exhibit decreased ability to activate the G protein (Pitcher et al., 1992; Freedman et al., 1995; Castellano and Bohm, 1997; Rockman et al., 2002). This process is generally slower than the homologous desensitization ($t_{1/2}$ of 3.5 min, vs ~20 sec for the β-ARK phosphorylation) (Castellano and Bohm, 1997; Mills, 2002; Violin et al., 2008).

### *1.6.3. Control of β-AR transcription*

β-ARs are decreased by 60-90% in studies performed in cell lines following sustained agonist stimulation (Harden, 1983; Sibley and Lefkowitz, 1985). Hadcock et al. have observed a 45% decrease in β-AR mRNA in MF-2 hamster vas deferens cells after 1 hr of isoproterenol treatment, implicating decreased receptor protein transcription (Hadcock and Malbon, 1988). In vivo, stimulation of the rat post-synaptic β-ARs through infusion of isoproterenol or NA has been associated with a downregulation within 7 days (Chang et al., 1982). Persistent stimulation of the receptors by i.p. administration of isoproterenol leads to a downregulation of the receptors (Kimura et al., 1993).

## 1.7. Phosphodiesterase-4

### *1.7.1. Phosphodiesterase superfamily*

Signal transduction cascades of the second messenger nucleotides cAMP and cyclic guanosine-monophosphate (cGMP) terminate with their catalysis to the corresponding mononucleotides adenosine-monophosphate (AMP) or guanosine-monophosphate (GMP) by the phosphodiesterase (PDE) family of enzymes in a process dependent on the presence of cofactors $Zn^{2+}$ or $Mg^{2+}$ (Liu et al., 2001; Laliberte et al., 2002; Zhao et al., 2003). To date, 21 genes have been discovered that encode approximately 50 different PDE enzyme isoforms grouped into 11 subfamilies (PDE1-11) according to the mononucleotide selectivity, amino acid sequence, kinetic properties and regulatory profile (Houslay and Adams, 2003; Wong et al., 2006; Omori and Kotera, 2007; Esposito et al., 2009; Zhang, 2009). cAMP is selectively broken down by the PDE4, 7 and 8 subfamilies, while PDE5, 6 and 9 are cGMP-specific and PDE1, 2, 3, 10 and 11 hydrolyze both cyclic nucleotides with equal affinity (Torphy, 1998; Conti and

Jin, 1999; Houslay and Adams, 2003; Omori and Kotera, 2007). Table 1-1 summarizes the properties of the PDE subfamilies.

PDE isozymes are distributed throughout the body, playing a part in physiological processes including vision (PDE6) (Lamb and Pugh, 2006), olfaction (PDE4) (Borisy et al., 1993), penile erection (PDE5) (Moreland et al., 1998), airway constriction (PDE4) (Sturton and Fitzgerald, 2002), memory formation (PDE2 and PDE4) (Barad et al., 1998; Monti et al., 2006; Reneerkens et al., 2009), cardiac contractility (PDE3 and PDE4) and inflammation (PDE4) (Barnette et al., 1998). Expression of PDE1, 2, 3, 4, 5, 7 and 9 have been reported in the cardiac tissues (Lugnier, 2006; Mongillo et al., 2006).

### *1.7.2. Phosphodiesterase-4 subfamily*

PDE4 isozymes are distinguished by their high affinity for cAMP ($K_m$ of 1–5 μM (Torphy et al., 1992; Houslay and Milligan, 1997; Omori and Kotera, 2007). This PDE subfamily was the subject of intense study due to the efficacy of PDE4 inhibitors in treatment of asthma and depression (Zeller et al., 1984; Bertolino et al., 1988). Recent genetic association studies have linked PDE4 with ischemic stroke (Gretarsdottir et al., 2002) and with spinal regeneration (Nikulina et al., 2004). Transcriptional variants of the four PDE4 genes (PDE4A, PDE4B, PDE4 C and PDE4D) encode over 20 distinct isoforms (Rao and Xi, 2009), classified as long, short and super-short depending on the presence of upstream conserved regions (UCR1 and UCR2) flanking a catalytic site comprising 270-400 amino acids common to all subtypes (Beavo, 1995; Conti and Jin, 1999) (Figure 1-5, Table 1-2). Differences in the N-terminus regions of PDE4 subtypes lead to distinct localized cellular compartments, differences in susceptibility to

Table 1-1: Comparison of properties of phosphodiesterase (PDE) enzymes.

| Subfamily | Genes | Expression | Substrate | Inhibitor | Property |
|---|---|---|---|---|---|
| PDE1 | PDE1A<br>PDE1B<br>PDE1C | Brain, heart, smooth muscle, lung[2,3,4,5,6] | cAMP/cGMP | zaprinast | $Ca^{2+}$-CaM-stimulated |
| PDE2 | PDE2A | Brain, heart, adrenal cortex, platelets[2,7,8] | cAMP/cGMP | EHNA, dipyridamole | cGMP-stimulated |
| PDE3 | PDE3A<br>PDE3B | Heart (PDE3A only)[1], brain, smooth muscle, kidneys, platelets[2,10] | cAMP/cGMP | Cilostamide, amrinone, milrinone | cGMP-inhibited[9] |
| PDE4 | PDE4A<br>PDE4B<br>PDE4C<br>PDE4D | Brain, heart, skeletal muscle, adipose tissue, immune cells, pancreas | cAMP | Rolipram, Ro 20-1724 | Characterized by rolipram inhibition |
| PDE5 | PDE5A | Brain, lung, smooth muscle, skeletal muscle, kidneys, platelets[2,11,12,13,154] | cGMP | Sildenafil, vardenafil | |
| PDE6 | PDE6A<br>PDE6C<br>PDE6D<br>PDE6G | Retinal rod and cone cells[15], pineal gland[2,16,17] | cGMP | Zaprinast, vardenafil | Phototransduction, high hydrolysis rate[15] |
| PDE7 | PDE7A<br>PDE7B | T-cells, brain[21,22], skeletal muscle[18,20], fetal tissues[19], lung, testes[21] | cAMP[18-19] | BRL50481[32] | Two PKA phosphorylation sites[21] |
| PDE8 | PDE8A<br>PDE8B | Thyroid gland, brain (PDE8B)[22,23], testis, spleen, colon, small intestine, ovary, placenta, kidneys[24] | cAMP[23] | | IBMX-insensitive |
| PDE9 | PDE9A | Brain[2,25,26] | cGMP | | |
| PDE10 | PDE10A | Brain[2,28] | cAMP/cGMP[27] | | |
| PDE11 | PDE11A | Skeletal muscle, prostate, testis, salivary glands[29], parasympathetic ganglia[30], brain[31] | cAMP/cGMP | | |

1 Osadchii et al., 2007
2 Reneerkens et al., 2009
3 Dent et al., 1998
4 Sonnenburg et al., 1998
5 Yan et al., 1994
6 Kostic et al., 1997
7 Ito et al., 1996
8 Martins et al., 1982
9 Movsesian et al., 2009
10 Reinhardt et al., 1995
11 Giordano et al., 2001
12 Hotston et al., 2008
13 Kotera et al., 2000
14 Yanaka et al., 1998
15 Cote, 2004
16 Holthues and Vollrath, 2004
17 Morin et al., 2001
18 Bloom and Beavo, 1996
19 Han et al., 1997
20 Michaeli et al., 1993
21 Sasaki et al., 2002
22 Perez-Torres et al., 2003
23 Kobayashi et al., 2003
24 Wang et al., 2001
25 Reyes-Irisarri et al., 2007
26 van Staveren et al., 2002
27 Soderling et al., 1999
28 Seeger et al., 2003
29 Makhlouf et al., 2006
30 Loughney et al., 2005
31 Wong et al., 2006
32 Smith et al., 2004

EHNA erythro-9-(2 hydroxy-3-nonyl)adenine
IBMX 3-isobutyl-1-methylxanthine

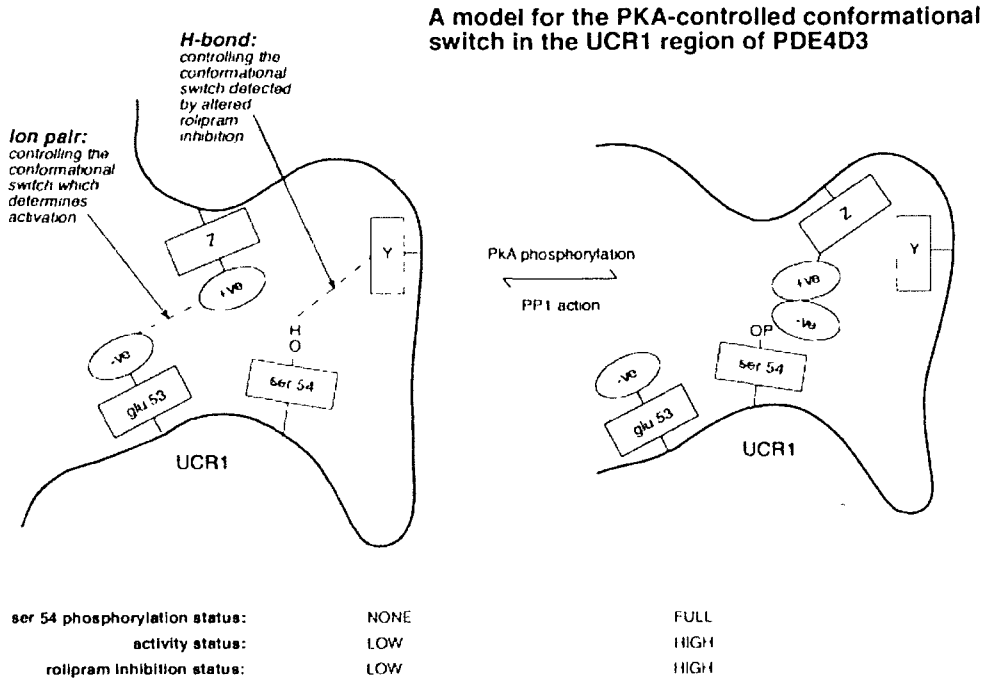


Figure 1-5: Proposed conformational change elicited by the PKA phosphorylation of the Ser54 residue in PDE4D3 isozyme. From Hoffman et al, 1999 (Hoffmann et al., 1998).

Table 1-2: Classification of PDE4 isozymes by the structure into long, short and super-short enzymes.

| Gene | Structure | Variant | Reference |
|---|---|---|---|
| PDE4A | *Long* | 4A4/5 | Terry et al., 2003; Abi-Gerges et al., 2009 |
| | | 4A8[1] | Abi-Gerges et al., 2009 |
| | | 4A10[1,2] | Rena et al., 2001; Abi-Gerges et al., 2009 |
| | | 4A11[2] | Rena et al., 2001 |
| | *Super-short* | 4A1[2] | Rena et al., 2001 |
| | *Dead-short* | 4A7[2] | Rena et al., 2001 |
| PDE4B | *Long* | 4B1[3] | Kostic et al., 1997 |
| | | 4B3[3] | Kostic et al., 1997 |
| | | 4B4[6] | Shepherd et al., 2003 |
| | *Short* | 4B2[3,4] | Kostic et al., 1997; Richter et al., 2005 |
| | *Super-short* | 4B5[7] | Cheung et al., 2007 |
| PDE4C | *Long* | 4C1[8] | Owens et al., 1997 |
| | | 4C2[8] | Owens et al., 1997 |
| | | 4C3[8] | Owens et al., 1997 |
| PDE4D | *Long* | 4D3[3,9] | Bolger et al., 1997; Kostic et al., 1997 |
| | | 4D4[4,9] | Bolger et al., 1997; Richter et al., 2005 |
| | | 4D5[9] | Bolger et al., 1997 |
| | | 4D7[4] | Richter et al., 2005 |
| | | 4D8[4] | Richter et al., 2005 |
| | | 4D9[4] | Richter et al., 2005 |
| | *Short* | 4D1[3,4,9] | Bolger et al., 1997; Kostic et al., 1997; Richter et al., 2005 |
| | *Super-short* | 4D2[3,4,9] | Bolger et al., 1997; Kostic et al., 1997; Richter et al., 2005 |
| | | 4D6[4] | Richter et al., 2005 |
| | | 4D10[10] | Chandrasekaran et al., 2008 |
| | | 4D11[10] | Chandrasekaran et al., 2008 |

phosphorylation, and interactions with different scaffolding proteins (Houslay et al., 2007).

## 1.8. PDE4 expression

PDE4 enzymes are expressed in virtually every tissue in the body, with the brain, heart, lung and skeletal muscle tissue exhibiting highest levels (McLaughlin et al., 1993; Engels et al., 1994; Houslay et al., 1998). mRNA quantification by real-time polymerase chain reaction (RT-PCR) has detected all four PDE4 subtypes in the human brain, liver, lung, kidney and cardiac tissue (Engels et al., 1994; Engels et al., 1995). Overall PDE4 mRNA expression in rat tissues is higher than in humans (Bian et al., 2004), while the relative levels of isozymes in the rat brain and heart are different from the human expression profile (Engels et al., 1994; Engels et al., 1995). PDE4A, B and D, but not the PDE4C, subtypes are found in the rat brain and heart tissues (Bolger et al., 1994; Engels et al., 1994; Kostic et al., 1997; Iona et al., 1998; Takahashi et al., 1999; Takahashi et al., 2002; Houslay and Adams, 2003; Abi-Gerges et al., 2009). In isolated ovine cardiac nuclei, 56% of the total cAMP-hydrolyzing activity is due to PDE4, with the rest accounted for by the PDE3 enzymes (Lugnier et al., 1999).

## 1.9. PDE4 regulation

### *1.9.1. PKA phosphorylation*

Cell permeable form of cAMP, dibutyryl-cAMP (db-cAMP), and agents that increase cAMP synthesis (e.g. isoproterenol by β-AR agonism or forskolin by AC activation) rapidly (within 15-30 min) elevate PDE4 activity (Sette et al., 1994; Verghese

et al., 1995; Chang et al., 1997; Liu and Maurice, 1999; Murthy et al., 2002). PDE4 activity in isolated monocytes increases 2-fold 18-24 hours after treatment with db-cAMP, returning to baseline levels after 48 hours of continous treatment (Verghese et al., 1995). Maximal PDE4 activity increase was observed in these cells after 4 hours of stimulation (Verghese et al., 1995). The ability of the PKA inhibitor H89 to block these increases in enzyme activity, as well as the PDE4-stimulating effect of the PKA activator 5,6-dichloro-1-β-D-ribofuranosyl benzimidazole 3',5'-cyclic monophosphate SP-isomer (cBIMPS) and membrane permeable cAMP analogue 8-Br-cAMP, implicate PKA phosphorylation of PDE4 in the observed increase in catalytic function (Alvarez et al., 1995; Chang et al., 1997; Liu and Maurice, 1999; Murthy et al., 2002). PKA-mediated phosphorylation of the PDE4 enzyme occurs at the Ser-54 residue in the UCR1 region of the long isoforms, disrupting the hydrogen bond, placing a negative charge at that position and switching the conformation of the entire enzyme to the high activity form (Sette and Conti, 1996; Hoffmann et al., 1998; Torphy, 1998; Liu and Maurice, 1999) (Figure 1-5). Ser54 phosphorylation was observed to affect only the long forms of the PDE4 isozymes, since the shorter isoforms lack the relevant UCR1 region (Sette and Conti, 1996; Richter et al., 2005). In addition to increased catalytic activity, PKA-phosphorylated PDE4 exhibits increased affinity for the inhibitor rolipram, with the $IC_{50}$ values decreased 6-15 times upon phosphorylation (0.68 μM to 0.11 μM with PDE4D3; 123 nM to 8 nM with PDE4A4) (Sette and Conti, 1996; Hoffmann et al., 1998; Laliberte et al., 2002), which has been recently confirmed in vivo (Itoh et al., 2010).

### *1.9.2. ERK phosphorylation*

Mitogen-activated protein kinase (MAPK) extracellular-signal regulated kinase 2 (ERK2) phosphorylates PDE4 isozymes at a site within the catalytic region (Liu and Maurice, 1999; MacKenzie et al., 2000), inhibiting the catalytic activity of the long isoforms and stimulating the short isoforms (Hoffmann et al., 1998; Zhang, 2009). Susceptibility of PDE4 isozymes to the regulation by the kinases of two distinct intracellular signaling pathways allows individual subtypes to differentially respond by increased expression and phosphorylation, depending on their immediate intracellular milieu, providing precise control over cAMP levels in the cellular compartments (Kostic et al., 1997).

### *1.9.3. Increased PDE4 enzyme expression*

Studies in vascular smooth muscle cells, human monocytes, human umbilical vein endothelial cells as well as rat tissues have demonstrated increased PDE4 expression and activity with sustained (> 2 hrs) increases in cAMP levels (Torphy et al., 1992; Engels et al., 1994; Manning et al., 1996; Rose et al., 1997; Torphy, 1998; Tilley and Maurice, 2002; Campos-Toimil et al., 2008). Increases in PDE4 activity were attenuated by the transcription inhibitor actinomycin-D or protein synthesis disruptor cycloheximide, implicating de novo protein synthesis (Torphy et al., 1992; Tenor et al., 1996; Erdogan and Houslay, 1997; Campos-Toimil et al., 2008).

### *1.9.4. Decreased PDE4 activity and expression*

Modulation of PDE4 activity and expression is susceptible to downregulation, as well as stimulation, by the intracellular cAMP levels. Administration of a non-selective

antagonist propranolol and 6-OHDA-induced destruction of the noradrenergic neurons reduce cAMP-catalyzing activity and PDE4 (PDE4A and B) expression in brain tissues (Ye et al., 1997; Farooqui et al., 2000).

### 1.10. PDE4 and cAMP compartmentalization

Considering that free diffusion of cAMP in the cytosol is estimated to occur rapidly (130–700 $\mu m^2$/sec) (Houslay et al., 2007), the specificity and variability of intracellular responses to the second messenger can only be explained by the presence of molecular barriers to the propagation of the signal. PDE subtypes underlie the formation of discrete regions of signal-amplification ("compartmentalization") by creating intracellular cAMP gradients through co-localization with the β-AR, AC, and the effector proteins. Involvement of PDE is demonstrated by the free diffusion of the β-AR initiated signal to propagate throughout the cell in the presence of the non-selective PDE inhibitor 3-isobutyl-1-methylxanthine (IBMX) (Jurevicius and Fischmeister, 1996; Houslay and Milligan, 1997). In the adult rat ventricular myocyte, PDE4 is the foremost catalytic enzyme that maintains intracellular cAMP compartments, with PDE3 inhibitors only affecting the free distribution if PDE4 activity is already suppressed (Leroy et al., 2008). Individual subtypes of PDE4 exist in discrete pools within the cell (Jin et al., 1998), suggesting that compartmentalization is maintained by a complex system of co-localization with distinct proteins. A-kinase anchoring protein (AKAP) is one of the scaffolding proteins that plays a role in compartmentalization by targeting PKA to the cell surface receptors, placing it to the proximity of AC and PDE4 (Bauman and Scott, 2002; Baillie et al., 2005).

## 1.11. Heart failure

### *1.11.1. Definition and aetiology*

Heart failure is a progressive pathological state defined by the inability of the heart to adequately meet the circulatory demands of the body (Bristow et al., 1982; Ramani et al., 2010), most frequently associated with coronary artery disease and/or hypertension (Ramani et al., 2010). A normal heart fails in its physiological function following a short-term injury, such as myocardial infarction (MI), or as a result of a sustained unfavourable condition such as valve disease or hypertension (Ramani et al., 2010). The tissue and systemic responses that follow cardiac dysfunction form the maladaptive cascade of alterations at the neurohormonal and histological level.

Using ischemic insult as an example, a heart that suffered a myocardial infarction undergoes a remodeling process that is initially compensatory, but can culminate in heart failure with a significant enough defect. At its most basic, post-infarct remodeling is a progressive change in the volume and geometry of the left ventricle (Bengel, 2009). The process itself can be divided into an early (first 72 hours) and late phase. The early phase involves local (peri-infarct) events, including the expansion of the necrosis around the infarct zone, degradation of extracellular collagen, wall thinning and ventricular dilatation, with possible externalization of β-AR (Maisel et al., 1985; Sutton and Sharpe, 2000; Dobrucki and Sinusas, 2010). Compensatory mechanisms are mobilized at this stage, with the altered hemodynamics stimulating the sympathetic adrenergic system, resulting in increasing catecholamine synthesis and release. In the late stages, myocyte hypertrophy occurs, with the heart distributing wall stresses more evenly across the intact

myocardium (Sutton and Sharpe, 2000). Coronary flow rate of the heart is significantly reduced in the ischemic area immediately following infarction, with a gradual increase over the next 14 days, likely due to anastomoses and collateral vessel formation, reaching control values after three months (Bester et al., 1972).

### *1.11.2. Heart failure as a hyperadrenergic state*

Studies published in 1964 initially found left ventricular NA to be decreased to 50% or less then normal levels in heart failure patients (Chidsey et al., 1963; Chidsey et al., 1963; Chidsey et al., 1964), leading to a period in which β-blockers were counterindicated in heart failure therapy and adrenergic agonists as inotropic agents saw wide use, resulting in increased mortality (Nony et al., 1994). Organ-specific tracer kinetic techniques have subsequently shown that the failing heart is actually in a hyperadrenergic state, with a NA spillover rate up to 50 times higher than normal levels (Thomas and Marks, 1978). Currently, it is recognized that the failing heart is sympathetically overstimulated, with the plasma NA concentration correlating directly with the severity of cardiac dysfunction (Thomas and Marks, 1978; Cohn et al., 1984; Swedberg et al., 1984; Leimbach et al., 1986; Eisenhofer et al., 1996; Bristow, 2000; Osadchii et al., 2007).

Increased sympathetic nervous system stimulation and resultant elevation of cardiac adrenergic tone is initially compensatory and aimed at re-establishing cardiac function through increasing contractility. With sustained sympathetic hyperactivity, persistent adrenergic stimulation turns maladaptive and pathogenic (Floras, 2003; Houser and Margulies, 2003). Adrenergic hyperactivity is a common factor in heart failure,

regardless of the underlying etiology (Leimbach et al., 1986; Eisenhofer et al., 1996; El-Armouche et al., 2003; Osadchii et al., 2007). Cardiac release of NA could be increased up to 20-fold in HF patients (Swedberg et al., 1984; Hasking et al., 1986) reaching levels observed in the heart of a healthy person at near maximal exercise exertion (Hasking et al., 1986; Patel et al., 1996). Similar increases in plasma and myocardial NA were observed in animal models of heart failure utilizing drug-induced, surgical and genetic models of heart failure in rabbits, rats, mice, hamsters and dogs (Tong et al., 1991; Ikegaya et al., 1992; van Veldhuisen et al., 1994; Yoshikawa et al., 1994; Takahashi et al., 2002; Lymperopoulos et al., 2007). In a number of animal models of heart disease, prolonged presence of heart failure may result in the depletion of cardiac NA, reducing the cardiac circulating levels (Vogel and Chidsey, 1969; Hajjar et al., 1993). Since heart failure is a hyperadrenergic state, use of β-AR blockers reduced mortality by 30-69% (Packer et al., 1996).

### *1.11.3. Alterations in β-AR expression and function*

In a first report of β-AR downregulation in the failing heart, Bristow et al. observed a 2-fold reduction in receptor levels, as established by studies on cardiomyocyte membranes obtained from NYHA level IV heart failure patients with severe functional defects (Bristow et al., 1982). In the three decades since, decreased β-AR levels were confirmed in human patients and animal cardiopathology models (Sanbe and Takeo, 1995; Akhter et al., 1997; Tse et al., 2000; Yoshida et al., 2001). Specifically, left anterior descending coronary artery (LAD) ligation reduced isoproterenol responsiveness (Yoshida et al., 2001), with a ~25% decrease in the total β-AR density (Sanbe and Takeo,

1995). Decreased $B_{max}$ of $^{125}$I-labeled $\beta_1$-AR antagonist (-)iodocyanopindolol in the right ventricular endomyocardial biopsy tissues has been observed in subjects with moderate (38.2%) or severe (57.7%) dysfunction (Fowler et al., 1986). The same series of experiments have shown a diminished contractile response in the failing heart to the $\beta_1$-selective agonist dobutamine and normal response to $Ca^{2+}$, suggesting that the contractile machinery of the cardiomyocytes remains functional (Fowler et al., 1986).

Adrenergic receptor density in heart failure is altered in a subtype-specific fashion. $\beta_1$-AR density decreases from 60 fmol/mg to ~35 fmol/mg in failing human hearts, while the expression of $\beta_2$-AR is not altered (~20 fmol/mg) (Satwani et al., 2004). In a rat model of ligation-induced ischemic heart failure, $\beta_1$-AR expression as a proportion of total β-AR decreases from 81.5% to 67.1% 10 weeks following infarct (Pfeffer et al., 1979; Witte et al., 2000). Spontaneously hypertensive rats in heart failure display a 25% decrease in total β-AR $B_{max}$ and increased relative proportion of $\beta_2$-AR from 44 to 53% (Xiao et al., 2003). Canine pacing-induced heart failure studies exhibit a change in $\beta_1/\beta_2$ ratio from 72/28 to 45/55, without a reduction in total β-AR density (Tse et al., 2000; Laurent et al., 2001).

GRK phosphorylation of the β-AR is increased in heart failure (Ungerer et al., 1993; El-Armouche et al., 2003), correlating with increased β-ARK1 expression and activity (Akhter et al., 1997; Choi et al., 1997). Induction of β-ARK1 with an inhibitor peptide in the ventricular myocytes isolated from failing hearts of a hypertensive rat model increased basal and isoproterenol-stimulated cAMP production and improved contractile function (Eckhart and Koch, 2002). Downregulation of β-AR in heart failure was postulated to proceed through the heterogenous desensitization processes, with the

receptors being sequestered into the endocytotic vesicles and rendered unresponsive to an agonist by internalization. Phosphorylation of $\beta_2$-AR by PKA has been shown to switch the receptor G-protein coupling from $G_{s\alpha}$ to the inhibitory $G_{i\alpha}$ subunit through the recruitment of β-arrestin to the receptor (Baillie et al., 2003).

*1.11.4. Alterations in the post-receptor cAMP signaling cascade*

In contrast to the well-characterized changes in the β-AR cell surface expression in pathological states, alterations in the signal transduction elements that follow receptor activation are still contentious, with proposed alterations illustrated in Figure 1-6. While some studies have reported a decrease in $G_{s\alpha}$ in human patients and animal disease models (Longabaugh et al., 1988; Kessler et al., 1989; Horn and Bilezikian, 1990; Yoshida et al., 2001), other groups reported normal protein expression and mRNA (Feldman et al., 1988; Sethi et al., 1994; Bohm, 1995), or even an increase (Ikegaya et al., 1992; Sethi et al., 1998; Movsesian et al., 2009). More consensus exists on the $G_{i\alpha}$ subunit, with a number of groups reporting increases in subunit activity (evaluated as the capability of the $G_{i\alpha}$ inhibitor pertussis toxin to remove inhibition of AC and catalyze ADP-ribosylation), mRNA levels and protein expression in heart failure (Feldman et al., 1988; Sethi et al., 1998).

Canine and rabbit studies have confirmed the decreases in AC activity in cardiomyocytes from failing hearts (Akhter et al., 1997; Tse et al., 2000). Following induction of myocardial infarction in male Sprague-Dawley rats (occlusion of the left coronary artery), AC activity in purified sarcolemmal preparations is decreased in the left and increased in the right ventricle (Sethi et al., 1997). In a canine model of pacing-

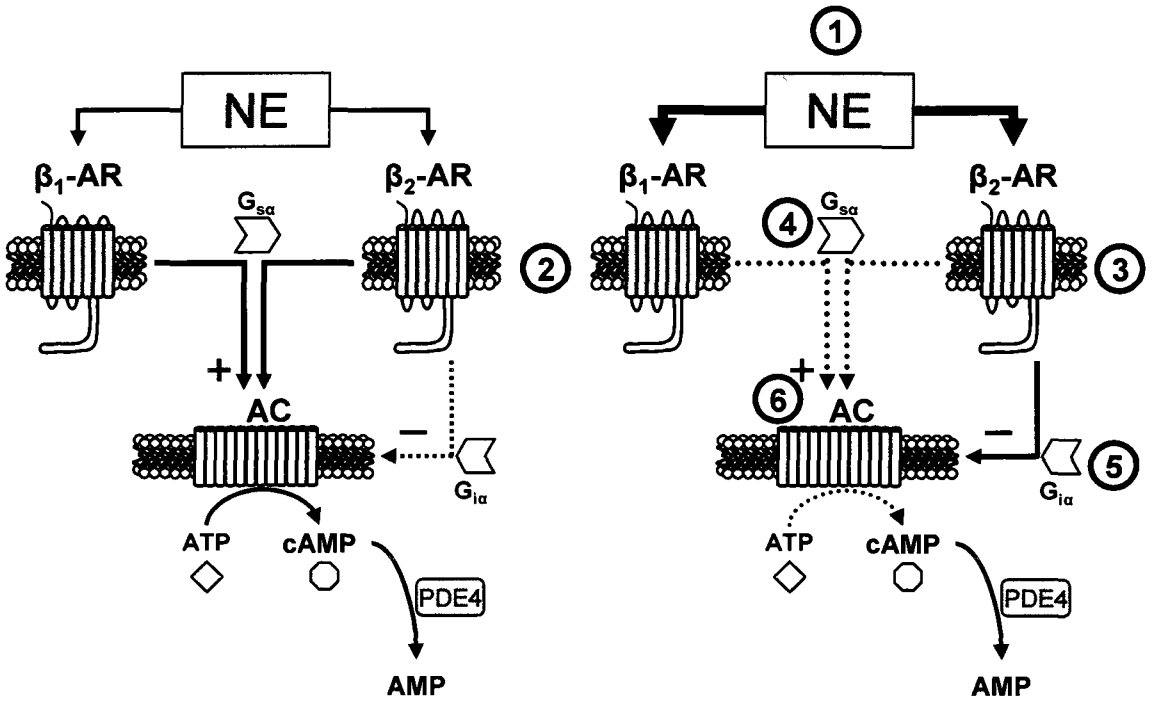


Figure 1-6: Schematic representation of the reported alterations in the activity of the components of NA signaling in heart failure. At physiological state, NA release stimulates post-synaptic $\beta_1$- and $\beta_2$-AR, which are linked to the activation of the AC by the $G_{s\alpha}$ subunit or, in case of $\beta_2$-AR, also to inhibition of the AC by the $G_{i\alpha}$ subunit. AC converts ATP to cAMP, which is broken down to adenosine monophosphate by the PDE4 enzyme. In heart failure, NA levels are elevated, increasing the stimulation of the post-synaptic receptors (1). Downregulation of the $\beta_1$-AR occurs through heterologous and homologous desensitization (2). $\beta_2$-AR signaling is switched to inhibit the AC more strongly (3). $G_{s\alpha}$ subunit expression is generally found to be unaltered in heart failure (4). $G_{i\alpha}$ subunit expression is elevated in heart failure (5). Finally, most studies with heart failure models show decreased activity and expression of the AC (6).

induced heart failure, responsiveness at the AC level to isoproterenol is diminished at 4 days of tachycardia. However, AC response to the direct activator forskolin is attenuated only at 24 days of pacing (Ping et al., 1997), suggesting a different time-course for downregulation of the individual components of the β-AR signal transduction. In other models, the response of AC activity to direct stimulation by the forskolin derivative colforsin daropate is preserved following LAD ligation (Sanbe and Takeo, 1995; Toyoshima et al., 1998; Yoshida et al., 2001), suggesting that some of the reported decreases in AC activity may reflect increased activity of the AC-inhibiting $G_{i\alpha}$ subunit.

### *1.11.5. Phosphodiesterase-4 in animal models of cardiac dysfunction*

Direct involvement of PDE4 in the pathogenesis of heart failure has been shown by the progressive development of cardiomyopathy in the genetic knockout of the PDE4D enzyme, without a reduction in β-AR levels (Lehnart et al., 2005). In human failing cardiac tissues, a reduction in RyR-bound PDE4D phosphorylation and activity has been observed (Lehnart et al., 2005). Pacing-induced cardiac failure in dogs with left ventricular hypertrophy displayed no change in PDE4 catalytic activity, despite significant decreases in $\beta_1$-AR density and AC activity (Tse et al., 2000). Conversely, PDE4 levels were slightly increased in the rat cardiomegaly model involving chronic (12 day) administration of isoproterenol (Tse et al., 1978). In the pressure-induced congestive heart failure rat model, 18 weeks on high-salt diet increases PDE4 mRNA levels and activity, in parallel with a decrease in cardiac fractional shortening (Takahashi et al., 2002). Similar model of hypertension-induced cardiac hypertrophy displays unchanged PDE4 levels despite the loss of acute responsiveness to isoproterenol, as evidenced by the

preserved contractile response to PDE4 inhibitors (Osadchii et al., 2005). Studies utilizing aortic banding to induce cardiac hypertrophy show β-AR desensitization with a concomitant reduction in PDE4A and PDE4B, and no change in PDE4D (Abi-Gerges et al., 2009). Cardiac hypertrophy resulting from chronic stimulation of β-AR receptors in rats exhibited preserved contractile response to PDEs, despite reduced inotropic response to agonists.

## 1.12. Cardiac PET imaging

### *1.12.1. Cardiac positron emission tomography imaging*

Positron emission tomography (PET) is a nuclear imaging technique that utilizes a three-dimensional quantification of radiolabeled tracer distribution within the body, as illustrated in Figure 1-7, to gain insight into physiological and pathological processes at the molecular level. A cyclotron-produced neutron-deficient radioisotope is incorporated into a molecule with a desired pharmacological profile and injected into a patient or experimental animal. The "tracer" distributes through the body according to its unique pharmacokinetic and pharmacodynamic properties. The unstable isotope decays by the emission of a positron, which travels a short distance through the body and annihilates with an electron to emit two anti-parallel γ-rays of 511 keV. PET cameras consist of photon-sensitive scintillation crystals arranged in a ring around the test subject that record the coincident events. Following electronic amplification of the signal, volumetric density of the decay events is calculated and corrected for scatter and attenuation, resulting in a three-dimensional PET "image". The distribution of the tracer depends on the nature of the labeled compound.

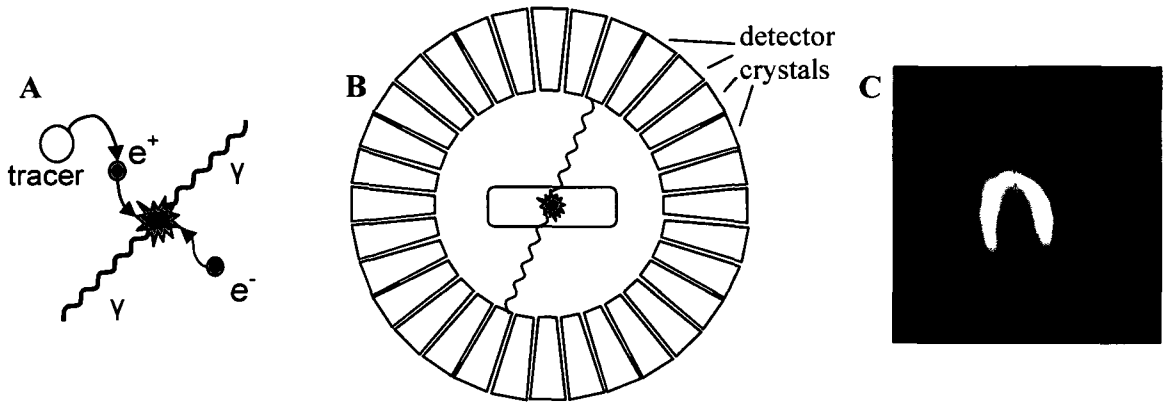


Figure 1-7: Radiolabeled tracer (a molecule of interest which has an incorporated neutron-deficient radioisotope) is injected into the subject, distributes according to the labeled compound's pharmacokinetic and pharmacodynamic profile and decays through emission of a positron ($e^+$) (A). Released positron annihilates with an electron ($e^-$) within the tissue, emitting two anti-parallel 511 keV γ-rays (photons). A ring of scintillation crystals detects coincident event (B), allowing the location and frequency of the tracer decay events to be calculated. Following corrections for scatter and attenuation, a three-dimensional PET image is obtained, representing the volumetric density of decays, and thereby the tracer distribution (C).

PET imaging is routinely applied in the evaluation of myocardial perfusion using tracers like [$^{13}$N]$NH_3$, [$^{15}$O]$H_2O$ and [$^{11}$C]CO (Di Carli and Dorbala, 2006). Recent years have seen major advances in myocardial imaging, moving beyond perfusion visualization towards high resolution and sensitivity in vivo evaluation of molecular targets such as transporter proteins, receptors and second messenger molecules (Chun et al., 2008; Bengel, 2009). A number of physiological processes in the myocardium have been targeted, including metabolism (with [$^{18}$F]FDG and [$^{11}$C]acetate), apoptosis (with [$^{18}$F]fluoroannexin), NA reuptake (with [$^{11}$C]hydroxyephedrine ([$^{11}$C]HED)) and post-synaptic receptors ([$^{11}$C]methylquinuclidinyl benzilate (MQNB), [$^{11}$C]CGP12177, [$^{11}$C]CGP12388, [$^{18}$F]fluorocarazolol, [$^{11}$C]ICI-OMe) (Grierson et al., 2004; Lautamaki et al., 2007; Shirani and Dilsizian, 2009).

### *1.12.2. PET noradrenergic imaging targets*

Once the involvement of NA signaling in the pathophysiology of heart failure, hypertension, obesity and other disorders was established, a number of techniques were devised to measure NA outflow and signaling. These included mathematical analysis of the heart rate variability and assessment of the firing of the sympathetic nerves by microneurography, evaluated by an electrode inserted into the peroneal nerve bundles (Floras, 2003; Vallbo et al., 2004; Charkoudian and Rabbitts, 2009). Alternatively, measurements of radiotracer dilution have been applied to quantify the plasma spillover of NA, reflecting the balance between NA release, reuptake and metabolism (Esler et al., 1984). Both techniques are relatively indirect, with microneurography measuring the sympathetic efferent signal onto the skeletal muscle and extrapolating to the cardiac

innervation, while spillover measurements provide no indication of the NA levels in the cardiac muscle itself. PET imaging provides a method for non-invasive direct measurements of NA release and uptake, as well as post-synaptic receptor signaling.

The predictive value of clinical PET imaging of pre- and post-synaptic aspects of adrenergic signal transduction in the heart has been demonstrated (Pietila et al., 2001; Higuchi and Schwaiger, 2006; Link and Caldwell, 2008). The single photon emission computed tomography (SPECT) agent metaiodobenzylguanidine (MIBG), labelled with $^{125}$I, provided the first imaging studies of the pre-synaptic NA uptake (Wieland et al., 1981). Since the initial studies, $^{123}$I-labeled MIBG is routinely used in the clinical assessment of cardiac adrenergic innervation with prognostic value (Agostini et al., 2008; Link and Caldwell, 2008). The NA-analogue [$^{11}$C]meta-hydroxyephedrine ([$^{11}$C]HED) has seen widespread use as a PET agent for the assessment of cardiac innervation and noradrenergic transmission (Ungerer et al., 2000; Pietila et al., 2001). $^{11}$C-labeled adrenaline has been applied to measure the myocardial catecholamine uptake, showing that a defect in noradrenergic innervation is larger than the defect in [$^{13}$N]$NH_3$-measured blood perfusion, with the mismatched area providing a substrate for initiation of ventricular arrhythmias (Sasano et al., 2008).

Post-synaptic receptor antagonists [$^{11}$C]CGP12177 and [$^{11}$C]CGP12388 can be used for quantification of β-adrenergic receptors (β-ARs) with in vivo PET studies. [$^{11}$C]CGP12388 PET imaging has demonstrated decreased receptor presence in idiopathic heart failure patients (de Jong et al., 2005). A growing volume of publications testifies to the clinical applicability of this tracer class in imaging cardiac disorders such as idiopathic, dilated or ischemic heart failure (Delforge et al., 1991; Van Waarde et al.,

1992; Elsinga et al., 2001; Delforge et al., 2002; Doze et al., 2002; de Jong et al., 2005; Link and Caldwell, 2008). It is therefore evident that non-invasive evaluation of the pre- and post-synaptic elements of the noradrenergic signaling cascade is of great value both in the clinical setting, as well as in the elucidation of neurohormonal dysfunction in the progression of cardiac pathologies.

### *1.12.3. Potential for PET imaging with $^{11}$C-labeled PDE4 inhibitor rolipram*

All PDE4 isozymes are inhibited by rolipram ((*R/S*)-4(3-cyclopentyloxy-4-methoxyphenyl)-2-pyrrolidone; Figure 1-8) (Houslay et al., 1998; Houslay et al., 2005; Lugnier, 2006). Clinically, rolipram has been tested as an antidepressant showing promising effectiveness in human and animal studies (Wachtel, 1983; Zeller et al., 1984; Bertolino et al., 1988), but failing to reach wide-spread application due to its emetic side-effects (Zeller et al., 1984; Esposito et al., 2009). In cardiac studies, rolipram has been found to potentiate the action of inotropic agents and modulate cardiac contractility (Kajimoto et al., 1997). Rolipram exists as (*R*)- and (*S*)- stereoisomers, with the (*R*)- form being 10-15 times more potent in eliciting antidepressant action (Wachtel, 1983) and ~20 times more effective at inhibiting PDE4 (Schneider et al., 1986). (*R*)-Rolipram reversibly binds PDE4 (Liu et al., 2001), inhibiting the enzyme activity with $IC_{50}$ values of 1–5 nM (Houslay et al., 1997; Houslay et al., 1998; Laliberte et al., 2000).

Both (*R*)- and (*S*)-rolipram have been labeled with C-11 with the aim of quantifying PDE4 levels in the tissues non-invasively using PET (DaSilva et al., 1997). Since the PDE4 expression and phosphorylation state is regulated by intracellular cAMP

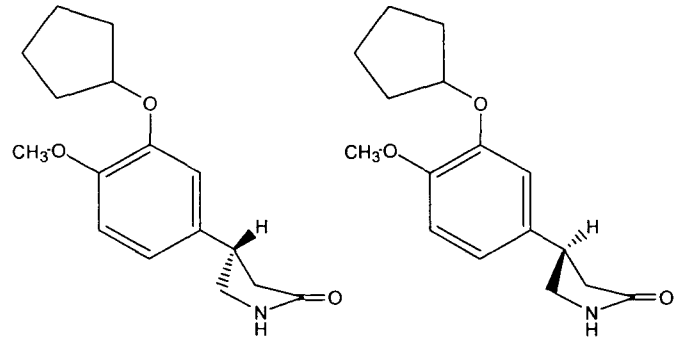


Figure 1-8: Structures of PDE4-specific inhibitors (*R*)-rolipram and (*S*)-rolipram.

levels, (*R*)-[$^{11}$C]rolipram binding was proposed as an index of PDE4 levels and, indirectly, a method of evaluating changes in cAMP signaling in the brain, heart and other PDE4-rich tissues (Lourenco et al., 1999; DaSilva et al., 2001; Lourenco et al., 2001).

Rolipram undergoes extensive metabolism, with six separate products of phase I metabolic reactions identified in the mammalian plasma following [$^{3}$H]rolipram injection (Figure 1-9) (Krause and Kühne, 1992; Krause and Kühne, 1993; Krause et al., 1993). Taking into consideration the location of the C-11 label on the rolipram molecule, a number of proposed metabolites would remain radioactive. The proportion of these labeled metabolites in the total detected radioactive signal needs to be quantified to obtain any meaningful measure of PDE4-specific binding of the unchanged (*R*)- and (*S*)-[$^{11}$C]rolipram tracers for PET imaging.

## 1.13. Hypotheses

The general hypothesis of this project was that (*R*)-[$^{11}$C]rolipram can detect alterations in cAMP-mediated PDE4 signaling a) following acute treatments affecting neurohormonal transmission; b) in rat models of adriamycin (ADR)-induced cardiotoxicity and c) post-MI remodelling. The secondary hypotheses of this project are: 1) cardiac PDE4 binding can be measured in animal models using (*R*)-[$^{11}$C]rolipram; 2) (*S*)-[$^{11}$C]rolipram has the potential to quantify non-specific binding of (*R*)-[$^{11}$C]rolipram in rat myocardium; 3) high performance liquid chromatography (HPLC) column-switch methods can evaluate radiolabeled metabolites of (*R*)-[$^{11}$C]rolipram in rat plasma and organs; 4) (*R*)-[$^{11}$C]rolipram can detect and correlate changes in PDE4 levels in vivo in

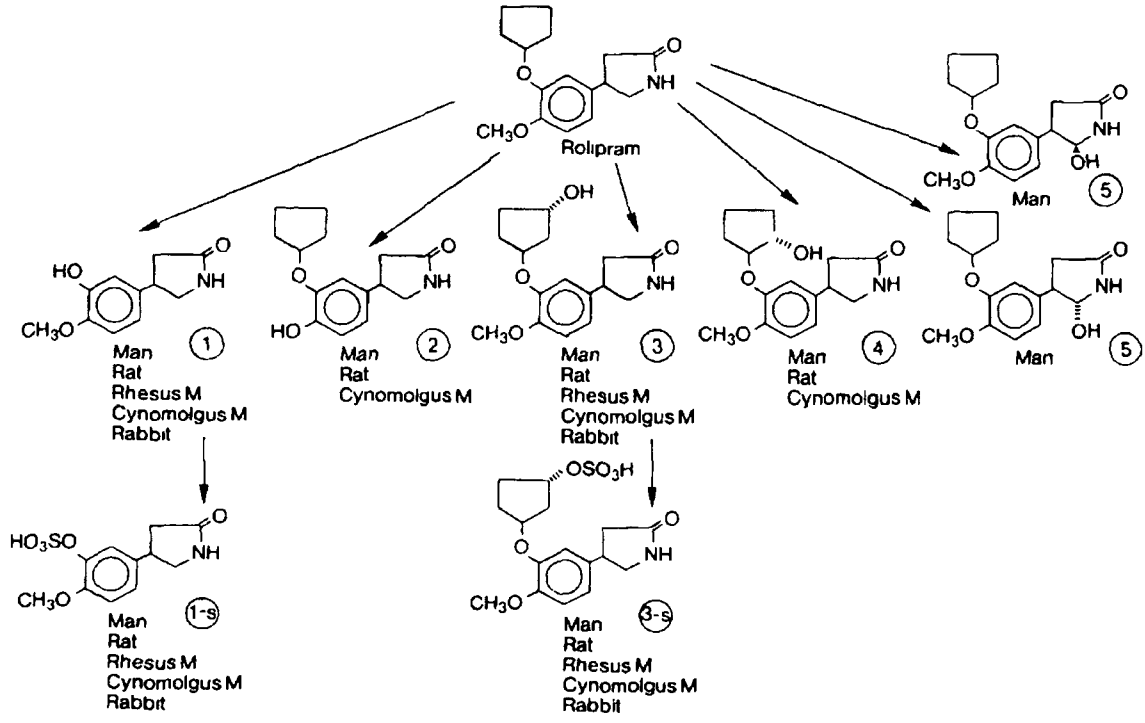


Figure 1-9: Metabolic pathways of rolipram, as elucidated by Krause et al., 1992. Six different metabolites are formed from the phase I biotransformation reactions. From Krause, 1992 (Krause and Kühne, 1992).

rat myocardium after acute treatments affecting cAMP levels and PDE4 regulation; 5) changes in adrenergic signaling can be assessed at the β-AR level (using [$^{3}$H]CGP12177) and PDE4 level (using (*R*)-[$^{11}$C]rolipram) following ADR treatment in rats; 6) (*R*)-[$^{11}$C]rolipram can measure changes in PDE4 levels in vivo in a rat myocardium undergoing remodelling following myocardial infarction and 7) alterations in (*R*)-[$^{11}$C]rolipram in vivo retention following myocardial infarction in animal models reflect in vitro changes in PDE4 enzyme expression and/or enzyme activity.

## 1.14. Objectives

The objectives were to: 1) prepare and purify (*R*)- and (*S*)-desmethylrolipram precursors for (*R*)- and (*S*)-[$^{11}$C]rolipram radiosynthesis; 2) characterize time course and PDE4 binding selectivity of (*R*)- and (*S*)-[$^{11}$C]rolipram in various rat heart compartments; 3) establish (*S*)-[$^{11}$C]rolipram potential to measure non-specific binding of (*R*)-[$^{11}$C]rolipram in various cardiac compartments; 4) evaluate metabolites of (*R*)- and (*S*)-[$^{11}$C]rolipram present in rat venous plasma, as well as in cardiac tissue using a novel "HPLC column-switching" method; 5) evaluate changes in (*R*)-[$^{11}$C]rolipram binding following various acute pharmacological treatments affecting cAMP levels and PDE4 regulation in normal rats; 6) evaluate alterations in (*R*)-[$^{11}$C]rolipram binding to PDE4 and [$^{3}$H]CGP12177 to β-AR, respectively, in ADR-induced cardiotoxicity; 7) evaluate alterations in (*R*)-[$^{11}$C]rolipram binding to PDE4 in myocardial remodelling following a myocardial infarction; and 8) establish whether in vivo changes in (*R*)-[$^{11}$C]rolipram binding to PDE4 correspond to in vitro changes in PDE4 expression and/or activity in rats following myocardial infarction.

## 1.15. Introduction to manuscripts

The following six manuscripts are listed in the order of publications.

### *1.15.1. Manuscript #1*

Prior to the experiments detailed in this manuscript, (*R*)-[$^{11}$C]rolipram has undergone basic characterization, providing preliminary data supporting its use in PET imaging of the brain. Manuscript #1 details the results of ex vivo biodistribution experiments measuring (*R*)-[$^{11}$C]rolipram retention in the whole heart, brain and lung tissues following treatments affecting adrenergic, histaminergic, dopaminergic and serotonergic transmission. Since all four neurotransmitters have receptors that are linked to cAMP regulation by the $G_{s\alpha}$ stimulatory subunit, sensitivity of (*R*)-[$^{11}$C]rolipram retention to pharmacological agents affecting NA, histamine and 5HT, but not dopamine, signaling supports the use of the tracer in future imaging studies with disorders that exhibit altered neurotransmitter levels.

### *1.15.2. Manuscript #2*

The second manuscript in this thesis expands on the concepts presented in the previous publication, which suggested potential for the use of (*R*)-[$^{11}$C]rolipram in evaluation of alterations in PDE4 levels and cAMP signaling in neurotransmitter signaling pathways in the heart. Biodistribution experiments presented in the manuscript #2 established specific binding of (*R*)-[$^{11}$C]rolipram to PDE4 in cardiac tissues, skeletal muscle, lungs, liver and pancreas, but not in the white and brown adipose tissue.

Administration of increasing doses of unlabeled (*R*)- and (*S*)-rolipram was used to establish a dose-response relationship and estimate $ED_{50}$ values for blocking (*R*)-[$^{11}$C]rolipram retention with both enantiomers. Co-administration of saturating doses of subtype-selective PDE inhibitors confirmed the selectivity of (*R*)-[$^{11}$C]rolipram binding to PDE4 over other PDE subtypes found in the heart. In vivo results were validated by in vitro autoradiography. Administration of (*S*)-[$^{11}$C]Rolipram with unlabeled (*R*)-rolipram, (*S*)-rolipram and Ro 20-1724 exposed PDE4-specific binding, albeit with lower affinity than the (*R*)-[$^{11}$C]rolipram enantiomer. This manuscript expands the applicability of in vivo quantification of PDE4 levels with (*R*)-[$^{11}$C]rolipram beyond the brain to the periphery in the heart, skeletal muscle, lungs and the pancreas, with potential use in cardiac disorders, diabetes and obesity.

### *1.15.3. Manuscript #3*

Manuscript #3 presents the quantification of radioactive metabolites in rat plasma, brain, heart, pancreas, skeletal muscle and brown adipose tissue following administration of (*R*)- and (*S*)-[$^{11}$C]rolipram. A column-switching HPLC technique measured the contribution of unchanged radiotracer to the total radioactivity signal. Labeled metabolites were found to be hydrophilic, and thus not likely to cross the cell membrane. Furthermore, co-administration of a saturating dose of unlabeled (*R*)-rolipram affected the relative proportion of the peak representing unchanged (*R*)-[$^{11}$C]rolipram, indicating that the metabolites do not bind PDE4 specifically. Findings of this study were combined with the results of PDE4-blocking studies of manuscripts #1 and #2 to identify the contributions of radioactive metabolites (44%), specific (15%) and non-specific (*R*)-

[$^{11}$C]rolipram binding (41%) to the total measured radioactive signal in plasma and tissues at 45 min following tracer administration.

*1.15.4. Manuscript #4*

Increased (*R*)-[$^{11}$C]rolipram binding following desipramine challenge was used to measure intracellular NA responsiveness in a rat ADR-induced cardiotoxicity model. Biodistribution studies using (*R*)-[$^{11}$C]rolipram, [$^{11}$C]HED (for evaluation of presynaptic innervation) and [$^{3}$H]CGP12177 (for quantifying β-AR binding) were performed on rats treated for two weeks with ADR in a protocol previously shown to elevate cardiac NA. Assessment of neurohormonal changes was correlated with evaluation of cardiac function using echocardiography. Baseline (*R*)-[$^{11}$C]rolipram and [$^{11}$C]HED retention were unchanged, [$^{3}$H]CGP12177 retention was diminished and (*R*)-[$^{11}$C]rolipram response to desipramine challenge was attenuated 3 weeks following last ADR injection. The multi-tracer approach in these studies detected decreased β-AR signaling that precedes cardiac dysfunction, suggesting potential for PET imaging in ADR cardiotoxicity and other forms of heart failure.

*1.15.5. Manuscript #5*

A review of the recent publications describing the use of (*R*)-[$^{11}$C]rolipram and PET imaging to measure alterations in PDE4 levels has been assembled for publication in Current Radiopharmaceuticals. (*R*)-[$^{11}$C]Rolipram is the first tracer that allows in vivo non-invasive quantification of cAMP-mediated PDE4 using PET. Due to the involvement of cAMP signaling in the proposed molecular mechanisms of depression, schizophrenia

and other neuropsychiatric disorders, great interest exists in imaging brain PDE4 using (*R*)-[$^{11}$C]rolipram and PET. Alterations in myocardial NA signaling in heart failure and PDE4 involvement in the control of cardiac contractility indicate potential for cardiac PET imaging using (*R*)-[$^{11}$C]rolipram. Manuscript #5 proposes a consensus on aspects of (*R*)-[$^{11}$C]rolipram characterization and applications, including presence of specific binding, PDE4-selectivity of tracer, safety profile, pharmacokinetics and potential PET imaging applications.

### *1.15.6. Manuscript #6*

Deployment of the Siemens Inveon$^{TM}$ small-animal PET camera at the University of Ottawa Heart Institute allowed full dynamic assessment of the tracer retention over a 60 minute scan. Rats underwent [$^{13}$N]$NH_3$ (to quantify myocardial blood flow and measure the infarct size) and (*R*)-[$^{11}$C]rolipram (to measure myocardial PDE4 in the non-infarcted myocardium). While $\beta_1$-AR expression was decreased 8 weeks following MI, myocardial blood flow in the non-infarcted myocardium was unchanged and in vivo (*R*)-[$^{11}$C]rolipram retention was increased. This study used (*R*)-[$^{11}$C]rolipram in vivo PET imaging to confirm the involvement of alterations in PDE4 enzyme and cAMP signaling in the intracellular pathological processes that follow changes in sympathetic regulation of the myocardium in heart failure.

# CHAPTER 2: MANUSCRIPT #1

Life Sciences 79 (2006) 356–364

# Increasing synaptic noradrenaline, serotonin and histamine enhances in vivo binding of phosphodiesterase-4 inhibitor (*R*)-[$^{11}$C]rolipram in rat brain, lung and heart

Celia M. Lourenco[a], Miran Kenk[a,b,c], Rob S. Beanlands[b] and Jean N. DaSilva[a,b,c,*]

[a] *PET Centre, Centre for Addiction and Mental Health, 250 College St., Toronto, Ontario, Canada, M5T 1R8*

[b] *Cardiac PET Centre, Division of Cardiology, University of Ottawa Heart Institute, 40 Ruskin St., Ottawa, Ontario, Canada, K1Y 4W7.*

[c] *Department of Cellular and Molecular Medicine, Faculty of Medicine, University of Ottawa, 451 Smyth Rd., Ottawa, Ontario, Canada, K1H 8M5.*

Received 16 August 2005; accepted 11 January 2006

*Corresponding author. Cardiac PET Centre, University of Ottawa Heart Institute, 40 Ruskin St., Ottawa, Ontario, Canada K1Y 4W7. Tel.: +1 613 7985555x19704; fax: +1 613 7615406.

*E-mail address*: jdasilva@ottawaheart.ca (J.N. DaSilva)



Doi: 10.1016/j.lfs.2006.01.010

**Contributions of authors**

Work performed in this manuscript was initiated at the Centre for Addiction and Mental Health in Toronto, ON and completed at the University of Ottawa Heart Insitute.. The design and execution of the experiments were performed jointly by the senior PhD student that initiated the project, PhD candidate Celia M. Lourenco and myself. Dr. Beanlands provided a clinical perspective on the data. Dr. DaSilva (supervisor) and I worked jointly on manuscript preparation and submission.

**Abstract**

Phosphodiesterase-4 (PDE4) is one of the main enzymes that specifically terminate the action of cAMP, thereby contributing to intracellular signaling following stimulation of various G protein-coupled receptors. PDE4 expression and activity are modulated by agents affecting cAMP levels. The selective PDE4 inhibitor (*R*)-rolipram labeled with C-11 was tested in vivo in rats to analyze changes in PDE4 levels following drug treatments that increase synaptic noradrenaline (NA), serotonin (5HT), histamine (HA) and dopamine (DA) levels. We hypothesized that increasing synaptic neurotransmitter levels and subsequent cAMP-mediated signaling would significantly enhance (*R*)-[$^{11}$C]rolipram retention and specific binding to PDE4 in vivo. Pre-treatments were performed 3 h prior to tracer injection, and rats were sacrificed 45 min later. Biodistribution studies revealed a dose-dependent increase in (*R*)-[$^{11}$C]rolipram uptake following administration of the monoamine oxidase (MAO) inhibitor tranylcypromine, NA and 5HT reuptake inhibitors (desipramine [DMI], maprotiline; and fluoxetine, sertraline, respectively), and the HA $H_3$ receptor antagonist (thioperamide), but not with DA transporter blockers GBR 12909, cocaine or DA $D_1$ agonist SKF81297. Significant increases in rat brain and heart reflect changes in PDE4 specific binding (total – nonspecific binding [coinjection with saturating dose of (*R*)-rolipram]). These results demonstrate that acute treatments elevating synaptic NA, 5HT and HA, but not DA levels, significantly enhance (*R*)-[$^{11}$C]rolipram binding. Use of (*R*)-[$^{11}$C]rolipram and positron emission tomography as an index of PDE4 activity could provide insight into understanding disease states with altered NA, 5HT and HA concentrations.

*Keywords:* cAMP; PDE4, Rolipram; Signal transduction; Brain and heart imaging; Positron emission tomography

**Introduction**

Phosphodiesterase-4 (PDE4) is the main enzyme that selectively hydrolyzes cAMP into 5'AMP following stimulation of various G protein-coupled receptors, including β-adrenergic (β-AR) and histamine (HA) $H_2$ receptors (Delgado et al., 2003; Xiang et al., 2005). By terminating the action of intracellular cAMP, PDE4 plays a key role in several cAMP-mediated signaling pathways. Disturbances in the cAMP-mediated signal transduction pathways of various neurotransmitters, such as noradrenaline (NA), serotonin (5HT), dopamine (DA) and HA, have been demonstrated in numerous neuropsychiatric and cardiovascular disorders (Wachtel, 1990; Cowburn et al., 1992; Feldman, 1993). Increasing cAMP levels through blocking of PDE4 enzymatic activity with PDE4 inhibitors such as rolipram (4-(3-cyclopentyloxy-4-methoxyphenyl-2-pyrrolidone) has been demonstrated to improve symptoms in a wide variety of disorders, including asthma (Torphy, 1998), chronic obstructive pulmonary disease (Sturton and Fitzgerald, 2002), atopic dermatitis (Hanifin et al., 1996), multiple sclerosis (Dinter et al., 1997), dementia (O'Connolly et al., 1988; Saletu et al., 1992), and depression (Wachtel, 1990). In cardiac studies, rolipram has been found to potentiate the action of inotropic agents and modulate cardiac contractility (Kajimoto et al., 1997).

PDE4 isozymes are distributed throughout the body. The four distinct genes, PDE4A, B, C, and D are widely expressed in the human brain, whereas PDE4A, B and D subtypes have been found in the mammalian heart and lung (Engels et al., 1994; Houslay et al., 1998). Most human inflammatory cells exhibit PDE4 activity. PDE4 is localized in both particulate and soluble cellular fractions from different tissues and cell lines (Schneider et al., 1986). The tritiated form of the more active enantiomer of (*R*)-rolipram was shown

to bind reversibly and stereospecifically with high affinity ($K_d$ 1–5 nM) to all subtypes of the $Mg^{2+}$-induced PDE4 conformation, which is the active holoenzyme complex (Houslay et al., 1998; Laliberte et al., 2000). Recently, we have demonstrated that (*R*)-rolipram labeled with carbon-11 binds selectively in vivo in rat brain, heart and lung, and that this binding can be significantly reduced by PDE4 inhibitors, indicating presence of specific binding in these organs (DaSilva et al., 2001; Lourenco et al., 2001). This tracer displayed potential for imaging the human brain with positron emission tomography (PET) (DaSilva et al., 2002).

PDE4 expression and activity are altered by changes in cAMP production (Houslay et al., 1998; Conti and Jin, 1999). In the short-term, an increase in intracellular cAMP levels causes phosphorylation of PDE4 enzymes by protein kinase-A (PKA), rapidly (within 15 min) increasing PDE4 activity and its affinity for rolipram (Sette et al., 1994; Madelian and La Vigne, 1996). Prolonged (>2 hours) elevation of cAMP levels leads to increased transcription of the PDE4 enzyme, increasing PDE4 expression in the tissues (Engels et al., 1994; Manning et al., 1996; Torphy, 1998).

Chronic treatments with the NA transporter (NAT) blocker desipramine (DMI), selective 5HT reuptake inhibitors (SSRI) fluoxetine or sertraline, or monoamine oxidase (MAO) inhibitor tranylcypromine significantly increased PDE4A and B mRNA and proteins in rat cerebral cortex (Takahashi et al., 1999; Ye et al., 2000). Miro et al. (Miro et al., 2002) reported upregulation of PDE4 mRNA 2 h following fluoxetine treatment. In vitro, PDE4 activity was upregulated within 2 h of incubation with HA (Delgado et al., 2003). Prolonged β-adrenoceptor stimulation using the $\beta_2$ agonist salbutamol increased total soluble PDE activity by 58%, which coincided with an elevation in the expression of

PDE4A and B, but not D, mRNA and protein (Manning et al., 1996). PDE4 A, B, and D were reported to be upregulated within 2 h in human monocytes, following exposure to dibutyryl-cAMP or rolipram (Verghese et al., 1995) or to salbutamol (Manning et al., 1996; Torphy, 1998).

The purpose of this study was to evaluate in vivo the changes in PDE4 specific binding as measured with (*R*)-[$^{11}$C]rolipram in rat brain, heart and lung, following acute treatments increasing synaptic NA, 5HT, HA or DA levels. We hypothesized that increasing synaptic neurotransmitter levels and subsequent cAMP-mediated signaling would enhance (*R*)-[$^{11}$C]rolipram retention and specific binding to PDE4. These experiments will provide the basis for future use of (*R*)-[$^{11}$C]rolipram and PET to image disorders with altered synaptic levels of NA, 5HT, HA or DA in neuropsychiatry or cardiovascular diseases, such as in depression, schizophrenia, Parkinson's disease or heart failure.

## Materials and methods

### *Animals*

All experiments were conducted in accordance with the recommendations of the Canadian Council on Animal Care and with approval from the Animal Care Committee at the Centre for Addiction and Mental Health, and University of Ottawa. Male Sprague-Dawley rats (Charles River, Montreal, Canada) were housed in groups of two and maintained on a 12-h light/dark cycle, with free access to food and water.

### *Chemicals*

All drugs were purchased from Sigma-Research Biochemical International, except for sertraline·HCl (Pfizer), cocaine·HCl (BDH) and SKF81297·HBr (a kind gift from SmithKline and Beecham, PA). DMI·HCl, tranylcypromine·HCl and thioperamide·HCl were dissolved in 0.9% sterile saline. Fluoxetine·HCl was dissolved in 5/95 ethanol/0.9% saline. Maprotiline·HCl, sertraline·HCl, GBR 12909, cocaine and SKF81297·HBr were dissolved in warm 5/20/75 ethanol/1,2-propanediol/0.9% saline. (*R*)-[$^{11}$C]rolipram was synthesized as previously described (DaSilva et al., 2001) with high radiochemical purity (>95%) and specific activity >400 mCi/μmol at the time of first injection.

*Biodistribution studies*

Experiments were carried out as previously described (Lourenco et al., 2001) with rats weighing 180–230g. For injections via a tail vein, rats were immobilized in a rodent restrainer (Harvard Apparatus, Canada) and the tail immersed in a warm water bath (~45 °C) for vasodilation. The dose of (*R*)-[$^{11}$C]rolipram administered was 0.8–2.0 mCi (29.6–74 MBq) in ~0.3 mL of the formulation. In each experiment, all animals received approximately the same mass dose (0.27–0.67 μg) of (*R*)-[$^{11}$C]rolipram. Rats were killed 45 min after radioligand injection. Concentration of radioactivity was measured in dissected organs and expressed as % injected dose per gram of tissue (%ID/g). This value was multiplied by rat body weight (%ID/g BW) to normalize for differences in body mass and allow meaningful comparisons.

*Drug treatments increasing synaptic neurotransmitters*

Treatments with tranylcypromine (1, 5, 10 and 20 mg/kg; $n$ = 4, 5, 8 and 6, respectively), DMI (1, 5, 10, 20, 30 and 40 mg/kg; $n$ = 4, 4, 9, 7, 9 and 4, respectively), maprotiline (5, 20, 30 and 40 mg/kg; $n$ = 4, 8, 8 and 4, respectively), sertraline (1, 5, 10, 20, 30 and 40 mg/kg; $n$ = 4, 3, 5, 7, 7 and 5, respectively), fluoxetine (0.2, 0.5, 1.0, 10, 20 and 30 mg/kg; $n$ = 4, 5, 4, 9, 4 and 4, respectively), thioperamide (1, 5, 7, 10, 20 and 30 mg/kg; $n$ = 4, 4, 4, 9, 8 and 4, respectively), GBR12909 (10 mg/kg; $n$ = 4), cocaine (20 mg/kg; $n$ = 4) and SKF81297 (3 and 10 mg/kg; $n$ = 4 and 5, respectively) were administered by intraperitoneal injection 3 h prior to the radiotracer. Control rats were administered vehicle solutions, 3 h prior to radiotracer. Drug treatments were selected based on doses commonly used to increase synaptic neurotransmitter levels (Johnson et al., 1980; Garcia-Sevilla and Zubieta, 1986; Giralt and Garcia-Sevilla, 1989; Oishi et al., 1989; Malagie et al., 1995; Takahashi et al., 1999; Zahniser et al., 1999; Budygin et al., Lett 2000 Mar 3), or exert effect on postsynaptic receptors (Arnt et al., 1988).

*Determination of PDE4 specific binding*

Selected drug treatments that displayed increases in (*R*)-[$^{11}$C]rolipram uptake were repeated in the presence of a saturating dose (1 mg/kg) of unlabeled (*R*)-rolipram (Lourenco et al., 2001), in order to block PDE4 and thus measure the non-specific binding of the radioligand. Rats were pretreated with i.p. administrations of DMI (10 mg/kg, $n$ = 4), tranylcypromine (10 mg/kg, $n$ = 4), maprotiline (30 mg/kg, $n$ = 5), fluoxetine (10 mg/kg, $n$ = 4), sertraline (40 mg/kg, n = 5) or thioperamide (10 mg/kg, $n$ = 9), 3 h prior to radiotracer. (*R*)-[$^{11}$C]rolipram was coinjected with a saturating dose of unlabeled (*R*)-rolipram (1.0 mg/kg) (Lourenco et al., 2001). Specific binding was

calculated by subtracting the %ID/g BW in the presence of the (*R*)-rolipram blocking dose (non-specific binding) from the %ID/g BW in the absence of (*R*)-rolipram (total binding). Percent change in specific binding was calculated as the percent difference in %ID/g BW values in organs of treated and control animals.

*Statistical analysis*

All data are expressed as means of %ID/g BW ± standard deviation, with % change values presenting the difference between the control and treated animals. Statistical analysis was carried out on the %ID/g data using one-way ANOVA followed by Bonferroni's post-hoc comparison test. To account for any pharmacokinetic effects that the pharmacological treatments may exert on radiotracer distribution, additional statistical analysis was performed, using a multivariate general linear model with blood as a covariate (mean comparison with Bonferroni confidence interval adjustment to obtain comparison between treatments). All analyses were performed using SPSS 12.0.1 statistical analysis software. Since no statistically significant difference was found in the tissue retention of radioactivity between rats pretreated with saline and 5/20/75 ethanol/1,2-propanediol/0.9% saline, the data from all vehicle-treated rats were pooled ($n$ = 44) and used in the statistical calculations. Differences with a $p$ value <0.05 were considered statistically significant.

**Results**

*Treatments increasing synaptic monoamines and histamine*

The highest uptake of radioactivity was observed in the brain, followed by the lung and heart. These three PDE4-rich organs displayed higher activity levels when compared to blood (see controls in Figures). Pretreatment with the nonselective MAO inhibitor tranylcypromine led to a dose-dependent increase in (*R*)-[$^{11}$C]rolipram retention, with significance observed at 10 and 20 mg/kg doses (Figure 2-1). Taking blood as a covariate, significant increases are observed with a 20 mg/kg dose in the brain, and 10 and 20 mg/kg dose in the heart. Figure 2-2A and B depict a dose-dependent enhancement in (*R*)-[$^{11}$C]rolipram retention after increasing synaptic NA following pretreatments with NAT inhibitors DMI and maprotiline. Higher doses elicited significant increases in PDE4-rich organs, while lower doses had no detectable effect. Increases determined to be significant with blood taken as a covariate are seen in the brain and heart with DMI and maprotiline. Increasing synaptic 5HT after pretreatment with SSRIs fluoxetine and sertraline also produced similar dose-response effects (Figure 2-3A and B), with significance observed in the heart at higher doses of fluoxetine (blood taken as a covariate). Pretreatments with the HA $H_3$ antagonist thioperamide increased (*R*)-[$^{11}$C]rolipram binding in a dose-dependent manner (Figure 2-4). Using blood as a covariate, radioactivity retention in the brain and heart, but not the lung, was significantly elevated at doses of 10, 20 and 30 mg/kg (Figure 2-4). Interestingly, using blood as a covariate, no effect on (*R*)-[$^{11}$C]rolipram retention was observed with high doses of DA reuptake inhibitor GBR 12909, catecholamine uptake inhibitor cocaine, and DA $D_1$ full agonist SKF81297 (Figure 2-5). Table 2-1 presents percent changes in (*R*)-[$^{11}$C]rolipram retention after treatments in comparison to controls.

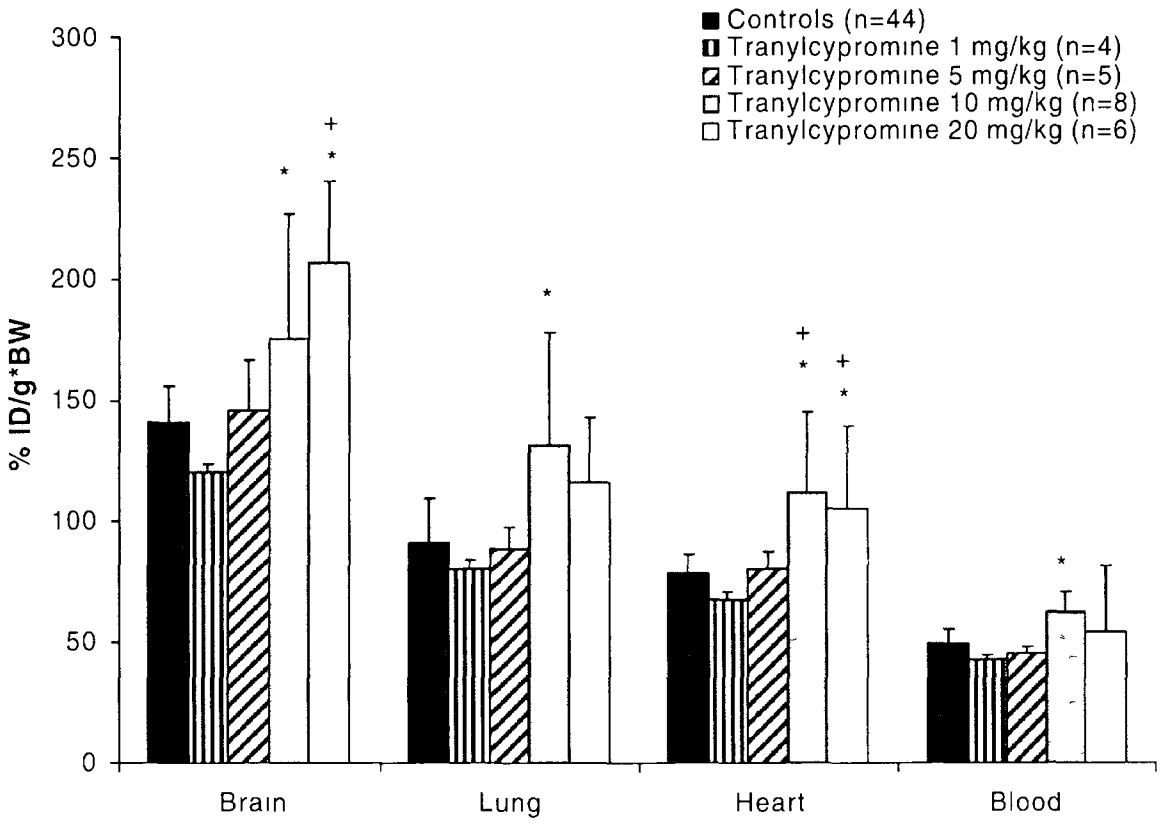


Figure 2-1: Dose-dependent effect of treatments with MAO inhibitor tranylcypromine on (*R*)-[$^{11}$C]rolipram binding. Data are presented as mean of percent injected dose per gram of tissue multiplied by body weight (%ID/g BW) ± standard deviation. * $p<0.05$ one-way ANOVA with Bonferonni post hoc, +$p<0.05$ general linear model, with blood as a covariate.

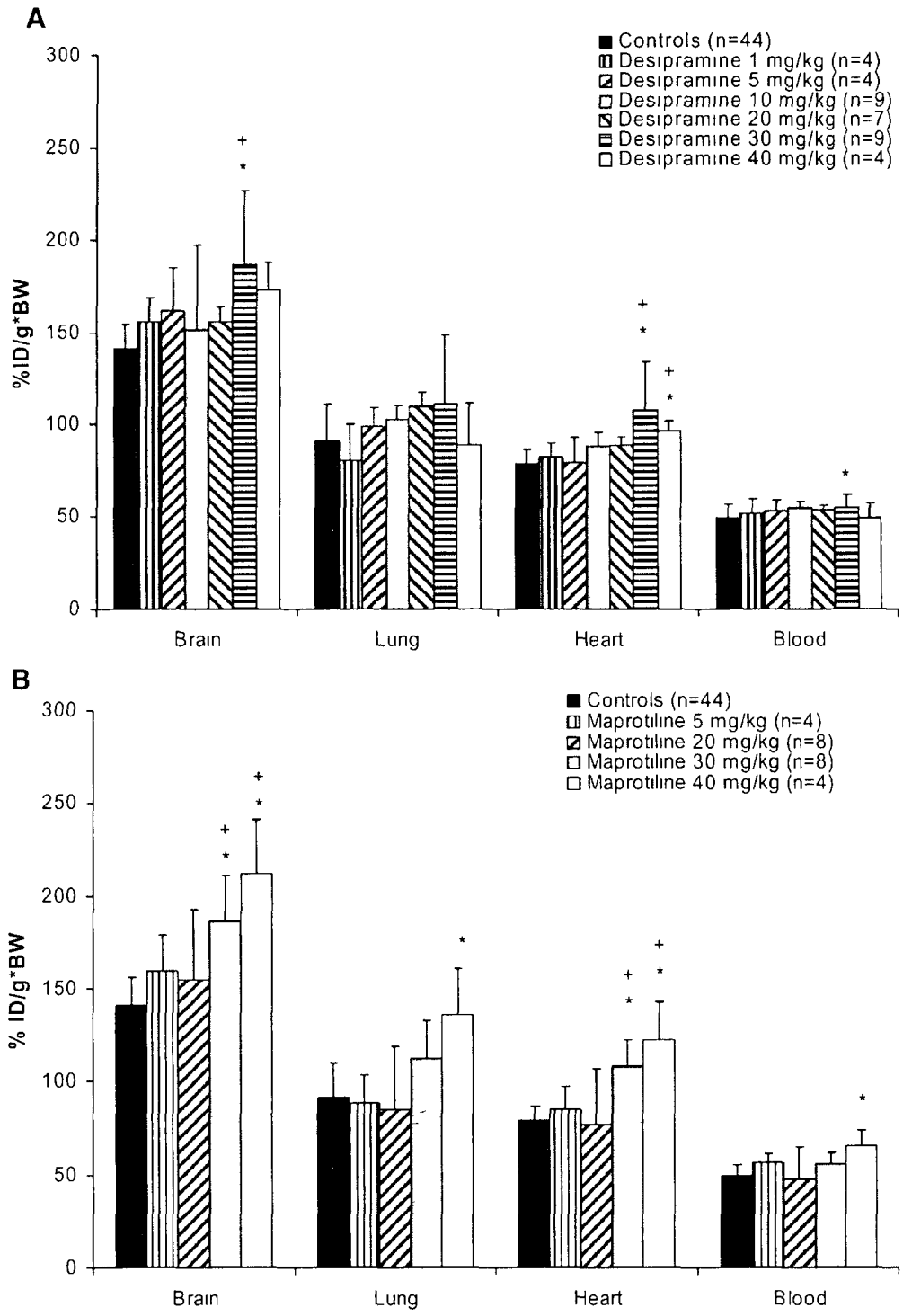


Figure 2-2: Dose-dependent effect of treatments with noradrenaline reuptake inhibitors desipramine (A) and maprotiline (B) on (*R*)-[$^{11}$C]rolipram binding. Data are presented as mean of percent injected dose per gram of tissue multiplied by body weight (%ID/g BW) ± standard deviation. *$p<0.05$ one-way ANOVA with Bonferonni post-hoc, +$p<0.05$ general linear model, with blood as a covariate.

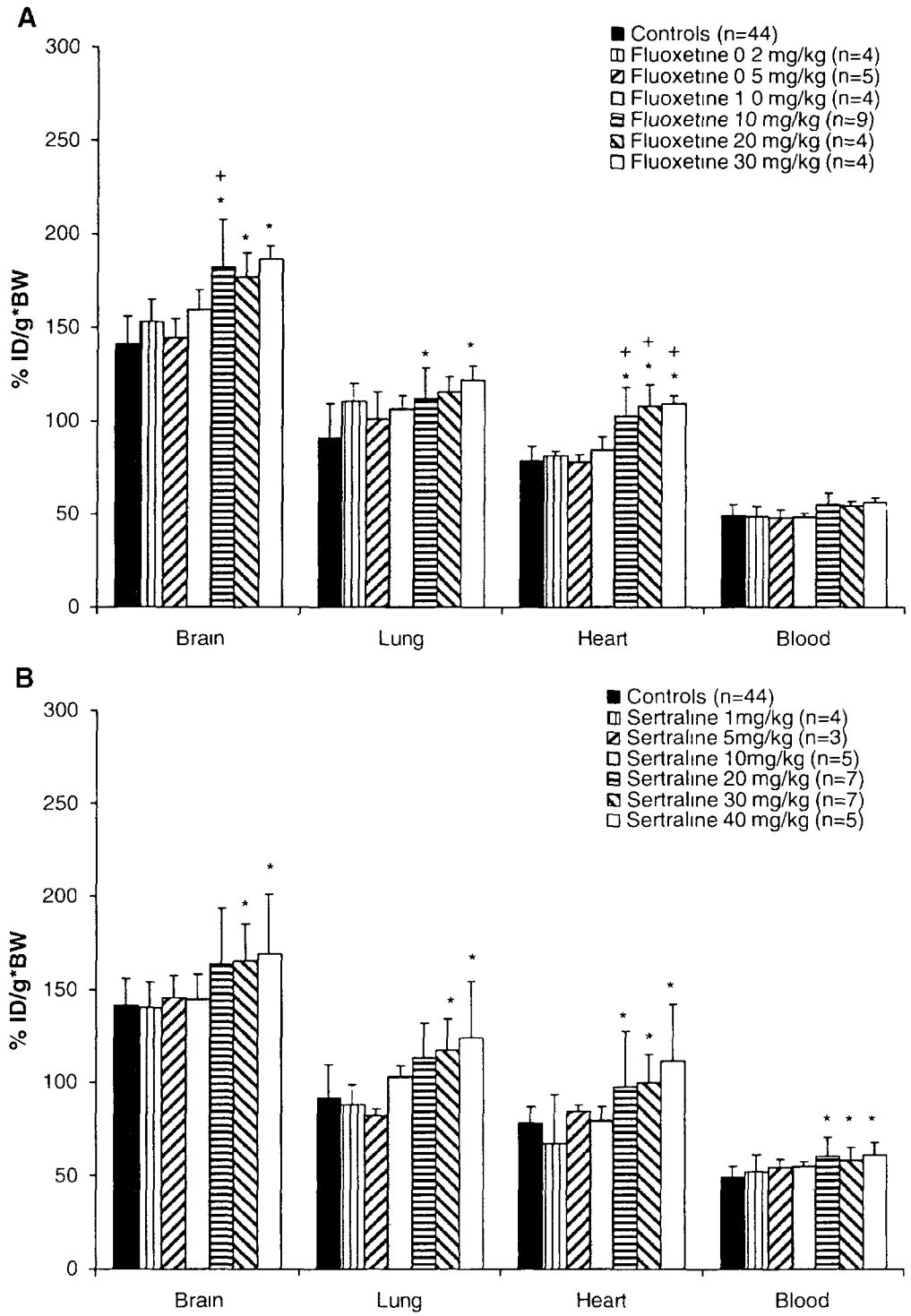


Figure 2-3: Dose-dependent effect of treatments with selective serotonin reuptake inhibitors fluoxetine (A) and sertraline (B) on (*R*)-[$^{11}$C]rolipram binding. Data are presented as mean of percent injected dose per gram of tissue multiplied by body weight (%ID/g BW) ± standard deviation. *$p<0.05$ one-way ANOVA with Bonferonni post hoc, +$p<0.05$ general linear model, with blood as a covariate.

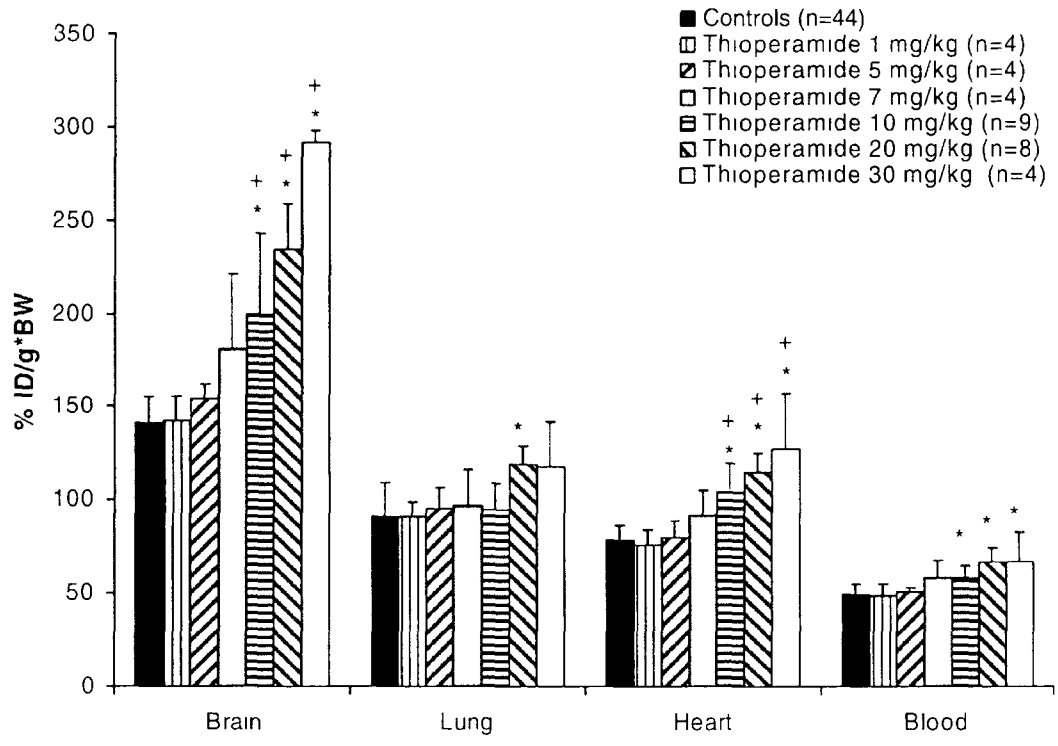


Figure 2-4: Dose-dependent effect of treatment with $H_3$ receptor antagonist thioperamide on (*R*)-[$^{11}$C]rolipram binding. Data are presented as mean of percent injected dose per gram of tissue multiplied by body weight (%ID/g BW) ± standard deviation. *$p<0.05$ one-way ANOVA with Bonferonni post hoc, +$p<0.05$ general linear model, with blood as a covariate.

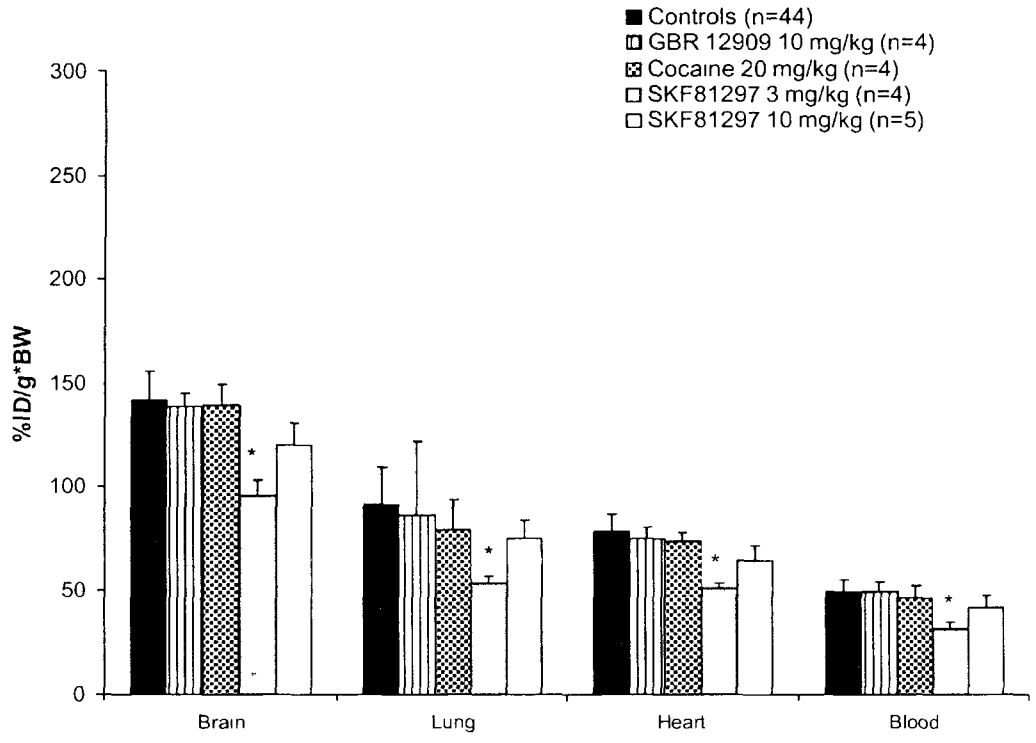


Figure 2-5: Effect of treatments increasing synaptic dopamine levels and $D_1$ agonist SKF81297 on (*R*)-[$^{11}$C]rolipram binding. Data are presented as mean of percent injected dose per gram of tissue multiplied by body weight (%ID/g BW) ± standard deviation. *$p<0.05$ one-way ANOVA with Bonferonni post hoc, +$p<0.05$ general linear model, with blood as a covariate.

Table 2-1: Percent change[a] in (*R*)-[$^{11}$C]rolipram retention in rat tissues following acute drug treatments.

| Treatment | | Percent change in tissue | | | |
|---|---|---|---|---|---|
| | | Brain | Lung | Heart | Blood |
| Tranylcypromine | 1 mg/kg | - 15 | - 12 | -13 | -13 |
| | 5 mg/kg | 3 | - 3 | 2 | - 9 |
| | 10 mg/kg | 24 | 44 | 43 | 27 |
| | 20 mg/kg | 34 | 27 | 34 | 10 |
| Desipramine | 1 mg/kg | 10 | - 12 | 4 | 5 |
| | 5 mg/kg | 14 | 9 | 1 | 8 |
| | 10 mg/kg | 7 | 13 | 12 | 11 |
| | 20 mg/kg | 10 | 20 | 13 | 9 |
| | 30 mg/kg | 32 | 22 | 37 | 12 |
| | 40 mg/kg | 22 | - 3 | 23 | 0 |
| Maprotiline | 5 mg/kg | 13 | - 4 | 8 | 14 |
| | 20 mg/kg | 10 | - 8 | - 2 | - 4 |
| | 30 mg/kg | 32 | 23 | 37 | 14 |
| | 40 mg/kg | 50 | 49 | 56 | 33 |
| Fluoxetine | 0.2 mg/kg | 8 | 21 | 4 | - 1 |
| | 0.5 mg/kg | 3 | 11 | - 1 | - 2 |
| | 1.0 mg/kg | 13 | 17 | 8 | - 1 |
| | 10 mg/kg | 29 | 23 | 31 | 13 |
| | 20 mg/kg | 25 | 27 | 38 | 12 |
| | 30 mg/kg | 32 | 34 | 39 | 15 |
| Sertraline | 1 mg/kg | - 1 | - 4 | - 14 | 6 |
| | 5 mg/kg | 3 | - 10 | 8 | 10 |
| | 10 mg/kg | 3 | 13 | 1 | 12 |
| | 20 mg/kg | 16 | 24 | 25 | 23 |
| | 30 mg/kg | 17 | 29 | 27 | 19 |
| | 40 mg/kg | 19 | 36 | 42 | 24 |
| Thioperamide | 1 mg/kg | 1 | 0 | - 3 | - 2 |
| | 5 mg/kg | 9 | 4 | 2 | 3 |
| | 7 mg/kg | 28 | 6 | 17 | 18 |
| | 10 mg/kg | 41 | 4 | 33 | 19 |
| | 20 mg/kg | 66 | 31 | 46 | 36 |
| | 30 mg/kg | 85 | 29 | 62 | 35 |
| GBR12909 | 10 mg/kg | - 2 | - 6 | - 5 | 0 |
| Cocaine | 20 mg/kg | - 1 | - 13 | - 18 | - 7 |
| SKF81297 | 3 mg/kg | - 33 | - 42 | - 35 | - 36 |
| | 10 mg/kg | - 15 | - 18 | - 18 | - 26 |

[a] Percent change in radiotracer retention (determined as percent injected dose per gram of tissue multiplied by weight of the rat) between the treated rats and the bank of controls ($n$ = 44). $n$ values for treatments are shown in figures.

Table 2-2: Percent change in specific binding of (*R*)-[$^{11}$C]rolipram following acute treatments increasing synaptic neurotransmission.

| | DMI | TRAN | MAP | FLUOX | SERT | THIO |
|---|---|---|---|---|---|---|
| Brain | 20.6 | 23.8 | 32.1 | 34.6 | 24.8 | 31.4 |
| Lung | 27.3 | 77.9 | 10.0 | 57.4 | 82.2 | - 52.7 |
| Heart | 21.6 | 67.5 | 48.4 | 65.2 | 80.7 | 1.8 |

Percent changes in specific binding of (*R*)-[$^{11}$C]rolipram following drug treatments. Specific binding was calculated by subtracting the %ID/g BW in the presence of the (*R*)-rolipram blocking dose (1 mg/kg i.v., coinjected with the radioligand) or non-specific binding, from the %ID/g BW in the absence of (*R*)-rolipram or total binding.
To determine total binding, rats were administered: DMI (10 mg/kg, 3 h prior to radioligand injection, $n = 9$); tranylcypromine (TRAN: 10 mg/kg, i.p., 3 h prior, $n = 8$); maprotiline (MAP: 30 mg/kg i.p., 3 h prior, $n = 8$); fluoxetine (FLUOX: 10 mg/kg, i.p., 3 h prior, $n = 9$); sertraline (SERT: 40 mg/kg i.p., 3 h prior, $n = 7$) or thioperamide (THIO: 10 mg/kg, i.p., 3 h prior, $n = 9$), injected with (*R*)-[$^{11}$C]rolipram and sacrificed 45 min later. To determine non-specific binding, animals were treated again with the drug challenges as above (DMI $n = 4$; TRAN $n = 4$; MAP $n = 5$; FLUOX $n = 4$; SERT $n = 5$; THIO $n = 9$), and then coinjected with a blocking dose of (*R*)-rolipram (1 mg/kg, i.v.), and sacrificed 45 min later.

*PDE4 specific binding determination*

Similar increases in PDE4 specific binding (20–35% change over controls) were obtained in the brain after selected drug treatments were repeated in the presence of (*R*)-rolipram, confirming that the changes in total tracer retention (Table 2-1) reflect (*R*)-[$^{11}$C]rolipram specific binding to PDE4 (Table 2-2). In periphery, equivalent changes in the specific binding were found only after treatments with NA reuptake inhibitors (10–49%). On the other hand, tranylcypromine and SSRIs produced a higher change in PDE4 specific binding in comparison to (*R*)-[$^{11}$C]rolipram total retention (57–83% vs. 23–44%, see Tables 2-1 and 2-2). Following thioperamide treatment, specific binding was decreased in the lung and remained unchanged in the heart, suggesting underlying changes in non-specific binding or tracer delivery.

A number of treatments at higher doses significantly affected (*R*)-[$^{11}$C]rolipram presence in the blood in comparison to the controls. Using blood as a covariate in statistical analysis allows for the effect of treatment on tracer binding to PDE4 to be analyzed, taking into account the different blood levels of (*R*)-[$^{11}$C]rolipram.

**Discussion**

Imaging post-receptor signal transduction with PET has potential not only in psychiatry (Fujita and Innis, 2000), but also in neurological and cardiovascular disorders. PDE4 is an essential component of the cAMP-mediated signal transduction and plays an important role in signaling and cell function by controlling cAMP levels formed following stimulation of several neurotransmitter systems. Previous studies demonstrated that PDE4 expression and activity are regulated by cAMP levels. (*R*)-[$^{11}$C]rolipram has

shown potential for measuring PDE4 expression and activity in in vivo studies (Lourenco et al., 2001). The use of (*R*)-[$^{11}$C]rolipram to measure PDE4 binding and as an indirect index of cAMP signaling with PET could provide insight into understanding several pathologies with altered cAMP levels, and their treatments.

In the studies reported here, we have shown that treatments elevating cAMP levels increased (*R*)-[$^{11}$C]rolipram retention in PDE4-rich organs brain, heart and lung, presumably through stimulating PDE4 expression and/or phosphorylation since an increase in PDE4 specific binding was also detected. Elevations in synaptic monoamines following administration of the MAO inhibitor tranylcypromine increased (*R*)-[$^{11}$C]rolipram binding to PDE4 in rat brain and heart. These results support the increases in PDE4 protein detected by immunoblot analysis following repeated treatments with antidepressants, including phenelzine, an irreversible MAO inhibitor (Ye et al., 2000).

In the brain, the noradrenergic system has been identified as one of the main neurotransmitter systems regulating PDE4 activity through stimulation of postsynaptic β-adrenergic receptors (Whalin et al., 1989; Ye et al., 2000). Higher doses used in our studies elicited an increase in brain (*R*)-[$^{11}$C]rolipram retention following administration of DMI or maprotiline, proving the susceptibility of PDE4 enzymes to regulation by synaptic NA levels in the brain. In cardiac tissues, PDE4 isozymes are involved in the regulation of NA signaling through the $\beta_1$-AR and $\beta_2$-AR which modulate cardiac contractility and overall function (Müller et al., 1990; Kajimoto et al., 1997; Koch et al., 2000; Xiang et al., 2005). Observed potentiation of PDE4 binding to (*R*)-[$^{11}$C]rolipram in the heart by NAT inhibitors confirms the responsiveness of cardiac PDE4 enzymes to enhanced NA signaling.

5HT reuptake inhibition by the SSRIs dose-dependently increased (*R*)-[$^{11}$C]rolipram binding to PDE4 in the brain, lungs and heart. Fluoxetine increases 5HT levels by inhibiting reuptake, causing a stimulation of postsynaptic 5HT receptors. $5HT_4$, $5HT_6$ and $5HT_7$ receptor subtypes are positively coupled to AC through the $G_{s\alpha}$ subunit (Ruat et al., 1993; Ruat et al., 1993; Torres et al., 1995), resulting in increased cAMP production with reported amplification of PDE4 expression in chronic studies (Takahashi et al., 1999; Ye et al., 2000). Increased brain retention of (*R*)-[$^{11}$C]rolipram are in line with the findings of Miro et al. (2002) that PDE4 expression is upregulated rapidly with fluoxetine administration. Recently detected presence and functional involvement of $5HT_4$ in cardiac tissues (Bach et al., 2001; Brattelid et al., 2004) suggest that the observed increase in (*R*)-[$^{11}$C]rolipram binding to PDE4 in the whole heart likely reflects the amplification of cAMP signaling through that receptor subtype.

Stimulation of dopaminergic signaling did not affect (*R*)-[$^{11}$C]rolipram binding to PDE4 in any of the organs studied. While SKF81297 did elicit a decrease in radioactivity, a corresponding decrease in blood activity levels was observed, indicating that diminished availability of tracer caused an artificially low retention value not likely due to function. Even though $D_1$ receptor is coupled to $G_{s\alpha}$ and its stimulation increases intracellular cAMP levels (Kebabian and Calne, 1979), modulation of cAMP signaling within the dopaminergic system following both enhanced synaptic DA or direct $D_1$ agonist stimulation did not affect (*R*)-[$^{11}$C]rolipram binding in our study. Makhay et al. (2001) reported that $D_1$ agonist SKF38393 does not substitute for rolipram in discriminative stimulus effect, which points to a lack of involvement of PDE4 in $D_1$-mediated signaling pathway. The DA $D_1$ system was previously shown to be associated

with PDE1 rather than PDE4 enzymes (Polli and Kincaid, 1994; Mori et al., 2000). These findings differ from the observations of Harada et al., (2002) who have detected a dose-dependent decrease in (*R*)-[$^{11}$C]rolipram specific binding in striatum and frontal cortex of conscious monkeys following treatment with a $D_1$ antagonist SCH23390. The same group also reported a dose-dependent increase of (*R*)-[$^{11}$C]rolipram binding in monkey stratum after methamphetamine treatment (Tsukada et al., 2001). Differences with the current study may relate to species differences. Thus, further work is required to clarify the role of PDE4 in DA-mediated signal transduction in vivo in various species.

Stimulation of HA synthesis and release through $H_3$ antagonism by thioperamide (Gomez-Ramirez et al., 2002) potentiated (*R*)-[$^{11}$C]rolipram binding to PDE4 in the brain in a dose-dependent manner. Postsynaptic $H_2$ receptors are known to be coupled to elevated AC activity (Lemos Legnazzi et al., 2000) and increase PDE4 activity 2- to 3-fold in blood mononuclear white cells (Delgado et al., 2003) and neutrophils (Dasi et al., 2000), explaining the increased radiotracer binding measured in our study. While radioactivity levels were significantly elevated in the heart following thioperamide injections, these increases were not blocked by (*R*)-rolipram, suggesting that changes in total binding are due to factors affecting non-specific binding of (*R*)-[$^{11}$C]rolipram. Cardiac $H_3$ receptors have been shown to behave as heterogenic receptors on presynaptic terminals, modulating release of NA in the heart (Levi and Smith, 2000). It was not possible to detect this interaction using (*R*)-[$^{11}$C]rolipram, as thioperamide treatment affected non-specific binding of the tracer in the periphery.

Lung retention of (*R*)-[$^{11}$C]rolipram exhibited a trend towards an increase following treatments affecting NA and 5HT signaling, but these changes did not reach

significance when blood is taken as a covariate. However, even though PDE4 subtypes are present in mammalian lungs, there is little potential to use (*R*)-[$^{11}$C]rolipram for lung imaging due to the low in vivo lung density (0.26 g/cm$^3$) in comparison to heart and liver (1.05 g/cm$^3$) in the chest area.

In conclusion, our present study indicates that (*R*)-[$^{11}$C]rolipram binding to PDE4 responds to acute treatments elevating synaptic NA, 5HT and HA, but not DA levels, demonstrating tracer selectivity for discrete functions. This work extends our prior characterization of (*R*)-[$^{11}$C]rolipram (Lourenco et al., 2001) and supports that it is a promising radioligand for non-invasive imaging of disorders with altered levels of those neurotransmitters. Work currently in progress is aimed towards analyzing the effects of various pharmacokinetic factors on (*R*)-[$^{11}$C]rolipram retention.

**Acknowledgements**

The authors thank the PET Centre staff for technical assistance, Dr. Rob deKemp for discussions, and Stephanie Thorn for help in preparing the manuscript. R.S.B. was supported by a Canadian Institutes of Health Research (CIHR) Scientist Award. This work was supported in part by a PhD scholarship from the Natural Sciences and Engineering Research Council of Canada (C.M.L.), Eli Lilly Canada Inc., and a grant from the CIHR MOP 62765.

# CHAPTER 3: MANUSCRIPT #2

Nuclear Medicine and Biology 34 (2007) 71 – 77

# In vivo selective binding of (*R*)-[$^{11}$C]rolipram to phosphodiesterase-4 provides the basis for studying intracellular cAMP signaling in the periphery

Miran Kenk[a,b], Michael Greene[a,b], James Thackeray[a,b], Robert A. deKemp[a], Mireille Lortie[a], Stephanie Thorn[a,b], Rob S. Beanlands[a,b], Jean N. DaSilva[a,b*]

[a]*Cardiac PET Centre, Division of Cardiology, University of Ottawa Heart Institute, Ottawa, Ontario, Canada, K1Y 4W7*

[b]*Department of Cellular and Molecular Medicine, Faculty of Medicine, University of Ottawa, Ottawa, Ontario, Canada, K1H 8M5*

Received 15 August 2006; received in revised form 25 September 2006; accepted 7 October 2006

* Corresponding author. Cardiac PET Centre, University of Ottawa Heart Insitute, Ottawa, Ontario, Canada K1Y 4W7. Tel.: +1 613 798 5555x19704; fax: +1 613 761 5406

*E-mail address:* jdasilva@ottawaheart.ca (J.N. DaSilva)

**Contributions of authors**

Experiments described in this manuscript were designed and executed by myself, with assistance from MSc candidate Michael Greene (analysis of white and brown adipose tissue data), and practical help from PhD candidates James Thackeray and Stephanie Thorn. Physicists Drs. Robert deKemp and Mireille Lortie provided input on the experiments needed for estimating in vivo parameters for use in future PET imaging. Dr. Beanlands provided a clinical perspective on the data. Work performed was supervised by Dr. Jean DaSilva.

**Abstract**

**Introduction:** Phosphodiesterase-4 (PDE4) enzymes specifically break down the second messenger cAMP, thereby terminating the intracellular signaling cascade that plays an essential role in neurohormonal modulation of many physiological systems. PDE4 activity and expression are regulated by cAMP levels, suggesting that measurement of PDE4 provides an index of intracellular cAMP signaling.

**Methods:** Male Sprague-Dawley rats were administered (*R*)- or the less active enantiomer (*S*)-[$^{11}$C]rolipram and sacrificed 30 min later with tracer retention measured in various tissues. Co-injections with saturating doses of unlabeled (*R*)-rolipram, (*S*)-rolipram and Ro 20-1724, as well as subtype-selective PDE inhibitors vinpocetine, Bay 60-7550, cilostazol and zaprinast were used to establish binding selectivity for PDE4 over PDE1, PDE2, PDE3 and PDE5 subtypes, respectively. Autoradiography was performed to substantiate results of biodistribution studies in the myocardium.

**Results:** In vivo (*R*)-[$^{11}$C]rolipram retention was dose-dependently reduced by co-injections of (*R*)-rolipram and (*S*)-rolipram ($ED_{50}$ values of 0.03 mg/kg and 0.2 mg/kg, respectively). Vinpocetine, Bay 60-7550, cilostazol and zaprinast had no effect on (*R*)-[$^{11}$C]rolipram binding, while (*R*)-rolipram and Ro 20-1724 reduced the tracer uptake to non-specific levels in PDE4-rich tissues.

**Conclusions:** In addition to brain, (*R*)-[$^{11}$C]rolipram binds selectively to PDE4 across all cardiac regions, skeletal muscle, lungs and pancreas, but not in the adipose tissues. In vivo findings were confirmed by in vitro autoradiography studies, suggesting that (*R*)-[$^{11}$C]rolipram can be applied to evaluate alterations in central and peripheral PDE4 levels and cAMP-mediated signaling.

*Keywords:* PDE4; cAMP; Rolipram; Intracellular signal transduction; Myocardial imaging; Positron emission tomography

## 1. Introduction

Cyclic 3',5'-adenosine monophosphate (cAMP) second messenger is an important component of signaling cascades initiated by a number of neurohumoral pathways modulating cardiac (Movsesian, 1998) and metabolic functions (Robidoux et al., 2004). Alterations in cAMP-mediated signaling have been reported in various disorders affecting a number of physiological systems, including asthma (Torphy, 1998), heart failure (Takahashi et al., 2002), dementia and depression (Wachtel, 1990).

Phosphodiesterase-4 (PDE4) is one of the main enzymes that specifically hydrolyse cAMP ($V_{max}$=0.3–11 μmol/(min/mg), $K_m$=2–8 μM) (Hughes et al., 1997), thereby terminating the intracellular signaling following stimulation of the $G_{s\alpha}$ subunit of various G protein-coupled receptors including β-adrenergic (β-AR), adenosine $A_2$ and histamine $H_2$ receptors (Movsesian, 1998; Torphy, 1998; Lourenco et al., 2006). PDE4 enzymes are distributed throughout the body, being present in all major organs (Engels et al., 1994; Hughes et al., 1997; Lourenco et al., 2001), with the greatest concentrations expressed in the brain (Schneider et al., 1986; Lourenco et al., 2001). High concentrations of PDE4 are also contained in the lungs, heart (Engels et al., 1994; Takahashi et al., 2002; Lourenco et al., 2006) and skeletal muscle (Enoksson et al., 1998). The pancreas is reported to express PDE4 enzymes (Hughes et al., 1997; Pyne and Furman, 2003), as do types of cells in the immune system (Torphy, 1998); however, platelets and red blood cells are devoid of PDE4 activity (Maurice et al., 2003). PDE4 has been shown to be expressed in white and brown adipose tissues (WAT and BAT), but to a much lesser extent than PDE3 (Nagaoka et al., 1998; Coudray et al., 1999). The four distinct PDE4 genes, PDE4A, B, C and D, are widely expressed in the human brain and skeletal muscle,

whereas PDE4C is absent in the remainder of the above-mentioned tissues (Hughes et al., 1997; Houslay et al., 1998). PDE4 activity and density are regulated acutely by intracellular cAMP levels via phosphorylation by protein kinase A (PKA) and extracellular signal-related kinase (short-term) (Laliberte et al., 2002), as well as by de novo protein synthesis following prolonged elevation in cAMP levels (long-term) (Engels et al., 1994; Manning et al., 1996; Houslay et al., 1998; Torphy, 1998).

The more active enantiomer of the widely used selective PDE4 inhibitor rolipram ((*R*)-4-(3-cyclopentyloxy-4-methoxyphenyl)-2-pyrrolidinone) binds reversibly and stereospecifically with high affinity ($K_d$=1–5 nM) to all subtypes of the $Mg^{2+}$-induced PDE4 conformation, which is the active holoenzyme complex (Houslay et al., 1998; Laliberte et al., 2000; Laliberte et al., 2002). The less active enantiomer (*S*)-rolipram binds to PDE4 with 10- to 30-fold lower affinity (Schneider et al., 1986; Hughes et al., 1997; Laliberte et al., 2000; Laliberte et al., 2002). From in vitro studies, binding of rolipram to PDE4 has been reported to occur at two sites, called the high- and low-affinity rolipram binding site (HARBS and LARBS, respectively) (Jacobitz et al., 1996; Souness and Rao, 1997).

Both enantiomers of rolipram have been radiolabeled in our laboratory with C-11 and tested for potential use in positron emission tomography (PET) imaging of brain disorders (DaSilva et al., 1997; Lourenco et al., 1999; DaSilva et al., 2001; Lourenco et al., 2001). The most active stereoisomer (*R*)-[$^{11}$C]rolipram has already found wide application in imaging brain cAMP signaling in rats (Fujita et al., 2005; Lourenco et al., 2006), monkeys (Tsukada et al., 2001; Harada et al., 2002; Tsukada et al., 2004), pigs (Parker et al., 2005) and humans (DaSilva et al., 2002). Due to their function in the

regulation of cardiac contraction, lipolysis and thermogenesis (conversion of food-derived energy into heat) (Nagaoka et al., 1998; Coudray et al., 1999; Collins and Surwit, 2001; Robidoux et al., 2004), the cAMP-specific PDE4 enzymes also present great interest for PET imaging in the periphery. (*R*)-[$^{11}$C]Rolipram and PET imaging would allow serial assessment of PDE4 and yield insight into the mechanisms underlying disorders such as heart failure, obesity and diabetes. This paper presents studies exploring in vivo binding selectivity of (*R*)-[$^{11}$C]rolipram in peripheral organs, with the goal of establishing its potential for use in evaluation of PDE4 regulation in myocardial and metabolic disorders.

## 2. Materials and methods

### *2.1. Materials*

(*R*)- and (*S*)-[$^{11}$C]rolipram were synthesized as previously described (DaSilva et al., 1997; DaSilva et al., 2001) with high radiochemical purity (>95%) and specific activity (10.7–58.5 GBq/μmol; 290–1580 mCi/μmol) at the time of first injection. All drugs were purchased from Sigma-Aldrich (Canada), except for Bay 60-7550, which was purchased from Axxora (San Diego, CA), and (*R*)-rolipram from Tocris (Ellisville, MI). Unlabeled (*R*)- and (*S*)-rolipram, as well as Bay 60-7550, Ro 20-1724 and vinpocetine, were dissolved in ethanol/propylene glycol/0.9% saline 5/20/75 (v/v/v), while cilostazol and zaprinast were dissolved in 0.9% saline/DMSO 2/1 (v/v).

### *2.2. Animals*

Male Sprague-Dawley rats (Charles River, Montreal, Canada) weighing 200–275 g were maintained on a 12-h light/dark cycle with free access to food and water. All animal experiments described herein were conducted according to the guidelines of the University of Ottawa Animal Care Committee and the Canadian Council on Animal Care for the use and care of laboratory animals. Competition studies were carried out as previously described for (*R*)- and (*S*)-[$^{11}$C]rolipram (Lourenco et al., 1999).

Briefly, nonanesthetized rats were killed by decapitation 30 min after injection of 18.5–59.2 MBq (0.5-1.6 mCi) of radiotracer (0.37–1.29 μg of cold mass injected). A blood sample was collected from the trunk into a heparinized tube and tissues quickly removed. The heart was dissected into right and left atria, right and left ventricle and septum. A sample of the skeletal muscle (quadriceps), lung, liver, intrascapular BAT, abdominal WAT, pancreas, as well as the entire brain, was also removed. All tissues were washed in saline, blotted and counted (decay-corrected) in a gamma-counter along with aliquots of injected solution as standards and then weighed. Radioactivity retained is expressed as percent of injected dose per gram (%ID/g) of tissue.

*2.3. Evaluation of PDE subtype binding selectivity*

To evaluate the susceptibility of (*R*)-[$^{11}$C]rolipram to blocking by unlabelled rolipram stereoisomers, (*R*)-rolipram (0.001–1 mg/kg) and (*S*)-rolipram (0.01–3 mg/kg) were co-injected with the radiotracer via the tail vein. The binding selectivity of (*R*)-[$^{11}$C]rolipram was evaluated by administration of high pharmacologic doses of unlabelled inhibitors of PDE subtypes; unlabeled (*R*)- and (*S*)-rolipram (1 and 3 mg/kg, co-injected iv, respectively), Ro 20-1724 (30 mg/kg, co-injected iv) (Kant et al., 1980), vinpocetine

(10 mg/kg ip, 15 min prior to tracer injection) (Sauer et al., 1988), Bay 60-7550 (3 mg/kg, co-injected iv) (Boess et al., 2004), cilostazol (10 mg/kg, co-injected iv) (Hotta et al., 1998) and zaprinast (10 mg/kg, co-injected iv) (Ng and Pang, 1998). (*S*)-[$^{11}$C]Rolipram was co-injected with Ro 20-1724 (30 mg/kg, iv), (*R*)-rolipram (1 mg/kg, iv) and (*S*)-rolipram (1, 3 and 10 mg/kg, iv). Control rats were administered vehicle solutions. The animals were sacrificed and the tissue concentration of radioactivity determined as described above.

*2.4. In vitro autoradiography studies*

Autoradiography studies were carried out with (*R*)- and (*S*)-[$^{11}$C]rolipram using methods adapted from Strome et al. (Strome et al., 2005). Briefly, short axis heart slices of 20 μm thickness were cut with a Leica cryostat (CM3050S, Leica Microsystems) at –18°C, thaw-mounted onto glass slides (three slices per slide) and kept at –80°C until the day of the experiment. Slides were pre-washed in incubation buffer (50 mM Tris–HCl, 120 mM NaCl, 5 mM KCl, 2 mM $CaCl_2$, 1 mM $MgCl_2$), incubated with 5 nM of (*R*)- or (*S*)-[$^{11}$C]rolipram for 45 min, washed three times for 1 min in cold (4°C) incubation buffer, dipped in saline and dried. A standard curve for storage imaging was obtained by placing 5-μl droplets of serial dilutions of the incubation buffer onto a thin-layer chromatography (TLC) plate (silica, Whatman). Three slides per PDE inhibitor were incubated with radiotracer in the presence of 10 μM vinpocetine, Bay 60-7550, cilostazol, zaprinast, Ro 20-1724 or racemic (*R/S*)-rolipram in 50 ml staining dishes. Dried slides and the TLC plate were exposed to the multisensitive storage phosphorus screen (Kodak Screen-K, BioRad) for 2 h in a light-impermeable cassette. The phosphor screen was

removed under dim lighting and scanned using a BioRad Personal Molecular FX Imager at 50-μm resolution. Analysis was performed using Quantity One software (BioRad, Philadelphia), producing a measure of total counts within a 5-mm$^2$ region drawn on the left ventricle, corrected for background signal. This value was correlated to activity, using a standard curve obtained from standards run within the same experiment, to obtain the radiotracer retention in Becquerel per cubic centimeter. Dividing this amount by the specific activity at the beginning of incubation resulted in a measure of protein binding, expressed in picomole per cubic centimeter. This procedure was repeated with another formulation of each tracer.

*2.5. Statistical Analysis*

All data are expressed as means of %ID/g ± S.D. Statistical analysis was carried out using one-way ANOVA followed by Bonferroni's post hoc comparison test. To account for any pharmacokinetic effects that the pharmacological treatments may exert on radiotracer distribution, additional statistical analysis was performed using a multivariate general linear model with blood as a covariate (mean comparison with Bonferroni confidence interval adjustment to obtain comparison between treatments). All analyses were performed using SPSS 14.0 statistical analysis software. Since no statistically significant difference was found in the tissue retention of radioactivity between rats pretreated with saline and other vehicles, the data from all vehicle-treated rats were pooled ($n$=12) and used in the statistical calculations. In statistical test used, differences with a $P$ value <.05 were considered statistically significant.

## 3. Results

### *3.1. (R)-[$^{11}$C]Rolipram in vivo binding selectivity studies*

Co-injections of (*R*)-rolipram dose-dependently blocked (*R*)-[$^{11}$C]rolipram retention in the brain, skeletal muscle, lungs (Figure 3-1A) and all cardiac regions (Figure 3-1B). Since cardiac uptake was uniform across all cardiac compartments (Figure 3-1B), for clarity and simplicity of expressing these data, the left ventricle is presented in following figures as the representative heart region. At a saturating dose of unlabeled (*R*)-rolipram (1 mg/kg iv), radiotracer retention was blocked by 81% in the brain and ~30% in heart regions (Table 3-1). (*S*)-Rolipram co-injections also dose-dependently reduced (*R*)-[$^{11}$C]rolipram uptake in the rat brain, myocardium, skeletal muscle and lungs (Figure 3-2; 69% reduction in the brain, 34% in the heart; Table 3-1). Both (*R*)- and (*S*)-rolipram co-injections reduced (*R*)-[$^{11}$C]rolipram retention to the same nonspecific levels, with the less active (*S*)- enantiomer needing a higher dose to elicit an equivalent effect. The $ED_{50}$ values in the brain and heart were determined to be 0.03 mg/kg for (*R*)-rolipram and 0.2 mg/kg for (*S*)-rolipram (Table 3-1).

Distribution of (*R*)-[$^{11}$C]rolipram was significantly reduced by co-injection with saturating doses of the selective PDE4 inhibitors Ro 20-1724 and (*R*)-rolipram in the brain, cardiac tissues, skeletal muscle, lungs and pancreas (Figure 3-3), whereas no effect was observed following treatments with high pharmacologic doses of vinpocetine, Bay 60-7550, cilostazol or zaprinast (selective PDE1, PDE2, PDE3 and PDE5 inhibitors, respectively; Figure 3-3). (*S*)-[$^{11}$C]Rolipram retention in tissues studied was not susceptible to blocking by the PDE4 inhibitors, including a high dose of (*S*)-rolipram (10 mg/kg) (Figure 3-4).

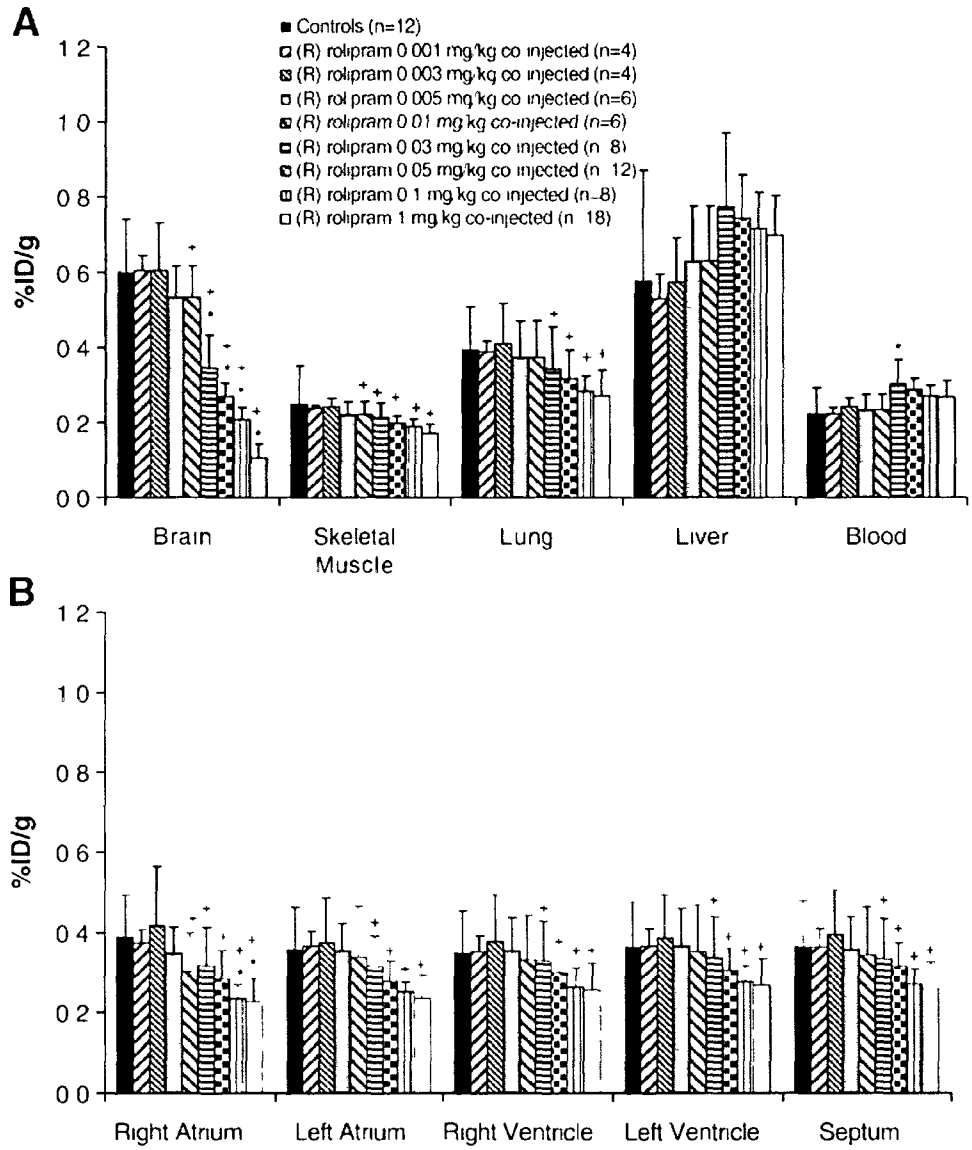


Figure 3-1: Effect of co-injection of (*R*)-rolipram (0.001–1 mg/kg iv) with (*R*)-[$^{11}$C]rolipram on radioactivity uptake in rat brain, skeletal muscle, lungs, liver, blood (A) and cardiac tissues (B). Nonanesthetized animals were sacrificed 30 min following radiotracer injection (18.5–59.2 MBq). Data are presented as mean %ID/g of tissue ±S.D. $^{*}P<.05$ one-way ANOVA compared to controls with Bonferonni post hoc; $^{+}P<.05$ compared to controls with the general linear model, using blood as a covariate.

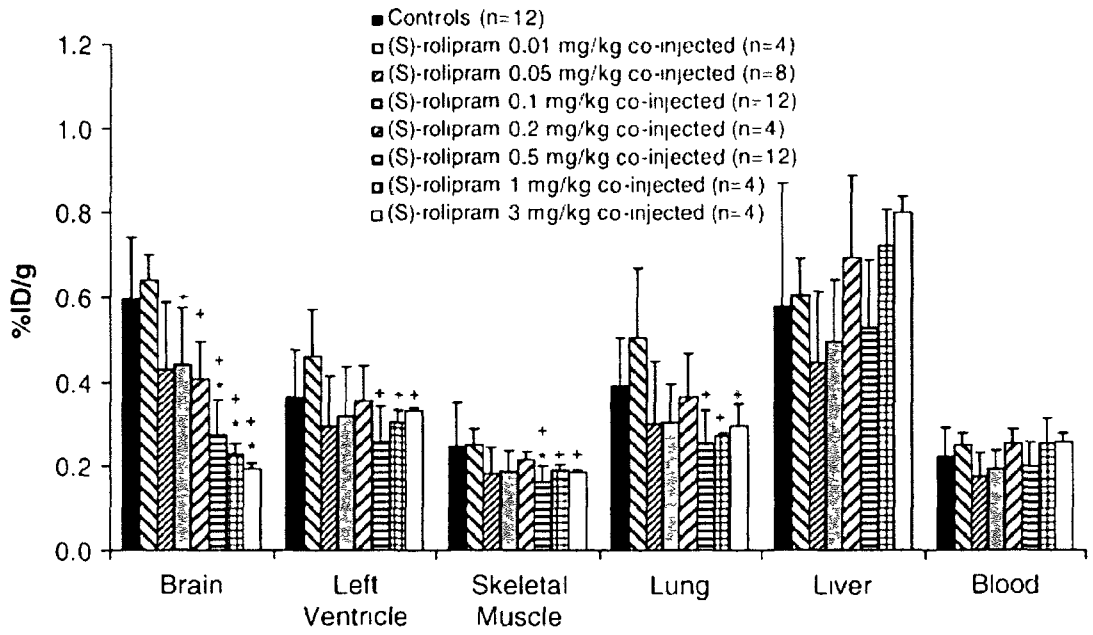


Figure 3-2: Effect of co-injection of (*S*)-rolipram (0.01–3 mg/kg iv) with (*R*)-[$^{11}$C]rolipram on radioactivity uptake in rat brain and peripheral tissues. Nonanesthetized animals were sacrificed 30 min following radiotracer injection (18.5–59.2 MBq). Data are presented as mean %ID/g of tissue±S.D. $^{*}P<.05$ one-way ANOVA compared to controls with Bonferonni post hoc; $^{+}P<.05$ compared to controls with the general linear model, using blood as a covariate.

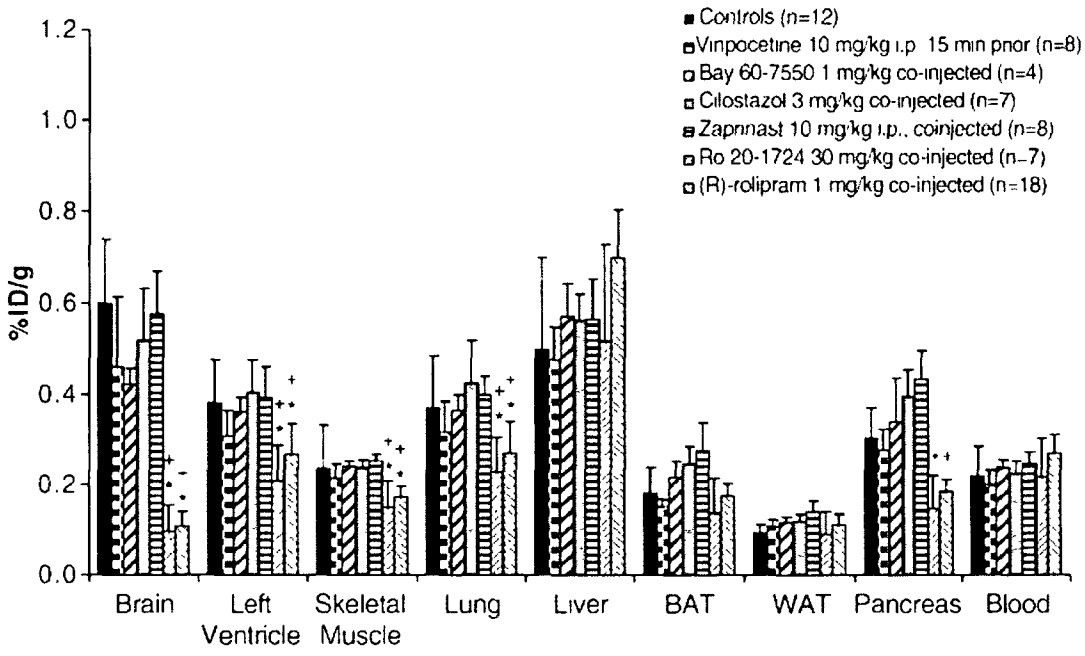


Figure 3-3: Effect of co-administration of (*R*)-[$^{11}$C]rolipram with PDE inhibitors vinpocetine (PDE1), Bay 60-7550 (PDE2), cilostazol (PDE3), zaprinast (PDE5), Ro 20-1724 (PDE4) and (R)-rolipram (PDE4) on (*R*)-[$^{11}$C]rolipram uptake in rat tissues. Nonanesthetized animals were sacrificed 30 min following radiotracer injection (18.5–59.2 MBq). Data are presented as mean %ID/g of tissue ±S.D. $^{*}P<.05$ one-way ANOVA compared to controls with Bonferonni post hoc; $^{+}P<.05$ compared to controls with the general linear model, using blood as a covariate. BAT=brown adipose tissue, WAT=white adipose tissue. For BAT, WAT and pancreas, $n$=4, for all other tissues, as depicted in the legend.

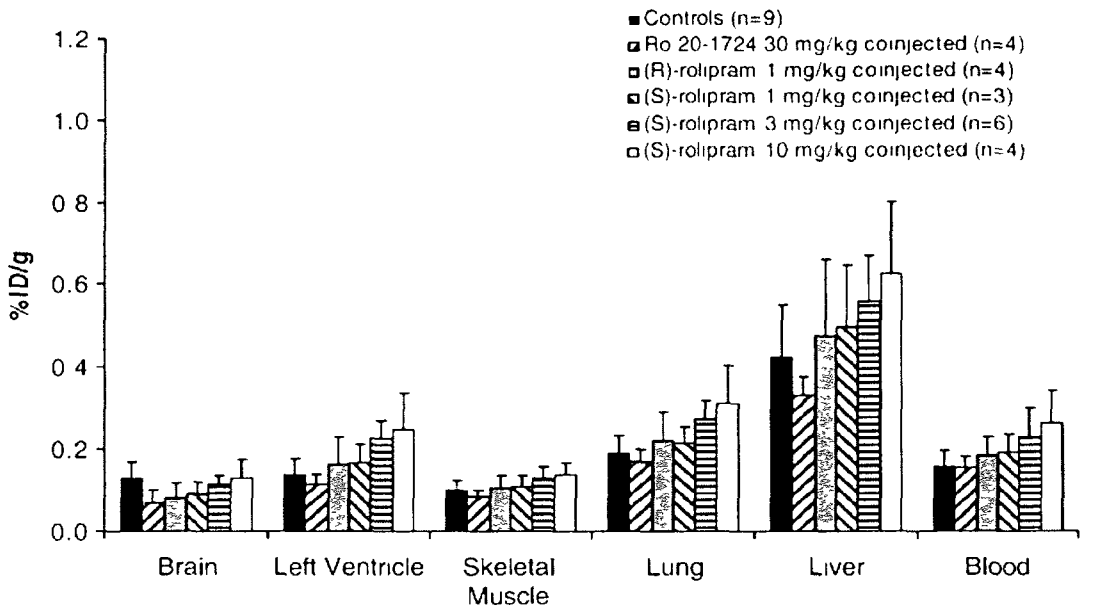


Figure 3-4: Effect of co-injection of (*S*)-[$^{11}$C]rolipram (18.5–59.2 MBq) with PDE4 inhibitors Ro 20-1724, (*R*)-rolipram and (*S*)-rolipram on radioactivity uptake in rats. Nonanesthetized animals were sacrificed 30 min following radiotracer injection. Data are presented as mean %ID/g of tissue ±S.D.

Table 3-1: Blocking of (*R*)-[$^{11}$C]rolipram retention in brain and left ventricle with unlabeled (*R*)-rolipram (1 mg/kg co-injected iv) and (*S*)-rolipram (3 mg/kg co-injected iv).

| | Control (%ID/g) | Blocked (%ID/g) | Blocking (% reduction) | $ED_{50}$ (mg/kg) |
|---|---|---|---|---|
| (*R*)-Rolipram | | | | |
| Brain | 0.60 | 0.11 | 81 | 0.03 |
| Left ventricle | 0.38 | 0.27 | 30 | 0.03 |
| (*S*)-Rolipram | | | | |
| Brain | 0.60 | 0.19 | 69 | 0.2 |
| Left ventricle | 0.38 | 0.25 | 34 | 0.2 |

Data are expressed as % change compared to (*R*)-[$^{11}$C]rolipram injection alone (% change=((radiotracer uptake with blocker–radiotracer uptake alone)/radiotracer uptake alone)*100).

*3.2. Autoradiography studies*

Retention of (*R*)-[$^{11}$C]rolipram was significantly blocked by 58 and 65% when cardiac tissues were incubated in the presence of PDE4 inhibitors (*R/S*)-rolipram and Ro 20-1724, respectively, while vinpocetine, Bay 60-7550, cilostazol and zaprinast had no significant effect (Figure 3-5). (*S*)-[$^{11}$C]Rolipram retention to cardiac slices showed no significant decreases when incubated with the PDE inhibitors (data not shown).

## 4. Discussion

Previous studies have shown the potential for using (*R*)-[$^{11}$C]rolipram as a radiotracer in the evaluation of the cAMP-mediated signaling in the brain (Lourenco et al., 1999; Lourenco et al., 2001; Tsukada et al., 2001; Harada et al., 2002; Tsukada et al., 2004; Fujita et al., 2005; Parker et al., 2005; Lourenco et al., 2006). Work performed to date has established binding selectivity of (*R*)-[$^{11}$C]rolipram for PDE4 over PDE1 in the brain and established the presence of specific binding in rat brain, lungs and the whole heart (Lourenco et al., 2001), with retention levels responding to treatments altering cAMP signaling (Lourenco et al., 2006). Imaging of intracellular second messenger components of post-receptor signal transduction has been proposed as a new direction for brain (Fujita and Innis, 2000) and cardiac (Chen et al., 2005) PET imaging, since alterations in signal-transduction cascades have been observed in neuropsychiatric and myocardial disorders. Current work was aimed to evaluate and establish the potential for using (*R*)-[$^{11}$C]rolipram as an in vivo marker of PDE4 binding in various PDE4-rich organs in the periphery.

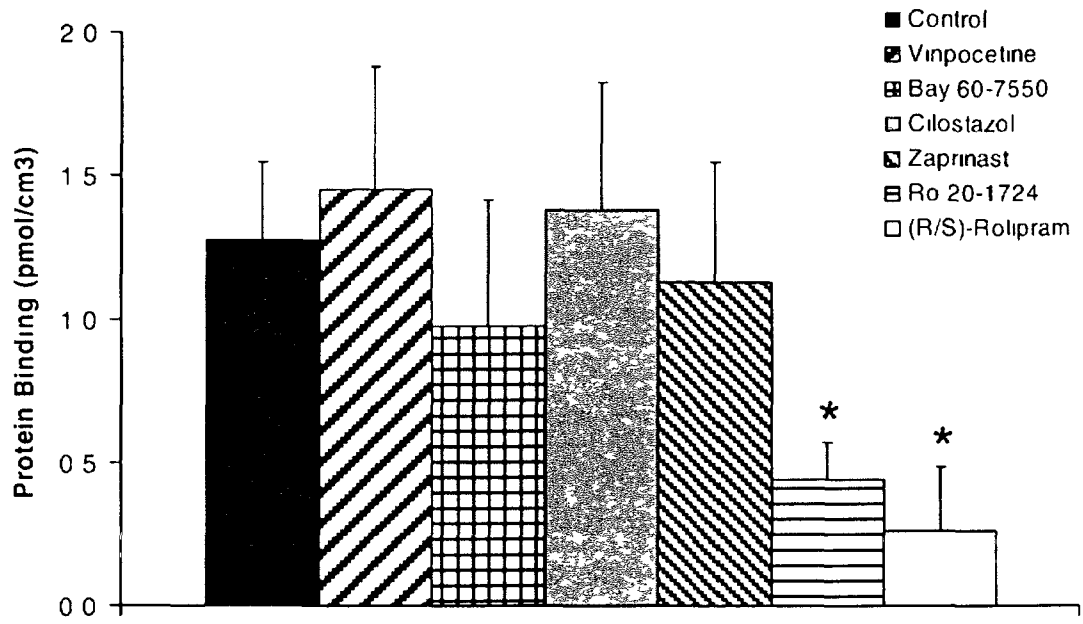


Figure 3-5 Myocardial protein binding, as evaluated using autoradiography studies Cardiac slices were incubated with 5 nM (*R*)-[$^{11}$C]rolipram with or without 10 μM inhibitors of PDE1 (vinpocetine), PDE2 (Bay 60-7550), PDE3 (cilostazol), PDE4 ((*R/S*)-rolipram, Ro 20-1724) or PDE5 (zaprinast). $^{*}P<.05$ one-way ANOVA compared to controls with Bonferonni post hoc.

Sympathetic nervous system control of cardiac contractility and heart rate occurs through modulation of NA signaling through β-AR present on cardiomyocytes. $\beta_1$- and $\beta_2$-AR coexist in the myocardium where they are positively coupled to $G_{s\alpha}$ and activate adenylyl cyclase following agonist binding, producing cAMP (Movsesian, 1998). While PDE3 and PDE4 isozymes represent the major cAMP-hydrolyzing activities in cardiac ventricular nuclei (Maurice et al., 2003; Lugnier, 2006), the presence of PDE1, PDE2, PDE5, PDE7 and PDE9 enzymes has also been observed in the heart (Lugnier et al., 1999). Increasing cAMP levels by PDE4 inhibition using Ro 20-1724 was reported to improve cardiac contractility and heart rate (Herzer et al., 1998), while treatment with rolipram enhanced isoproterenol-induced cAMP accumulation in the rat myocardium (Xiang et al., 2005).

Alterations in NA signaling and downstream cAMP-mediated signal transduction have been reported in animal models of obesity, with an associated impairment in NA-stimulated lipolysis and thermogenesis (Levin et al., 1983; Collins and Surwit, 2001). Increased NA and cAMP levels with corresponding down-regulation of $\beta_3$-AR were reported in obese rodent BAT (Bronnikov et al., 1999; Robidoux et al., 2004). Additionally, PDE4 has been found to be a major cAMP-catalyzing enzyme in the skeletal muscle of mice (Bloom, 2002), with suggested influence on thermogenesis. In combination with the involvement of PDE4 isozymes in modulation of lipolysis in adipocytes (Enoksson et al., 1998), PDE4 regulation of cAMP may thus play an important role in pathologies involving energy homeostasis, such as diabetes and metabolic syndrome. In fact, PDE4 was reported to modulate glucose-induced insulin

release through PKA signaling in the pancreatic islets (Renstrom et al., 1997; Pyne and Furman, 2003). Imaging of (*R*)-[$^{11}$C]rolipram as an index of PDE4 binding and cAMP signaling may thus be beneficial to understanding and treating diabetes and other metabolic conditions.

The 30-min time point was selected for the biodistribution studies presented here on the basis of previously published time-course experiments (Lourenco et al., 2001), which displayed a good tissue/blood signal ratios at this sacrifice time. The observed dose-dependent blockade of (*R*)-[$^{11}$C]rolipram retention in the brain, cardiac tissue and lungs by (*R*)- and (*S*)-rolipram confirms our previous observations (Lourenco et al., 2001), and indicates that specific binding to PDE4 is present in peripheral tissues in addition to the brain. Higher doses of (*S*)-rolipram were required to block (*R*)-[$^{11}$C]rolipram binding to PDE4 ($ED_{50}$ of 0.03 and 0.2 mg/kg for (*R*)- and (*S*)-rolipram, respectively), in accordance with the lower affinity of the (*S*)- enantiomer for the enzyme in vitro (~10× lower) (Schneider et al., 1986). As expected, high doses of inhibitors of PDE1, PDE2, PDE3 and cGMP-specific PDE5 exhibited no effect on (*R*)-[$^{11}$C]rolipram binding. These results were confirmed by in vitro autoradiography studies in myocardial tissues. This observation is in line with previous studies reporting rolipram to bind selectively to PDE4 (Schneider et al., 1986; Lourenco et al., 2001). Selectivity of (*R*)-[$^{11}$C]rolipram for PDE4 over other PDE subtypes was also observed in the skeletal muscle, pancreas and lung, with radioactivity retention in those tissues displaying susceptibility to blocking by treatments with PDE4 inhibitors only. Selective inhibitors of PDE7 and PDE9 were not tested despite their presence in the heart as insensitivity of

PDE7 to rolipram has been well established (Gardner et al., 2000; Lugnier, 2006), and PDE9 is being expressed at low concentrations in the heart (Maurice et al., 2003).

Even though in vitro investigations have implicated PDE2, PDE3 and PDE4 in metabolic regulation in WAT and BAT (Nagaoka et al., 1998; Coudray et al., 1999), PDE4 activity in these tissues is reportedly low (~1–9 pmol/[min/mg]), with PDE3 being a major contributor to cAMP hydrolysis (five and four times higher than PDE4 in WAT and BAT, respectively) (Nagaoka et al., 1998). The inability to detect in vivo PDE4-specific binding in adipose tissues with (*R*)-[$^{11}$C]rolipram may be attributed to both the low PDE4 density in adipose tissues and specific activity of the tracer that is too low to allow study of these sites without saturation.

While (*R*)-[$^{11}$C]rolipram binding in the lungs was shown in this study to be specific for PDE4, any imaging applications of the tracer in this tissue would be made difficult by the low density of the tissue (0.26 g/cm$^3$ for lungs, compared to 1.05 g/cm$^3$ in the heart). High retention of (*R*)-[$^{11}$C]rolipram observed with uptake expressed per gram of tissue would not translate to a high signal contrast between the lung uptake and surrounding tissue in a volumetric expression (activity/cubic millimeter of tissue) relevant to PET imaging (Muzik et al., 1993).

Rolipram binds to PDE4 enzymes at two distinct sites (HARBS and LARBS; $K_d$=~0.7 and 40 nM, respectively) (Schneider et al., 1986; Jacobitz et al., 1996; Souness and Rao, 1997). Central (*R*)-rolipram binding to HARBS ($IC_{50}$=~2–5 nM) was reported to correlate with behavioural effects (Schmiechen et al., 1990). While it has been argued that HARBS are only present in the brain and not in the periphery (Schneider et al., 1986; Zhao et al., 2003), specific binding of (*R*)-[$^{11}$C]rolipram obtained in this study as well as

in our previously published findings (Lourenco et al., 2001; Lourenco et al., 2006) indicates the presence of saturable HARBS in cardiac tissues, skeletal muscle, lungs and pancreas. $ED_{50}$ values of 0.03 mg/kg obtained in our study for inhibition of tracer binding by unlabelled (*R*)-rolipram in vivo in the cardiac tissues indicate that at tracer doses it is unlikely that the observed specific binding of (*R*)-[$^{11}$C]rolipram reflects retention at the LARBS. Since the active form of PDE4, which exhibits high affinity binding to rolipram and accounts for HARBS binding, is dependent on the presence of $Mg^{2+}$ cations at the catalytic site (Laliberte et al., 2000; Xu et al., 2000; Liu et al., 2001), conditions in the physiological milieu are likely to favor the active holoenzyme conformation of the PDE4 enzyme. It is thus likely that the in vivo conditions in our experiments preserve the HARBS in the periphery, accounting for the discrepancy with the previously published in vitro results.

Overall, lower levels of PDE4-specific binding were observed in the peripheral tissues (30–40% of total binding) in comparison to the brain (~80%). This may reflect higher PDE4 levels in the brain, higher levels of nonspecific binding, or the presence of radiolabeled metabolites of (*R*)-[$^{11}$C]rolipram in the periphery. Further studies are currently being performed to analyze the presence of radiolabeled metabolites in peripheral tissues. In contrast to the observations in the brain (Lourenco et al., 2001), use of (*S*)-[$^{11}$C]rolipram may be suitable for measuring (*R*)-[$^{11}$C]rolipram nonspecific binding in the periphery, as very little specific binding was observed with the less active enantiomer at the specific activities used in this study. Work is currently in progress by our group using large animals, addressing the pharmacokinetic issues and the potential use of less active enantiomer in tracer kinetic modeling and imaging.

In conclusion, our present study indicates that (*R*)-[$^{11}$C]rolipram, unlike the (S)-enantiomer, binds selectively to PDE4 in the brain, myocardium, lungs, skeletal muscle and pancreas, but not in the BAT and WAT. Involvement of PDE4 enzymes in post-synaptic regulation of cAMP signaling in a number of receptor signal transduction cascades provides a rationale for applications of (*R*)-[$^{11}$C]rolipram in evaluating changes in intracellular cAMP signaling. Observations presented here expand on previous work that established the potential for use of (*R*)-[$^{11}$C]rolipram as a PET tracer in the brain, opening up possible applications for this radiotracer in PET imaging of PDE4 and cAMP signaling in cardiac and metabolic disorders.

**Acknowledgments**

The authors acknowledge the contributions of the University of Ottawa Heart Institute Cardiac PET Centre radiochemistry staff (Samantha Mason, Paul Colletta, Anthony DiNardo and Jeff Collins) in the preparation of radiotracers and would like to thank Elissa Strome and Doris Doudet (University of British Columbia/TRIUMF PET Group) for help with the autoradiography methods, as well as the University of Ottawa Heart Institute Animal Care and Veterinary Staff (Rick Seymour and Dan de Vette) for assistance with experiments in animals. This work was supported by a grant from Canadian Institutes for Health Research (CIHR) MOP62765.

# CHAPTER 4: MANUSCRIPT #3

Nuclear Medicine and Biology 35 (2008) 515 – 521

# Use of a column-switching high-performance liquid chromatography method to assess the presence of specific binding of (*R*)- and (*S*)-[$^{11}$C]rolipram and their labeled metabolites to the phosphodiesterase-4 enzyme in rat plasma and tissues

Miran Kenk[a,b], Michael Greene[a,b], Mireille Lortie[a], Robert A. deKemp[a], Rob S. Beanlands[a,b], Jean N. DaSilva[a,b,*]

[a]*Cardiovascular PET Molecular Imaging Program, Division of Cardiology, University of Ottawa Heart Institute, Ottawa, Ontario, Canada, K1Y 4W7*

[b]*Department of Cellular and Molecular Medicine, Faculty of Medicine, University of Ottawa, Ottawa, Ontario, Canada, K1H 8M5*

Received 27 September 2007; received in revised form 20 December 2007; accepted 22 January 2008

* Corresponding author. Cardiac PET Centre, University of Ottawa Heart Institute, 40 Ruskin Street, Ottawa, Ontario, Canada, K1Y 4W7. Tel.: 1 613 798 5555x19704; fax:1 613 761 5406

*E-mail address:* jdasilva@ottawaheart.ca (J.N. DaSilva).

**Contributions of authors**

Experiments executed in this manuscript were performed by myself and MSc candidate Michael Greene (analysis of metabolites in pancreas and brown adipose tissue), under guidance and supervision of Dr. Jean DaSilva. Drs Robert deKemp and Mireille Lortie provided input on the relevance of obtained data for the interpretation of PET data, guiding the experiments. Dr. Rob Beanlands provided input on the physiological aspects of the data.

**Abstract**

**Introduction:** To complement recent studies using the high-affinity $^{11}$C-labeled phosphodiesterase-4 (PDE4) inhibitor (*R*)-rolipram and the less active enantiomer (*S*)-[$^{11}$C]rolipram for in vivo quantification of PDE4 levels, we evaluated the presence of radiolabeled metabolites and their potential binding to PDE4 in the rat plasma, brain, heart, pancreas, skeletal muscle and brown adipose tissue.

**Methods:** A reverse-phase capture and analytical HPLC column-switch method was used to detect (*R*)-[$^{11}$C]rolipram, (*S*)-[$^{11}$C]rolipram and their radiolabeled metabolites in rat plasma and tissue extracts. The relative proportion of PDE4-specific binding of the radiotracers and their labeled metabolites was analyzed following co-injections with a saturating dose of unlabeled (*R*)-rolipram at 45 min post-tracer injection in tissue extracts.

**Results:** Radiolabeled metabolites were found in the plasma (72-75% of total radioactive signal), and in the heart, skeletal muscle, pancreas and brown adipose tissue (44-52%), but not in the brain. In comparison to polar labeled metabolites, the proportion of unchanged (*R*)-[$^{11}$C]rolipram was reduced in PDE4-rich organs by co-injection of unlabeled (*R*)-rolipram. Conversely, no changes were obtained in brown adipose tissue, or with (*S*)-[$^{11}$C]rolipram, suggesting that radiolabeled metabolites of (*R*)-[$^{11}$C]rolipram display no specific binding to PDE4.

**Conclusions:** Radiolabeled hydrophilic metabolites are unlikely to compete with (*R*)-[$^{11}$C]rolipram for PDE4-specific retention. However, due to the high proportion of the radioactive metabolites in the total radioactive signal, any kinetic modeling calculations

in the peripheral tissues will need to take into account the presence of labeled metabolites.



*Keywords:* $^{11}$C-Labeled metabolites; HPLC; Imaging cAMP-mediated signaling; PDE4; Positron emission tomography

## 1. Introduction

Cyclic 3',5'-adenosine monophosphate (cAMP)-mediated signal transduction is initiated following agonist binding on a number of G protein-coupled receptors. This second messenger is produced following activation of adenylyl cyclase by the stimulatory subunit of the G protein ($G_{s\alpha}$), and hydrolyzed by the phosphodiesterase (PDE) superfamily of enzymes, comprising at least 11 different families. Enzymes of the PDE4 subfamily (PDE4A-D) are selective for cAMP and are characterized by susceptibility to inhibition by rolipram (Houslay, 2001). Density and activity of the PDE4 enzymes are regulated by intracellular cAMP levels through increased protein expression (long-term) (Houslay, 2001) and increased phosphorylation by protein kinase A or extracellular signal-regulated kinase (Laliberte et al., 2002). PDE4 is expressed in the brain, heart, lungs, skeletal muscle, pancreas and, to a lower extent, in the white and brown adipose tissues (Wachtel, 1990; Nagaoka et al., 1998; Torphy, 1998; Pyne and Furman, 2003). Modulation of the enzyme has been associated with affective disorders and memory in the brain (Wachtel, 1990), as well as in the inflammatory mechanisms of asthma (Torphy, 1998). Cardiac PDE4 plays a role in regulating myocardial contractility (Takahashi et al., 2002), while PDE4 in the skeletal muscle, adipose tissues and the pancreas regulates metabolic processes, including thermogenesis and glucose homeostasis (Nagaoka et al., 1998; Pyne and Furman, 2003).

Rolipram binding to PDE4 is stereospecific and reversible, with (*R*)-rolipram exhibiting high affinity ($K_d$ 1-5 nM) and the (*S*)-rolipram enantiomer 10- to 30-fold lower affinity (Schneider et al., 1986). We have recently reported that $^{11}$C-labeled (*R*)-rolipram in tracer doses binds to PDE4 selectively in PDE4-rich organs such as the brain, heart,

lungs, skeletal muscle and pancreas, but not in the adipose tissues (Kenk et al., 2007). Conversely, (*S*)-[$^{11}$C]rolipram displayed no PDE4-specific binding. The lower levels of PDE4-specific binding observed in rat PDE4-rich peripheral tissues (30-40% of total binding at 30 min postinjection and ~41% at 45 min) compared to the brain (80% at both time points) (Lourenco et al., 2001; Kenk et al., 2007) may reflect higher PDE4 expression in the brain, higher nonspecific binding and/or the presence of radiolabeled metabolites in the periphery. Prior to using (*R*)-[$^{11}$C]rolipram to measure PDE4 levels noninvasively by positron emission tomography (PET), it is important to ascertain the presence and proportion of $^{11}$C-labeled metabolites in the tissues of interest for kinetic modeling calculations in quantitative studies. At least six labeled metabolites were separated by HPLC in rat plasma following administration of $^{3}$H-labeled racemic rolipram (Krause and Kühne, 1992).

The purpose of this study was to evaluate the proportion of unchanged (*R*)-[$^{11}$C]rolipram, (*S*)-[$^{11}$C]rolipram and their $^{11}$C-labeled metabolites (if any) in plasma and tissues of interest, using a sensitive column-switch HPLC method. Additionally, this procedure was applied to determine the relative proportion of PDE4-specific binding of unchanged radiotracers in comparison to the total radioactivity following co-injections of a saturating dose of unlabeled (*R*)-rolipram.

## 2. Materials and Methods

### *2.1. Chemicals*

Acetonitrile, methanol, urea and ammonium formate were purchased from Sigma (Sigma-Aldrich, Canada). Unlabeled (*R*)-rolipram (Tocris Bioscience, Missouri) was

dissolved in 5/20/75 ethanol/propylene glycol/saline (v/v/v). (*R*)-[$^{11}$C]Rolipram and (*S*)-[$^{11}$C]rolipram were synthesized as previously described (DaSilva et al., 2001) with high radiochemical purity and specific activity (12.6-40.2 GBq/ μmol; 341-1489 mCi/μmol at the time of injection in animals).

*2.2. In vivo metabolism studies*

All experiments were conducted in accordance with the recommendations of the Canadian Council on Animal Care and with approval from the Animal Care Committee at the University of Ottawa. Male Sprague-Dawley rats ($n$=28 total; Charles River, Montreal, Canada) were housed in groups of two and maintained on a 12-h light/dark cycle, with free access to food and water. Rats weighed 250-500 g at the time of the experiment. For injections via a tail vein, rats were immobilized in a rodent restrainer (Harvard Apparatus, Canada) and the tail warmed under a heat lamp for vasodilation. In each experiment, all animals received 0.8–12.0 mCi (29.6–444 MBq) of (*R*)-[$^{11}$C]rolipram or (*S*)-[$^{11}$C]rolipram in 0.2–0.3 mL of the formulation, corresponding to a mass dose of 0.2–7.8 μg. Rats were sacrificed at either 30 or 45 min following radiotracer administration by decapitation, with blood collected from the trunk. Heart, brain and samples of quadriceps skeletal muscle, brown adipose tissue and pancreas were rapidly dissected and placed on ice ($n$=3 for each tissue).

*2.3. Ex vivo sample preparation*

Plasma samples for HPLC analysis were prepared following blood centrifugation (3000×g, 5 min). Dissected tissue samples were homogenized in 10 mL 80/20

EtOH/water (v/v) using a Polytron homogenizer (PT 1200, Kinematica AG, Lutzen), then centrifuged (82000×g) for 15 min. Supernatant was collected and evaporated, then redissolved in $CH_3CN$ (200 μL) and 1 mL 1/99 $CH_3CN$/water (v/v). Plasma and tissue solutions were filtered through 0.22 μm Cathivex-GS (Millipore, Ireland) syringe filters and injected onto the HPLC system.

*2.4. Chromatography conditions and analyses*

A modification of the HPLC column-switch method developed by Hilton et al. (Hilton et al., 2000) (see Scheme 1 from Hilton et al. for illustration) was used to quantify tissue and plasma metabolites. Eluted solvents were analyzed by two detectors in series: a UV absorbance detector (Waters 486) and a dual bismuth germanium oxide (BGO) HPLC coincidence radiation detector (Bioscan), linked to a chromatography data integration system (PeakSimple with attached PC running PeakSimple data analysis software, version 3.29). Eluted radioactivity levels were recorded in real time, with detected peaks integrated and subsequently corrected for radioactive decay and noise. It is important to note that radioactivity detection was not saturated, allowing proper analysis of the proportion of each peak relative to each other. Columns used in the analysis were Column 1: a capture column made from a refillable guard column (Alltech In-Line capture column, 2×20 mm; Mandel, Canada) with 2-μm frits (2-mm filter elements, Alltech) hand-packed with polymeric reverse phase sorbent (Oasis HLB; Waters Corp.); and Column 2: an analytical column (Aqua C18 5 μm 125 A 250×4.60 mm; Phenomenex). In Step 1 (at the time of sample injection, 0–4 min), Solvent 1 [1/99 acetonitrile/water (v/v) at 2 ml/min] was eluted using a Waters 510 pump through a six-

port valve onto Column 1 and, downstream, to the four-port valve that directs the outflow to the detectors (see Ref. (Hilton et al., 2000)). Step 2 (4–6 min): 4 min after sample injection, when the UV absorbance subsides to baseline (see Figures 4-1, 4-2 and 4-3), switching both the six- and four-port valves redirects the flow of Solvent 1 to waste; and Solvent 2 [45/55 acetonitrile/0.1 M ammonium formate (v/v) at 1 ml/min, delivered by the second Waters 510 pump] back-flushes the capture column onto Column 2 and to the detectors. Step 3 (6–20 min): after the solvent front is observed by UV (2–3 min following switch), the six-port valve is returned to its original position, allowing the capture column to be re-equilibrated and prepared for the next sample injection. At the end of analysis, the four-port valve is switched back to the initial state, prior to the next injection. Under these experimental conditions, up to 4 ml of plasma or tissue homogenate extracts can be injected onto the system without clogging the capture column. Administration of large volumes can compensate for the radioactive decay, especially at later time points after injection of radiotracer in animals. The capture column could sustain at least five consecutive sample injections, before it needed to be repacked.

*2.5. Control analysis*

Control experiments were carried out with (*R*)-[$^{11}$C]rolipram or (*S*)-[$^{11}$C]rolipram added to blood, brain and heart (as representative peripheral tissue) obtained from untreated rats to establish whether the radioactivity peaks are affected by factors outside the biotransformation processes in vivo and determine recovery capabilities. Blood and tissues were incubated with radiotracers for 30 or 45 min at 37°C then homogenized,

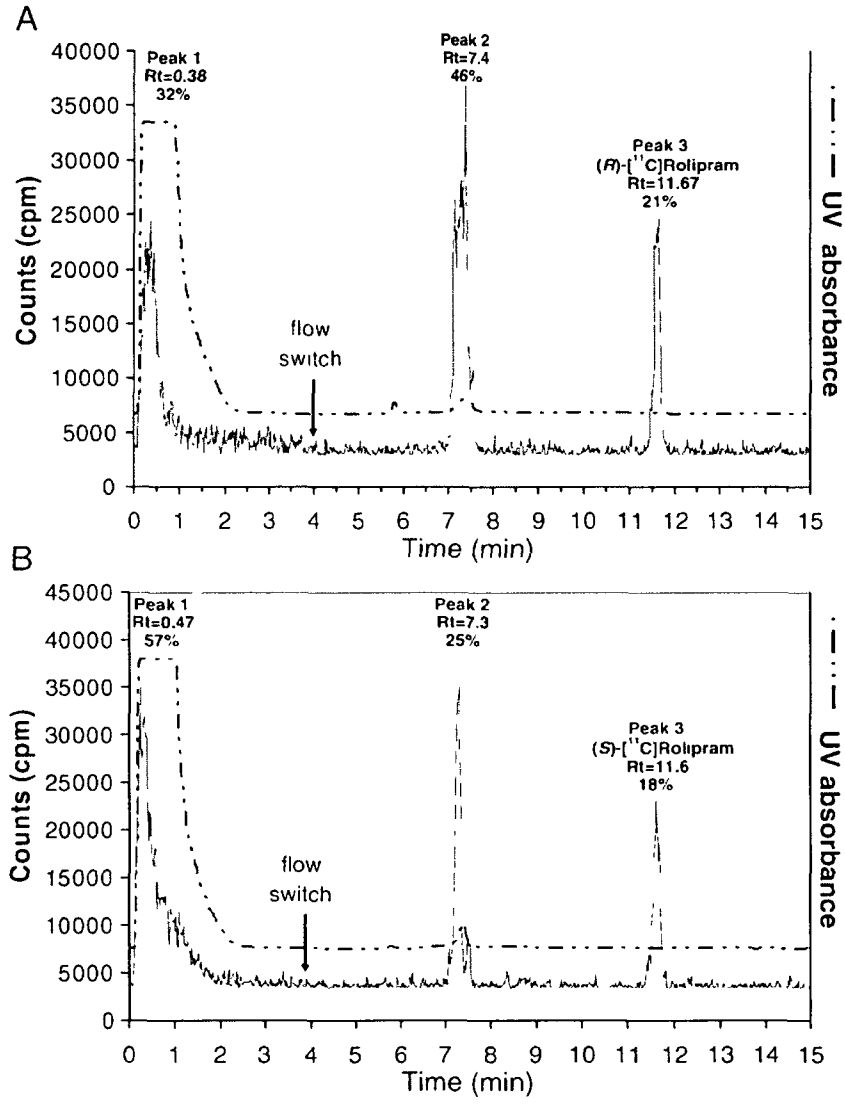


Figure 4-1: Sample chromatogram depicting the radioactive peaks with the injection of plasma, 45 min following (*R*)-[$^{11}$C]rolipram (A) or (*S*)-[$^{11}$C]rolipram (B) administration. Columns and solvents were switched at 4 min.

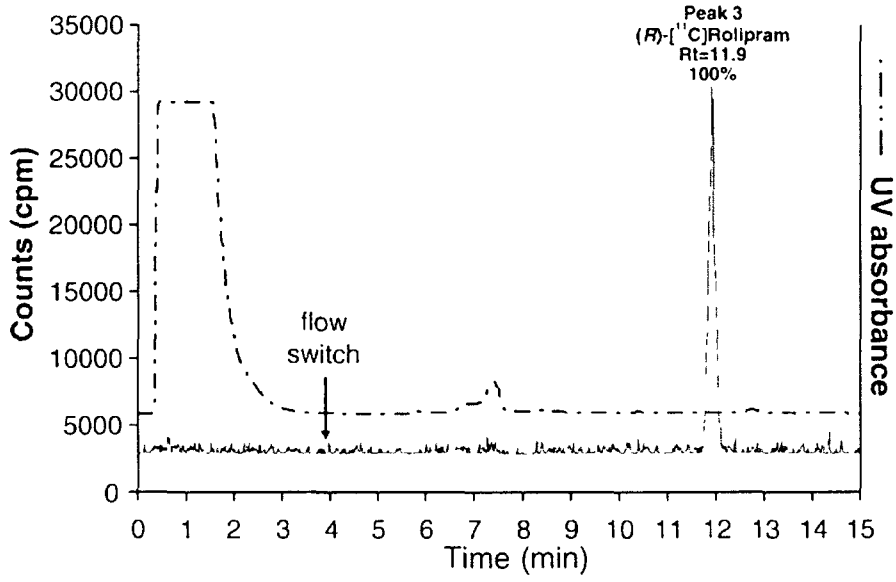


Figure 4-2: Sample chromatogram depicting the radioactive peaks with the injection of brain homogenate, 45 min following (*R*)-[$^{11}$C]rolipram administration. Columns and solvents were switched at 4 min.

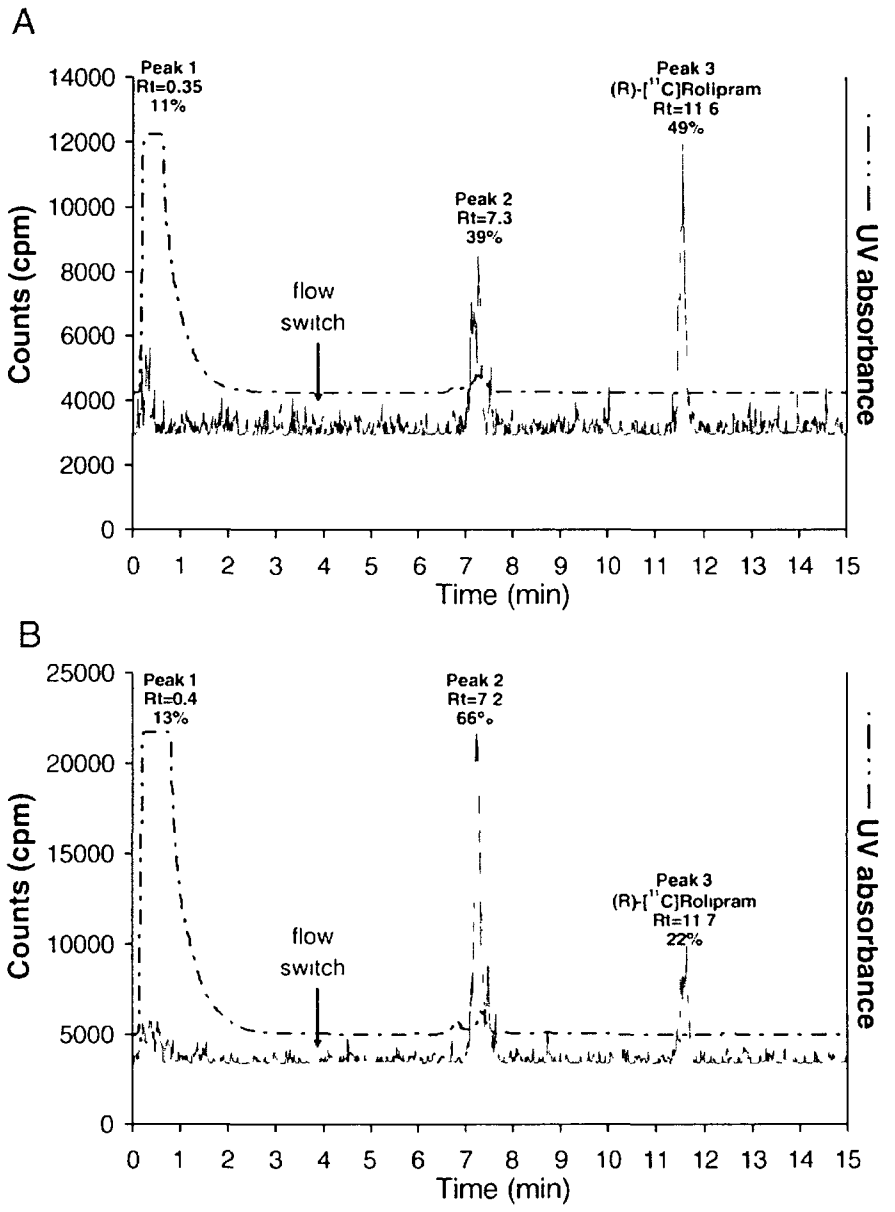


Figure 4-3: Sample chromatogram depicting the radioactive peaks with the injection of heart homogenate, 45 min following (*R*)-[$^{11}$C]rolipram administration (A) and co-injected with a blocking dose of unlabeled (*R*)-rolipram (B). Columns and solvents were switched at 4 min.

centrifuged and filtered as above, prior to injection on the HPLC system. In order to determine whether protein binding affects retention of unchanged radiotracers and radiolabeled metabolites at the capture column, urea (6.65 M) was added to samples of plasma obtained at 45 min following (*R*)-[$^{11}$C]rolipram injection, as well as to plasma from a control rat spiked with authentic (*R*)-[$^{11}$C]rolipram.

### *2.6. Determination of specific binding*

Rats were co-injected with a blocking dose of unlabeled (*R*)-rolipram (1.0 mg/kg (Kenk et al., 2007)) to evaluate the nonspecific binding of (*R*)-[$^{11}$C]rolipram and (*S*)-[$^{11}$C]rolipram in the tissues of interest ($n$=3). Retained radioactivity levels in these conditions represent nonspecifically retained tracer and labeled metabolites. Tracer-specific binding corresponds to the difference between nonblocked (total binding) and blocked (nonspecific binding) tissue levels.

### *2.7. Statistical analyses*

Statistical analysis was carried out using one-way ANOVA followed by Bonferroni's post-hoc comparison test. All analyses were performed using SPSS 14.0 statistical analysis software. Differences with a $P$ value <.05 were considered statistically significant.

## 3. Results

### *3.1. Method validation*

HPLC analysis of blood and heart incubated 30 or 45 min at 37°C with (*R*)-[$^{11}$C]rolipram or (*S*)-[$^{11}$C]rolipram displayed only one peak corresponding to the unchanged radiotracer with consistent retention times ($R_t$) (data not shown), proving that labeled metabolite peaks detected following tracer administration in rats are products of in vivo metabolic processes, not resulting from breakdown of the radiotracers in the blood of the animals.

### *3.2. Analysis of labeled metabolites of (R)-[$^{11}$C]rolipram and (S)-[$^{11}$C]rolipram in plasma*

Following administration of (*R*)-[$^{11}$C]rolipram or (*S*)-[$^{11}$C]rolipram, three distinct radioactivity peaks were detected in the rat plasma, with retention times of <30 s, approximately 7.4 min and 11.6 min (Figure 4-1). Injections of authentic (*R*)-[$^{11}$C]rolipram or (*S*)-[$^{11}$C]rolipram formulations identified the third radioactivity peak [retention time 11.6 min] as unchanged radiotracer. Peak 1 corresponds to hydrophilic labeled metabolites eluted from the capture column ($R_t$ <30 s). Peak 2 ($R_t$ 7.4 min) represents hydrophilic labeled metabolites that elute close to the solvent front of the analytical column, 3.4 min after column and solvent switch. Slightly reduced presence of unchanged radiotracer relative to preceding two peaks is observed at 45 min compared to 30 min following (*R*)-[$^{11}$C]rolipram or (*S*)-[$^{11}$C]rolipram injection (Table 4-1).

Urea was added to the injected samples to disrupt protein binding, maximize elution of the macromolecules (e.g., protein) and retention of radiolabeled compounds by the capture column sorbent (Hilton et al., 2000). The proportion of unchanged radiotracer (Peak 3) was not affected by the addition of urea, but it did alter the ratios of Peak 1 and

Table 4-1: Labeled metabolites in the plasma of rats administered (*R*)-[$^{11}$C]rolipram or (*S*)-[$^{11}$C]rolipram 30 and 45 min following radiotracer administration and effect of addition of urea.

| | Time | Peak 1 * | Peak 2 * | Peak 3 * |
|---|---|---|---|---|
| (*R*)-[$^{11}$C]Rolipram | 30 min | 30.6±1.1 | 41.5±1.8 | 27.8±0.7 |
| | 45 min | 32.5±7.4 | 42.5±6.2 | 25.0±4.9 |
| | 45 min + urea | 22.4±3.5 | 49.6±2.2 | 28.1±5.7 |
| (*S*)-[$^{11}$C]Rolipram | 30 min | 51.5±5.8 | 19.9±1.0 | 28.5±4.8 |
| | 45 min | 55.9±2.2 | 23.2±4.3 | 20.9±6.5 |

* Peak 1: Hydrophilic metabolites eluting from the capture column; Peak 2: hydrophilic metabolites eluting at the analytical column solvent front; Peak 3: unchanged radiotracer. $n$=2–5 rats per study.

Peak 2 (Table 4-1). Since there was no effect on retention of unchanged radiotracers relative to the labeled metabolite peaks, deproteinization with urea was not deemed necessary in further sample preparations.

*3.3. Analysis of labeled metabolites of (R)-[$^{11}$C]rolipram and (S)-[$^{11}$C]rolipram in tissues*

In the brain homogenates, only the peak corresponding to unchanged (*R*)-[$^{11}$C]rolipram (Figure 4-2) or (*S*)-[$^{11}$C]rolipram was observed 45 min following tracer injection. Conversely, radiolabeled metabolite peaks of both radiotracers were detected in the homogenates of the heart (as representative peripheral tissue; Figure 4-3A), brown adipose tissue, skeletal muscle and the pancreas (Table 4-2) at similar levels (44–56% of total radioactivity detected in the tissue samples).

*3.4. PDE4-specific binding of $^{11}$C-labeled metabolites*

Co-administration of unlabeled PDE4 inhibitor (*R*)-rolipram with radiotracers significantly reduced the peak corresponding to unchanged (*R*)-[$^{11}$C]rolipram in the heart (as representative peripheral tissue; Figure 4-3B), skeletal muscle and pancreas (from 47.9–55.9% to 17.5–25.3% of the total detected radioactivity) but not in the brown adipose tissue, while unchanged (*S*)-[$^{11}$C]rolipram peak was unaffected (Table 4-2).

**4. Discussion**

Determination of the presence and proportion of labeled metabolites vs. unchanged radiotracer in plasma is essential in establishing metabolite- and decay-corrected plasma time–activity curves used in pharmacokinetic modeling for the

Table 4-2: Proportion of labeled metabolites and unchanged (*R*)-[$^{11}$C]rolipram or (*S*)-[$^{11}$C]rolipram in the tissue homogenates of rats 45 min following tracer administration in rats.

| | **Tissue** | **Peak 1*** | **Peak 2*** | **Peaks 1+2*** | **Peak 3*** |
|---|---|---|---|---|---|
| (*R*)-[$^{11}$C]Rolipram | Heart (*n*=3) | 9.3±2.3 | 34.7±11.9 | 44.0 | 55.9±14.0 |
| | –Blocked | 13.0±8.2 | 64.7±4.0 | 77.7 | 22.3±4.3 * |
| | Skeletal muscle (*n*=3) | 9.1±6.5 | 39.0±3.1 | 48.2 | 51.8±6.8 |
| | –Blocked | 19.3±10.5 | 63.1±6.9 | 82.4 | 17.5±4.3 * |
| | Pancreas (*n*=3) | 11.1±10.2 | 40.9±15.3 | 52.0 | 47.9±6.3 |
| | –Blocked | 15.5±5.2 | 59.2±5.2 | 74.7 | 25.3±0.1 * |
| | Brown adipose tissue (*n*=3) | 16.2±1.9 | 34.3±6.6 | 50.2 | 49.5±8.2 |
| | –Blocked | 21.1±2.8 | 36.1±13.5 | 57.2 | 42.8±15.9 |
| (*S*)-[$^{11}$C]Rolipram | Heart (*n*=3) | 19.7±3.0 | 36.4±0.3 | 56.1 | 43.9±2.6 |
| | –Blocked | 21.4±9.4 | 36.4±4.6 | 57.8 | 42.2±13.6 |
| | Skeletal muscle (*n*=3) | 19.2±8.9 | 35.0±10.0 | 54.2 | 45.8±8.5 |
| | –Blocked | 33.8±10.5 | 29.1±9.4 | 62.9 | 37.1±11.6 |
| | Pancreas (*n*=3) | 28.0±2.5 | 24.0±3.8 | 52.0 | 48.0±5.3 |
| | –Blocked | 39.4±13.6 | 11.1±5.8 | 50.5 | 49.5±9.0 |
| | Brown adipose tissue (*n*=3) | 28.6±7.1 | 16.4±3.0 | 45.0 | 55.0±6.4 |
| | - Blocked | 28.7±7.9 | 14.6±1.8 | 43.3 | 56.8±6.5 |

* Blocking of radiotracer retention was evaluated by co-injection of 1.0 mg/kg of unlabeled (*R*)-rolipram. Peak 1: Hydrophilic metabolites eluting from the capture column; Peak 2: hydrophilic metabolites eluting at the analytical column solvent front; Peak 3: unchanged radiotracer. All blocking studies are *n*=3. *$P$<.05 One-way ANOVA with Bonferroni post hoc.

quantification of (*R*)-[$^{11}$C]rolipram retention. Quantitative analysis of relative proportions of unchanged radiotracer and metabolites in the tissues of interest is a crucial component in the creation and verification of these kinetic models. The column-switch method developed by Hilton et al. (Hilton et al., 2000) displays the sensitivity and reliability required for rapid serial analysis of the radioactivity present in tissue and plasma samples. This method was used in the present study to quantify the proportions of unchanged radiotracers and their labeled metabolites. Removal of macromolecules from plasma and tissue samples through the capture column and observation of the elution pattern by UV absorbance prevent loading of macromolecules onto the analytical column and allow serial injections without clogging the system.

Since the 45-min time point was best suited for observing PDE4 alterations in vivo (Lourenco et al., 2006), the ex vivo tissue evaluations were done at that time point. In the brain homogenates, only the peak corresponding to the unchanged (*R*)-[$^{11}$C]rolipram or (*S*)-[$^{11}$C]rolipram was observed, indicating that labeled metabolites do not cross the blood–brain barrier. This finding is in agreement with our previous analysis using thin-layer chromatography (Lourenco et al., 2001). Conversely, hydrophilic radiolabeled metabolites of both radiotracers were detected in the homogenates of the heart, brown adipose tissue, skeletal muscle and the pancreas at similar levels (44–56% of total radioactivity detected in the tissue samples).

It is important to note that *O*-demethylated metabolites are no longer radioactive and are not of interest at tracer doses. Metabolism of rolipram has been previously shown to proceed through ether cleavage at the methoxy and pentyloxy groups and hydroxylation of the pentyl and pyrrolidone rings, followed by Phase II reaction resulting

in formation of hydrophilic sulphate metabolites (Krause and Kühne, 1993). Different biotransformation products were previously observed in rats, rabbits, primates and humans (Krause and Kühne, 1992). Krause and Kühne (Krause and Kühne, 1993) found three to five distinct metabolites in the plasma and reported a half-life of 1–3 h in all species following oral administration of (*R/S*)-rolipram. Our method detected two distinct groups of radiolabeled metabolites, both more hydrophilic than the unchanged (*R*)-[$^{11}$C]rolipram or (*S*)-[$^{11}$C]rolipram. These polar hydrophilic metabolites elute either from the capture column or at the solvent front of the analytical reverse phase column, and are unlikely to penetrate the cell membrane. Our findings showed no difference in relative proportions of labeled metabolites produced in vivo following administration of (*R*)-[$^{11}$C]rolipram or (*S*)-[$^{11}$C]rolipram, which is in accordance with previous work reporting that the chiral center of rolipram is not affected by biotransformation pathways in rats (Krause and Kühne, 1993).

The results presented here show that in the periphery, at 45 min postinjection, the combined proportion of hydrophilic radiolabeled metabolites of (*R*)-[$^{11}$C]rolipram accounts for 44–52% of the total activity present in the homogenates of the rat heart, skeletal muscle, pancreas and brown adipose tissue. Reduction of retention of (*R*)-[$^{11}$C]rolipram relative to labeled metabolites following co-injection with cold (*R*)-rolipram confirms recent in vivo biodistribution work that established the presence of (*R*)-[$^{11}$C]rolipram specific binding in these PDE4-rich organs (Kenk et al., 2007). No effect was observed with (*S*)-[$^{11}$C]rolipram or the hydrophilic labeled metabolites, since their retention is not reduced by a saturating dose of cold (*R*)-rolipram, suggesting the absence of specific binding to PDE4. Since the labeled metabolites did not display

binding to PDE4, no attempts were made to identify their structure and further determine their binding characteristics. While cAMP signaling and a number of PDE subtypes have been implicated in the modulation of metabolic processes in adipocytes, it was previously reported that PDE4 is not a major enzyme hydrolyzing cAMP in comparison to PDE3 (Nagaoka et al., 1998), probably explaining the lack of effect observed in the brown adipose tissue.

From our previous biodistribution work at 45 min postinjection, 41% of the total cardiac (*R*)-[$^{11}$C]rolipram radioactive signal is susceptible to blocking by the saturating dose of unlabeled (*R*)-rolipram and therefore reflects specific binding to PDE4 (Lourenco et al., 2001). The graphical representation presented in Figure 4-4 illustrates the proportions involved in the total myocardial signal: i.e., 44% labeled metabolites (Table 4-2), 41% specific binding (Lourenco et al., 2001), with the remaining activity (15%) corresponding to the nonspecific binding of (*R*)-[$^{11}$C]rolipram. Whereas in the brain, the proportions of the signal published in Ref. (Lourenco et al., 2001) correspond to 88% specific binding and 12% nonspecific binding. Interestingly, a similar proportion of nonspecific binding is observed in both tissues.

Recent biodistribution studies with (*R*)-[$^{11}$C]rolipram in the peripheral tissues have detected a large proportion of radioactive signal resistant to blocking by saturating doses of (*R*)-rolipram in comparison to the brain following (*R*)-[$^{11}$C]rolipram administration (Kenk et al., 2007). The results presented here suggest that a large portion of this nonspecific signal is due to the presence of radiolabeled metabolites which do not exhibit binding to the PDE4 enzyme and, to a lesser extent, to nonspecific binding of unchanged (*R*)-[$^{11}$C]rolipram (12–15% of total signal) at 45 min postinjection. These

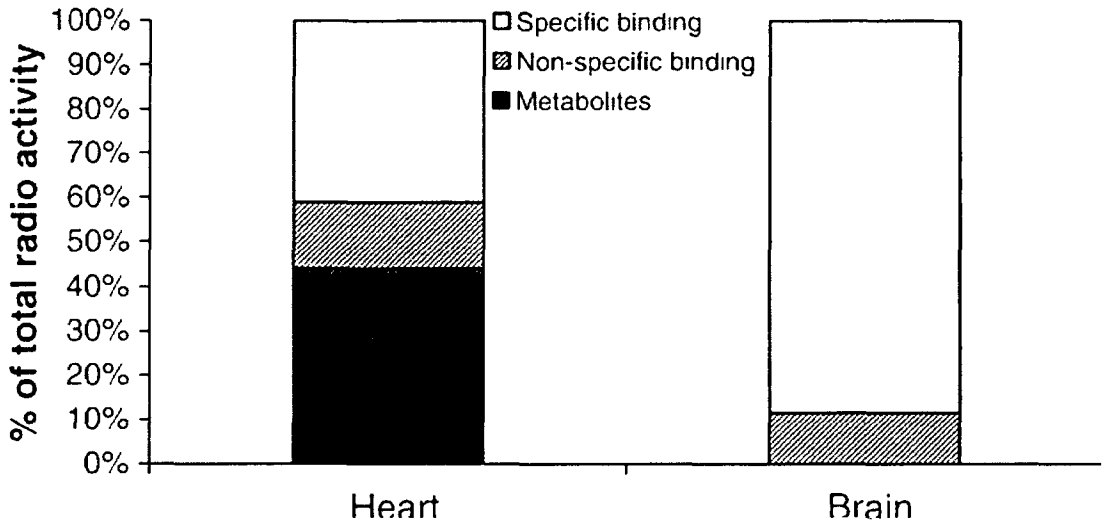


Figure 4-4: Proportions of radioactive signal accounted for by labeled metabolites, specific and nonspecific binding in the heart (representative peripheral tissue) and brain homogenates in rats at 45 min postinjection of (*R*)-[$^{11}$C]rolipram. Specific binding (□) reflects the proportion of the radiotracer retention that can be blocked by (*R*)-rolipram co-injection (41% and 88% in the heart and brain, respectively), as ascertained using biodistribution methods in Ref. (Lourenco et al., 2001). Metabolite proportion (■) is determined by HPLC column-switch methods (44% in the heart, not detected in the brain). (*R*)-[$^{11}$C]Rolipram nonspecific binding (□) corresponds to the remaining portion of radioactivity (15% in the left ventricle, 12% in the brain).

findings indicate that kinetic modeling of data obtained from (*R*)-[$^{11}$C]rolipram PET imaging in peripheral organs will likely need to account for the presence of labeled metabolites in the plasma and the peripheral organs. However, in vivo, the hydrophilic labeled metabolites are not expected to cross the cell membrane and bind to PDE4 intracellularly.

In conclusion, polar hydrophilic radiolabeled metabolites of (*R*)- and (*S*)-[$^{11}$C]rolipram are present following tracer administration in plasma and homogenates of cardiac, skeletal muscle, pancreas and brown adipose tissues, but not the brain. Relative retention of unchanged (*R*)-[$^{11}$C]rolipram was susceptible to blocking by co-injected (*R*)-rolipram in PDE4-rich tissues, unlike the labeled metabolites and the less active (*S*)-[$^{11}$C]rolipram stereoisomer. Radiolabeled hydrophilic metabolites are thus unlikely to compete with (*R*)-[$^{11}$C]rolipram PDE4-specific retention. Since these radioactive metabolites account for approximately 44–52% of the total radioactive signal at 45 min postinjection, any kinetic modeling calculations in the peripheral tissues will need to take into account the presence of radiolabeled metabolites. This study emphasizes the need to perform metabolite studies for quantitative PET imaging with novel radiotracers.

**Acknowledgments**

The authors acknowledge the contributions of the University of Ottawa Heart Institute Cardiac PET Centre radiochemistry staff (Samantha Mason, Paul Colletta, Anthony DiNardo and Jeff Collins) in preparation of radiotracers, Stephanie Thorn and James Thackeray in animal experiments and the University of Ottawa Heart Institute Animal Care and Veterinary Staff (Rick Seymour and Dan de Vette) for help with

maintenance and housing of experimental animals. This work was supported by a grant from Canadian Institutes for Health Research (CIHR) MOP62765.

# CHAPTER 5: MANUSCRIPT #4

Journal of Nuclear Cardiology 17(2010) 254 – 263

# Alterations of pre- and postsynaptic noradrenergic signaling in a rat model of adriamycin-induced cardiotoxicity

Miran Kenk, BSc,[a,b] James T. Thackeray, BSc, MSc,[a,b] Stephanie L. Thorn, BSc, MSc,[a,b] Karan Dhami, BSc, MD,[c] Benjamin J. Chow, MD, FRCPC, FACC, FASNC,[a] Kathy J. Ascah, MD, FRCPC,[d] Jean N. DaSilva, PhD,[a,b] and Rob S. Beanlands, MD, FRCPC, FACC[a,b]

From the National Cardiac PET Centre, Division of Cardiology (Department of Medicine),[a] University of Ottawa Heart Institute, Ottawa, ON, Canada; Department of Cellular and Molecular Medicine,[b] and Faculty of Medicine,[c] University of Ottawa, Ottawa, ON, Canada; Echocardiography Laboratory, Division of Cardiology,[d] University of Ottawa Heart Institute, Ottawa, ON, Canada

Received for publication Jun 24, 2009; final revision accepted Dec 19, 2009.

Miran Kenk was supervised by Jean N. DaSilva; Karan Dhami was supervised by Rob S. Beanlands; James T. Thackeray was co-supervised by Jean N. DaSilva and Rob S. Beanlands.

The study was supported in part by the Heart and Stroke Foundation of Ontario (HSFO) Program Grant on Molecular Function and Imaging (Grant #PRG6242) and a Canadian Institutes of Health Research (CIHR) grant FRN78520. B.J. Chow was supported by a CIHR New Investigator Award #MSH-83718. J.T. Thackeray was supported by a PhD Ontario Graduate Scholarship in Science and Technology. S.L. Thorn was supported by a PhD Ontario Graduate Scholarship. K. Dhami was supported by a University of Ottawa summer studentship funded from the HSFO and Canadian Institute for Health Research. R.S. Beanlands is a Career Investigator supported by the Heart and Stroke Foundation of Ontario.

**Contributions of authors**

Experiments described in this manuscript were designed and executed by myself, in collaboration with PhD candidates James Thackeray and Stephanie Thorn, with guidance and supervision by Drs. Robert Beanlands and Jean DaSilva. The medical student Karan Dhami participated in the execution of the experiments and helped with the interpretation of the data. Dr. Benjamin Chow provided the clinical perspective on the problem of ADR cardiotoxicity, and helped with the experimental design. Dr. Kathy Ascah guided the acquisition and interpretation of echocardiographic data.

**Abstract**

*Background.* Altered sympathetic nervous system signaling is known to play a role in the cardiotoxicity of the anthracycline chemotherapeutic agents, but the interaction of pre- and postsynaptic function is not well understood.

*Methods and Results.* Our aim was to study the noradrenergic signaling in an established rat model of adriamycin cardiotoxicity (15 mg/kg administered i.p. over 2 weeks) using radiotracers having potential applicability for imaging with positron emission tomography (PET). Ex vivo biodistribution was performed 1 and 3 weeks post-adriamycin treatment with the noradrenaline analogue [$^{11}$C]*meta*-hydroxyephedrine ([$^{11}$C]HED), β-adrenergic receptor antagonist [$^{3}$H]CGP12177, and phosphodiesterase-4 inhibitor (*R*)-[$^{11}$C]rolipram. Cardiac function (echocardiographic parameters) and heart/body weight ratio were not affected. Myocardial retention of [$^{11}$C]HED, [$^{3}$H]CGP12177, and (*R*)-[$^{11}$C]rolipram were unchanged 1 week post-adriamycin. Compared to controls, 3 weeks post-treatment [$^{3}$H]CGP12177 uptake decreased (left ventricle free wall and septum; $P < 0.05$), while [$^{11}$C]HED and (*R*)-[$^{11}$C]rolipram uptake were unaffected. Following acute increase in myocardial noradrenaline levels with desipramine treatment, (*R*)-[$^{11}$C]rolipram retention increased in the left atrium, right ventricle, left ventricle free wall and septum ($P < 0.05$) in vehicle-, but not adriamycin-treated animals.

*Conclusion.* Our results suggest that adriamycin-induced toxicity exhibits no change in presynaptic noradrenaline uptake, but decreased β-adrenergic receptors in cardiac tissues, supporting a role for PET imaging of noradrenaline signaling in the study of anthracycline cardiotoxicity. (J Nucl Cardiol 2010)

Key Words: Positron emission tomography tracers · myocardium · adriamycin, rolipram · CGP 12177 · meta-hydroxyephedrine · cAMP

## INTRODUCTION

Adriamycin (doxorubicin, ADR) is an anthracycline chemotherapeutic agent used in treatment of leukemias, lymphomas, and a number of solid tumours (Minotti et al., 2004). Its application is limited by the severe cardiac side effects occurring at cumulative doses exceeding 550 mg/m$^2$ (Lefrak et al., 1973; Minotti et al., 2004). The congestive heart failure that develops is characterised by hypotension, tachycardia, decreased QRS voltage and cardiac dilatation, culminating in ventricular failure that can be refractory to inotropic drugs and mechanical circulatory assistance (Singal et al., 1987; Weinberg and Singal, 1987; Minotti et al., 2004). Despite numerous techniques proposed to detect biochemical, neurohormonal, anatomical, and functional changes associated with ADR treatment, cardiac tissue biopsy remains the most accurate means of diagnosing early toxicity (Bristow et al., 1981; Panjrath and Jain, 2006; Dranitsaris et al., 2008). At present no reliable noninvasive method exists for assessing ADR-induced cardiac damage before the critical ADR dose is reached and the irreversible cascade of rapid myocardial deterioration is initiated. The heterogeneity of the patient response to ADR observed in the clinical setting necessitates improved noninvasive techniques for early detection of cardiotoxicity (Bristow et al., 1981; Marchandise et al., 1989; Dranitsaris et al., 2008).

The molecular mechanism of ADR cardiotoxicity is not well understood, but is believed to involve free radical formation, apoptosis, defects in intracellular iron transport and altered myocardial energy metabolism (Singal et al., 1987; Beanlands et al., 1994; Minotti et al., 2004; L'Ecuyer et al., 2006; Tokarska-Schlattner et al., 2006). ADR administration has also been associated with altered adrenergic signaling in the heart, with separate studies identifying changes in noradrenaline (NA) levels (Tong et al., 1991;

Nousiainen et al., 2001), presynaptic NA uptake-1 transporter (NAT) function (Kawada et al., 2000), and postsynaptic β-adrenergic receptor (β-AR) density (Yoshikawa et al., 1994; Kizaki et al., 2004). However, a comprehensive evaluation of these different levels of sympathetic nervous system (SNS) signaling has not been conducted. In addition, there is limited data on alterations in postsynaptic neurohormonal signalling that follows stimulation of surface β-AR and how these changes impact downstream second messenger systems such as cAMP.

We have recently developed and evaluated the radiolabelled phosphodiesterase-4 (PDE4) inhibitor (*R*)-[$^{11}$C]-rolipram (Lourenco et al., 2006; Kenk et al., 2007). This tracer provides an index of cAMP activity and as such, a means to evaluate cAMP-mediated signaling in the heart. Distribution of the β-adrenergic antagonist [5,7-$^{3}$H]CGP12177 reflects β-adrenergic receptor density in the heart (van Waarde et al., 1992). [$^{11}$C]*meta*-Hydroxyephedrine ([$^{11}$C]HED) is a NA analogue commonly used in cardiac positron emission tomography (PET) studies to evaluate NA function and SNS innervation (Raffel and Wieland, 2001), with demonstrated potential in small animal cardiac imaging (Tipre et al., 2008). Cardiac [$^{11}$C]HED retention has been shown to be inversely modulated by NA (deGrado et al., 1993; Raffel and Wieland, 2001; Thackeray et al., 2007).

Our objective was to characterize the early alterations in SNS signaling in a model of ADR-induced cardiotoxicity that precedes physiological manifestations of cardiac dysfunction. This study explored alterations in NA signaling associated with ADR-induced cardiotoxicity at presynaptic (NA reuptake), postsynaptic (adrenergic receptors), and intracellular second messenger (PDE4) sites.

## METHODS

### Animals

Male Sprague-Dawley rats (Charles River, Montreal, Canada) initially weighing 200-275 g were maintained on a 12-h light/dark cycle with free access to food and water. All animal experiments described herein were conducted according to the guidelines of the University of Ottawa Animal Care Committee and the Canadian Council on Animal Care for the use and care of laboratory animals.

### ADR Treatment

Adriamycin (doxorubicin·HCl, Pharmacia Canada Inc., Mississauga, Ontario) was administered by six i.p. injections of 2.5 mg/kg each over 14 days, for a cumulative dose of 15 mg/kg. This model has been widely applied to induce ADR cardiotoxicity (Weinberg and Singal, 1987; Tong et al., 1991; Li et al., 2000; Ohkura et al., 2003). Control rats were injected with equivalent volumes of 0.9% saline solution. Injection site was observed during and following ADR administration to monitor for local tissue necrosis that could result from ADR extravasation.

### Materials

[$^{11}$C]HED radiosynthesis (specific activity 13.3-21.7 GBq/μmol; 359.5-586.5 mCi/μmol) was carried out according to the methods described by Rosenspire et al (Rosenspire et al., 1990) and routinely used for clinical studies (Link et al., 2003). (*R*)-[$^{11}$C]Rolipram (specific activity 19.7-64.9 Gbq/μmol; 532-1754 mCi/μmol) was synthesized as previously described.(DaSilva et al., 2001) Tritiated radiotracer [5,7-$^{3}$H](-

)CGP12177 (specific activity 33 mCi/μmol) was purchased from Perkin Elmer (Boston, MA).

**Echocardiography**

The VisualSonics Vevo 770 high-resolution imaging system was used to evaluate cardiac function before ADR treatment (baseline), and at 1 and 3 weeks following the last ADR injection. Rats were anaesthetised with 1-2% isoflurane. Parasternal long and short axis views were recorded in B- and M-mode using a 710B scanhead (VisualSonics, Toronto, Ontario) at the transducer frequency of 37.5 MHz (70 μm axial resolution, 15 mm focal length, and 20 mm field of view). Heart rate was recorded during the image acquisition.

M-mode still images were used to measure left ventricle internal diameter (left ventricle diastolic and systolic dimensions; LVDD and LVSD), left ventricle posterior wall (LVPW), and intra-ventricular septum (IVS) thickness at end diastole and peak systole. These dimensions were used to calculate the left ventricular volume in diastole and systole (LVDV, LVSV), stroke volume (SV), ejection fraction (EF), fractional shortening (FS), and left ventricular mass (LV mass) as follows:

$$LVDV = (7/(2.4+LVDD)) \times LVDD^3$$

$$LVSV = (7/(2.4+LVSD)) \times LVSV^3$$

$$SV = LVDV - LVSV$$

$$EF = ((LVDV - LVSV)/LVDV) \times 100\%$$

$$FS = ((LVDD - LVSD)/LVDD) \times 100\%$$

$$LV\ mass = 1.053 \times (((LVDD + LVPW + IVS)^3) - LVDD^3$$

**Biodistribution Studies**

Biodistribution studies were performed 1 and 3 weeks following the last ADR injection. On the day of the experiment, conscious rats were administered [$^{11}$C]HED (62.9-74.0 MBq (1.7-2.0 mCi); 0.52-1.00 μg of cold mass injected) co-injected with [$^{3}$H]CGP12177 (0.3 MBq (8 μCi); 6.8 ng of cold mass) or (*R*)-[$^{11}$C]rolipram (48.1-55.5 MBq (1.3-1.5 mCi); 0.20-0.78 μg of cold mass) dissolved in approximately 0.2 mL of saline via a tail vein. Animals were sacrificed by decapitation 30 minutes following [$^{11}$C]HED/[$^{3}$H]CGP12177 or 45 minutes following (*R*)-[$^{11}$C]rolipram. A blood sample was collected from the trunk into a heparinized tube and tissues quickly removed. The heart was dissected into right and left atria, right and left ventricle free wall (RA, LA, RV, LV) and intra-ventricular septum. A sample of the skeletal muscle (quadriceps) was also removed. All tissues were washed in saline, blotted and counted (decay-corrected) in a Packard Cobra II gamma-counter (Perkin Elmer, Boston, MA) with aliquots of the injected solution as standards and then weighed. Radioactivity retained is expressed as percent of injected dose per gram of tissue (%ID/g).

For tritiated radiotracers, tissue retention was quantified using scintillation techniques following solubilization and decoloration.(van Waarde et al., 1992)Tissue samples (approximately 0.1 g) were solubilized using NCS-II tissue solubilizer (Amersham Biosciences; incubation with shaking for 4 h at 50°C), and the resulting solution decolorized using isopropanol and hydrogen peroxide (30°C for 30 minutes). Glacial acetic acid (60 μL) was added to counteract chemiluminescence. Following addition of 10 mL of scintillation fluid (Biodegradable Counting Scintillant, Amersham

Biosciences), radioactivity was counted in a liquid scintillation counter (1219 RackBeta, LKB Wallac), and expressed as tissue uptake ((cpm recovered/g tissue)/(cpm injected/body weight)).

**Post-DMI studies**

To evaluate responsiveness at the PDE4 level to acutely increased NA, a subgroup of ADR- and vehicle-treated rats were administered desipramine·HCl (DMI, 20 mg /kg; Sigma-Aldrich Inc, St Louis, MO) i.p., 3 h prior to (*R*)-[$^{11}$C]rolipram injection. Tracer administration and tissue processing were performed as described above.

**Statistical Analysis**

All data are expressed as mean ± standard deviation. [$^{11}$C]HED, [$^{3}$H]CGP12177 and (*R*)-[$^{11}$C]rolipram data were compared using one-way ANOVA to detect differences between ADR-treated and control groups. The *P* values of individual tests were adjusted for multiple comparisons using the Bonferroni method. All tests used $P < 0.05$ for the critical value of statistical significance.

## RESULTS

**Animals**

ADR-treated animals showed virtually no weight gain during the 14 days of treatment (Figure 5-1; days 0–14), with some recovery in body weight after the last injection. Earliest mortality was observed 2 days following last ADR injection, with 7%

of the animals lost by 1 week and 33% by 3 weeks. At 3 weeks post-ADR, rats exhibited piloerection, ungroomed appearance, pale skin, and large volumes of ascites.

**Physiological Indices**

Echocardiographic studies showed no difference in ejection fraction or fractional shortening between ADR-treated rats and controls at baseline, 1 and 3 weeks following drug administration (Table 5-1). No difference in heart rate was observed between ADR- and saline-treated rats. Whole heart weights of ADR-treated rats were significantly smaller than those of control animals on postmortem analysis. Heart weight to body weight ratios were not different (Table 5-2).

**Biodistribution Studies**

*[$^{11}$C]HED*: A general trend towards an increase was observed at 1 week post-ADR in cardiac tissues, without reaching significance ($P$ values of 0.032, 0.077, 0.010, 0.071, 0.192 in RA, LA, RV, LV, and septum, respectively, with the critical value of statistical significance adjusted for this multiple comparison being $P < 0.006$). [$^{11}$C]HED uptake was similar between treated and untreated rats at 3 weeks following ADR (Figure 5-2).

*[$^{3}$H]CGP12177*: Compared to controls, treatment with ADR significantly decreased the retention of [$^{3}$H]CGP12177 in cardiac regions, reaching statistical significance in the LV and septum ($P < 0.006$), with a trend toward significance in the RA, LA, and RV ($P$ values of 0.030, 0.080, and 0.020, respectively) at 3 weeks post-ADR, but not at the earlier time point (Figure 5-3).

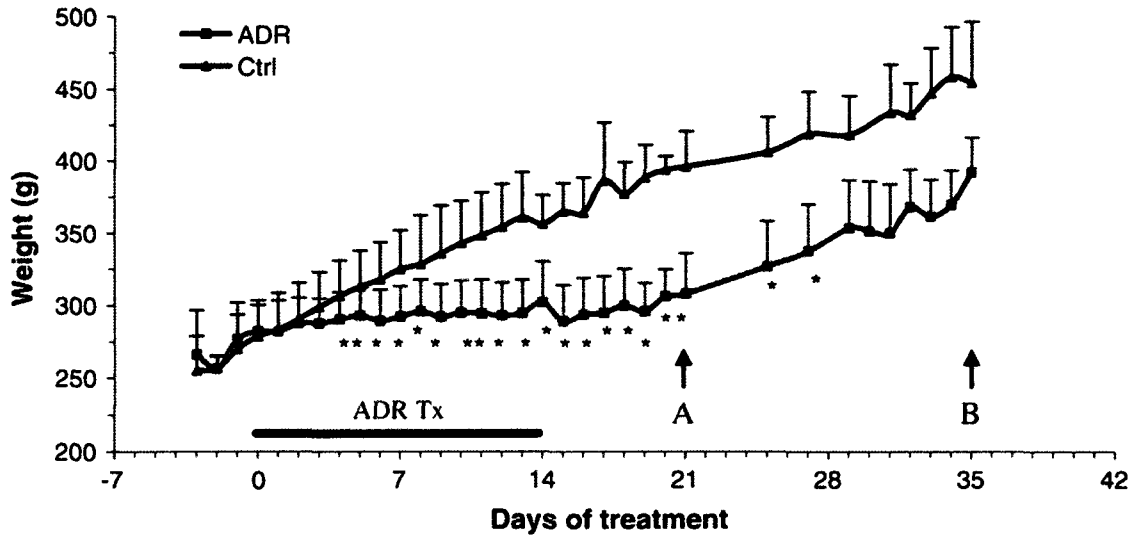


Figure 5-1: Weights of ADR- and vehicle-treated rats over the duration of the experiment. Day 0 represents the first ADR injection. ADR was administered in six i.p. injections over 2 weeks, with echocardiography and tracer distribution evaluated 7 (point A) or 21 days (point B) following last ADR injection. -3 to 21 days of treatment: ADR $n$ = 43, controls $n$ = 24; 21-35 days: ADR $n$ = 15, controls $n$ = 12. *$P$ < 0.05. One-way ANOVA compared to saline-treated controls.

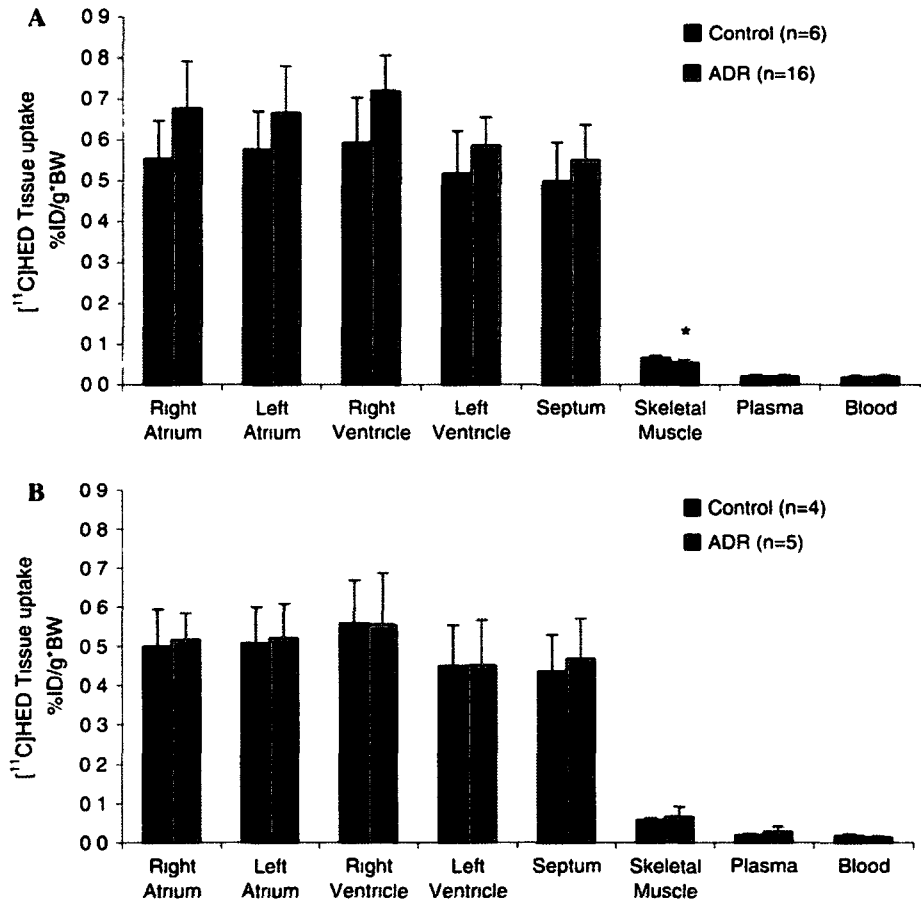


Figure 5-2: [$^{11}$C]HED retention 30 minutes following radiotracer administration is unchanged in cardiac tissues and decreased in the skeletal muscle 1 week (**A**) and unchanged 3 weeks post-ADR (**B**) in comparison to the saline-treated controls. *$P < 0.05$. One-way ANOVA compared to saline-treated controls.

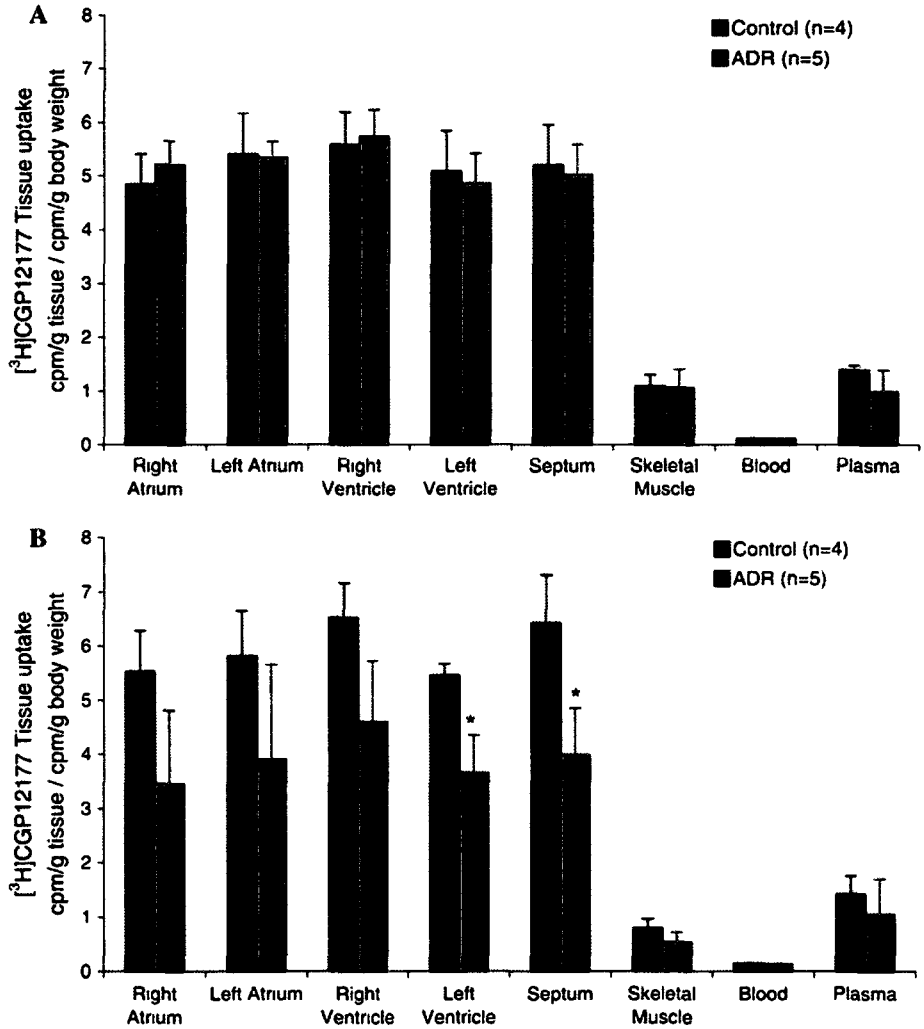


Figure 5-3: [$^3$H]CGP12177 retention 30 minutes following tracer administration is unchanged 1 week (**A**) and significantly decreased in the LV and septum (**B**) 3 weeks following ADR treatment, in comparison to the saline-treated controls. $*P < 0.05$. One-way ANOVA compared to saline-infused controls.

Table 5-1: Echocardiography results

| | LV Vol; d (μL) | LV Vol; s (μL) | SV (μL) | % EF | % FS | LV mass (mg) | HR (bpm) |
|---|---|---|---|---|---|---|---|
| Baseline (n = 37) | 209.9 ± 43.9 | 48.0 ± 17.6 | 161.9 ± 39.3 | 76.8 ± 9.2 | 47.2 ± 7.8 | 577.0 ± 115.3 | 385.7 ± 23.8 |
| 1 Week | | | | | | | |
| Controls (n = 9) | 292.6 ± 66.3 | 66.4 ± 23.9 | 226.2 ± 52.8 | 77.3 ± 6.0 | 47.7 ± 6.0 | 949.9 ± 184.6 | 354.6 ± 35.2 |
| ADR (n = 15) | 258.7 ± 39.0 | 70.2 ± 22.4 | 188.5 ± 31.4 | 73.1 ± 7.2 | 43.7 ± 6.2 | 725.9 ± 237.5 | 345.7 ± 46.7 |
| 3 Weeks | | | | | | | |
| Controls (n = 4) | 350.6 ± 48.3 | 96.3 ± 39.6 | 254.3 ± 25.1 | 73.2 ± 8.7 | 44.3 ± 7.6 | 979.6 ± 170.1 | 342.0 ± 49.7 |
| ADR (n = 4) | 251.3 ± 39.2 | 56.0 ± 19.5 | 195.4 ± 25.6 | 78.1 ± 6.0 | 48.4 ± 6.2 | 758.5 ± 107.1 | 379.3 ± 23.5 |

* $P < 0.05$ using one-way ANOVA, compared to the baseline; ADR, Adriamycing; EF, ejection fraction; FS, fractional shortening; HR, heart rate

Table 5-2: Postmortem analysis of heart size.

| | **Heart weight (g)** | **Body weight (g)** | **Ratio ($\times 10^3$)** |
|---|---|---|---|
| 1 Week | | | |
| Controls (n = 10) | 1.06 ± 0.1 | 428.7 ± 47.8 | 2.48 ± 0.3 |
| ADR (n = 23) | 0.88 ± 0.1 * | 296.6 ± 22.8 * | 2.97 ± 0.3 |
| 3 Weeks | | | |
| Controls (n = 12) | 1.18 ± 0.1 | 449.6 ± 32.2 | 2.62 ± 0.2 |
| ADR (n = 15) | 0.93 ± 0.1 * | 365.3 ± 27.0 * | 2.55 ± 0.2 |

* $P < 0.05$ using one-way ANOVA analysis, compared to controls. *ADR*, Adriamycin.

*(R)-[$^{11}$C]Rolipram*: No difference in (*R*)-[$^{11}$C]rolipram uptake was observed between ADR-treated and control animals at 1 or 3 weeks post-treatment (Figure 5-4). DMI-stimulation elicited a significant increase in (*R*)-[$^{11}$C]rolipram uptake in control rats in the LA, RV, LV and septum ($p<0.05$), but not in ADR-treated animals 3 weeks following ADR administration (Figure 5-5).

## DISCUSSION

A cardiotoxic "threshold" has been postulated by Bristow et al, below which uninjured tissues can compensate and preserve normal cardiac contraction, with functional indices deteriorating rapidly once this critical degree of damage is surpassed (Bristow et al., 1981). Assessment of cumulative subclinical damage that precedes overt symptomatic congestive heart failure could be valuable in predicting the safe dose of anthracyclines on a patient-specific basis (Dranitsaris et al., 2008). In the early stages of ADR-induced heart failure, elevated catecholamine levels have been proposed to compensate for cytotoxic damage and maintain cardiac output (Thomas et al., 2004). With subthreshold myocardial toxicity that does not exhibit contractile dysfunction, only morphological studies (i.e., invasive tissue biopsy) or neurohormonal changes could predict outcome and guide the ADR chemotherapy (Bristow et al., 1981). In this study, despite the absence of any change in the echocardiography-measured physiological indices or relative heart size at 3 weeks post-ADR, we observed decreased postsynaptic β-AR measured using [$^{3}$H]CGP12177 and diminished responsiveness to acute elevations in NA levels measured using (*R*)-[$^{11}$C]rolipram with DMI pretreatment.

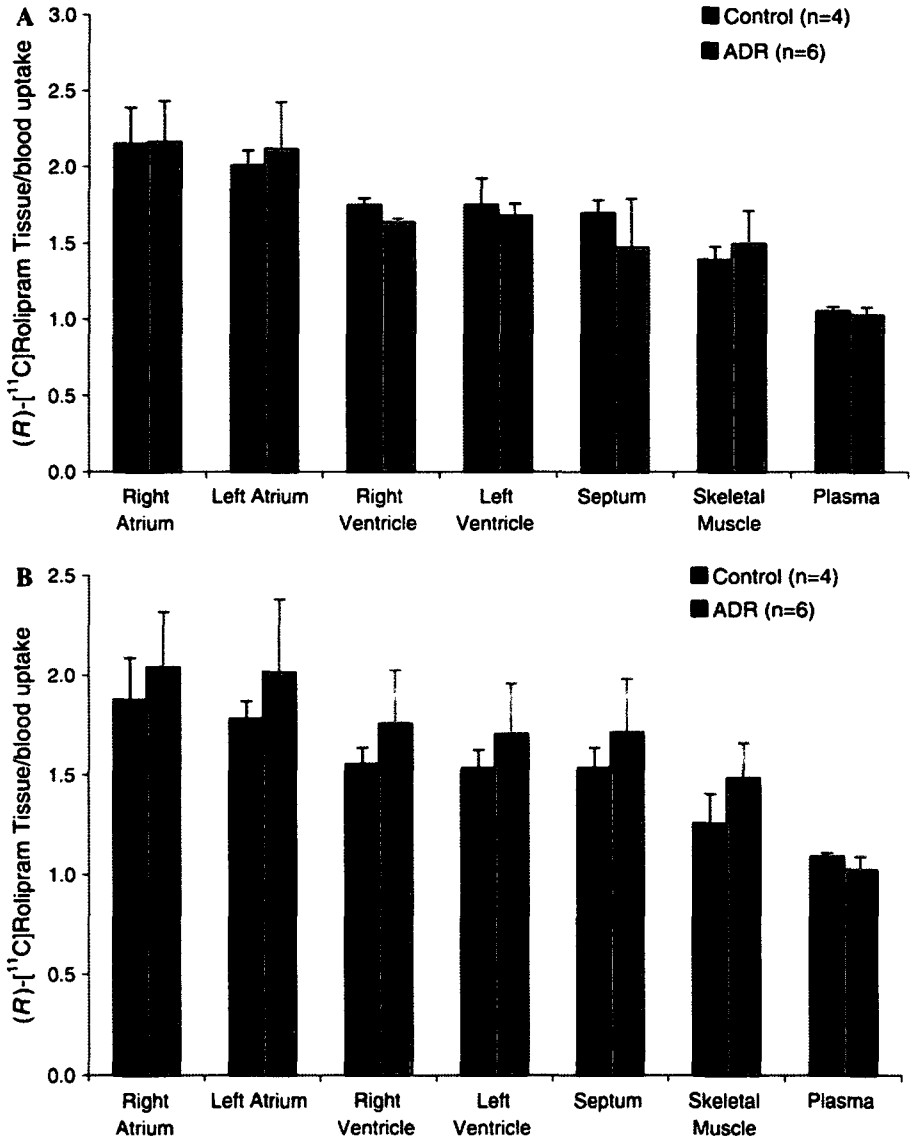


Figure 5-4: Retention of (*R*)-[$^{11}$C]rolipram 45 minutes following tracer administration is not altered by treatment with ADR, as assayed 1 (**A**) and 3 weeks (**B**) following last ADR injection.

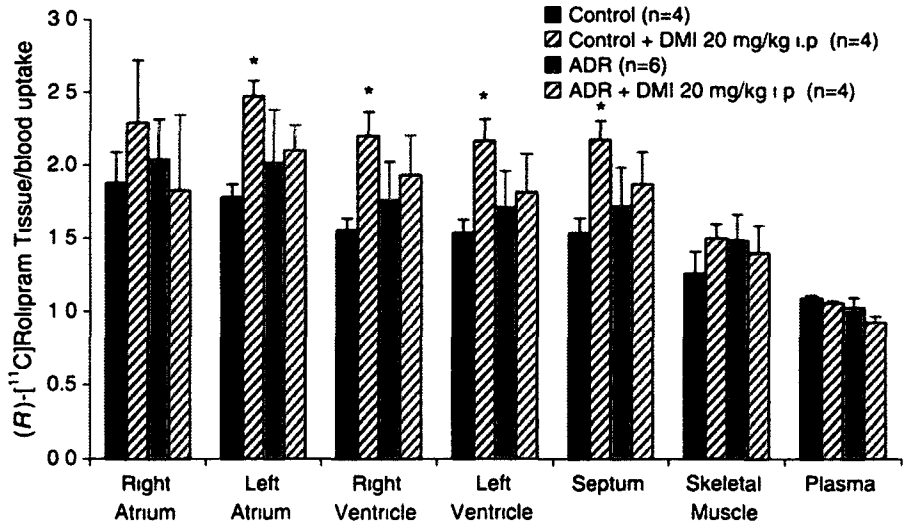


Figure 5-5: Three weeks following end of ADR treatment, the increase in (*R*)-[$^{11}$C]rolipram retention 45 minutes following radiotracer administration in response to DMI (20 mg/kg i.p., 3 h prior to radiotracer) is attenuated in the cardiac tissues in comparison to saline-treated animals. $^{*}P < 0.05$. One-way ANOVA compared to saline-treated controls, with Bonferroni post hoc correction for multiple comparisons.

The NA analogue and "false" neurotransmitter [$^{11}$C]HED is taken up into the presynaptic varicosity by NAT (uptake-1) and freely diffuses through the vesicles and plasma membrane back into the synaptic cleft (Raffel and Wieland, 2001). Its tissue uptake is therefore is therefore dependent on NAT expression (uptake-1), as well as on local NA levels (Thackeray et al., 2007). It is not susceptible to the metabolic breakdown that follows postsynaptic uptake (uptake-2) and terminates the presence of NA (Raffel and Wieland, 2001). While uptake-2 could affect NA-analogue tracers (Degrado et al., 1995), Tipre et al. (Tipre et al., 2008) have shown the kinetics of HED in rats to correspond to those observed in isolated hearts and in human clinical imaging. In our study, [$^{11}$C]HED retention showed a trend toward an elevation in the non-LV heart regions and was decreased in the skeletal muscle at 1 week post-ADR, but remained unchanged in all tissues at the 3 week time point. Therefore, despite an ~80% elevation in myocardial NA levels reported by Tong et al. (Tong et al., 1991) at the 3 week time point using an identical animal model, our results suggest that no presynaptic dysfunction can be detected using [$^{11}$C]HED at this 3 week stage in the progression of ADR cardiotoxicity. Studies with iodine-125-metaiodobenzylguanidine ($^{125}$I-MIBG), a NA and [$^{11}$C]HED analogue used in single photon emission computed tomography (SPECT) imaging, have shown no change in uptake after 3 weeks of ADR administration (2 mg/kg, once a week) and a decrease in uptake at 7 weeks, detected once the cardiac dysfunction is clearly observed (Wakasugi et al., 1992).

Published studies using alternative chronic ADR administration protocols have shown a decrease of approximately 20% in $\beta_1$-AR mRNA (Kizaki et al., 2004). Desensitization of β-AR has been previously shown following prolonged stimulation,

proceeding through receptor phosphorylation (short-term) and receptor downregulation through decreased expression (long-term) (Bristow et al., 1982; Hausdorff et al., 1990). Since previous studies have shown NA to be increased at 3 weeks post-ADR,(Tong et al., 1991) the diminished [$^{3}$H]CGP12177 binding likely reflects the downregulation of β-ARs. However, the hydrophilic nature of CGP12177 limits its binding to the receptors expressed at the cell membrane (Van Waarde et al., 1995), suggesting that the observed reduction in tracer retention reflects decreased cell surface receptor presence through both internalization and decreased expression.

(*R*)-[$^{11}$C]Rolipram retention and specific binding have been previously shown to increase by ~30% following acute elevation of synaptic NA levels through administration of reuptake inhibitor DMI (Lourenco et al., 2006). The observed increase in binding likely reflects elevated PDE4 expression (Engels et al., 1994; Manning et al., 1996) and phosphorylation, which increases the affinity of rolipram for PDE4 subtypes (Sette et al., 1994; Madelian and La Vigne, 1996). Baseline (*R*)-[$^{11}$C]rolipram uptake is not altered between control and ADR-treated rats. This finding may be explained by the opposing factors of increased NA levels and decreased surface β-AR balancing each other out and resulting in normal signaling output at the intracellular postreceptor level. Alternatively, one can speculate that compensatory factors such as adenylyl cyclase downregulation, decreased $G_s$ activity or increased $G_i$ activity following β2-AR stimulation may lead to cAMP levels and PDE4 activity and expression remaining unchanged at this point in the development of ADR cardiotoxicity at 3 weeks post-ADR (Calderone et al., 1991; Fu et al., 1994; Kizaki et al., 2004). Further experiments need to be performed to elucidate intracellular processes involved. In the current study, the diminished response to DMI

administration correlates with decreased [$^{3}$H]CGP12177 retention, as reduced surface β-AR presence potentially translates to decreased cAMP production.

Our findings with [$^{3}$H]CGP12177 can be translated into clinical studies using $^{11}$C-labelled CGP1277 and its isopropyl analogue CGP12388, developed for PET application (de Jong et al., 2005). While [$^{11}$C]HED and (*R*)-[$^{11}$C]rolipram could provide insight into the molecular alterations involved in ADR cardiotoxicity at later time points, [$^{11}$C]CGP12177 and related compounds hold promise for early detection of cardiotoxicity. Retention of these tracers could provide an in vivo index of cardiac β-AR expression and binding using serial noninvasive quantitative studies. Clinically, this information would be useful in directing ADR therapy, by detecting cardiotoxicity before it reaches levels that manifest physiologically. In vivo PET evaluation of β-AR expression and signaling could theoretically be used in other forms of heart failure. Further clinical studies are required in this regard.

Mortality observed in our study corresponds to the previously published losses with this model (30% reported by Tong and Ganguly) (Tong et al., 1991). Animals exhibited characteristics of ADR toxicity, with decreased body weight gain and ascites (Tong et al., 1991; Li et al., 2000).

**Study Limitations**

One potential limitation of this study is the lack of information on the cardiac flow kinetics in individual groups, which may play a role in the differences in tracer

uptake through the effect on the tracer extraction fraction. Additionally, caution should be exercised when extrapolating data on noradrenergic signalling from animal models, due to potential species differences in factors that drive catecholamine kinetics (Tipre et al., 2008). Pretreatment with DMI prior to (*R*)-[$^{11}$C]rolipram was only performed at 3 weeks following ADR administration. This DMI challenge was not performed at 1 week for logistical reasons, so we do not know if the alterations to second messenger response may have occurred earlier. Tissue NA levels were not measured as part of our experiments. Other groups have, however, quantified the myocardial NA levels with an identical disease model (Tong et al., 1991). No alterations in LV function were observed at the evaluated time points, preventing a direct correlation between changes in tracer retention and alterations in physiological parameters of LV performance. Previous studies have reported changes in LV ejection fraction following ADR treatment occurring at later time points (6 weeks) following the last injection (Ohkura et al., 2003). The 3 week protocol used here results in rapid and subacute toxicity, compared to the cardiac dysfunction that results from the human chemotherapy regimen, which progresses more slowly with weekly or less frequent ADR administration (Swain et al., 2003). Findings presented here warrant further investigation of neurohormonal PET imaging in patients being treated with anthracyclines.

## CONCLUSIONS

In an animal model, ADR-induced toxicity exhibits decreased postsynaptic β-AR assessed by [$^{3}$H]CGP12177, and impaired intracellular signalling response at the PDE4

level evaluated using (*R*)-[$^{11}$C]rolipram and DMI challenge. Reduced β-ARs and downstream impairment of second messenger signaling response appeared early in this ADR-toxicity model and may precede changes in LV function. The potential therefore exists for use of imaging with PET, particularly [$^{11}$C]CGP12177 derivatives and other β-AR tracers, to study the progression of ADR cardiotoxicity or other forms of heart failure.

**Acknowledgements**

The authors thank Samantha Mason, Jeffrey Collins, and Paul Colletta for their assistance in radiotracer production in the radiochemistry laboratory, Kathryn Williams for guidance in statistical analysis and Animal Care and Veterinary Staff for help with handling and monitoring of experimental animals.

# CHAPTER 6: MANUSCRIPT #5

Current Radiopharmaceuticals (To be submitted)

# PET measurements of cAMP-mediated phosphodiesterase-4 with (*R*)-[$^{11}$C]rolipram

Miran Kenk[1,2], Adam Thomas[1,2], Mireille Lortie[1], Rob deKemp[1,2], Rob S. Beanlands[1,2] and Jean N. DaSilva[1,2*]

[1]*National Cardiac PET Centre, Division of Cardiology, University of Ottawa Heart Institute, 40 Ruskin St., Ottawa, Ontario, Canada, K1Y 4W7*

[2]*Department of Cellular and Molecular Medicine, Faculty of Medicine, University of Ottawa, 451 Smyth Rd., Ottawa, Ontario, Canada, K1H 8M5*

*MK was supervised by JND*

The study was supported in part by the Canadian Institutes of Health Research (CIHR) grant FRN78520 and the Heart and Stroke Foundation of Ontario (HSFO) Program Grant on Molecular Function and Imaging (grant #PRG6242). R. S. Beanlands is a Career Investigator supported by the Heart and Stroke Foundation of Ontario.

* Address correspondence to this author at the:
Jean N. DaSilva, Ph.D.
Professor, Dept. of Medicine (Cardiology) and
Cellular and Molecular Medicine, University of Ottawa
Head, PET Radiochemistry, National Cardiac PET Centre,
University of Ottawa Heart Institute
40 Ruskin Street, Ottawa, Ontario, Canada, K1Y 4W7
Tel.: 1 613 798 5555 (ext 19704); fax: 1 613 761 5406
*E-mail address:* jdasilva@ottawaheart.ca

**Contribution of authors**

I performed the literature review and wrote the manuscript, with editing help and corrections from Dr. Jean DaSilva and Adam Thomas. Drs. Rob de Kemp and Mireille Lortie provided input on the kinetic modeling and occupancy portions of the manuscript, with Dr. Robert Beanlands' guidance on PET imaging and clinical applications. This review will be submitted to the Current Radiopharmaceuticals.

**ABSTRACT**

Cyclic adenosine monophosphate (cAMP) is the common second messenger in signal-transduction cascades originating at a number of monoamine receptors involved in neurotransmission, cardiac function and smooth muscle contraction. Altered regulation of cAMP synthesis (at receptors, G-protein subunits or adenylyl cyclase) and breakdown (phosphodiesterase (PDE)) has been implicated in a number of pathologies. The PDE4 inhibitor (*R*)-rolipram, and the less active (*S*)- enantiomer, have been labeled with carbon-11 and characterized by in vivo and in vitro experiments for use in the evaluation of altered PDE4 levels in the brain and cardiac tissues. (*R*)-[$^{11}$C]Rolipram has been shown to bind selectively to PDE4 over other PDE isozymes, with specific binding reflecting approximately 80 and 40% of the total detected radioactivity in the brain and the heart, respectively. Tracer retention in PDE4-rich tissues is increased by cAMP-elevating treatments, as detected by in vivo PET studies and ex vivo biodistribution experiments. In vivo PET imaging studies display strong region-specific signal in the brain and heart, as evaluated in rats, pigs, monkeys and humans. Reduced noradrenaline-mediated signal transduction was observed in animal models of obesity and anthracycline-induced cardiotoxicity using (*R*)-[$^{11}$C]rolipram. Given the critical role of cAMP at the intersection of multiple hormonal pathways, with a good safety profile and well-characterized pharmacokinetics, (*R*)-[$^{11}$C]rolipram PET imaging provides a novel tool for serial monitoring of cAMP-mediated signaling at the PDE4 level, yielding insight into pathological progression with potential for directing therapy.

**Keywords:** cyclic adenosine-monophosphate, phosphodiesterase-4, positron emission tomography tracers, rolipram.

## ABBREVIATIONS AND ACRONYMS

| | |
|---|---|
| $^{11}$C | carbon-11 |
| $^{18}$F | fluorine-18 |
| $^{13}$N | nitrogen-13 |
| AC | adenylyl cyclase |
| β-AR | β-adrenergic receptor |
| BDNF | brain-derived neurotrophic factor |
| cAMP | cyclic adenosine-monophoshpate |
| cGMP | cyclic guanosine-monophosphate |
| CRE | cyclic adenosine-monophosphate response element |
| CREB | cyclic adenosine-monophosphate response element binding protein |
| DPBB | 12-deoxyphorbol 13-isobutyrate-20-butyrate |
| DAG | diacetylglycerol |
| DV | distribution volume |
| $ED_{50}$ | effective dose eliciting 50% of maximal response |
| ERK | extracellular signal-regulated kinase |
| GPCR | G protein-coupled receptor |
| $IP_3$ | inositol trisphosphate |
| HARBS | high-affinity rolipram binding site |
| HPLC | high-performance liquid chromatography |
| IBMX | 3-isobutyl-1-methylxanthine |
| LAH | lithium aluminium hydride |
| LARBS | low-affinity rolipram binding site |

| | |
|---|---|
| MBP-C | myosin binding protein C |
| NA | noradrenaline |
| PDE | phosphodiesterase |
| PET | positron emission tomography |
| $PIP_2$ | phosphatidylinositol 4,5-bisphosphate |
| PKA | protein kinase A |
| PKC | protein kinase C |
| PLB | phospholamban |
| PLC | phospholipase C |
| RT-PCR | real-time polymerase chain reaction |
| RyR | ryanodine receptor $Ca^{2+}$ channel |
| SERCA | sarcoplasmic reticulum calcium pump |
| TBAOH | tetrabutylammonium hydroxide |
| UCR | upstream conserved region |

# INTRODUCTION

## Cyclic adenosine monophosphate signaling

Second messengers cyclic adenosine monophosphate (cAMP) and cyclic guanosine monophosphate (cGMP) transmit and modulate the extracellular signal from the plasma membrane G protein-coupled receptors (GPCRs) to the intracellular effector proteins (Beavo and Brunton, 2002). cAMP was first discovered in 1957 as the second messenger to the hormone adrenaline and has since been identified as a key component of the intracellular signal-transduction of the dopamine, serotonin and histamine receptors (Bristow et al., 1989; Beavo and Brunton, 2002). At the molecular level, agonist binding to the cell surface receptor detaches the G protein $\alpha_S$ subunit, which stimulates the adenylyl cyclase (AC) to increase cAMP production. Activation of receptors coupled to the inhibitory $\alpha_i$ subunit, such as $\beta_2$-AR, decrease the activity of AC upon activation and reduce cAMP levels.

Elevated cAMP levels cause the catalytic subunit of the protein kinase A (PKA) to disassociate from the regulatory subunit and phosphorylate intracellular effector proteins (Beavo and Brunton, 2002). For example, in the brain, activation of cAMP-response element (CRE) transcription factor by the PKA-phosphorylated CRE binding protein (CREB) is considered to be a major component of cAMP-mediated antidepressant effects (Thome et al., 2000; Tardito et al., 2006). CRE activation modulates the transcription of more than 100 genes, including brain-derived neurotrophic factor (BDNF), anti-apoptotic protein Bcl-2 and other proteins involved in neural growth and plasticity (Tardito et al., 2006) (Figure 6-1A). Conversely, in the myocardium, activation of PKA following β-AR stimulation modulates the L-type $Ca^{2+}$ channels, the ryanodine

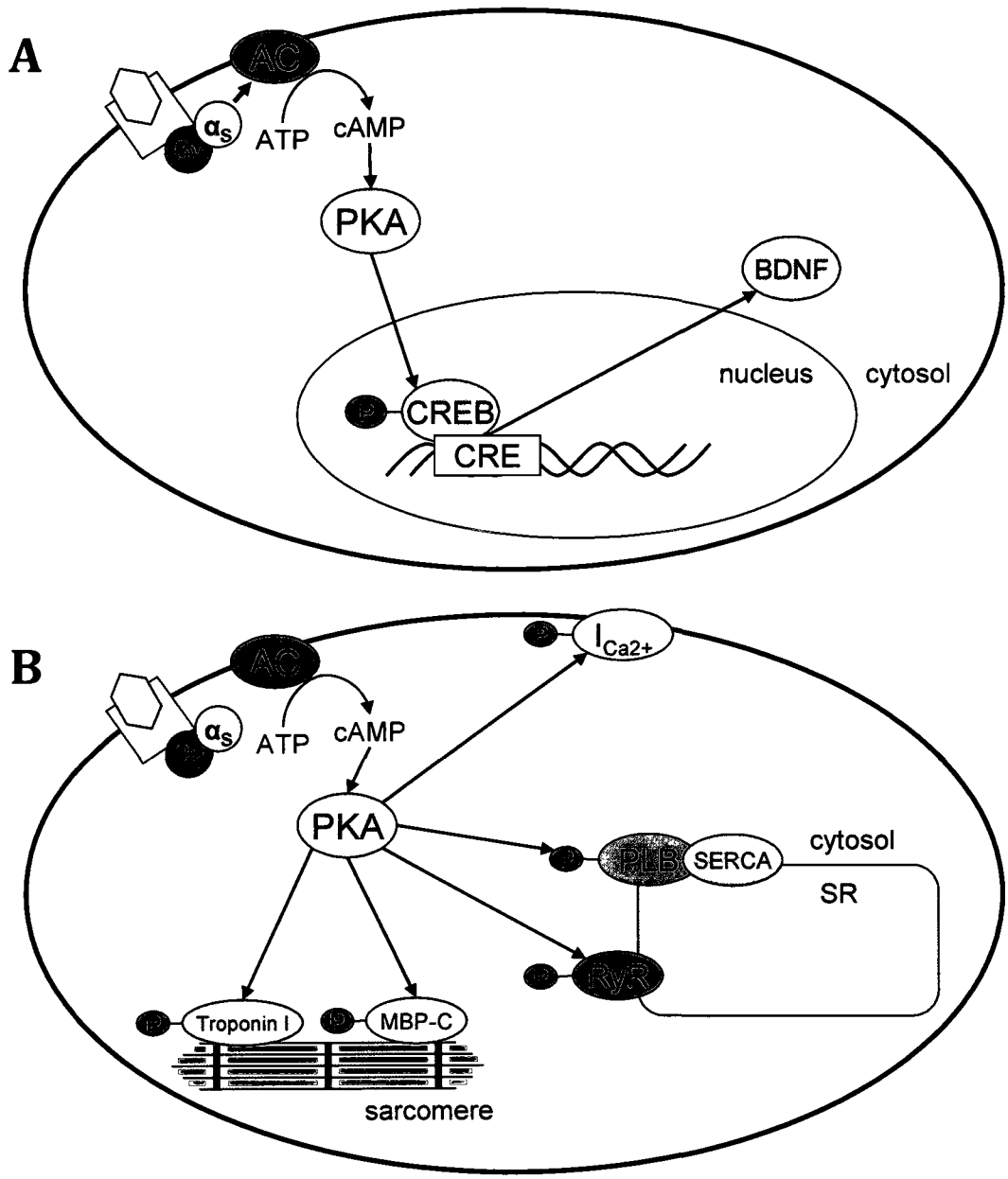
A
AC
$\alpha_s$
ATP
cAMP
PKA
BDNF
nucleus
cytosol
CREB
CRE
B
$I_{Ca2+}$
AC
$\alpha_s$
ATP
cAMP
PKA
PLB
SERCA
cytosol
SR
RyR
Troponin I
MBP-C
sarcomere

Figure 6-1: cAMP 2$^{nd}$ messenger signaling in a neuron (A) and cardiomyocytes (B), showing examples of intracellular effector proteins. Activation of a GPCR causes stimulation of AC-mediated cAMP generation, increasing intracellular levels. cAMP elevation stimulates protein kinase A (PKA) activity. In the neuron, phosphorylation of cAMP response-element binding protein (CREB) in the nucleus stimulates transcription of genes that affect cell plasticity and growth. In the cardiomyocytes, PKA activation results in increased influx of $Ca^{2+}$ through activation of $Ca^{2+}$ channels on the plasma membrane ($I_{Ca2+}$) and the ryanodine receptors $Ca^{2+}$ channels (RyR) on the sarcollemal reticulum. Phosphorylation of the phospholamban (PLB) removes sarco/endoplasmic reticulum $Ca^{2+}$-ATPase (SERCA) inhibition, increasing $Ca^{2+}$ influx into the cytosol. Additionally, phosphorylation of the troponin and myosin binding protein C (MBP-C) increases efficiency of contraction by sensitizing the sarcomere proteins to $Ca^{2+}$.

receptors $Ca^{2+}$ channels (RyR), troponin I, myosin binding protein C (MBP-C) and phospholamban (PLB) among other effectors. Ultimately, cAMP-mediated cardiac PKA activation affects $Ca^{2+}$ influx into the cytosol, thereby increasing the strength of cardiomyocytes contraction (Figure 6-1B). Physiologically, tissue-dependent modulation of cell function implicates cAMP in the control of processes ranging from thermogenesis to memory formation, with abnormal levels and responsiveness associated with pathological states (Yoshida et al., 2001).

**Phosphodiesterase enzyme superfamily**

Phosphodiesterase (PDE) enzymes terminate the cAMP and cGMP signal by catalyzing the second messengers to their respective inactive 5'-adenosine monophosphate derivatives in a process dependent on the presence of cofactors $Zn^{2+}$ or $Mg^{2+}$ (Liu et al., 2001; Laliberte et al., 2002; Zhao et al., 2003). Genetically, this protein family is highly conserved through evolution, attesting to its physiological importance (Davis et al., 1989; Beavo, 1995; Conti and Jin, 1999; Conti and Beavo, 2007). Twenty-one genes encoding approximately 50 different phosphodiesterase enzyme isoforms are grouped into 11 subfamilies (PDE1-11) according to amino acid sequence, kinetic properties and regulatory profile (Houslay and Adams, 2003; Wong et al., 2006; Esposito et al., 2009; Zhang, 2009). PDE4, 7 and 8 subfamilies exhibit specificity for cAMP, while PDE5, 6 and 9 are cGMP-specific and PDE1, 2, 3, 10 and 11 hydrolyze both cyclic nucleotides with equal affinity (Torphy, 1998; Conti and Jin, 1999; Houslay and Adams, 2003). PDE isozymes are distributed throughout the body, playing a part in physiological processes including vision (PDE6) (Lamb and Pugh, 2006), olfaction (PDE4) (Borisy et

al., 1993), penile erection (PDE5) (Moreland et al., 1998), airway constriction (PDE4) (Sturton and Fitzgerald, 2002), memory formation (PDE2 and PDE4) (Barad et al., 1998; Monti et al., 2006; Reneerkens et al., 2009), cardiac contractility (PDE3 and PDE4) and inflammation (PDE4) (Barnette et al., 1998).

**Phosphodiesterase-4 enzymes**

One of the most studied PDE subfamilies are the PDE4 isozymes, which have been a target of pharmacological interventions in treatment of major depression (Zeller et al., 1984; Bertolino et al., 1988) and asthma (Houslay et al., 2005), as well as, more recently, a target in genetic association studies linking PDE4 with ischemic stroke (Gretarsdottir et al., 2003). Four genes (PDE4A, PDE4B, PDE4C and PDE4D) encode over 20 isoforms (Rao and Xi, 2009), classified by structure as long, short and super-short depending on the presence of upstream conserved regions (UCR1 and UCR2) flanking a common catalytic site (Figure 6-2). All PDE4 isozymes break down cAMP with a $K_m$ of ~1 μM (Houslay et al., 1997) at the catalytic site located in a conserved region of 270-300 amino acids (Beavo, 1995; Conti and Jin, 1999). The uniqueness of individual isozymes arises from their N-terminus regions, leading to distinct regulation, intracellular localization and interactions with specific proteins (Houslay et al., 2007).

A major and relatively recent addition to the understanding of cAMP signaling and the role of PDE isozymes is the concept of cAMP signal compartmentalization. Intracellular localization of cAMP effects is achieved through the sequestering of AC-mediated cAMP generation and its breakdown (by PDE enzymes) to distinct cellular compartments, forming intracellular gradients of cAMP concentration (Jin et al., 1998; Zaccolo and

Pozzan, 2002; Terry et al., 2003; Houslay et al., 2007). Initially, the large number of PDE4 subtypes was believed to facilitate differential regulation of short and long isoforms, however, it is now known that the differences in isozymes relate to intracellular modulator protein interactions with PDE leading to precise regulation of pools of cAMP around sites such as β-ARs or RyR (Perry et al., 2002; Baillie et al., 2003; Bolger et al., 2003; Lynch et al., 2005). As an example, the N-terminal domain of PDE4A4 (and its rodent equivalent, PDE4A5) dictates redistribution of the enzyme intracellularly when exposed to inhibitors Ro 20-1724 and RS25344 (Terry et al., 2003). Most PDE4 subtypes are capable of interacting with β-arrestin, which provides dynamic regulation of the cAMP signal initiated by β-AR activation, in parallel with the modulation of adrenergic sensitivity by the processes of receptor internalization and downregulation (Perry et al., 2002; Lynch et al., 2005).

**PDE4 expression**

PDE4 expression is ubiquitous throughout a variety of organs, with the greatest levels observed in the brain, heart, lung and skeletal muscle (McLaughlin et al., 1993; Engels et al., 1994; Houslay et al., 1998). Real-time polymerase chain reaction (RT-PCR) studies quantifying mRNA expression have detected all four PDE4 subtypes in human brain, liver, lung, kidneys and hearts (Engels et al., 1994; Engels et al., 1995). Heterogeneous PDE4 expression within the human and rat brain was reported, with the regions of the cerebral cortex, the olfactory system, cerebellum, striatum and the hippocampus exhibiting high PDE4 mRNA and protein levels (Kaulen et al., 1989; Engels et al., 1994; Engels et al., 1995; Shakur et al., 1995; Iwahashi et al., 1996; Zhang

et al., 1999; Farooqui et al., 2000; D'Sa et al., 2005; Richter et al., 2005; Dlaboga et al., 2008).

Species differences have been reported in the PDE4 mRNA levels, with different relative expression of PDE4 isozymes in the brain and heart detected in rats, compared to human tissue (Engels et al., 1994; Bian et al., 2004). Additionally, the overall PDE4 mRNA expression in most rat tissues is higher than in humans (Bian et al., 2004). While the relative tissue expression and importance of individual subtypes is still contentious, it has been established that PDE4A, B and D are present in the rat brain (Bolger et al., 1994; Iona et al., 1998; Takahashi et al., 1999) and heart (Engels et al., 1994; Kostic et al., 1997; Takahashi et al., 2002; Abi-Gerges et al., 2009) tissues with minimal expression of PDE4C in those two organs.

**PDE4 regulation**

PKA-mediated phosphorylation increases PDE4 activity within 15 minutes of elevated cAMP levels, as evidenced by the ability of the PKA inhibitor H89 to block increases in enzyme activity (Chang et al., 1997). Phosphorylation of the PDE4 enzyme at the Ser-54 residue in the UCR1 region of the long isoforms (Figure 6-3) results in the disruption of a hydrogen bond and placement of a negative charge at that position, putting the enzyme in the high activity form (Sette and Conti, 1996; Hoffmann et al., 1998; Torphy, 1998; Liu and Maurice, 1999). This phosphorylation was observed to affect only the long forms of the PDE4 isozymes (Richter et al., 2005), since the shorter isoforms lack the relevant UCR1 region. In addition to increased catalytic activity, PKA-phosphorylated PDE4 has been shown to exhibit increased affinity for the inhibitor

rolipram ((*R/S*)-4(3-cyclopentyloxy-4-methoxyphenyl)-2-pyrrolidone; Figure 6-4), with the $IC_{50}$ values decreased 6-15 times upon phosphorylation (0.68 μM to 0.11 μM with PDE4D3; 123 nM to 8 nM with PDE4A4) (Sette and Conti, 1996; Hoffmann et al., 1998; Laliberte et al., 2002), which has been recently confirmed in vivo (Itoh et al., 2010).

In addition to the activation of PDE4 activity by the β-AR-cAMP-PKA cascade, mitogen-activated protein (MAP) kinase extracellular receptor kinase 2 (ERK2) activation results in phosphorylation at a site within the catalytic region. Catalytic activity of long PDE4 isoforms phosphorylated at this site is inhibited (Hoffmann et al., 1999), while the short isoforms are stimulated (Zhang, 2009). A second ERK-phosphorylation site has been suggested on the long isoform PDE4D3 that may increase enzyme activity and induce translocation (Liu and Maurice, 1999). Additionally, activation of the MAP kinase signaling pathways through the protein kinase C reduces the stability of PDE4D mRNA in vascular smooth muscle cells (Liu et al., 2000). The dual regulation of PDE4 provides a mechanism for complicated spatial and temporal regulation of the cAMP signal, allowing distinct cellular pockets to exhibit different cAMP responses to receptor stimulation, depending on the PDE4 subtype present. As an example, thyroid-stimulating hormone has been shown to increase PDE4D3 enzymes in the soluble and particulate fraction of the quiescent FRTL-5 thyroid cell, while long-term TSH exposure increases PDE4D2 primarily in the soluble fraction (Jin et al., 1998). Regulation of PDE4 expression can also be isozyme-specific, with individual subtypes exhibiting different susceptibility to increased expression and phosphorylation (Kostic et al., 1997), providing precise control over cAMP levels in the cellular compartments.

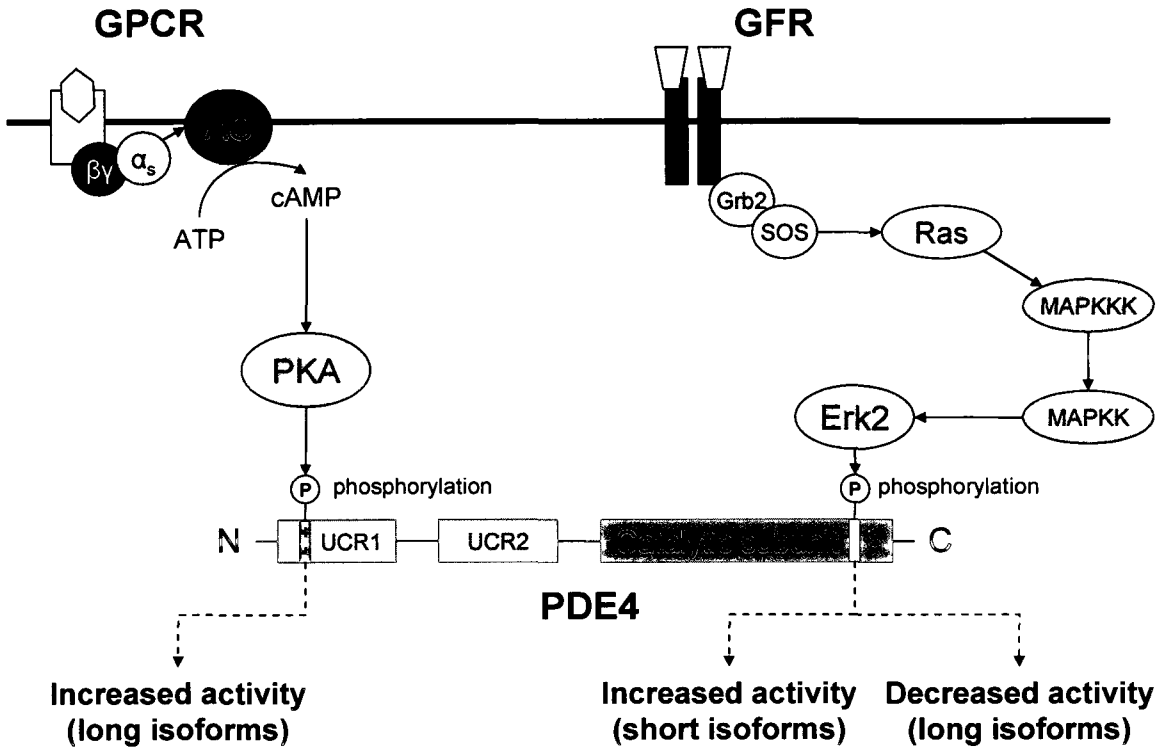


Figure 6-3: Regulation of PDE4 by phosphorylation at two distinct sites on the molecule, following activation of the GPCR and tyrosine kinase receptor (growth factor receptor; GFR) pathway. Activated PKA phosphorylates the long isoforms of PDE4 at the Ser54 site of the upstream conserved region 1 (UCR1), increasing the enzyme's catalytic activity. Phosphorylation of the PDE4 enzyme by Erk2 MAP kinase on a Ser site in the catalytic subunit inhibits the catalytic activity of long isoforms and activates the short isoforms.

Sustained elevation in cAMP levels (> 2 hours) increases enzyme expression and activity through increased PDE4 gene transcription (Torphy et al., 1992; Engels et al., 1994; Manning et al., 1996; Rose et al., 1997; Torphy, 1998; Tilley and Maurice, 2002; Campos-Toimil et al., 2008). Tilley et al. have demonstrated that administration of activators of PKA (dibutyryl-cAMP) or AC (forskolin) increase PDE4 activity by approximately 55% in vascular smooth muscle cells within 5 hours of drug treatment in a transcription-dependent process (Tilley and Maurice, 2002). Conversely, inhibition of PDE4 transcription with actinomycin-D or disruption of protein synthesis by cycloheximide has been shown to attenuate cAMP-dependent increases in PDE4 expression (Torphy et al., 1992; Tenor and Schudt, 1996; Erdogan and Houslay, 1997), implicating de novo protein synthesis.

A chronic blockade of β-AR with propranolol has been shown to decrease cAMP hydrolysis (Ye and O'Donnell, 1996) and PDE4 protein density in the rat cerebral cortex (Ye et al., 1997). Destruction of noradrenergic neurons with intracerebral administration of 6-hydroxydopamine reduces PDE4A and PDE4B expression in the rat hypothalamus, showing regulation of these two PDE4 subtypes by the noradrenergic system (Farooqui et al., 2000). These studies indicate that PDE4 expression and activity respond to both increases and decreases in the cAMP levels, with the potential for using measurements of PDE4 as an indirect index of intracellular cAMP levels. At the most basic level, the immediate response to increased cAMP levels is an elevation in PDE4 activity by PKA phosphorylation. With a persistent cAMP elevation, PKA-mediated processes initiate gene transcription and de novo protein synthesis, increasing PDE4 expression in the cell.

## PDE4 INHIBITORS

The first agents used for inhibition of phosphodiesterase enzymes were the xanthine derivatives caffeine, theophylline and 3-isobutyl-1-methylxanthine (IBMX) (Wells and Kramer, 1981; Yasui and Komiyama, 2001). Theophylline has been used clinically for the past five decades for treatment of asthma. However, xanthine derived PDE inhibitors exhibited relatively low potency in inhibiting PDE isozymes, very little subtype selectivity and adenosine receptor antagonist action (Yasui and Komiyama, 2001), rendering them ineffective compared to modern agents.

Intense interest in the second generation of PDE4 inhibitors that selectively affect the low $K_m$, cAMP-specific PDE4 subfamily was caused by the ability of these agents to inhibit platelet aggregation and elicit cardiotonic effects (Weishaar et al., 1985). Rolipram, zardaverine, filaminast, mesopram and piclamilast were considered for anti-inflammatory applications, but were dropped from clinical trials due to the emetic side effects. From this generation of PDE4-specific inhibitors, rolipram, Ro 20-1724, ICI 63-197 have exhibited behavioural effects on rats that suggested the effectiveness in elevating brain cAMP (Wachtel, 1982) and thus potential for treatment of major depression (Wachtel, 1983; Wachtel, 1983; Wachtel, 1988). Clinical studies have established efficacy (Zeller et al., 1984), accompanied with high occurrence of side-effects, including nausea and vomiting (Bertolino et al., 1988).

In addition to anti-depressive applications, an ongoing challenge for the pharmaceutical industry has been to enhance subtype specificity and increase anti-inflammatory and bronchorelaxant effects of PDE inhibitors, while reducing side effects (Manning et al., 1999). Presently, a degree of specificity has been achieved, with recently

synthesized compounds showing 17-fold specificity for PDE4A and B over PDE4D (Manning et al., 1999). This refinement in developmental chemistry has allowed several PDE4 inhibitors to warrant clinical trials or approval by regulatory agencies for treatment of COPD (roflumilast and olgemilast), psoriasis (apremilast), asthma (MEM1414) and rheumatoid arthritis (GRC 4039) (Pages et al., 2009).

**Rolipram**

Archetypal PDE4-selective inhibitor rolipram has been tested as an antidepressant, showing promising effectiveness in human and animal studies (Wachtel, 1983; Zeller et al., 1984; Bertolino et al., 1988; Esposito et al., 2009). In cardiac studies, rolipram has been found to potentiate the action of inotropic agents and modulate cardiac contractility (Kajimoto et al., 1997). Rolipram exists as (*R*)- and (*S*)- stereoisomers, with the (*R*)- form being 10–15 times more potent in eliciting antidepressant action (Wachtel, 1983) and ~20 times more effective at inhibiting PDE4 (Schneider et al., 1986). (*R*)-Rolipram reversibly binds to PDE4 (Liu et al., 2001), inhibiting the enzyme activity with $IC_{50}$ values of 0.1–1 μM (Houslay et al., 1997).

PDE4 exhibits a high- and low-affinity rolipram binding site (HARBS and LARBS, respectively). Presence of two rolipram binding sites on the PDE4 enzyme has been shown, with the possibility that the two sites may actually be two distinct forms or states of the enzyme (Torphy et al., 1992; McLaughlin et al., 1993; Jacobitz et al., 1997; Torphy, 1998; Liu et al., 2001; Houslay and Adams, 2003; Zhao et al., 2003), with $K_i$ values of ~1–10 nM and ~50–1000 nM, respectively (McLaughlin et al., 1993; Barnette et al., 1995; Barnette et al., 1996; Jacobitz et al., 1996; Houslay and Adams, 2003). While

studies by Zhao et al. using [$^{3}$H]rolipram and [$^{3}$H]piclamilast detected no HARBS in the peripheral tissues and only 50–65% of total rolipram binding in the brain (Zhao et al., 2003), other groups have shown the presence of both sites in the brain and the periphery (Kelly et al., 1996). Conflicting data from in vitro studies likely results from the dependence of HARBS on the presence of $Mg^{2+}$cofactor to induce its holoenzyme conformation (Liu et al., 2001; Zhao et al., 2003) and alter the phosphorylation state of the enzyme (Sette and Conti, 1996; Hoffmann et al., 1998; Torphy, 1998). In a physiological milieu, it would be expected that intracellular $Mg^{2+}$ levels would satisfy the enzyme cofactor dependence for functionality (Houslay and Adams, 2003). Three-dimensional X-ray crystallography of the PDE4 enzyme structure points to the presence of a catalytic site with highly conserved residues that binds two metal atoms and has been proposed as a potential site for rolipram binding (Xu et al., 2000). Based on mutation studies, PKA phosphorylation was suggested to increase rolipram binding to PDE4 through the formation of an ion-pair between the phosphorylated Ser54 in the UCR1 with a residue within the catalytic subunit (Hoffmann et al., 1998).

## PATHOLOGIES INVOLVING ALTERATIONS IN cAMP REGULATION

### Asthma and inflammatory disorders

Due to the expression of PDE4 isozymes in the lungs and inflammatory tissues, PDE4 inhibitors are undergoing rigorous investigation as a treatment for asthma. PDE4 inhibitor imbudilast is currently used in the Asian markets for control of asthma, while a number of other compounds are in clinical trials (Houslay et al., 2005). Pharmacologic

inhibition of PDE4 activity suppresses the release of pro-inflammatory factors histamine, and tumor necrosis factor-α from the cells of the immune system (Barnette et al., 1998). Despite their effectiveness, wide application of PDE4 inhibitors is limited by the emetic effect.

**Neuropsychiatric disorders**

All PDE isozymes (except PDE11) are expressed to a varying degree in the brain (Makhlouf et al., 2006; Wong et al., 2006; Reneerkens et al., 2009), The past three decades have seen continued research into the involvement of PDE4 in the molecular mechanism of depressive disorders (Wachtel, 1983; Duman et al., 1997), due to the involvement of the enzymes in the termination of monoamine signaling (Zhang et al., 1999; Farooqui et al., 2000; Delgado et al., 2003; Zhao et al., 2003; Lynch et al., 2005; Lourenco et al., 2006). PDE4-selective inhibitors exhibit characteristics common to the antidepressant drugs in animal models, such as potentiation of yohimbine lethality and inhibition of reserpine-induced hypothermia, as well as hypokinesia and reduced escape failures in the learned helplessness rat model of depression (Wachtel, 1983; Wachtel and Schneider, 1986; O'Donnell and Zhang, 2004). These effects were found to occur even with the blockade of β-AR or dopaminergic receptors, indicating that the antidepressant site of action of PDE4 inhibitors is located downstream of the receptor (Wachtel and Schneider, 1986).

In a simplified proposed cascade of antidepressant action, increased synaptic monoamines activate G protein-coupled receptors, stimulating cAMP generation and PKA activation. Phosphorylation of CRE by PKA induces binding to CREB, resulting in

increased transcription and expression of the modulator of neural plasticity BDNF (Duman et al., 1997; Itoh et al., 2004). Increasing intracellular cAMP was proposed as the common factor in the action of pharmaceutical agents affecting noradrenergic and serotonergic signaling, unifying the antidepressant mechanisms of selective serotonin reuptake inhibitors, monoamine oxidase inhibitors and tricyclic antidepressants (Duman et al., 1997). Learned helplessness rat model of depression exhibited reduced PDE4 expression (Itoh et al., 2003), while electroconvulsive seizure therapy and chronic antidepressant drug administration have been shown to upregulate PDE4 enzymes (Takahashi et al., 1999; Cho et al., 2000; Zhao et al., 2003; D'Sa et al., 2005). Inhibition of PDE4 in the brain was reported to reverse cognitive defects arising from sleep deprivation in rats (Vecsey et al., 2009). The involvement of cAMP and PDE4 in the mechanisms of both pathogenesis and antidepressant action makes in vivo quantification of enzyme activity and expression a promising target (Fujita and Innis, 2000).

**Cardiac disorders**

In cardiac tissues, cAMP activation of PKA modulates the phosphorylation of a number of intracellular proteins which regulate $Ca^{2+}$ influx and therefore the strength of cardiomyocyte contraction. Generated cAMP is hydrolyzed mostly by PDE3 and PDE4 isozymes in the myocardium, which display distinct intracellular localization (Mongillo et al., 2004). While PDE3 enzymes localize primarily to the intracellular membrane, PDE4B and D subtypes are found in clusters throughout the myocardial cytosol, associated with the membrane, and in high density at the M and Z line of the sarcomere (Mongillo et al., 2004). Adult rat cardiomyocytes also show cAMP- and cGMP-

hydrolyzing PDE2 activity (Mongillo et al., 2006), as well as the presence of cGMP-specific PDE1 (Nikolaev et al., 2006). Functionally, cardiac PDE4 subtypes break down the cAMP generated following β-AR activation within the sympathetic branch of the autonomic nervous system (Katano and Endoh, 1990; Katano and Endoh, 1992; Cui and Green, 2003; Xiang and Kobilka, 2003; Mongillo et al., 2004; Nikolaev et al., 2006). Increased cardiac adrenergic tone and decreased post-synaptic response to NA are common factors in heart failure, regardless of the underlying etiology (Leimbach et al., 1986; Eisenhofer et al., 1996; Osadchii et al., 2007), making measurement of adrenergic signaling at receptor and post-receptor second messenger level a tempting novel target for in vivo quantification.

Progressive cardiomyopathy observed in a mouse model of genetic PDE4D gene inactivation despite the lack of change in β-adrenergic receptors directly implicates PDE4 in the pathogenesis of heart failure (Lehnart et al., 2005). In human failing cardiac tissues, a reduction in RyR-bound PDE4D phosphorylation and activity has been observed (Lehnart et al., 2005). Furthermore, heart failure induced by aortic banding reduced cAMP generation by 32% and decreased overall PDE4A and PDE4B expression, while PDE4D was unchanged (Abi-Gerges et al., 2009). Conversely, Takahashi et al. have observed an increase in PDE3 and PDE4 activities in a pressure-induced congestive heart failure rat model (Takahashi et al., 2002). The same study reported an increase in cardiac cAMP levels compared to the age-matched controls at the age of 11 weeks, when the rats are merely hypertensive, followed by a decrease at 18 weeks, once the animals develop congestive heart failure (Takahashi et al., 2002). The contradictions between the

two findings suggest cAMP regulation and PDE4 levels may be altered in a time-dependent fashion in pathology.

## IMAGING SIGNAL TRANSDUCTION

### Post-synaptic 2$^{nd}$ messenger signaling

As important cellular switches and common components of a number of neurotransmitter signal-transduction cascades, non-invasive quantification of secondary messenger systems in living tissues could provide mechanistic insights into alterations of signal transduction pathways in disease states. Additionally, since signaling cascade defects may precede functional impairments, evaluation of intracellular components of cell signaling at different stages in disease progression could provide clinically significant information and help guide therapy. A number of radiolabeled ligands have been proposed for in vivo evaluation of molecular targets in the post-receptor cascades (Figures 6-4 and 6-5).

*[$^{11}$C]rolipram and [$^{11}$C]Ro20-1724*

Specific PDE4 inhibitors rolipram and Ro20-1724 were initially labeled with C-11 by DaSilva et al. (DaSilva et al., 1997), and their retention compared using biodistribution studies for potential as indices of PDE4 binding, and indirectly, of cAMP signaling (Lourenco et al., 1999). Both radiotracers bound PDE4 specifically in the brain, with [$^{11}$C]rolipram exhibiting three times higher regional expression and greater specific binding (approximately 80% vs. ~50%) than [$^{11}$C]Ro20-1724 (Lourenco et al., 1999). (*R*)-[$^{11}$C]rolipram was developed through further studies as a PET tracer used for the evaluation of PDE4 levels and alterations in cAMP signaling pathways.

**Phosohodiesterase-4**

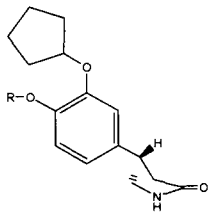

R= $^{11}CH_3$–

(*R*)-[$^{11}$C]rolipram

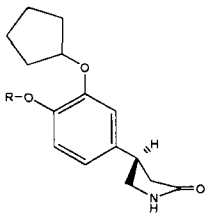

(*S*)-[$^{11}$C]rolipram

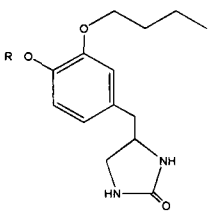

[$^{11}$C]Ro20-1724

**Adenylyl cyclase**

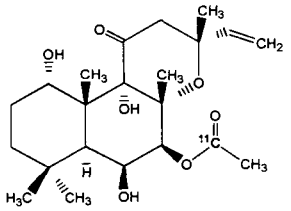

[$^{11}$C]forskolin

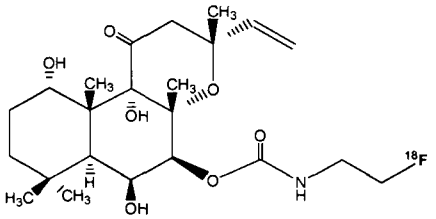

[$^{18}$F]forskolin

**Phosphoinositide turnover**

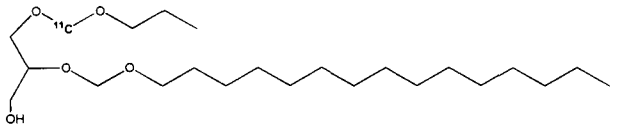

[$^{11}$C]DAG

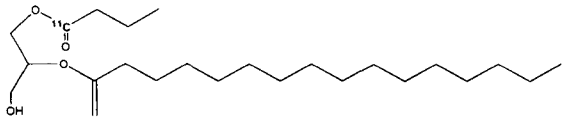

*sn*-1,2-[$^{11}$C]DAG

**Arachidonic acid**

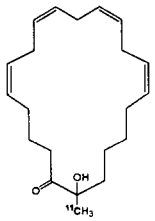

[$^{11}$C]arachidonic acid

**Protein kinase A**

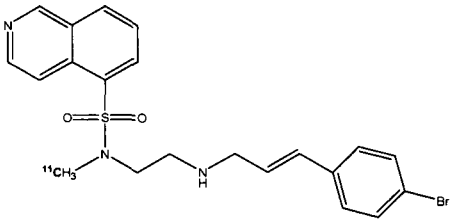

[$^{11}$C]isoquinoline-5-sulfonamide

**Protein kinase C**

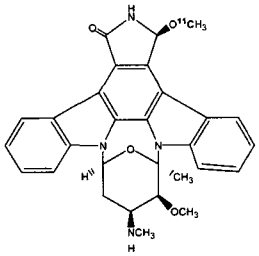

[7β-methoxy $^{11}$C]methoxy staurosporine

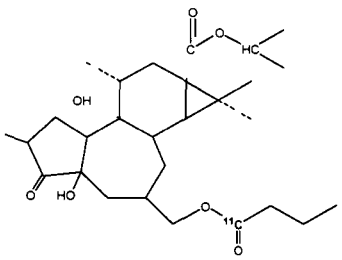

[$^{11}$C]DPBB

Figure 6-4: Structures of radioligands evaluated for imaging of signaling targets; phosphodiesterase-4 ((*R*)-[$^{11}$C]rolipram, (*S*)-[$^{11}$C]rolipram and [$^{11}$C]Ro20-1724 R = $CH_3$- for unlabeled derivatives), adenylyl cyclase ([$^{11}$C]forskolin and [$^{18}$F]forskolin), phosphoinositide turnover ([$^{11}$C]DAG and *sn*-1,2-[$^{11}$C]DAG), arachidonic acid ([$^{11}$C]arachidonic acid), protein kinase A ([$^{11}$C]isoquinoline-5-sulfonamide) and protein kinase C ([7β-methoxy $^{11}$C]methoxy staurosporine and [$^{11}$C]DPBB).

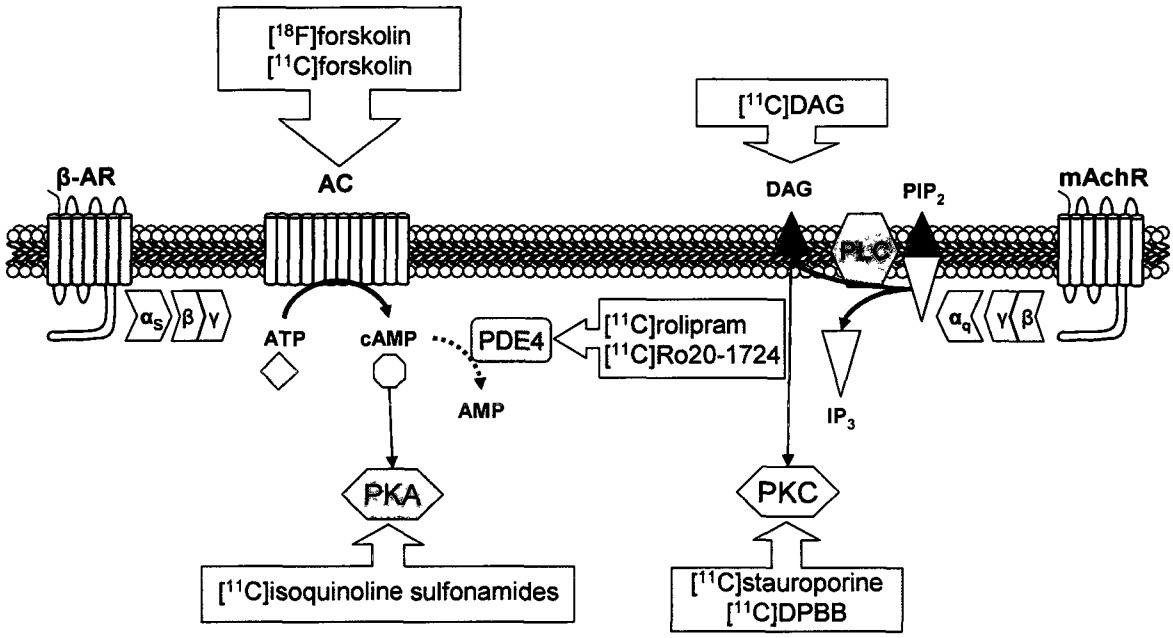


Figure 6-5: Examples of tracers with potential for imaging components of the cAMP and PLC signaling pathways following activation of the G protein coupled receptors (GPCRs). β-AR stimulation activates the adenylyl cyclase (AC), which has been studied using $^{11}$C- and $^{18}$F-labeled inhibitor forskolin. AC stimulation increases cAMP levels, activating protein kinase A (PKA) and increasing phosphodiesterase-4 (PDE4) levels. (*R*)- and (*S*)-[$^{11}$C]rolipram have been used for quantification of PDE4 expression and activity. Attempts have been made to quantify PKA using $^{11}$C-labeled isquinoline sulfonamides. Following mAchR activation, the $\alpha_q$ subunit of the GPCR stimulates phospholipase C (PLC) to break phosphatidyl 4,5-bisphosphate ($PIP_2$) into inositol trisphosphate ($IP_3$) and diacylglycerol (DAG), which activates protein kinase C (PKC). [$^{11}$C]DAG has been used to measure the activation of the IP3/DAG signaling cascade, while $^{11}$C-labeled stauroporine and $^{11}$C-labeled phorbol esters, including 12-deoxyphorbol 13-isobutyrate-20-[1-$^{11}$C]butyrate ([$^{11}$C]DPBB), have been assessed for PKC imaging.

*[$^{11}$C]Arachidonic acid*

Regional incorporation of arachidonic acid labeled with C-11 is used as an index of phospholipase $A_2$ activity in vivo (Esposito et al., 2007), reflecting changes in the stimulation of cell surface receptors that utilize this pathway, including serotonin 5-HT2 receptors (Basselin et al., 2009).

*[7β-methoxy $^{11}$C]methoxy-stauroporine*

Tracers based on phorbol esters, molecules which incorporate into the protein kinase C (PKC)/ diacylglycerol (DAG)/ phosphoinositide ($IP_3$) signaling pathway, have been tested using ex vivo techniques, showing retention of 12-deoxyphorbol 13-isobutyrate-20-[1-$^{11}$C]butyrate ([$^{11}$C]DPBB) to be susceptible to displacement by unlabeled inhibitors (Ohmori et al., 1993). Radiolabeling of the inhibitor stauroporine as [7β-methoxy $^{11}$C]methoxy-stauroporine was aimed at imaging brain PKC localization, but failed to establish a radiochemical yield sufficient for positron emission tomography (PET) imaging (Sasaki et al., 1996).

*[$^{11}$C]Diacylglycerol*

Within the PKC signaling pathway, $^{11}$C-labeled DAG (1-[1-[$^{11}$C]butyryl-2-palmitoyl-rac-glycerol) has been applied for in vivo PET imaging of the myocardium in rats with experimentally-induced myocardial infarction, as well as in human heart failure patients (Chida et al., 2000; Otani et al., 2005). [$^{11}$C]DAG is metabolized within the phosphoinositide cycle, with the radioactivity uptake reflecting the activation of the $IP_3$/DAG second messenger cascade (Otani et al., 2005). Studies imaging PKC signaling pathway using PET display potential for analysis of post-MI remodeling in the

myocardium, mediated by angiotensin II, endothelin-I and $\alpha_1$-adrenergic receptors (Chida et al., 2000; Otani et al., 2005).

*[$^{18}$F]Fluoroethylcarbamoyl-forskolin, [$^{11}$C]forskolin and $^{11}$C-labeled isoquinolinesulfonamide*

The GPCR-AC-cAMP-PKA axis has provided a number of targets for non-invasive quantification by PET tracers. $^{18}$F-labeled carbamate analog of forskolin, 7-(2-[$^{18}$F[fluoroethyl) carbamoyl forskolin, was tested for AC imaging in the brain (Kiesewetter et al., 2000). Despite the high in vitro affinity for AC of the candidate compound, in vivo studies in primates and ex vivo studies in rats exhibited low and non-specific uptake of the tracer in the brain (Kiesewetter et al., 2000). Sasaki et al. tested [$^{11}$C]forskolin in rats, reporting high signal uptake and susceptibility to displacement by unlabeled forskolin in the heart (Sasaki et al., 1993). Recent efforts were geared towards labeling isoquinolinesulfonamide PKA inhibitors, testing a number of candidate tracers by ex vivo biodistribution techniques (Vasdev et al., 2008).

## PDE4 IMAGING

### (*R*)-[$^{11}$C]Rolipram

Rolipram labeled with C-11 has been applied for evaluation of changes in the cAMP signaling pathway in rat, monkey, pig and human (DaSilva et al., 1997; Lourenco et al., 1999; Tsukada et al., 2001; DaSilva et al., 2002; Fujita et al., 2005; Parker et al., 2005). (*R*)- and (*S*)-desmethylrolipram precursors are synthesized by dealkylation of (*R/S*)-rolipram with iodotrimethylsilane, followed by separation of (*R*)- and (*S*)-precursors through chiral high performance liquid chromatography (HPLC) to >99%

optical purity (DaSilva et al., 2001). (*R*)- and (*S*)-[$^{11}$C]rolipram are synthesized by O-[$^{11}$C]methylation of respective phenolic precursors with [$^{11}$C]methyl iodide in the presence of tetrabutylammonium hydroxide (TBAOH) (DaSilva et al., 1997). Initial radiosyntheses of (*R*)- and (*S*)-[$^{11}$C]rolipram yielded specific activities of 18–93 GBq/μmol (>500–2500 mCi/μmol) at end-of-synthesis using the wet (lithium aluminium hydride; LAH) method (Tsukada et al., 2001; Fujita et al., 2005; Parker et al., 2005; Fujita et al., 2007; Kenk et al., 2007).

**(*R*)-[$^{11}$C]rolipram safety profile**

Human and animal studies performed with unlabeled (*R/S*)-rolipram show a good toxicological safety profile. Emetic side-effects of rolipram occur at doses of 0.1 mg/kg i.v. (in dogs) (Heaslip and Evans, 1995), while a dose of 1.0 mg/kg t.i.d. has been well tolerated in human clinical studies (Zeller et al., 1984; Bertolino et al., 1988). With specific activities of 185–370 GBq/μmol (5000–10000 mCi/μmol) becoming routinely achievable, the cold mass that would be administered in a human PET imaging study for a 370–555 MBq (10–15 mCi) injection would range from 0.3–4.1 μg. This amount of unlabeled (*R*)-rolipram would not be expected to elicit any negative effects. Administration of (*R*)-[$^{11}$C]rolipram in imaging studies with healthy volunteers and rats elicited no change in heart rate, blood pressure and respiratory rate (DaSilva et al., 2002; Fujita et al., 2005; Sprague et al., 2008).

Extrapolation of ex vivo rat dosimetry data to estimate human dose yielded absorbed dose estimates (for a 370 MBq (10 mCi) injected dose) of 1.4 μGy/MBq (51.9 μGy/mCi) for the whole body, with the highest absorbed dose in the urinary bladder wall,

small intestine and liver (14.2, 7.6 and 5.3 μGy/MBq; 525.9, 281.5 and 196.3 μGy/mCi) (Lourenco et al., 2001). Subsequent studies using PET imaging have estimated the effective dose absorbed by high-exposure organs at 4.8 μGy/MBq (177.8 μGy/mCi)from human PET studies and 1.4 μGy/MBq (51.9 μGy/mCi) from monkey imaging (Sprague et al., 2008), reflecting species differences in metabolic pathways. Both studies have concluded that the exposure of human subjects is well within safety limits, considering the standard effective dose of $^{11}$C-labeled receptor tracers is ~3–6 μGy/MBq (111.1–222.2 μGy/mCi) (International commission on radiological protection (ICRP), 2008). By comparison, the adult dose of commonly used clinical PET imaging agent [$^{18}$F]fluorodeoxyglucose ([$^{18}$F]FDG) is 10–90 μGy/MBq (370.4–3333.3 μGy/mCi) (International commission on radiological protection (ICRP), 2008), far higher than with (*R*)-[$^{11}$C]rolipram. In rats and monkeys, excretion of (*R*)-[$^{11}$C]rolipram was predominantly urinary, while the hepatobilliary route plays a major role in humans (DaSilva et al., 2002; Sprague et al., 2008).

**Ex vivo / in vitro characterization of [$^{11}$C]rolipram binding**

Biodistribution studies have been used to define the time-course of both $^{11}$C-labeled enantiomers of rolipram (Lourenco et al., 1999). High uptake of (*R*)-[$^{11}$C]rolipram was observed in the PDE4-rich brain, lungs, heart, skeletal muscle and pancreas, with the rank order of signal retention matching PDE4 densities determined by in vitro methods (Lourenco et al., 1999; Lourenco et al., 2001; Kenk et al., 2007). (*R*)- and (*S*)-[$^{11}$C]rolipram uptake reaches maximal values 5 min following tracer administration (Lourenco et al., 2001). Activity retained in tissues following (*S*)-

[$^{11}$C]rolipram administration decays with higher clearance than the (*R*)- enantiomer (Lourenco et al., 2001).

(*R*)- and (*S*)-[$^{11}$C]rolipram biodistribution studies displayed a large amount of reversible binding of (*R*)-[$^{11}$C]rolipram in the brain (~80%) and the heart (30-40%) that could be displaced by co-administration of unlabeled (*R*)-rolipram or a structurally distinct PDE4 inhibitor, Ro 20-1724 (Lourenco et al., 2001). Co-administration of (*R*)-[$^{11}$C]rolipram with a range of doses of unlabeled (*R*)- or (*S*)-rolipram generated dose-response curves with $ED_{50}$ values of 0.04 and 0.5 mg/kg, respectively (Lourenco et al., 2001; Kenk et al., 2007). Despite the lower affinity for PDE4, ~50% of brain (*S*)-[$^{11}$C]rolipram retention was susceptible to blocking by (*R*)-rolipram, indicating the presence of specific binding. However, a much lower tissue contrast was observed in the tissues following (*S*)-[$^{11}$C]rolipram administration compared with (*R*)-[$^{11}$C]rolipram, reflecting the lower affinity of the (*S*)- stereoisomer for the PDE4 enzyme (Lourenco et al., 2001).

In the heart, biodistribution studies have estimated (*R*)-[$^{11}$C]rolipram specific binding to account for 30–40% of the total detected signal (Lourenco et al., 2006; Kenk et al., 2007). Retention of (*R*)-[$^{11}$C]rolipram in cardiac regions, skeletal muscle, lungs and pancreas was unaffected by administration of inhibitors of PDE1, 2, 3 and 5 isozymes, demonstrating binding selectivity for the PDE4 isoforms over other PDE enzymes (Lourenco et al., 2001; Kenk et al., 2007). This result was validated using in vitro autoradiography studies (Kenk et al., 2007). Conversely, specific binding of (*R*)-[$^{11}$C]rolipram was absent in the adipose tissues. Overall, ex vivo and in vitro characterization demonstrates that (*R*)-[$^{11}$C]rolipram is a suitable imaging agent for

evaluating PDE4 in the brain, myocardial tissues, skeletal muscle and pancreas, but not the adipose tissues (Kenk et al., 2007).

**(*R*)- and (*S*)-[$^{11}$C]rolipram metabolism**

Studies performed with $^{3}$H- and $^{14}$C-labeled rolipram have shown extensive metabolism of rolipram, with the elimination of labeled rolipram in rats proceeding in a 4:1 ratio through renal to biliary routes (60% of activity excreted through urine and 15% through feces), with a significant amount of enterohepatic recirculation (Krause and Kühne, 1988; Krause et al., 1989).

Six separate metabolism products have been identified in rat, rabbit, monkey and human plasma (Krause and Kühne, 1992; Krause and Kühne, 1993), resulting from phase I cleavage of the methoxy and pentyloxy groups, or hydroxylation of the pentyloxy ring (at positions 2 of 3) (Krause and Kühne, 1993). Of phase II metabolic reactions, only sulphation conjugated metabolites were detected, with no glucuronidation (Davis and Daly, 1979). One of the proposed metabolic pathways involves the removal of the $^{11}$C-labeled methyl group resulting in the formation of an unlabeled metabolite (Krause and Kühne, 1992). However, according to the findings of Krause and Kuhne, the main metabolite is the hydroxylated cyclopentyl ring that would retain its radioactive label, even after subsequent sulphation (Krause and Kühne, 1992). Lack of involvement of the chiral center in the biotransformation reactions is reflected in the similar pharmacokinetics of (*R*)- and (*S*)-rolipram (Krause et al., 1989; Krause and Kühne, 1993).

Multiple radiolabeled metabolites have been observed in the plasma and peripheral tissues (Lourenco et al., 2001; Kenk et al., 2008), accounting for ~75% of the total plasma radioactive signal, and 44–52% of the observed signal in the heart, skeletal muscle, pancreas and brown adipose tissue 45 min following tracer injection in rats (Kenk et al., 2008). It has been established by thin layer chromatography and HPLC that metabolism of (*S*)- and (*R*)-[$^{11}$C]rolipram occurs outside the brain, with hydrophilic radiolabeled metabolites unable to cross the blood brain barrier (Krause and Kühne, 1988; Lourenco et al., 2001; DaSilva et al., 2002; Fujita et al., 2005; Parker et al., 2005; Fujita et al., 2007; Kenk et al., 2008), simplifying (*R*)-[$^{11}$C]rolipram application for cerebral PET imaging (Pike, 2009).

Parker et al. detected no change in blood radioactivity and metabolites in pigs following administration of (*R*)-[$^{11}$C]rolipram with increasing doses of unlabeled (*R*)-rolipram (Parker et al., 2005), suggesting that the metabolic pathways are not sensitive to cold rolipram. Conversely, Fujita et al. reported differences between input functions of high (71.4 ± 10 GBq/μmol; 1920 ± 270 mCi/μmol) and low specific-activity (0.19 and 0.37 GBq/μmol; 5 and 10 mCi/μmol) (*R*)-[$^{11}$C]rolipram injections (Fujita et al., 2005).

While the labeled hydrophilic metabolites do not bind specifically to PDE4 (Kenk et al., 2008), their significant presence necessitates their inclusion in the kinetic modeling of (*R*)- and (*S*)-[$^{11}$C]rolipram for PET quantification of PDE4 in the peripheral tissues. Studies performed on rat tissue homogenates obtained 45 minute following radiotracer administration demonstrate that the radioactivity observed in the heart comprises 41% specific binding, 44% labeled metabolites and 15% non-specific binding (Kenk et al.,

2008). Metabolites of the (*R*)- and (*S*)- enantiomers formed in rats show no difference in relative proportions (Kenk et al., 2008).

Plasma protein binding has been estimated at 96% in human plasma (DaSilva et al., 2002), 81 and 83% in dogs ((*R*)- and (*S*)-[$^{11}$C]rolipram, respectively) (Lortie et al., 2006). In rats, plasma protein binding is similar for both (*R*)- and (*S*)-[$^{11}$C]rolipram enantiomers, with values reported in the 65-75% range (Lourenco et al., 2001; Fujita et al., 2005; Fujita et al., 2007; Itoh et al., 2009). Incorporating plasma protein binding with the contribution of radiolabeled metabolites to the total detected radioactivity signal, Lortie et al. have established a kinetic two-compartment model in canine studies consisting of specific and non-specific binding compartments with a parallel compartment for the labeled metabolites. This model provides an excellent fit to the PET data in the canine myocardium, and could be applied with modifications to small-animal studies with rats and mice (Lortie et al., 2006; Lortie et al., 2009 (Submitted)). The same study also established that the Logan approach of quantifying tracer retention results in some bias, which is consistent across scans (Lortie et al., 2009 (Submitted)).

**In vivo PET studies with (*R*)-[$^{11}$C]rolipram**

Early PET imaging studies with (*R*)-[$^{11}$C]rolipram in monkeys, rats and pigs detected high region-specific tracer uptake in the brain cortex, striatum, hippocampus and thalamus (Tsukada et al., 2001; DaSilva et al., 2002; Harada et al., 2002; Fujita et al., 2005; Parker et al., 2005). Radioactive in vivo signal was susceptible to blocking by unlabeled (*R*)-rolipram (Fujita et al., 2005; Parker et al., 2005). Due to the observed wide distribution of (*R*)-[$^{11}$C]rolipram and the ubiquitous PDE4 expression throughout the

brain, no reference region can be used to simplify the quantification of the tracer specific binding (DaSilva et al., 2002; Gee et al., 2002; Parker et al., 2005).

In vivo PET imaging measured the affinity of (*R*)-[$^{11}$C]rolipram to be an order of magnitude higher than (*S*)-[$^{11}$C]rolipram (Parker et al., 2005), confirming the in vitro observations. Furthermore, in vivo PET-derived $K_d$ values are higher (1.0 nM using PET, compared to 5.5 nM with in vitro techniques) than those obtained by in vitro binding assays performed with brain homogenates (Itoh et al., 2009). Specific binding was determined to account for the 86-90% of the PET-detected signal in the brain (Fujita et al., 2005; Itoh et al., 2009), which is comparable to the 81% measured using ex vivo biodistribution experiments (Kenk et al., 2007; Kenk et al., 2008).

Canine cardiac imaging studies have shown high (*R*)-[$^{11}$C]rolipram uptake in the left ventricle, with high contrast between the myocardium and the surrounding tissues (Kenk et al., 2006). Lung retention detected with biodistribution studies does not extend into potential for PDE4 imaging with (*R*)-[$^{11}$C]rolipram due to lower tissue density (0.26 g/cm$^3$) compared to the heart (1.05 g/cm$^3$, respectively) and surrounding organs. Despite the interest in PDE4 as a factor in bronchial dilatation and respiratory disorders, high lung retention of the tracer (as expressed in counts per g of tissue) would therefore not translate to high contrast in vivo imaging, since the signal would be distributed over a larger volume (Kenk et al., 2007).

**Injectable cold mass**

Hume at al. have performed an extensive study on acceptable occupancy for ligand tracer PET imaging (Hume et al., 1998), establishing the relationship between

receptor occupancy, injected activity, specific activity and the $ED_{50}$ of the radiotracer, and the weight of the animal studied. While the increase in PET equipment resolution has been a field of intense development, the limitations on sensitivity still set the minimal detectable injected dose of the radiotracer. To maintain receptor occupancy that allows kinetic modeling, high specific activities are necessary, dictated by the affinity of the radiotracer for its target (quantified as $ED_{50}$). In practical terms, tracers with high affinity require higher specific activity or lower injected dose (Hume et al., 1998). Jagoda et al. have set the threshold of acceptable occupancy for imaging studies at 5% (Jagoda et al., 2004).

Binding quantification is only possible if the receptor is not saturated and the binding curve is still in its linear (first-order kinetics) stage (Parker et al., 2005). Fujita et al. maintained receptor occupancy with unlabeled (*R*)-rolipram below 5% by injecting 110 MBq (3 mCi) of tracer to 300 g rats only if the specific activity is above 37 GBq/μmol (1000 mCi/μmol) (Fujita et al., 2005), assuming the $ED_{50}$ to be 0.05 mg/kg. At this occupancy, they observed no positive correlation between the specific activity and tracer distribution in brain regions, suggesting that satisfactory occupancy is attained. Recent studies performed by Thomas et al. have calculated the $ED_{50}$ for blocking (*R*)-[$^{11}$C]rolipram uptake in myocardial tissue to be ~0.03 mg/kg using Logan distribution volumes (Thomas et al., 2010), confirming the values obtained by biodistribution experiments at a single time point (Kenk et al., 2007). Given this $ED_{50}$ value, achievable specific activities and sensitivity of the small-animal PET equipment would permit imaging studies to be performed at <0.7% occupancy with injections of ~1.0 mCi (37

MBq; specific activity 37-111 GBq/μmol (1000–3000 mCi/μmol) in ~500 g rats, well below the 5% limit,.

**Quantification of PDE4-specific (*R*)-[$^{11}$C]rolipram binding**

Early imaging studies used a 2-tissue compartment model to fit (*R*)-[$^{11}$C]rolipram radioactivity retention in the human and rat brain (DaSilva et al., 2002; Fujita et al., 2005; Itoh et al., 2009). In rat PET imaging studies, time-activity curves were computed using a 2-tissue compartment model with the distribution volume (DV) representing the non-displaceable ($K_1/k_2$) uptake fixed to the DV obtained with saturating dose of (*R*)-rolipram (Itoh et al., 2009). Alternately, Logan graphical analysis has been applied previously to quantify (*R*)-[$^{11}$C]rolipram uptake in the porcine brain regions of interest by Parker et al., producing reproducible results (Parker et al., 2005).

The difference in affinities of (*R*)- and (*S*)-[$^{11}$C]rolipram stereoisomers for the PDE4 enzyme has led to the proposal of using the retention of the less active (*S*)-enantiomer to measure non-specific binding of (*R*)-[$^{11}$C]rolipram, simplifying quantification of PDE4-specific retention (Gee et al., 1998; Lourenco et al., 2001; Gee et al., 2002; Lortie et al., 2009 (Submitted)). In theory, a two-scan protocol in which PDE4-specific tracer binding is calculated by comparing the (*R*)- and (*S*)-[$^{11}$C]rolipram scans would overcome the lack of PDE4-free brain reference region and facilitate parameter estimates. Assuming that (*S*)-[$^{11}$C]rolipram does not exhibit measurable PDE4-specific binding, a scan with this enantiomer yields a measure of non-specific (*R*)-[$^{11}$C]rolipram binding and could provide an estimate of $K_1/k_2$ kinetic constants, which could be applied in the same subject to estimate the $k_3$ and $k_4$ parameters. A number of studies have

produced data that supports this proposition. Imaging studies in the monkey brains have shown region-specificity of (*R*)-, but not (*S*)-[$^{11}$C]rolipram (Tsukada et al., 2001; Harada et al., 2002), suggesting absence of (*S*)-[$^{11}$C]rolipram PDE4-specific binding. Very little displacement of (*S*)-[$^{11}$C]rolipram has been observed with the high dose of unlabeled (*R*)-rolipram (Gee et al., 2002). Initial studies by Parker et al. supported the use of (*S*)-[$^{11}$C]rolipram to measure the non-specific binding and thereby quantify PDE4-specific binding of (*R*)-[$^{11}$C]rolipram, since very similar time-activity curves were obtained with both stereoisomers in the presence of a blocking dose of rolipram (Parker et al., 2005). These findings were confirmed in canine cardiac imaging studies, where volumes of distribution reflecting non-displaceable components of (*R*)- and (*S*)-[$^{11}$C]rolipram uptake were not significantly different in canine hearts (Lortie et al., 2009 (Submitted)). Several groups have applied (*S*)-[$^{11}$C]rolipram scans to quantify (*R*)-[$^{11}$C]rolipram brain studies and eliminate changes in local blood flow as a factor in observed (*R*)-[$^{11}$C]rolipram alterations (Tsukada et al., 2001; Harada et al., 2002; Itoh et al., 2010).

While binding of (*S*)-rolipram to PDE4 exhibits 10-20× lower affinity than that of the (*R*)- enantiomer, early studies performed with biodistribution techniques, as well as subsequent PET imaging experiments, have shown the presence of measurable PDE4-specific (*S*)-[$^{11}$C]rolipram binding in the brain and peripheral tissues (Lourenco et al., 2001; Parker et al., 2005). Use of (*S*)-[$^{11}$C]rolipram is based on the assumption that pharmacokinetics of the two stereoisomers are identical, and (*S*)-[$^{11}$C]rolipram retention is not dependent on PDE4-specific binding. Incorporation of (*S*)-[$^{11}$C]rolipram as the non-specific component of (*R*)-[$^{11}$C]rolipram uptake in modeling is complicated by the presence of labeled metabolites in the periphery, as well as the reported difference in the

non-specific tracer retention reported by Lourenco et al. with biodistribution studies in rat tissues (Lourenco et al., 2001) and Parker et al. using distribution volumes of PET imaging of porcine brains (Parker et al., 2005). (*S*)-[$^{11}$C]Rolipram retention may include a small portion of PDE4-specific binding and the estimate of pharmacokinetics with (*S*)-[$^{11}$C]rolipram may therefore underestimate the (*R*)-[$^{11}$C]rolipram PDE4-specific binding.

**(*R*)-[$^{11}$C]rolipram sensitivity to alterations in cAMP signaling**

Following studies on imaging feasibility and specific binding of (*R*)-[$^{11}$C]rolipram for PDE4, the tracers were applied to measure changes in intracellular PDE4 levels. Initial biodistribution studies have shown increased (*R*)-[$^{11}$C]rolipram retention following administration of AC activator forskolin (Lourenco et al., 1999). Similarly, pre-treatment with desipramine, a NA reuptake inhibitor, results in increased (*R*)-[$^{11}$C]rolipram binding to PDE4 (Lourenco et al., 1999), likely through the stimulation of adrenergic receptors by the elevated synaptic NA levels. Administration of pharmacological agents increasing monoamine signaling (serotonergic, adrenergic, histaminergic) increased (*R*)-[$^{11}$C]rolipram retention in the brain and heart (Lourenco et al., 2006), in agreement with the recognized involvement of cAMP in these signaling systems. Notably, increasing cardiac levels of NA by administration of desipramine 3 hours prior to the radiotracer has been shown to increase retention of (*R*)-[$^{11}$C]rolipram by ~20%, as quantified using Logan graphical analysis of small-animal PET radioactive signal (Thomas et al., 2010).

PET measurements using the difference between (*R*)- and (*S*)-[$^{11}$C]rolipram uptake have shown that methamphetamine administration increased PDE4 levels in the monkey brain, likely through increased dopamine release (Tsukada et al., 2001). This

effect was blocked by the $D_1$ selective inhibitor SCH23390, but not by raclopride, a $D_2$ selective inhibitor, suggesting the involvement of $D_1$ receptors only (Tsukada et al., 2001). Conversely, ex vivo experiments by Lourenco et al. showed an increase in (*R*)-[$^{11}$C]rolipram specific binding following administration of drugs that increase noradrenergic and serotonergic, but not dopaminergic signaling (cocaine, GBR12909 or SKF81297) (Lourenco et al., 2006).

The use of PDE4 inhibitors for therapy of major depression and the involvement of PDE4 isozymes in the molecular processes underlying the function of many antidepressants has led to the interest in applying (*R*)-[$^{11}$C]rolipram for in vivo monitoring of drug therapy. Chronic administration of antidepressant imipramine in rats did not affect PDE4 levels, as evaluated by (*R*)-[$^{11}$C]rolipram PET, [$^{3}$H]rolipram binding assays and immunoblotting against individual PDE4 subtypes (Fujita et al., 2007). These findings conflict with the widely reported increases in PDE4 subtypes following chronic antidepressant administration (Ye et al., 1997; Takahashi et al., 1999; Ye et al., 2000; Zhao et al., 2003).

In PET studies with conscious rats, PKA activating agent dibutyryl-cAMP increased (*R*)-[$^{11}$C]rolipram specific binding by 10% when infused into the striatum (compared to the contralateral, saline-infused striatum), while Rp-cAMPs, a PKA inhibitor, decreased the tracer uptake by 9.1% (Itoh et al., 2009). These results provide in vivo confirmation of the in vitro regulation of the PDE4 binding to rolipram by phosphorylation.

## (*R*)-[$^{11}$C]ROLIPRAM IN ANIMAL MODELS OF DISEASE

**Aged monkeys**

PDE4-specific binding is significantly decreased in brain PET scans of aged monkeys (78 and 75% in the striatum and frontal cortex, respectively) compared to younger animals, as quantified using the difference between (*R*)-[$^{11}$C]rolipram and (S)-[$^{11}$C]rolipram uptake (Harada et al., 2002). While the authors suggest a link between these changes and decreased $D_1$ receptor presence and responsiveness, in vitro validation was not performed to support these findings.

**Diet-induced obesity**

Alterations in sympathetic nervous system signaling have been previously implicated in the pathogenesis of obesity (Landsberg, 1986; Levin et al., 1997; Collins and Surwit, 2001; Dulloo, 2002), with diet-induced obese rats exhibiting higher sympathetic tone (Levin et al., 1983; Levin and Dunn-Meynell, 2000). Dysfunctional intracellular NA responsiveness was detected at the PDE4 level in the diet-induced obese rats, but not diet-resistant animals using (*R*)-[$^{11}$C]rolipram (Greene et al., 2009).

**Adriamycin-induced cardiotoxicity**

The use of highly effective anthracycline chemotherapeutic agents is limited by the onset of cardiotoxic effects (Lefrak et al., 1973) associated with altered cardiac sympathetic stimulation (Tong et al., 1991). No change in basal (*R*)-[$^{11}$C]rolipram uptake was detected between rats treated with adriamycin (doxorubicin) and vehicle. In parallel with a decrease in [$^{3}$H]CGP12177 retention and unchanged [$^{11}$C]HED uptake, a diminished response of (*R*)-[$^{11}$C]rolipram uptake to desipramine challenge was observed

3 weeks following the last injection of adriamycin (Kenk et al., 2010). This study demonstrates the potential of (*R*)-[$^{11}$C]rolipram in multi-tracer PET evaluation of the progression of NA signaling dysfunction within anthracycline chemotherapy.

## CONCLUSIONS

As a common component of various signaling pathways, assessment of changes in cAMP signaling through in vivo quantification of PDE4 activity and expression is a promising target that could provide insight into molecular mechanisms that underlie a number of pathological processes. Due to the involvement of altered cAMP signal transduction cascade in major depression, schizophrenia, heart failure, obesity, diabetes and asthma, the ability to detect altered PDE4 levels has potential for elucidation of molecular mechanisms of drugs such as β-AR blockers, antidepressants, bronchodilators, cardiac inotropes and emerging pharmaceutical agents with novel mechanisms of action. (*R*)-[$^{11}$C]Rolipram has been characterized for applications in the quantification of PDE4 enzyme activity and expression. The tracer exhibits 1) an acceptable toxicological profile; 2) specific and selective binding to PDE4; 3) heterogeneous in vivo retention, with high contrast between PDE4-rich organs of interest and surrounding tissues and 4) sensitivity to selected treatments altering cAMP signaling. Based on the favorable characterization profile of (*R*)-[$^{11}$C]rolipram, it has promising future applications in serial imaging of disease progression, guiding treatment and testing novel therapies.

# CHAPTER 7: MANUSCRIPT #6

Circulation (To be submitted)

# Reduced $\beta_1$-adrenergic receptor expression is associated with increased phosphodiesterase-4 inhibitor (*R*)-[$^{11}$C]rolipram retention in normally-perfused myocardium 8 weeks following myocardial infarction

Miran Kenk[a,b], Stephanie L. Thorn[a,b], Jennifer Renaud[a], Maria Kolajova[a], Ran Klein[a], Marc Lamoureux[a], Robert deKemp[a,b], Rob S. Beanlands[a,b] and Jean N. DaSilva[a,b*]

[a]*National Cardiac PET Centre, Division of Cardiology, University of Ottawa Heart Institute, 40 Ruskin St., Ottawa, Ontario, Canada, K1Y 4W7*

[b]*Department of Cellular and Molecular Medicine, Faculty of Medicine, University of Ottawa, 451 Smyth Rd., Ottawa, Ontario, Canada, K1H 8M5*

*MK was supervised by JND;*
*SLT was supervised by JND;*
*RK and ML were supervised by RdK;*
*Abbreviations:* β-AR, β-adrenergic receptor; DV, distribution volume; ECG, electrocardiogram; EKV, ECG-based Kilohertz visualization; EF, ejection fraction; FS, fractional shortening; GAPDH, glyceraldehyde 3-phosphate dehydrogenase; HLA, horizontal long axis; HR, heart rate; HU, high uptake; LAD, left anterior descending coronary artery; LVEDV, left ventricle end-diastolic volume; LVESV, left ventricle end-systolic volume; MBF, myocardial blood flow; MI, myocardial infarction; [$^{13}$N]$NH_3$, [$^{13}$N]-ammonia; NA, noradrenaline; NAT, noradrenaline transporter; PDE, phosphodiesterase; SA, short axis; SV, stroke volume; VLA, vertical long axis

* *Corresponding author:*
Jean N. DaSilva, PhD
*E-mail address:* jdasilva@ottawaheart.ca

**Contributions of authors**

The animal model described in this manuscript has been implemented and evaluated by PhD student Stephanie Thorn and myself, under supervision and guidance of Dr. Jean DaSilva. Jennifer Renaud (MSc) and Dr. Ran Klein facilitated the analysis of the data by designing and optimizing the FlowQuant software to allow quantitation of [$^{13}$N]$NH_3$ and (*R*)-[$^{11}$C]rolipram retention. Marc Lamoureaux (MSc) provided input on using [$^{13}$N]$NH_3$ for measuring myocardial blood flow in rats using small-animal PET imaging. Maria Kolajova (research associate) contributed to the execution and analysis of the in vitro studies. Dr. Robert deKemp added insight into the kinetic modeling and quantification of both tracers. Dr. Rob Beanlands participated in the interpretation of the data and provided a clinical perspective on the animal model of heart failure.

**Abstract**

Heart failure is associated with compensatory sympathetic overactivity, leading to pathologic changes in norepinephrine release, post-synaptic β-adrenergic receptor (β-AR) expression and intracellular cAMP signal transduction. A rat model of surgically-induced myocardial infarction has been used to evaluate the alterations in cAMP-specific phosphodiesterase-4 (PDE4) using (*R*)-[$^{11}$C]rolipram with positron emission tomography (PET), 8-12 weeks following the ligation of the left anterior descending coronary artery. Cardiac function, infarct size and myocardial blood flow were assessed non-invasively using echocardiography and [$^{13}$N]$NH_3$ PET. Changes in the β-adrenergic receptors (β-AR) and PDE4 protein expression, as well as PDE4 enzyme activity were evaluated at 8-12 weeks post-myocardial infarction. Ejection fraction and fractional shortening were reduced in rats that underwent myocardial infarction compared to the sham-treated animals, confirming cardiac dysfunction. Altered adrenergic signaling was evident from decreased expression of $\beta_1$-AR. Distribution volumes reflecting (*R*)-[$^{11}$C]rolipram retention in the non-infarcted region of the left ventricle were significantly increased by 17% in rats that underwent ligation surgery, despite no change in myocardial blood flow in non-ischemic regions. In vitro studies detected no change in PDE4 enzyme activity or PDE4A, B or D subtype expression in the left ventricle homogenates. Elevated in vivo (*R*)-[$^{11}$C]rolipram retention suggests that the normally-perfused myocardium exhibits increased PDE4 levels even with the downregulation of the $\beta_1$-AR adrenergic receptors 8 weeks following myocardial infarction.

***Key Words:*** Positron emission tomography, rolipram, noradrenergic signal transduction, infarct, cAMP, phosphodiesterase-4

## INTRODUCTION

The sympathetic nervous system regulates heart rate and cardiac contractile strength by releasing noradrenaline (NA) and stimulating post-synaptic β adrenergic receptors (β-AR) (Brodde, 1993; Dzimiri, 1999). Both $\beta_1$- and $\beta_2$-AR subtypes are coupled by the G-protein $\alpha_S$ subunit to adenylyl cyclase, increasing the production of the second messenger cyclic adenosine 4,5-monophosphate (cAMP) (Brodde, 1993; Dzimiri, 1999) and thus activating protein kinase A (PKA). Subsequent phosphorylation of the intracellular effector proteins L-type $Ca^{2+}$ channels, ryanodine receptors and troponin by PKA increases $Ca^{2+}$ influx and sensitivity in the cardiomyocytes (Osadchii, 2007), resulting in chronotropic and inotropic effects (Dzimiri, 1999).

The intracellular cAMP signal is terminated through the conversion to AMP by the phosphodiesterase (PDE) family of enzymes (Dzimiri, 1999). The cAMP-selective rolipram-sensitive PDE4 subfamily comprises products of four genes (PDE4A-D) encoding multiple variants classified as short or long by the presence of the upstream conserved regions (Houslay, 2001). PDE4A, B and D subtypes account for approximately 50% of cAMP catalysis in the rat cardiomyocytes (Shahid and Nicholson, 1990; Lugnier et al., 1999; Maurice et al., 2003; Osadchii, 2007), while PDE4C subtype is not detected in rat hearts (Kostic et al., 1997). PDE4 activity and expression are regulated by the intracellular levels of cAMP through phosphorylation by PKA of the long isoforms, which increases catalytic activity within 15 minutes of increased cAMP (Houslay, 2001; Laliberte et al., 2002). Sustained elevation in intracellular cAMP levels results in increased PDE4 protein expression, through the PKA-mediated activation of cAMP response element binding protein and increased PDE4 transcription (Houslay, 2001).

PDE4 activity is also susceptible to modulation by the mitogen-activated protein kinase (MAPK) signaling pathway, with phosphorylation by the extracellular signal-related kinase (ERK2) reducing the catalytic activity of the long isoforms and stimulating short PDE4 enzymes (Hoffmann et al., 1999; Baillie et al., 2000).

$^{11}$C-labeled PDE4 inhibitor (*R*)-rolipram has been recently characterized for use in PET imaging of cardiac PDE4 in vivo (Lourenco et al., 2006; Kenk et al., 2007). Ex vivo biodistribution and in vitro autoradiography studies have shown (*R*)-[$^{11}$C]rolipram to bind cardiac PDE4 specifically, with selectivity for the PDE4 subtype over other cardiac PDE enzymes (Kenk et al., 2007). In vivo, (*R*)-[$^{11}$C]rolipram shows a high contrast between the myocardium and surrounding tissues, with distribution volumes (DVs) derived using Logan graphical analysis providing a quantitative measure of tracer retention (Thomas et al., 2010). (*R*)-[$^{11}$C]Rolipram provides an indirect index of cAMP signaling and a means to evaluate intracellular cAMP-mediated signaling in the heart.

Heart failure, the final common pathway for most forms of cardiac disease, is characterized by a compensatory increase in sympathetic drive and cardiac NA release in response to the reduction in cardiac output (Katz, 1986; Summers et al., 1995). Sustained elevation in myocardial NA levels causes direct toxicity (Haft, 1974), initiates maladaptive processes including cardiac remodeling (McDonald et al., 1994) and leads to β adrenergic receptor (β-AR) desensitization and altered signal transduction in the left ventricle (Bristow et al., 1982; Feldman, 1993; Akhter et al., 1999; Dzimiri, 1999; Laurent et al., 2001), ultimately resulting in increased mortality (Cohn et al., 1984).

Non-invasive measurement of changes in the PDE4 levels would provide insights into the alterations of the intracellular cAMP-mediated signal transduction in heart failure.

The aim of this study was to evaluate changes in PDE4 levels using (*R*)-[$^{11}$C]rolipram PET imaging and myocardial blood flow (MBF) with [$^{13}$N]$NH_3$ at late time-points (8-12 weeks) following surgically-induced myocardial infarction. In vivo findings are correlated with in vitro quantification of changes in β-AR and PDE4 protein expression, as well as PDE4 activity in tissue homogenates.

## MATERIALS AND METHODS

*Animals.* Sixty-three male Sprague-Dawley rats (Charles River, Montreal, Canada) initially weighing 200-275 g were maintained on a 12-hour light/dark cycle with free access to food and water. All animal experiments described herein were conducted according to the guidelines of the University of Ottawa Animal Care Committee and the Canadian Council on Animal Care for the use and care of laboratory animals. No mortality or adverse physiological responses were observed during echocardiography studies, or [$^{13}$N]$NH_3$ or (*R*)-[$^{11}$C]rolipram PET scans.

*LAD ligation.* Rats ($n$=48) were anaesthetized with 2% isoflurane, intubated and attached to a ventilator. Left anterior descending coronary artery (LAD) ligation was performed as previously described (Higuchi et al., 2008), inducing a myocardial infarction (MI). Briefly, a cranio-caudal incision was made on the chest and the pectoral muscles blunt dissected apart, exposing the third and fourth intercostal space. A thoracotomy was performed and the thymus retracted to allow localization of the pulmonary trunk and the left atrium. Silk suture (6-0) was driven using a small curved needle under the LAD, and the ligature tied. An additional suture was used if the blanching of the myocardium was not observed downstream of the ligation. A large portion of the left ventricle in the LAD-

ligated animals was observed to be affected (blanched at time of ligation, thinned at dissection; Figure 7-1). Ribs were stitched together using vicryl suture (3-0) and the air gently squeezed out of the thoracic cavity. Pectoral muscles were re-positioned and the wound closed by staples. Animals were recovered using ventilation with high oxygen. Buprenorphine was administered twice daily by s.c. injection for post-operative analgesia and animals monitored for 3 days following surgery. In 15 sham animals, the heart was exposed and the cavity sealed without ligating the LAD.

*Echocardiography studies.* Animals underwent echocardiographic studies 1, 7 and 11 weeks following surgery using the Vevo 770 high-resolution imaging system (VisualSonics, Toronto, Ontario). Rats were anaesthetized with isoflurane (1–2%) and hair removed from the abdomen. Parasternal long axis and short axis views were recorded in B- and M-mode, with the motion of the cardiac walls recorded by summation across several cycles using the ECG-based kilohertz visualization (EKV) mode (Cherin et al., 2006). The 716B scanhead was used, at the transducer frequency of 23.5 MHz, focal length of 17.5 mm and a field of view of 32 mm. M-mode recordings were used to visually confirm the presence of the infarct and observe the wall motion abnormality. B-mode EKV cine loops were used to delineate the shape of the left ventricle (endocardial and epicardial edge, as well as the major axis) at systole and diastole, allowing calculation of the left ventricle volume. Measured dimensions were used to calculate the ejection fraction (EF), fractional shortening (FS), stroke volume (SV) and the mass of the left ventricle using manufacturer-provided software (Vevo 770 3.0, VisualSonics).

*Radiochemistry.* [$^{13}$N]$NH_3$ was synthesized using routine clinical protocols. (*R*)-[$^{11}$C]Rolipram (specific activity 37-128 GBq/μmol; 997-3459 mCi/μmol) was

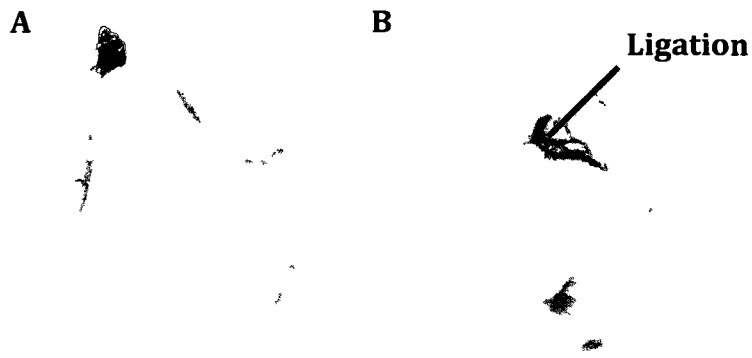


Figure 7-1: Representative post-mortem photographs of a sham-treated (A) and infarcted (B) heart, showing the location of the ligation and the scarred appearance of the ischemic left ventricle.

synthesised as previously described (DaSilva et al., 2001). Tritiated [5,7-$^{3}$H](-)CGP12177 (specific activity 33 mCi/μmol) was purchased from Perkin-Elmer (Boston, MA).

*[$^{13}$N]NH$_3$ PET imaging.* PET scans using [$^{13}$N]NH$_3$ were performed 1 week following surgery (Figure 7-2), as well as coupled with the (*R*)-[$^{11}$C]rolipram scans 8-12 weeks post-MI. Rats were anaesthetized with isoflurane (1-2%) and a 26G catheter inserted into the tail vein. Animals were positioned in the Siemens Inveon$^{TM}$ small animal PET scanner (Siemens, Knoxville, TN; 12.7 cm axial field-of-view, spatial resolution ≤ 1.4 mm) and administered 44.4–125.8 MBq (1.2–3.4 mCi MBq) [$^{13}$N]NH$_3$ in a bolus injection (<1.0 mL volume) via tail vein. List-mode data were gathered over 30 minutes, followed by a 10 min transmission scan. PET data was histogrammed into 20 frames (12×10sec, 3×60 sec and 5×300 sec) and reconstructed on a 128×128 image matrix with 0.34×0.34×0.80 mm pixel size using ordered-subsets expectation maximization 3D/maximum a posteriori (OSEM3D/MAP; β=1.0 OSEM3D iterations=2 MAP iterations=18). Corrections for detector dead-time, isotope decay, detector efficiencies, randoms, scatter and attenuation were incorporated in the image reconstruction. In-house developed software FlowQuant© was used to orient the left ventricle and generate relative uptake polar maps from the last 28 min of the scan data. Myocardial blood flow (MBF) polar maps were generated (representing flow in mL/min/g) using the 0–2

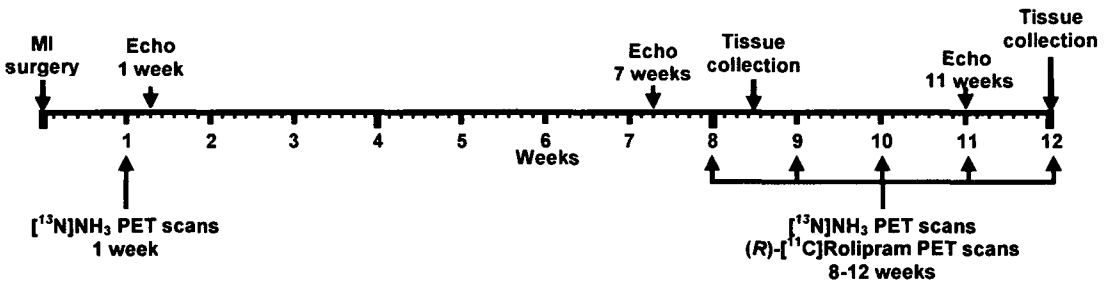


Figure 7-2: Timeline of experiments performed on myocardial infarction rats. Echocardiography was performed at 1, 7 and 11 weeks following LAD ligation to observe the progression of cardiac dysfunction. Rats underwent an early [$^{13}$N]$NH_3$ scan 1 week following surgery to establish the presence of a perfusion defect. (*R*)-[$^{11}$C]rolipram and second [$^{13}$N]$NH_3$ PET scans were performed between 8 and 12 weeks following LAD ligation. Tissues used for heart weight measurements, in vitro experiments and histology were collected by sacrificing a subset of rats at 8 and 12 weeks post-MI.

min data and a one tissue compartment model. Mean blood flow of the high uptake (>75% of the maximal observed blood flow) regions of the polar map were used to evaluate any changes in regional tissue perfusion.

*(R)-[$^{11}$C]Rolipram PET imaging.* Full dynamic data were acquired for 60 minutes following i.v. administration of 14.8–33.3 MBq (0.4–0.9 mCi; injected cold mass of 0.05–0.12 μg) of (*R*)-[$^{11}$C]rolipram via the tail vein in anaesthetized animals 8 to 12 weeks post-infarct. Data was histogrammed into 26 frames (12×10 sec, 3×60 sec and 11×300 sec). Image reconstruction was performed as previously described (Thomas et al., 2010). FlowQuant© software was used to perform Logan graphical analysis with a constant recovery coefficient (0.6) and generate (*R*)-[$^{11}$C]rolipram DV values from the 20–60 min portion of the PET scan.

*Heart weight.* Rats (*n*=20) were sacrificed by decapitation 8 or 12 weeks following LAD ligation. Hearts were dissected out and weighed.

*Histology.* Hearts dissected out following sacrifice were preserved in 4% paraformaldehyde, embedded in paraffin and sliced into 5 μm-thick short-axis slices. Tissue slides were stained using standard histological techniques for the Masson trichrome and Hematoxylin/eosin stains. Imaging of slices was performed using a Lecia microscope connected to Leica workstation software (Leica Microsystems Inc., Richmond Hill, Ontario).

*Protein immunoblotting for β-AR and PDE4.* Changes in β-AR and PDE4 protein expression were assessed in rat heart tissue with immunoblot techniques using the Bio-Rad western blot system (Bio-Rad Laboratories, Ltd., Mississauga, Ontario) for SDS – PAGE and Western blot analysis, according to manufacturer's instructions. Briefly,

hearts were excised, flash-frozen and pulverized using a mortar and pestle under liquid $N_2$. Aliquots of powdered tissue were homogenized using a Polytron Homogenizer (2 × 15 sec) in lysis buffer (25 mM Tris·HCl, 2% Triton X100, pH 7.8), containing protease inhibitors (Complete protease inhibitor cocktail, Roche Canada, Mississauga, Ontario) and lysed for 20 min on ice. Lysates were centrifuged for 10 min at 12000×g. Aliquots of supernatant were collected and stored at -80°C. Protein concentration was determined using the Pierce Bicinchoninic acid (BCA; Novagen, San Diego, USA) protein assay. Samples of the protein mixture were run on 8% Tris-glycine reducing SDS-PAGE, and separated proteins were transferred to a PVDF (polyvinylidene fluoride) membranes. After transfer, the membranes were treated for 1 h with blocking solution (150 mM NaCl, 10 mM Tris, 1% Tween20 and 5% skim milk, pH 8) and incubated with primary antibodies using manufacturer-recommended dilutions. Primary antibodies used were; anti-$\beta_1$-AR rabbit polyclonal antibody (abcam, ab3546), anti-$\beta_2$-AR rabbit polyclonal antibody (Santa Cruz Biotechnology, Inc., H-20sc-569), anti-PDE4A polyclonal rabbit antibody (FabGennix Inc., PDE4-112AP), anti-PDE4B polyclonal rabbit antibody (Santa Cruz Biotechnology, Inc., H-56 sc-25812) and anti-PDE4D polyclonal rabbit antibody (Santa Cruz Biotechnology, Inc., H-69 sc-25814). A mouse monocolonal antibody against glyceraldehydes 3-phosphate dehydrogenase (GAPDH; Santa Cruz Biotechnology, Inc., 6C5, sc-32233) was used as a loading control (see appendix for details). Adsorbed antibodies were detected with horseradish peroxidase-conjugated appropriate secondary immunoglobulins and enhanced chemiluminescence substrate. The protein bands were visualized and analysed using a Fluor Chem HD image station (Alpha Innotech, San Leandro, CA) equipped with charge-coupled device camera and AlphaEase

FC IS-990 image analysis software (Alpha Innotech). Data were expressed as a ratio of the target protein to the GAPDH protein band intensities, normalized to the mean of sham controls for each membrane.

*Measurement of PDE4 activity.* PDE4-mediated breakdown of cAMP in the cardiac tissue was measured using a PDE4 Enzymatic Assay Kit (PDEasy-200, FabGennix; Frisco, Texas), based on the methods first described by Thompson and Appleman (Thompson and Appleman, 1971). Non-infarcted left ventricular tissue from MI and control rats were excised, flash-frozen, powdered and stored at -80°C. Immediately before the assay, powdered aliquots were homogenized as described above, substituting a SolO buffer (FabGennix) for lysis buffer. Extracted protein (concentration in reaction vial 0.2 mg/mL) was added to incubation mixtures containing manufacturer-provided buffers, and (in blocked samples) (*R/S*)-rolipram (500 μM). Following addition of [$^{3}$H]cAMP substrate (1 μM final concentration), tubes were incubated for 10 min with shaking at 34°C. The reaction was terminated by boiling the sample for 3 min. The PDE4 reaction product 5'-AMP was then hydrolyzed by incubation of the assay mixture with Crotalus Atrox snake venom for 15 min at 34°C. To separate the resulting [$^{3}$H]adenosine from [$^{3}$H]AMP and [$^{3}$H]cAMP, pre-activated ion exchange resin (FabGennix) was added to each tube, mixed by vortexing and incubated on ice for 15 min. Tubes were centrifuged at 13000×g for 2 min, the supernatant containing unbound [$^{3}$H]adenosine mixed with scintillation fluid (BCS-NA scintillation cocktail, Amersham) and counted using a β-scintillation counter (1219 RackBeta liquid scintillation counter, LKB Wallac, Perkin-Elmer). PDE4 activity was defined as the fraction of cAMP PDE activity inhibited by

100 μM rolipram and expressed as pmol of cAMP hydrolyzed per minute per mg of protein.

*Statistical analysis.* All data are expressed as mean +/- SD. Data were compared using one-way ANOVA with $p<0.05$ considered significant.

## RESULTS

Among the rats that underwent MI surgery, all fatalities occurred during recovery or within the first 48 hours, with 15 out of 48 (31%) MI rats dying at these early time points.

*Echocardiography.* Echocardiography studies detected a regional abnormality in the left ventricle anterior lateral wall motion, as depicted in the representative short axis M-mode images (Figure 7-3). Quantitation of systolic and diastolic ventricular dimensions showed no change at 1 week following ligation, while MI rats exhibited significantly decreased EF and FS at 7 and 11 weeks post-surgery, compared to sham-treated controls (Table 7-1). Left ventricle mass estimated using the echocardiography analysis software showed no change between MI and sham-treated animals. Heart rate recordings obtained during the echocardiography studies showed no significant changes between the two groups at any of the time points assessed.

*[$^{13}$N]$NH_3$ infarct measurement.* FlowQuant© PET image analysis software generated reproducible polar maps displaying [$^{13}$N]$NH_3$ uptake following left ventricle re-orientation and quantification of the radioactive signal in the myocardium (Figure 7-4). In rats that underwent LAD ligation surgery, a defect in [$^{13}$N]$NH_3$ uptake was observed in the segments of the polar maps corresponding to the anterolateral areas of the left ventricle. The size of the defect induced by LAD ligation ranged from 24.1 to 59.6%

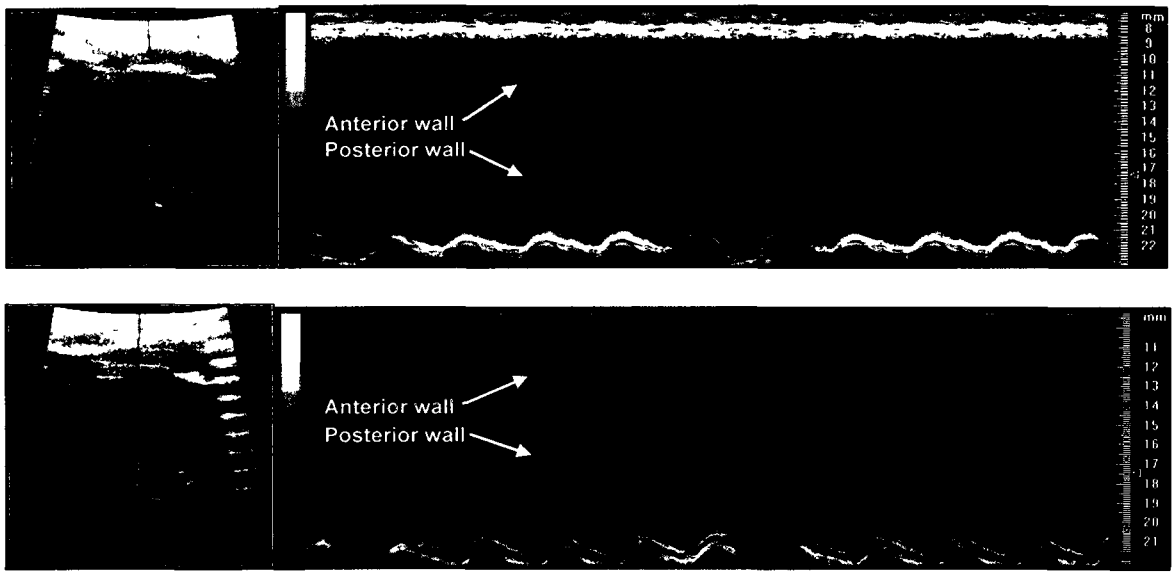


Figure 7-3: Representative short-axis M-mode echocardiography of MI (A) and sham-treated (B) rat 11 weeks following surgery, showing the absence of normal contractile motion in the anterior wall of the left ventricle of the rat that underwent LAD ligation.

Table 7-1: Cardiac function in post-MI rat model, evaluated by echocardiography 1, 7 and 11 weeks post-MI.

| | | LVEDV (μL) | LVESV (μL) | SV (μL) | % EF | % FS | LV mass | HR (bpm) |
|---|---|---|---|---|---|---|---|---|
| **1 Weeks** | **Sham (n=8)** | 385.7 ± 85 | 116.4 ± 47 | 269.3 ± 55 | 70.2 ± 7 | 65.0 ± 10 | 899.2 ± 163 | 358.9 ± 26 |
| | **MI (n=16)** | 404.9 ± 90 | 139.8 ± 45 | 265.1 ± 78 | 65.0 ± 10 | 47.4 ± 9 | 899.2 ± 163 | 359.9 ± 34 |
| **7 Weeks** | **Sham (n=7)** | 523.8 ± 104 | 121.6 ± 63 | 402.2 ± 97 | 76.8 ± 10 | 57.4 ± 10 | 1442.6 ± 309 | 335.7 ± 30 |
| | **MI (n=13)** | 670.0 ± 141 | 267.4 ± 127 | 402.6 ± 105 | 61.1 ± 13 * | 42.6 ± 12 * | 1373.5 ± 321 | 314.7 ±44 |
| **11 Weeks** | **Sham (n=3)** | 483.8 ± 95 | 125.2 ± 23 | 358.6 ± 82 | 73.8 ± 5 | 52.0 ± 6 | 1319.1 ± 361 | 322.0 ± 64 |
| | **MI (n=7)** | 659.7 ± 173 | 306.0 ± 128 | 353.7 ± 106 | 54.3 ± 10 * | 36.5 ± 9 * | 1597.0 ± 206 | 315.9 ± 36 |

* $p<0.05$, one-way ANOVA

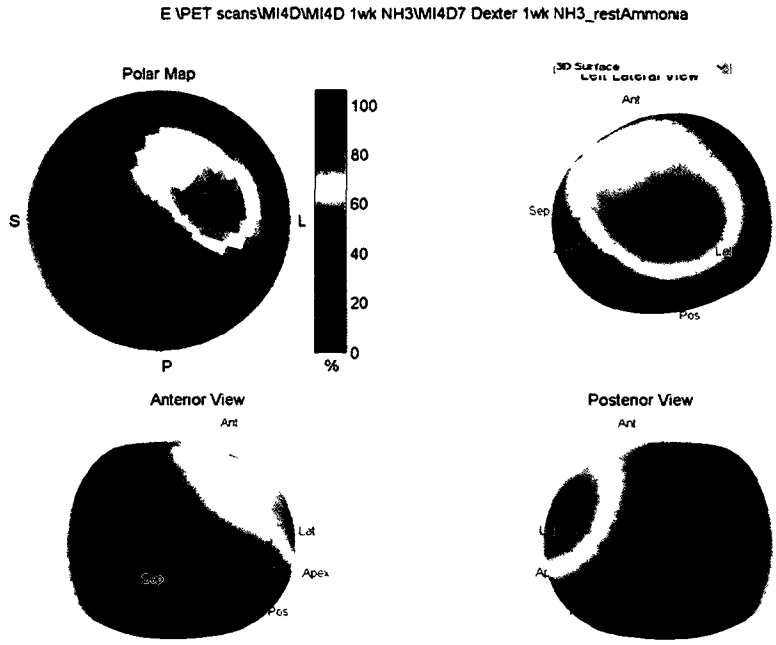


Figure 7-4: Representative polar map displaying left ventricle [$^{13}$N]$NH_3$ relative uptake determined by PET imaging and produced following reorientation of the myocardium using FlowQuant© software. Areas with low tracer uptake correspond to the infarcted region.

(mean 44.3% ± 11.6) of the total left ventricle area. Application of the one-compartment kinetic model to the data, with the left ventricle lumen radioactivity taken as the input function, generated reproducible MBF values, as previously published by Lamoureux et al. (Lamoureux et al., 2010 (Submitted)). In the non-infarcted myocardium, there was no detectable difference in MBF between the MI and sham-treated animals (2.9 ± 0.3 ml/min per g and 3.0 ± 0.3 mL/min per g, respectively).

*(R)-[$^{11}$C]rolipram imaging.* Uptake of (*R*)-[$^{11}$C]rolipram produced clearly delineated images of the myocardium, showing an anterolateral wall defect in tracer uptake corresponding to the area of low [$^{13}$N]$NH_3$ uptake (Figure 7-5). Quantification of tracer retention in the non-infarcted area of the left ventricle as Logan slope values resulted in a 17.3% significant increase ($P < 0.01$, one-way ANOVA) in DV values of MI rats compared to shams (Figure 7-6).

*Heart mass measurements.* Weights of the hearts of MI-treated rats were generally higher than those of sham-treated controls (Table 7-2). Once expressed relative to the rat body weight, however, there was no difference between the MI and sham-treated rats at both 8 and 12 weeks following infarct induction.

*In vitro experiments.* Staining with Masson Trichrome and Hematoxylin and Eosin stains has confirmed the presence of wall thinning and fibrosis in the scar (Figures 7-7 and 7-8), confirming the infarcted area identified by PET imaging. $\beta_1$-AR expression was reduced by 21% (p=0.019) in the MI-treated rats, as compared to the sham-treated controls, without a change in the $\beta_2$-AR subtype (Figure 7-9). PDE4 subtypes A, B and D showed no difference between the MI rats and sham-treated controls (Figure 7-10). Assessment of PDE4 activity in homogenates prepared from the hearts of MI and non-infarcted sham

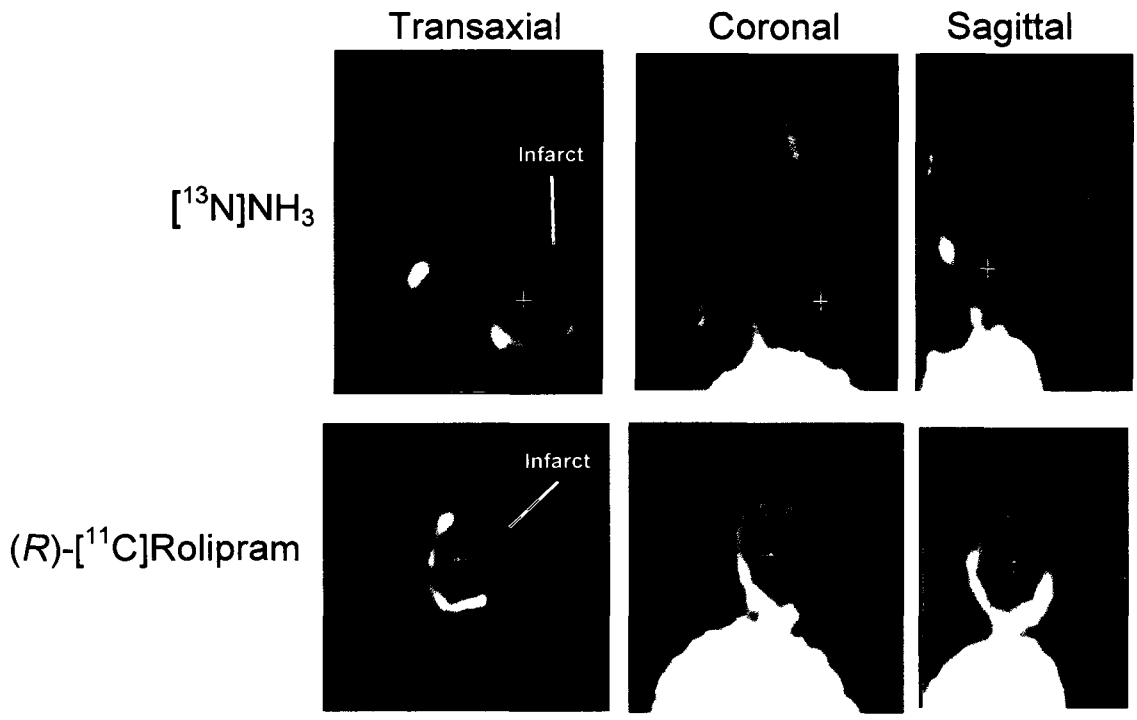


Figure 7-5: PET images obtained following [$^{13}$N]NH$_3$ and (*R*)-[$^{11}$C]rolipram administration in rats that underwent LAD ligation (MI), displaying the transaxial, coronal and sagittal orientations. The area showing decreased tracer uptake corresponds to the perfusion defect in both [$^{13}$N]NH$_3$ and (*R*)-[$^{11}$C]rolipram images.

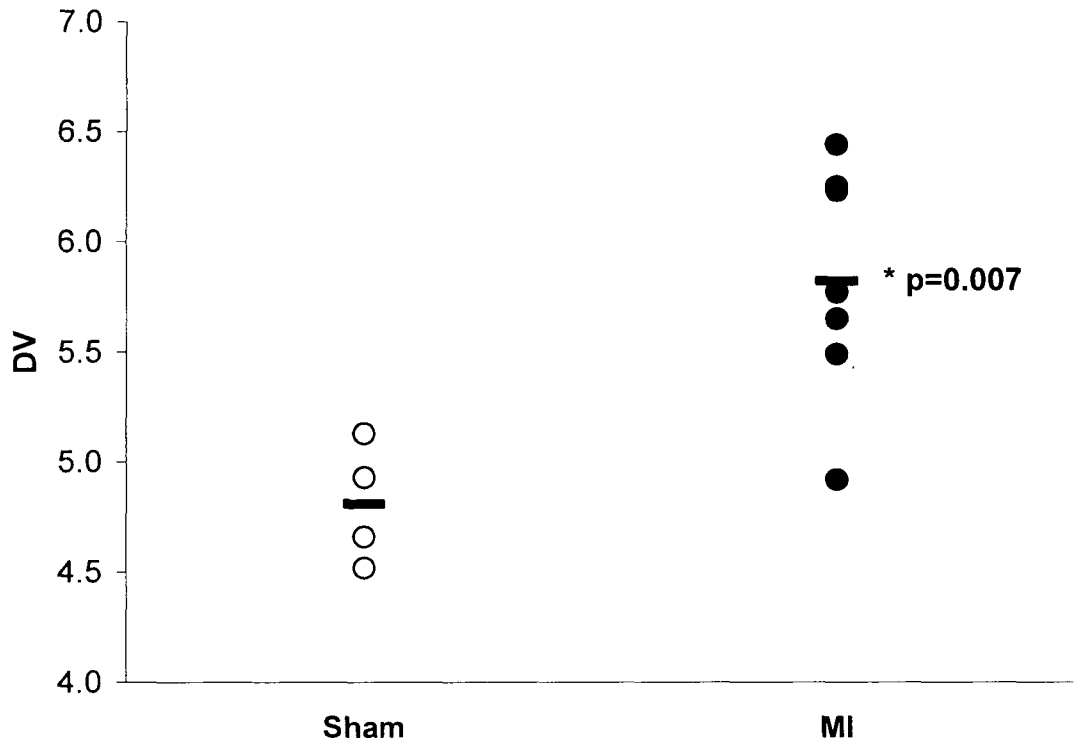


Figure 7-6: Logan DV values calculated from (*R*)-[$^{11}$C]rolipram PET scans of rats that underwent MI (●, n=8) or sham surgery (○, n=4), with mean values marked (—). Significance was evaluated with one-way ANOVA.

Table 7-2: Heart weights of MI and sham-treated rats, as measured at sacrifice.

| | | **Heart weight (g)** | **Body weight (g)** | **Heart weight/ body weight** |
|---|---|---|---|---|
| **8 weeks** | **Sham (n=8)** | 1.29 ± 0.15 | 507.6 ± 60.8 | 0.0026 ± 0.0002 |
| | **MI (n=12)** | 1.39 ± 0.11 | 538.2 ± 42.1 | 0.0026 ± 0.0002 |
| **12 weeks** | **Sham (n=3)** | 0.98 ± 0.07 | 516.7 ± 51.6 | 0.0019 ± 0.0002 |
| | **MI (n=4)** | 1.14 ± 0.07 | 551.4 ± 69.8 | 0.0021 ± 0.0003 |

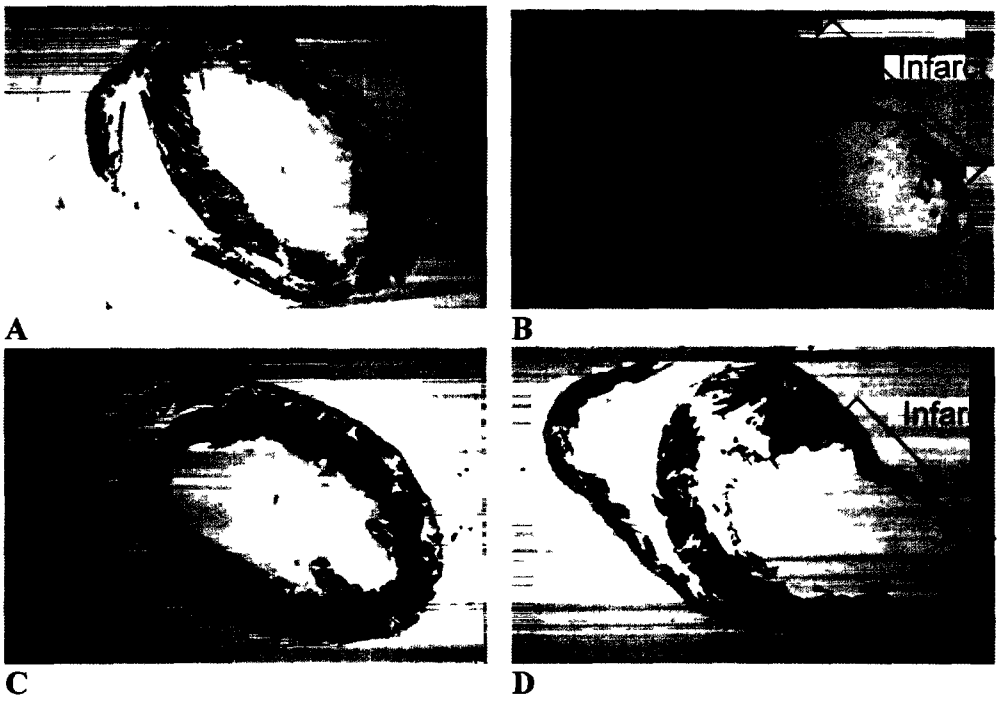


Figure 7-7: Hematoxyllin-Eosin (A, B) and Masson Trichrome stain image (C, D) (1× magnification) of the short-axis cardiac slices from sham (A, C) and MI (B, D) rats, 8 weeks post MI.

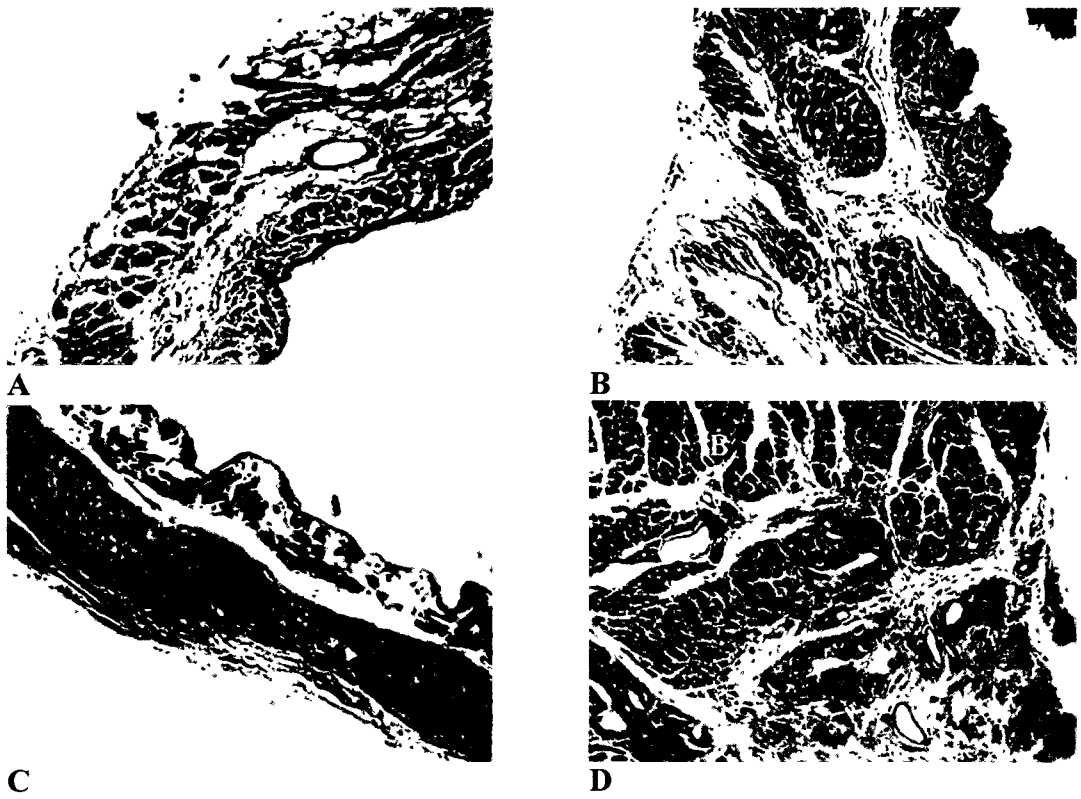


Figure 7-8: Hematoxyllin-Eosin (A, B) and Masson Trichrome stain image (C, D) (100× magnification) of the infarct scar (A, C) and peri-infarct area (B, D), 8 weeks post-MI.

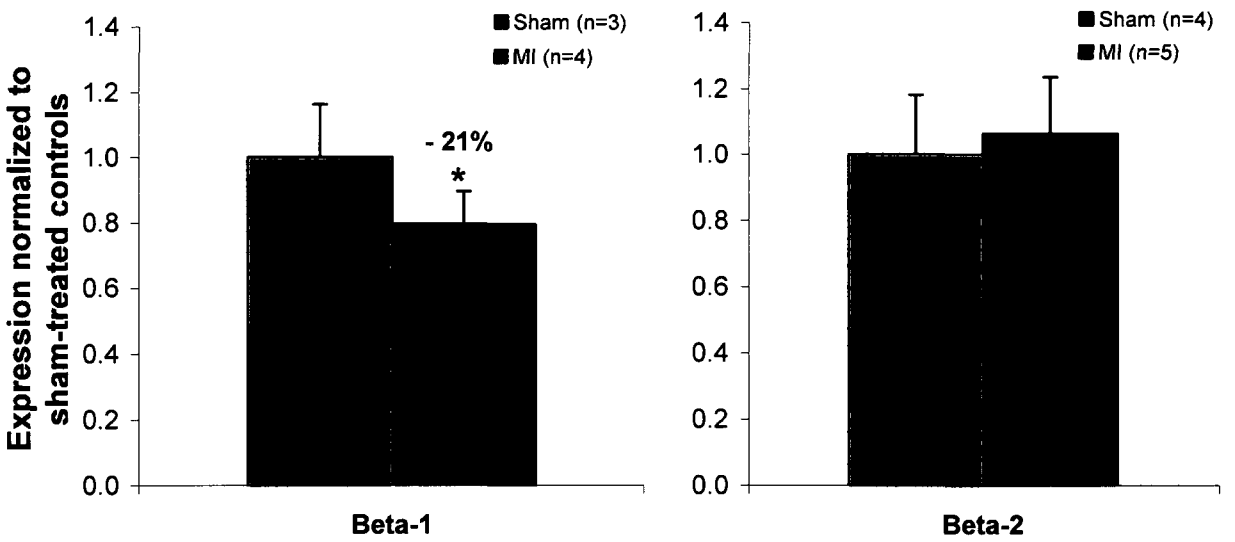


Figure 7-9: Western blot quantification of $\beta_1$- and $\beta_2$-AR expression in the non-infarcted left ventricle homogenates at 8 weeks post-MI. Band intensity is normalized to GAPDH, then expressed as ratio to sham-treated controls. * $p<0.05$ one-way ANOVA compared to sham-treated controls.

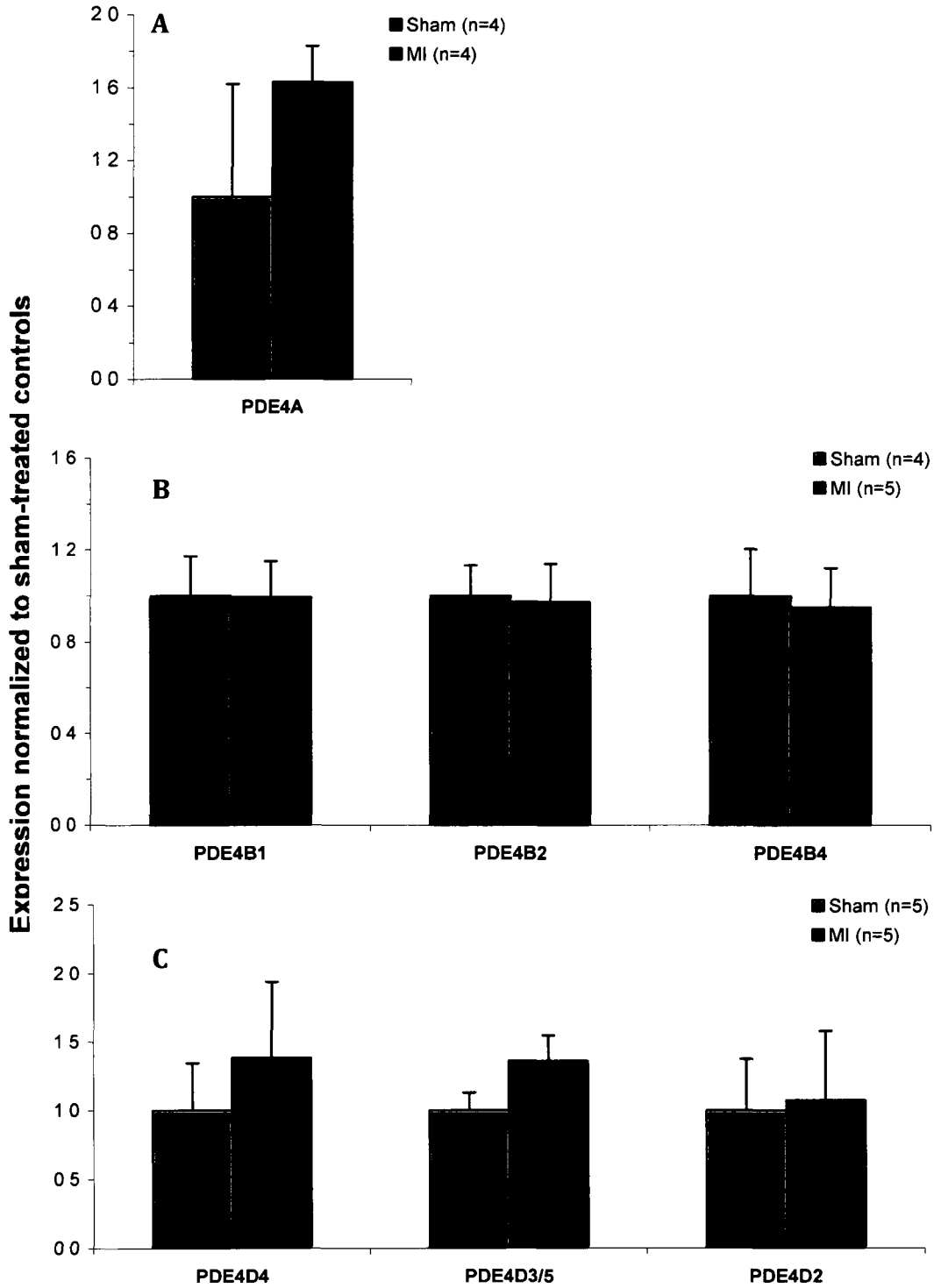


Figure 7-10: Western blot quantification of PDE4A (A), PDE4B (B) and PDE4D (C) subtype expression in the non-infarcted left ventricle homogenates at 8 weeks post-MI. Data is normalized to GAPDH, then expressed as a ratio to sham-treated controls.

rats exhibited no difference in PDE4 cAMP-catalyzing activity (Figure 7-11) between MI and controls.

## DISCUSSION

A variety of animal models of heart failure have been proposed, ranging from pharmacological (isoproterenol (Osadchii et al., 2007), anthracycline (Tong et al., 1991; Kenk et al., 2010)), surgical (myocardial infarction (Ahmet et al., 2005), aortic banding (Abi-Gerges et al., 2009)) and genetic (TNF-α overexpression (Shusterman et al., 2009)) with varying degrees of invasiveness, severity and clinical relevance. Rats in the current study exhibited a functional defect in cardiac function at 7 and 12 weeks following LAD ligation, as evidenced by the changes in EF and FS measured with echocardiography. The values obtained correspond to previously reported post-MI changes (EF and FS decreased by ~25-50% following infarction (Wu et al., 2004; Suuronen et al., 2007; Swaney et al., 2007; Rodriguez-Porcel et al., 2008)). The progressive nature of cardiac dysfunction has been reported in this animal model, with measurable defects observed 4 weeks post-surgery (Sanbe et al., 1993). Larger decreases have been reported using M-mode echocardiography analysis in Wistar rats following LAD ligation (FS values of 37% in sham treated vs. 19% in LAD-ligated rats), likely due to different echocardiographic methods used (Lee et al., 2010). In this study, wall motion abnormality was observed in the anterolateral portion of the left ventricle in the short axis B-mode cine videos. The presence of a fibrous scar was confirmed by histology at the anteriolateral left ventricle, the area perfused by the LAD. Despite expected dilatation and structural remodelling of

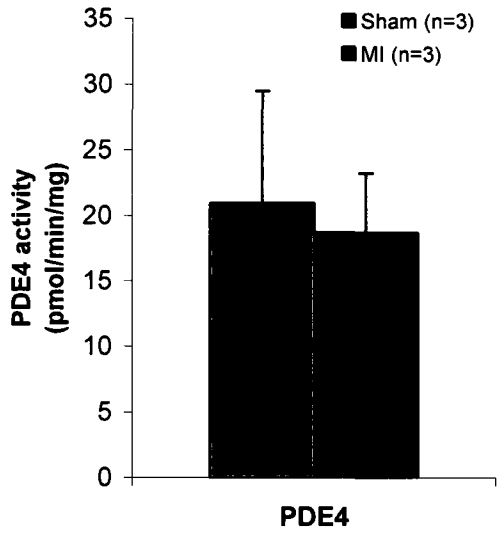


Figure 7-11: PDE4 enzyme activity in the homogenates of non-infarcted portions of the LV of MI and sham-treated rats, expressed as pmol of cAMP hydrolyzed per min per mg of protein. PDE4 activity was determined by incubating the first (cAMP-hydrolyzing) step in the presence of (*R/S*)-rolipram.

the left ventricle post-infarct, no change was observed in the heart weight/body weight ratios, possibly due to the loss of myocardial mass in the scar region in the MI animals.

It has previously been shown that the area of reduced [$^{13}$N]$NH_3$ uptake correlates with the perfusion defect, making [$^{13}$N]$NH_3$ PET an appropriate non-invasive technique for evaluating the area of the myocardium affected by ischemia (Kudo et al., 2002). [$^{13}$N]$NH_3$ PET scans confirmed the localization of the infarct, displaying a myocardial uptake defect in the polar map segments corresponding to the left ventricle anterior free wall. In the context of previously reported rat MI experiments, the observed infarct sizes would be classified as moderate (~30%) (Gosselin et al., 1998; Yoshida et al., 2001). It is important to note that the presence of the infarct did not affect the MBF values calculated in the non-infarcted (high-uptake) region of the left ventricle, suggesting that the blood flow, and therefore delivery of (*R*)-[$^{11}$C]rolipram, in the intact myocardium is not affected.

A unifying factor in the presumed mechanism of heart dysfunction in animal models of heart failure is the sustained sympathetic hyperactivity (Tong et al., 1991; Lymperopoulos et al., 2007), with a resulting decrease in post-synaptic responsiveness to the adrenergic agonists. In parallel with the elevation of cardiac NA levels, NA reuptake is decreased (Bohm et al., 1995; Eisenhofer et al., 1996) and post-synaptic responsiveness to adrenergic agonists diminished (Dzimiri, 1999). Desensitization of β-AR in heart failure proceeds in part through a selective downregulation of cardiac $\beta_1$-AR (Haft, 1974; Feldman, 1993; Xiao et al., 1999), producing a shift in the $\beta_1$-AR/$\beta_2$-AR ratio from 4:1 towards 1:1 in failing cardiomyocytes of rabbits, mice, dogs and humans (Bristow et al., 1989; Akhter et al., 1997; Akhter et al., 1999l; Koch et al., 2000; Laurent

et al., 2001; Pavoine and Defer, 2005). While in the normal heart the $\beta_2$-AR are strongly coupled to activation of adenylyl cyclase (Levy et al., 1993; Brodde et al., 2001; Steinberg and Brunton, 2001; Pavoine and Defer, 2005), in the failing heart $\beta_2$-AR were found to be uncoupled from $G_{\alpha s}$ and switch to inhibiting adenylyl cyclase through the $G_{\alpha i}$ subunit (Kiuchi et al., 1993; Bristow, 2000). Downstream of the β-AR, failing hearts exhibit increased $G_{\alpha i}$-proteins (Tse et al., 2000; Yoshida et al., 2001), as well as diminished myocardial adenylyl cyclase activities (Feldman et al., 1987; Feldman, 1993; Tse et al., 2000; Eckhart and Koch, 2002). In vivo PET studies display clinical predictive value of imaging presynaptic NA reuptake with [$^{11}$C]HED (Pietila et al., 2001) and have been used to confirm the downregulation of β-AR using [$^{11}$C]CGP12177 (Merlet et al., 1993; Delforge et al., 2002).

Retention and specific binding of (*R*)-[$^{11}$C]rolipram have been previously shown to increase by ~30% following treatments that increase cAMP, including NA-elevating agents (Lourenco et al., 2006; Kenk et al., 2010; Thomas et al., 2010). (*R*)-[$^{11}$C]Rolipram has been previously applied by our group in animal models of obesity and adriamycin-induced heart dysfunction, showing reduced responsiveness to acutely increased NA levels in these hyperadrenergic states (Greene et al., 2009; Kenk et al., 2010). Recent experiments have characterized the retention of (*R*)-[$^{11}$C]rolipram in the rat myocardium using small animal PET imaging (Thomas et al., 2010). High uptake and contrast were found between the myocardium and surrounding tissue, as well as reproducible quantification of the tracer uptake using DV values derived using the Logan graphical analysis (Thomas et al., 2010). In the current experiments, using full kinetic analysis of tracer distribution, a defect in (*R*)-[$^{11}$C]rolipram uptake was observed in the area of the

myocardium corresponding to the reduced [$^{13}$N]$NH_3$ uptake and the fibrotic scar identified by histology. As determined using quantitative analysis, (*R*)-[$^{11}$C]rolipram retention was increased by 17% in the non-infarcted portions of the left ventricle 8-12 weeks following LAD ligation, with no changes in MBF.

Cardiac infarction and contractile dysfunction observed in this animal model is correlated with a ~20% downregulation of $\beta_1$-AR expression, as detected by the immunoblotting techniques. As expected, no difference in $\beta_2$-AR expression was observed between MI and sham-treated rats, confirming the widely reported subtype-specific $\beta_1$-AR downregulation (Bristow et al., 1982; Feldman, 1993; Akhter et al., 1999; Bristow, 2000; Laurent et al., 2001). In analyzing anti-PDE4 western blots, molecular weights obtained from the literature were used to identify individual observed subtypes (Kostic et al., 1997; MacKenzie et al., 2000; Dodge et al., 2001; Rena et al., 2001; Richter et al., 2005). Despite a trend towards an increase in PDE4A subtypes, no change was detected in the expression of any of the subtypes recognized by the antibodies. In vitro PDE4 enzyme activity assays performed on frozen LV non-infarcted tissue of MI and sham-treated rats failed to detect a difference in PDE4 activity, in agreement with the pacing-induced HF model (Tse et al., 2000), but in contrast to the studies performed in the aortic banding or hypertensive rats (Takahashi et al., 2002; Abi-Gerges et al., 2009).

At normal NA levels, a downregulation in $\beta_1$-AR would be expected to reduce PDE4-specific (*R*)-[$^{11}$C]rolipram binding due to diminished cAMP formation and thus reduced enzyme levels. The increased (*R*)-[$^{11}$C]rolipram retention observed in the presence of decreased $\beta_1$-AR expression could tentatively be explained by the overstimulation of the

β-AR on the cell surface by the elevated NA levels in cardiac dysfunction maintains elevated levels of intracellular signaling compared to baseline.

Studies evaluating alterations in adrenergic signaling downstream of the NA receptors have produced contradictory findings, with reports showing $G_{\alpha s}$ expression to be increased (Feldman et al., 1989; Sethi et al., 1998), decreased (Yoshida et al., 2001) or unchanged (Fu et al., 1994), depending on the animal model utilized. PDE4 activity and expression are elevated two-fold in a pressure-induced congestive heart failure model using salt-sensitive hypertensive rats, compared to salt-insensitive controls (Takahashi et al., 2002). Conversely, in a rat cardiac hypertrophy model, PDE4 activity is decreased by 53% in parallel with a 60% decrease in PDE4A and D subtype expression (Abi-Gerges et al., 2009). In a canine model using aortic valve placation and rapid pacing, no changes were observed in PDE4 enzyme activity (Tse et al., 2000). While the exact effect of cardiac dysfunction on PDE4 is still contentious, (*R*)-[$^{11}$C]rolipram PET imaging provides a novel in vivo technique for assessing PDE4 enzymes in their physiological milieu.

*Limitations*

Tissue NA levels were not measured as part of our experiments. Other groups have, however, quantified the myocardial catecholamine levels following LAD ligation, showing increased NA in the cardiac tissues and plasma (Lymperopoulos et al., 2007; Lee et al., 2010). Invasive hemodynamic assessment of cardiac function such as quantification of end-diastolic and end-systolic pressures was not performed since the focus of the study was on non-invasive evaluation. It has been suggested that PDE4

involvement in the control of cardiac function is exerted through localization with effector and modulator proteins such as β-arrestin and ryanodine receptor, creating subcellular compartments of cAMP (Lehnart et al., 2005). (*R*)-[$^{11}$C]Rolipram binds to PDE4 localized in the particulate and cytosolic portions of the cell, and is intended to serve as a tissue-level index of PDE4. (*R*)-[$^{11}$C]Rolipram binding does not differentiate between different subtypes, but rather can serve as an index of total intracellular PDE4. Western blot experiments are limited by the selectivity of the commercially-available antibodies to the individual subtypes, potentially leaving other PDE4 subtypes present in the heart undetected. Enzyme activity assay, performed on the tissue obtained from non-anaesthetized rats, in contrast to its use in cell cultures, is susceptible to a loss of sensitivity due to the deterioration of the enzyme at sample collection or the homogenate preparation steps. Findings presented here warrant further testing of the animal model, as well as support further investigation of neurohormonal PET imaging in heart failure patients. The lack of changes in PDE4 activity and expression as evaluated using in vitro methods emphasizes the need for non-invasive techniques capable of assessing impaired cAMP signaling in living organs, as evidenced by the importance of intracellular second messenger in a number of pathological states.

In conclusion, a LAD-ligation heart failure rat model, (*R*)-[$^{11}$C]rolipram PET imaging detects an increase in PDE4 tracer binding in non-ischemic tissue 8-12 weeks post-infarct, suggesting an increase in PDE4 levels at late stage of disease progression despite a downregulation of $\beta_1$-AR and normal perfusion. This study confirms the involvement of alterations in PDE4 enzymes and cAMP signaling in the intracellular pathological

molecular processes that follow changes in cardiac sympathetic regulation in heart failure.

**Acknowledgements**

The study was supported in part by a Canadian Institutes of Health Research (CIHR) grant FRN78520 and the Heart and Stroke Foundation of Ontario (HSFO) Program Grant on Molecular Function and Imaging (grant # PRG6242). S. L. Thorn was supported by a Heart and Stroke Foundation PhD Scholarship. R. S. Beanlands is a Career Investigator supported by the Heart and Stroke Foundation of Ontario. The authors thank Samantha Mason, Jeffrey Collins, Julian Walcott, Elena Dobrota and Paul Coletta for their assistance in radiotracer production in the radiochemistry laboratory, Myra Kordos and Julia Lockwood for technical assistance with PET imaging and Animal Care and Veterinary Staff for help with handling and monitoring of experimental animals.

**Manuscript #6 Appendix**

**Linearity of GAPDH as an internal control**

In our Western blot experiments, the intensity of bands representing PDE4A, B and D were normalized to the expression of GAPDH. β-actin and GAPDH (Figure 7-12) are the most commonly used internal controls for immunoblotting experiments, due to the ubiquitous expression in a range of tissues. GAPDH was selected for our studies due to the lack of any change in protein expression in cardiac disease states, the strength of the signal and ease of use. Linearity of the GAPDH expression has been established between 10 and 70 μg of loaded protein mass by plotting the amount of loaded protein against band intensity, with high observed correlation (Figure 7-13).

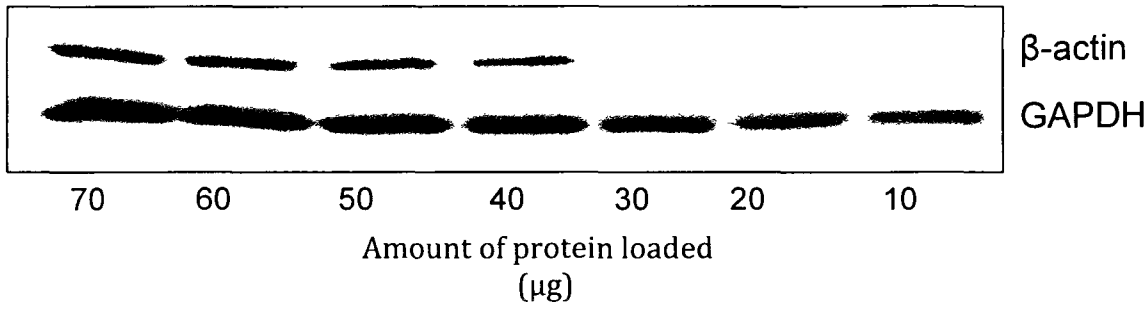


Figure 7-12: Representative Western blot with increasing amounts of loaded internal standards β-actin and GAPDH corresponding to the more intense bands. Gel electrophoreses were run as described in the Manuscript #6 Methods section.

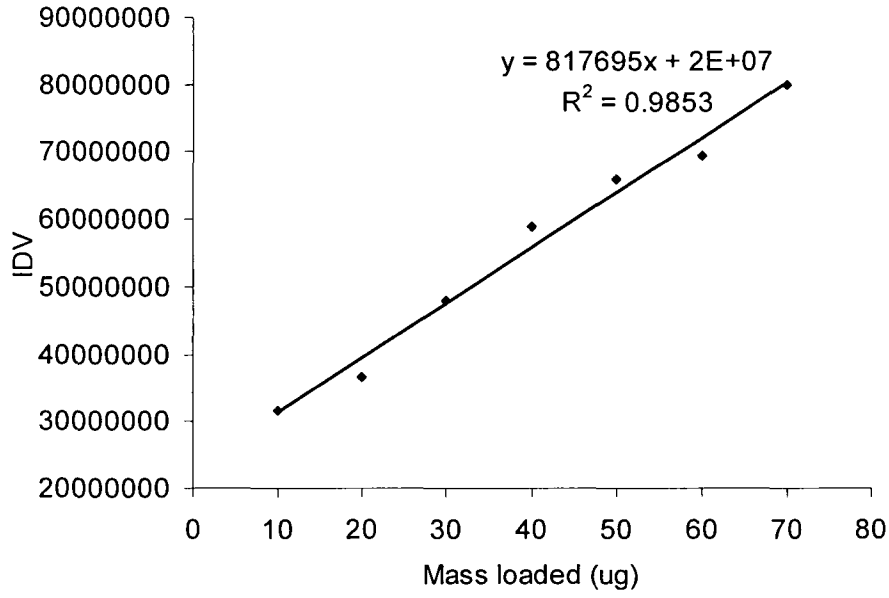


Figure 7-13: Correlation between integrated density values (IDV) and mass of GAPDH loaded on the electrophoresis gel. Results were obtained from one Western blot gel.

# CHAPTER 8: GENERAL DISCUSSION

Despite recent advances in the diagnosis and treatment of heart failure, mortality and morbidity remain high (Lloyd-Jones et al., 2010). Due to the overactivation of the sympathetic nervous system in cardiac disorders, β-blockers are commonly used as a first-line therapy to alleviate the pathogenic effects of adrenergic hyperactivity (Bristow, 2000; Rockman et al., 2002). The elucidation of the pathological processes that underlie disease development and therapy are limited by the available techniques. Currently, assessment of adrenergic innervation relies on measurements of indirect surrogate markers, such as muscle sympathetic nerve activity or plasma NA outflow from the heart, providing incomplete and potentially misleading data. Molecular intracellular mechanisms are generally analyzed by in vitro experiments performed on post-mortem or invasively-obtained tissue samples, or in cultured cell lines, with limited applicability to the living organism. Recent developments with PET tracers have provided novel tools for non-invasive assessment of sympathetic signaling components at the presynaptic NAT level and at the postsynaptic cell surface receptor, with proven clinical predictive value. The second messenger cAMP is a key element in the coupling of adrenergic cell surface receptors to the contractile machinery of the ventricular myocyte, with alterations in cAMP generation and degradation reported in cardiac disorders. The specific PDE4 inhibitor (*R*)-[$^{11}$C]rolipram has been characterized through the work presented in this thesis for non-invasive evaluation and quantification of changes in PDE4 enzymes, with the goal of indirectly assessing changes in cAMP signal transduction in cardiac dysfunction.

## 8.1. (*R*)-[$^{11}$C]rolipram and (*S*)-[$^{11}$C]rolipram characterization

This thesis continues the work initiated at the Centre for Addiction and Mental Health in Toronto, Ontario by Drs. Jean DaSilva and Celia Lourenco, which included the preliminary characterization of (*R*)-[$^{11}$C]rolipram for PET imaging of alterations in PDE4 signaling in the brain (Lourenco et al., 1999; Lourenco et al., 2001; DaSilva et al., 2002). The presence of specific binding of (*R*)-[$^{11}$C]rolipram to PDE4 in the myocardium, lungs, skeletal muscle and pancreas (Lourenco et al., 2006) suggests potential for applications of (*R*)-[$^{11}$C]rolipram in peripheral tissues. Treatments altering cAMP levels by affecting noradrenergic and serotonergic neurotransmission increased (*R*)-[$^{11}$C]rolipram specific binding in the brain, lung and the whole heart tissue. Following detection of saturable specific binding in the peripheral tissues, (*R*)-[$^{11}$C]rolipram was used for evaluation of cAMP-mediated PDE4 in cardiac diseases and disorders such as diabetes and metabolic syndrome. Work performed by MSc candidate Michael Greene in our lab has applied the PDE4-specific binding and responsiveness of (*R*)-[$^{11}$C]rolipram with DMI challenge to demonstrate dysfunctional intracellular response and altered NA signal transduction at the PDE4 level in peripheral tissues of diet-induced obese rats (Greene et al., 2009).

An important finding from the ex vivo characterization studies is the lack of blocking of (*R*)-[$^{11}$C]rolipram by doses of unlabeled (*R*)-rolipram below 0.005 mg/kg. The tracer formulation injected into the animal contains unlabeled (*R*)-rolipram formed during radiosynthesis from the reaction of desmethylrolipram precursor with non-radioactive $CH_3I$, with the "cold" dose determined by the specific activity (expressed as activity per moles of compound). The presence of unlabeled (*R*)-rolipram in the tracer formulation competes for binding to PDE4 (expressed as occupancy) through saturable kinetics (Hume et al., 1998). The tracer binding kinetics must be kept in the linear range

by limiting the receptor occupancy to 5% to generate pharmacologically meaningful measurements (Jagoda et al., 2004). Elucidation of the $ED_{50}$ contributes to the applications of (*R*)-[$^{11}$C]rolipram for PET imaging, since values of 0.05, 0.03 and 0.005 mg/kg have been proposed by different groups (Fujita et al., 2005; Parker et al., 2005; Thomas et al., 2008). Lower affinity for PDE4 observed with (*S*)-rolipram confirms previously reported in vitro differences in stereoisomer binding (Schneider et al., 1986; Parker et al., 2005).

In setting general considerations for radioligand selectivity and design, Pike et al. list high selectivity for the target receptor, high affinity, antagonist action, stereoselectivity, low toxicity, low (or measurable) metabolism and amenability to labelling (Pike et al., 2000). It is clear from our characterization studies that (*R*)-[$^{11}$C]rolipram satisfies these criteria, suggesting that, from a design point of view, it is a promising PET tracer.

## 8.2. (*R*)-[$^{11}$C]rolipram and (*S*)-[$^{11}$C]rolipram metabolism and pharmacokinetics

Column-switch HPLC quantification (relative presence) of polar hydrophilic radiolabeled metabolites that don't bind PDE4 identifies the components of the radioactive signal detected in tissues following tracer administration (Figure 3-4). While column-switch HPLC methods are commonly used for metabolite analysis in plasma (Hilton et al., 2000), we optimized the method for the analysis of tissue homogenates. This technique was subsequently utilized by other students in the group for the analysis of radiolabeled metabolites of [$^{11}$C]HED (by PhD candidate James Thackeray)

(Thackeray et al., 2007), [$^{11}$C]methyl-candesartan (by MSc candidate Sheryn Kirkpatrick) and [$^{11}$C]methyl-losartan (by MSc candidate Rawad Antoun).

Estimation of radiotracer retention using a ratio between a region of interest and a reference region devoid of receptors (e.g. cerebellum for quantification of DA receptors with [$^{11}$C]raclopride (Hume et al., 1992; Lammertsma et al., 1996) is common in PET imaging. This approach can not be applied to (*R*)-[$^{11}$C]rolipram, since PDE4 is present in virtually every tissue. An alternative approach would be to use the comparison between the (*R*)- and (*S*)-[$^{11}$C]rolipram, as discussed in chapter 6. If the only difference between (*S*)-[$^{11}$C]Rolipram and (*R*)-[$^{11}$C]rolipram retention is caused by the ~10× higher affinity of the (*R*)- stereoisomer for PDE4, a (*S*)-[$^{11}$C]rolipram PET scan could provide a measure of (*R*)-[$^{11}$C]rolipram non-specific binding and metabolites (providing an estimate of the $k_1$, $k_2$, $k_{1met}$ and $k_{2met}$ parameters in the model depicted in Figure 8-1), eliminating the need for arterial blood sampling, patient-specific metabolite analysis, and thus facilitating quantification of PDE4-specific binding. While it is not uncommon for stereoisomers of a compound to exhibit differences at the level of absorption, distribution, metabolism or elimination (Brocks, 2006; Lu, 2007), we observed no difference in the relative proportion of radiolabeled metabolites to unchanged tracer between the two stereoisomers using HPLC methods in rats. Our results confirm the findings of Krause et al., who found no differences between the pharmacokinetics of (*R*)- and (*S*)-rolipram in healthy volunteers (Krause et al., 1990). While it is conceivable that disease states may affect cytochrome P450 activity, the difference observed in vivo in binding confirms the conservation of stereochemistry.

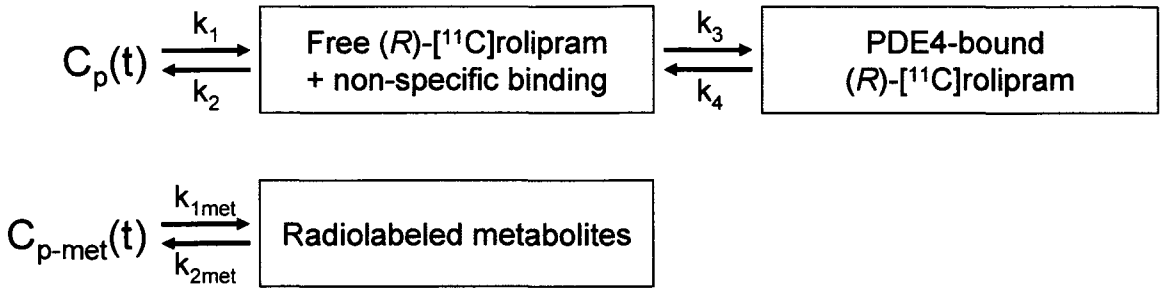


Figure 8-1: Proposed dual-input two-compartment model, adapted from Lortie et al., 2006 (Lortie et al., 2006).

## 8.3. Multi-tracer PET imaging

The unique nature of in vivo non-invasive PET imaging provides potential for serial assessment of multiple targets in a patient, interrogating more than one physiological property at a time. As an example, diminished blood perfusion (as evaluated by [$^{13}$N]$NH_3$) but normal glucose metabolism ([$^{18}$F]FDG) in cardiac PET imaging are indications of poorly-perfused but metabolically active and viable cells, or "hibernating" myocardium (Brunken et al., 1986). Similarly, a mismatch between the presynaptic sympathetic nervous system function and post-synaptic β-AR, evaluated using [$^{11}$C]HED and [$^{11}$C]CGP12177 PET, was proposed to represent local arrhythmogenic conditions, with greater mismatch correlating with a worse clinical outcome (Caldwell et al., 2008). Evaluation of adriamycin (ADR) toxicity described in manuscript #4 utilizes a similar multi-tracer approach, using [$^{11}$C]HED biodistribution for determining pre-synaptic sympathetic nervous system innervation, [$^{3}$H]CGP12177 for quantifying β-AR density and (*R*)-[$^{11}$C]rolipram for measuring changes in PDE4. While baseline (*R*)-[$^{11}$C]rolipram and [$^{11}$C]HED retention did not change at the 45 min post-tracer time-point, β-AR were decreased in cardiac tissue. This study identified the post-synaptic receptors as a promising imaging target in ADR cardiotoxicity. The observation that presynaptic and post-receptor elements of NA signaling are not altered is valuable in elucidation of the mechanism of ADR cardiotoxicity. It is important to note that ADR-induced cardiotoxicity is a hyperadrenergic state similar to obesity, diabetes and heart failure. Ungerer et al. have shown that [$^{11}$C]HED-measured presynaptic sympathetic nervous system activity doesn't correlate with β-AR levels, but relates to β-ARK expression, suggesting that evaluation of multiple sites of the β-AR signaling is

warranted (Ungerer et al., 2000). Editorial comments by Dr. Bengel on the ADR publication recognize the multi-tracer approach for the evaluation of cardiac pathologies as "an important early step" (Bengel, 2010). The limitations of in vitro studies that measure the signaling cascade components in conditions outside of the physiological environment can be complemented by the multi-tracer approach with PET imaging.

## 8.4. (*R*)-[$^{11}$C]Rolipram imaging in anthracycline chemotherapy

Our findings of altered β-AR density and decreased (*R*)-[$^{11}$C]rolipram response to acute elevation in NA with no associated change in basal PDE4 or presynaptic sympathetic nervous system function have implications for the clinical management of chemotherapy with cardiotoxic agents. Clinical applications of ADR and other anthracyclines are hindered by the onset of the congestive heart failure, limiting the cumulative doses to 550 mg/m$^2$ for all patients (Swain et al., 2003). Current proposed methods of evaluating ADR-induced cardiotoxicity are limited to invasive tissue biopsies, or echocardiographic measurements which are capable of detecting disease only if the cardiac contraction is significantly compromised (Bristow et al., 1981; Panjrath and Jain, 2006; Dranitsaris et al., 2008). Molecular imaging has potential for improving the treatment protocols and extending the therapy for the patients that are less susceptible to ADR toxicity (Panjrath and Jain, 2006). [$^3$H]CGP12177 retention and (*R*)-[$^{11}$C]rolipram responsiveness to acute elevations in NA levels are decreased prior to detectable cardiac functional defect (as assessed by echocardiography), suggesting that clinical imaging with $^{11}$C-labeled β-AR inhibitors CGP12177 or CGP12388, as well as (*R*)-[$^{11}$C]rolipram with a DMI challenge, could be used to evaluate cardiotoxic alterations in the

noradrenergic pathway. In vivo insight into individual tolerance to ADR and other anthracyclines can be used to adapt the treatment doses for the patient. Continuing the chemotherapy regimen past the current dose limit and stopping at the first appearance of β-AR downregulation (evaluated by PET) could customize chemotherapy and increase the patient benefit from the anthracycline, while avoiding cardiotoxicity.

## 8.5. (*R*)-[$^{11}$C]Rolipram imaging following myocardial infarction

LAD occlusion is a commonly-used rat model of heart failure, with cardiac dysfunction (established by a change in echocardiographic parameters) shown to occur early following myocardial infarction. Availability of the Siemens Inveon$^{TM}$ small-animal PET camera at the University of Ottawa Heart Institute has made *full* kinetic imaging studies with (*R*)-[$^{11}$C]rolipram and [$^{13}$N]$NH_3$ possible, as opposed to a single time-point assessment with biodistribution. Increases in (*R*)-[$^{11}$C]rolipram retention in the non-infarcted portion of the left ventricle were observed 8 weeks following myocardial infarction, with the MBF remaining normal. $\beta_1$-AR downregulation was observed at the same time-point by Western blot techniques, likely as a consequence of adrenergic overstimulation. The increase in (*R*)-[$^{11}$C]rolipram retention likely reflects increased binding to PDE4, due to increased affinity (through PKA phosphorylation) and/or increased $B_{max}$ (elevated expression of the enzyme). Since cAMP levels regulate PDE4 phosphorylation and expression, this finding may reflect increases in cAMP levels, despite reported alterations in the elements of the signal transduction cascade.

It has been previously reported that in heart failure, $\beta_1$-AR is downregulated (Pfeffer et al., 1979; Witte et al., 2000), $\beta_2$-AR signaling is uncoupled from the

stimulatory $G_{\alpha s}$ subunit and the $G_{\alpha i}$ is upregulated (Feldman et al., 1988; Sethi et al., 1998), while the overall AC activity is decreased (Akhter et al., 1997; Tse et al., 2000). Despite these compensatory changes aimed at reducing the intracellular cAMP levels, it is conceivable that in a living tissue, the overwhelming increase reported in the myocardial synaptic NA results in elevated cAMP. Figure 8-2 illustrates the concept of increased NA levels (e.g. DMI blocking the presynaptic NAT) with normal β-AR signaling and preserved β-AR signal transduction eliciting a major increase in cAMP levels (2$^{nd}$ panel), reflected in elevated (*R*)-[$^{11}$C]rolipram retention. Following $\beta_1$-ARdownregulation and compensatory changes downstream of the receptors, the increased sympathetic nervous system signal is partially attenuated at the second messenger level (3$^{rd}$ panel), resulting in elevated (*R*)-[$^{11}$C]rolipram PDE4 binding. Alternatively, the increase in PDE4 enzyme activity may be a result of a non-cAMP dependent pathway (possibly with the involvement of the PKC/ERK) as part of the intracellular mechanisms aimed at attenuating the β-AR signal.

In contrast to the evaluation of cardiac dysfunction in ADR-treated rats which showed no change in the baseline (*R*)-[$^{11}$C]rolipram uptake, full kinetic studies post-MI detected increased retention. In addition to the differences between the cardiac dysfunction induced by pharmacological or surgical insult, this difference may be due to increased sensitivity of the in vivo imaging for 60 min following tracer administration, as opposed to the evaluation of a single time-point with biodistribution.

In vitro techniques used to validate the in vivo increase in (*R*)-[$^{11}$C]rolipram failed to detect any change in PDE4 activity (assessed by the enzyme activity assay) or expression (evaluated by western blot techniques). These findings can be interpreted as

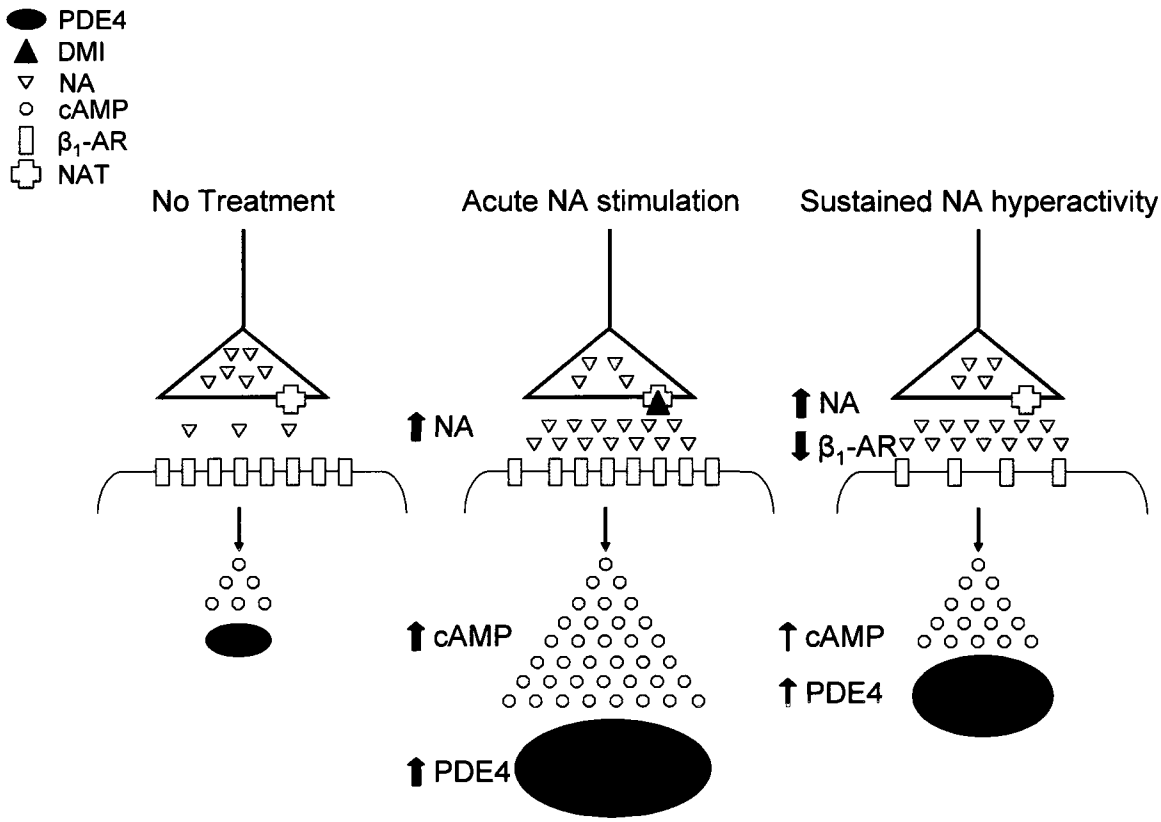


Figure 8-2: A schematic representation of the proposed alterations in the NA/cAMP/PDE4 signaling cascade. An acute elevation in synaptic NA elicited through inhibition of presynaptic reuptake by DMI results in elevated post-synaptic intracellular cAMP levels and increased PDE4. Sustained release of synaptic NA observed in heart failure causes a downregulation in post-synaptic β-AR, attenuating the NA stimulation of the post-receptor cAMP second messenger signal. Adapted from Duman et al., 1997 (Duman et al., 1997).

limitations of in vitro assessment of intracellular signaling. Enzyme activity assay measures the PDE4 cAMP-hydrolyzing activity in the tissue homogenates without differentiating the contributions of individual PDE4A-D subtypes. Changes in enzyme activity could reflect altered affinity of PDE4 for cAMP or the expression of the enzyme. The processing of tissues harvested from sacrificed animals would likely degrade the sensitive enzymes or change their phosphorylation state, affecting the accuracy and sensitivity of these assays. While applicable in cell cultures, analysis of PDE4 activity would therefore require a greater change such that it would be observable in processed tissue samples.

Western blot studies with commercially-available antibodies measure the expression of the individual subtypes (PDE4A, B and D), but may not detect each individual isoform. Interestingly, the expression of the PDE4A subtype showed a trend towards an increase in immunoblotting techniques. Enzymes in this subtype are known to be responsive to NA stimulation (Farooqui et al., 2000), and therefore may change in the hyperadrenergic state found in heart failure. The lack of any alterations in PDE4 activity assays could therefore be explained by the involvement of PDE4A7 subtype, a "dead-short" form of PDE4 which exhibits no catalytic activity (Johnston et al., 2004), but could conceivably still bind (*R*)-[$^{11}$C]rolipram. Due to the lack of a pan-PDE4 antibody that would detect all PDE4A-D subtypes, we evaluated only the expression of PDE4A, B and D isozymes using specific antibodies. PDE4C expression was not assessed, since the isozyme has been reported to be absent from cardiac tissue. Speculatively, cardiac expression of the PDE4C subtype may be upregulated in disease states, increasing the binding of (*R*)-[$^{11}$C]rolipram and possibly leading to the discrepancy between the

increased tracer DVs observed in vivo PET studies and the lack of change in the Western blot results.

## 8.6. (*R*)-[$^{11}$C]Rolipram PET applications in drug development

The development of novel PET tracers and increasing availability of low-cost small-animal cameras provide increasing opportunities for PET imaging in drug development (Rudin et al., 2004; Riemann et al., 2008). The non-invasive nature of PET imaging permits serial monitoring of changes in cAMP-mediated NA signal transmission at the level of PDE4 before and during therapy in the same subject. Despite the current interest in the development of selective inhibitors of PDE4 (using rolipram as a starting compound) (Pages et al., 2009) and the potential implications in therapy, applications of (*R*)-[$^{11}$C]rolipram in the development of improved PDE inhibitors would be limited by its lack of PDE4A, B, C or D subtype-selectivity.

PET imaging of PDE4 could play a role in the development of novel therapies, both within and beyond the noradrenergic system. (*R*)-[$^{11}$C]Rolipram can be used, alone or in a multi-tracer paradigm, to detect dysfunction in NA signal transduction and follow the reversal of defect through serial scans. Non-invasive imaging could thus be used to help elucidate the mechanism of action of current therapies, such as β-blockers or angiotensin receptor inhibitors. Unlike $^{11}$C-labeled β-AR antagonists, (*R*)-[$^{11}$C]rolipram would not be affected by the use of commonly-prescribed β-blockers since it monitors the noradrenergic system at a site downstream of the receptor.

Recent studies have shown increased expression of $G_{s\alpha}$-coupled 5HT4 receptors in human heart failure (Bach et al., 2001; Levy et al., 2008). It is conceivable that novel

therapies aimed at these receptors could reach clinical testing. Unlike current tracers targeting changes in NA reuptake and β-AR expression, (*R*)-[$^{11}$C]rolipram responds to alterations in cAMP-mediated 5HT signaling (as presented in chapter 4) and could therefore potentially assist in drug development and guide therapy.

## 8.7. (*R*)-[$^{11}$C]Rolipram PET imaging in differentiating heart disease

Genetic polymorphisms in $\beta_1$- and $\beta_2$-AR have been associated with altered intracellular AC activation and differences in the post-receptor signal transduction cascade (Mason et al., 1999; Rosskopf and Michel, 2008). As illustrated by the S49G and G389R single nucleotide polymorphisms, the Gly49 variant expressed in 25% of the white population is more susceptible to β-AR downregulation (Levin et al., 2002), while the Arg389 variant couples more effectively to the $G_{s\alpha}$ (Mason et al., 1999). Current therapy does not take these polymorphisms into account, treating all heart failure based strictly on measurable symptoms and disease history. Correlating the β-AR polymorphisms to differences in intracellular cAMP levels and responsiveness to treatment is a promising new application of PET imaging (Shirani and Dilsizian, 2008). Genetic differences in β-AR indistinguishable by conventional methods may present with different phenotypes when assessed using a technique that interrogates the intracellular components beyond the receptor. Variation in the sympathetic dysfunction between patients based on genetic differences and disease variants necessitates more individualized therapy, and could play a role in personalized therapy of heart failure (Floras, 2003; Knuuti and Bengel, 2008; Dobrucki and Sinusas, 2010).

As initially postulated by Bristow and Anderson, there are differences in the behaviour of components of the adrenergic signal transduction pathway between the idiopathic and ischemic heart failure (Bristow et al., 1991). Components of the signaling cascade downstream of the receptors show different degrees of AC stimulation and vary in the severity of uncoupling of receptors from the contractile response (Bristow et al., 1991). While imaging surface receptors and presynaptic NA reuptake would not detect these differences, imaging of PDE4 with (*R*)-[$^{11}$C]rolipram in conjunction with presynaptic and receptor-level imaging, could quantify these functionally important factors. A multi-tracer approach could thereby differentiate between types of cardiac dysfunction and provide a more precise diagnosis. PET imaging was already proposed as a method to clarify the differences in the pathophysiological mechanisms that underlie ischemic from idiopathic dilated cardiomyopathy (de Jong et al., 2002).

## 8.8. Conclusions

(*R*)-[$^{11}$C]Rolipram biodistribution and autoradiography studies demonstrated binding selectivity for PDE4 isozymes over other cardiac PDE subtypes. Tracer uptake is sensitive to treatments that affect cAMP signaling through serotonergic, noradrenergic and histaminergic neurotransmission. (*R*)-[$^{11}$C]rolipram has been shown to possess the properties desired in a PET radioligand for cardiac imaging. (*R*)-[$^{11}$C]Rolipram detected reduced NA signal transduction at the PDE4 level that precedes cardiac dysfunction in an ADR-induced rat model of cardiotoxicity. (*R*)-[$^{11}$C]rolipram in combination with other tracers therefore has potential in detecting NA signaling dysfunction and could help determine the safe limits for the anthracycline chemotherapeutic agents in human

patients. Small-animal PET imaging with (*R*)-[$^{11}$C]rolipram displays increased PDE4 binding in the non-infarcted left ventricle 8 weeks following myocardial infarction in spite of decreased β-adrenergic receptor expression and normal myocardial blood flow. As a result of the research presented in this thesis, (*R*)-[$^{11}$C]rolipram PET holds promise for non-invasive assessment of alterations in cAMP-mediated signaling. (*R*)-[$^{11}$C]Rolipram applicability in animal models of cardiac diseases provides the rationale for PET imaging impaired intracellular cAMP-mediated NA signaling.

## 8.9. Future direction

The development of a kinetic model describing the in vivo retention of (*R*)- and (*S*)-[$^{11}$C]rolipram is the immediate next step in the development of tracer for wide clinical applications. The deployment of high-resolution high-sensitivity small-animal PET cameras enables future studies with (*R*)-[$^{11}$C]rolipram in different animal models of heart dysfunction, such as cardiomegaly induced by chronic isoproterenol administration, dilated cardiomyopathy resulting from aortic banding, and potentially a full kinetic PET evaluation of ADR-induced cardiotoxicity. [$^{18}$F]Fluoro-alkyl/aryl rolipram derivatives would increase clinical applicability of PDE4 imaging due to the longer half life of the radionucleide (109.7 min, vs. 20.4 min for C-11), allowing the tracer to be shipped to near-by PET imaging centres (within 6 hours transportation) without an on-site cyclotron. Furthermore, $^{18}$F-labeled ligands can be produced at higher specific activity than C-11 due to the lack of F-19 in the reaction mixture as opposed to $CO_2$. High specific activity would remove any complications arising from occupancy of binding site by the non-labeled molecules, allowing more reliable quantification of tracer binding in tissues.

Multi-tracer approaches using (*R*)-[$^{11}$C]rolipram in combination with [$^{11}$C]HED and [$^{11}$C]CGP12388 will be explored with the goal of serial, non-invasive assessment of pre- and post-synaptic NA signaling in the same subjects. In parallel, ethics approval has already been obtained for myocardial PET studies with (*R*)-[$^{11}$C]rolipram in healthy human volunteers, with future potential for diagnosis and evaluation of therapy in cardiac patients at the University of Ottawa Heart Institute.

# CHAPTER 8: REFERENCES

Abi-Gerges, A., W. Richter, F. Lefebvre, P. Mateo, A. Varin, C. Heymes, J. L. Samuel, C. Lugnier, M. Conti, R. Fischmeister and G. Vandecasteele (2009). "Decreased expression and activity of cAMP phosphodiesterases in cardiac hypertrophy and its impact on beta-adrenergic cAMP signals." Circ Res **105**(8): 784-92.

Agostini, D., H. J. Verberne, W. Burchert, J. Knuuti, P. Povinec, G. Sambuceti, M. Unlu, M. Estorch, G. Banerjee and A. F. Jacobson (2008). "I-123-mIBG myocardial imaging for assessment of risk for a major cardiac event in heart failure patients: insights from a retrospective European multicenter study." Eur J Nucl Med Mol Imaging **35**(3): 535-46.

Ahlquist, R. P. (1948). "A study of the adrenotropic receptors." Am J Physiol **153**(3): 586-600.

Ahmet, I., E. G. Lakatta and M. I. Talan (2005). "Pharmacological stimulation of beta2-adrenergic receptors (beta2AR) enhances therapeutic effectiveness of beta1AR blockade in rodent dilated ischemic cardiomyopathy." Heart Fail Rev **10**(4): 289-96.

Ahn, S., C. D. Nelson, T. R. Garrison, W. E. Miller and R. J. Lefkowitz (2003). "Desensitization, internalization, and signaling functions of beta-arrestins demonstrated by RNA interference." Proc Natl Acad Sci U S A **100**(4): 1740-4.

Akhter, S. A., A. D. Eckhart, H. A. Rockman, K. Shotwell, R. J. Lefkowitz and W. J. Koch (1999). "In vivo inhibition of elevated myocardial beta-adrenergic receptor kinase activity in hybrid transgenic mice restores normal beta-adrenergic signaling and function." Circulation **100**(6): 648-53.

Akhter, S. A., C. A. Skaer, A. P. Kypson, P. H. McDonald, K. C. Peppel, D. D. Glower, R. J. Lefkowitz and W. J. Koch (1997). "Restoration of beta-adrenergic signaling in failing cardiac ventricular myocytes via adenoviral-mediated gene transfer." Proc Natl Acad Sci U S A **94**(22): 12100-5.

Alexander, R. W., L. T. Williams and R. J. Lefkowitz (1975). "Identification of cardiac beta-adrenergic receptors by (minus) [3H]alprenolol binding." Proc Natl Acad Sci U S A **72**(4): 1564-8.

Alvarez, R., C. Sette, D. Yang, R. M. Eglen, R. Wilhelm, E. R. Shelton and M. Conti (1995). "Activation and selective inhibition of a cyclic AMP-specific phosphodiesterase, PDE-4D3." Mol Pharmacol **48**(4): 616-22.

Armour, J. A. (2004). "Cardiac neuronal hierarchy in health and disease." Am J Physiol Regul Integr Comp Physiol **287**(2): R262-71.

Arnt, J., K. P. Bøgesø, J. Hyttel and E. Meier (1988). "Relative dopamine $D_1$and $D_2$ receptor affinity and efficacy determine whether dopamine agonists induce hyperactivity or oral sterotypy in rats." Pharmacol Toxicol **62**: 121-130.

Azevedo, E. R. and J. D. Parker (1999). "Parasympathetic control of cardiac sympathetic activity: normal ventricular function versus congestive heart failure." Circulation **100**(3): 274-9.

Bach, T., T. Syversveen, A. M. Kvingedal, K. A. Krobert, T. Brattelid, A. J. Kaumann and F. O. Levy (2001). "5$HT_{4A}$ and 5-$HT_{4B}$ receptors have nearly identical pharmacology and are both expressed in human atrium and ventricle." Naunyn Schmiedebergs Arch Pharmacol **363**(2): 146-60.

Baillie, G. S., S. J. MacKenzie, I. McPhee and M. D. Houslay (2000). "Sub-family selective actions in the ability of Erk2 MAP kinase to phosphorylate and regulate

the activity of PDE4 cyclic AMP-specific phosphodiesterases." Br J Pharmacol **131**(4): 811-9.

Baillie, G. S., J. D. Scott and M. D. Houslay (2005). "Compartmentalisation of phosphodiesterases and protein kinase A: opposites attract." FEBS Lett **579**(15): 3264-70.

Baillie, G. S., A. Sood, I. McPhee, I. Gall, S. J. Perry, R. J. Lefkowitz and M. D. Houslay (2003). "beta-Arrestin-mediated PDE4 cAMP phosphodiesterase recruitment regulates beta-adrenoceptor switching from Gs to Gi." Proc Natl Acad Sci U S A **100**(3): 940-5.

Barad, M., R. Bourtchouladze, D. G. Winder, H. Golan and E. Kandel (1998). "Rolipram, a type IV-specific phosphodiesterase inhibitor, facilitates the establishment of long-lasting long-term potentiation and improves memory." Proc Natl Acad Sci U S A **95**(25): 15020-5.

Barak, L. S., S. S. Ferguson, J. Zhang and M. G. Caron (1997). "A beta-arrestin/green fluorescent protein biosensor for detecting G protein-coupled receptor activation." J Biol Chem **272**(44): 27497-500.

Barnette, M. S., J. O. Bartus, M. Burman, S. B. Christensen, L. B. Cieslinski, K. M. Esser, U. S. Prabhakar, J. A. Rush and T. J. Torphy (1996). "Association of the anti-inflammatory activity of phosphodiesterase 4 (PDE4) inhibitors with either inhibition of PDE4 catalytic activity or competition for [3H]rolipram binding." Biochem Pharmacol **51**(7): 949-56.

Barnette, M. S., S. B. Christensen, D. M. Essayan, M. Grous, U. Prabhakar, J. A. Rush, A. Kagey-Sobotka and T. J. Torphy (1998). "SB 207499 (Ariflo), a potent and selective second-generation phosphodiesterase 4 inhibitor: in vitro anti-inflammatory actions." J Pharmacol Exp Ther **284**(1): 420-6.

Barnette, M. S., M. Grous, L. B. Cieslinski, M. Burman, S. B. Christensen and T. J. Torphy (1995). "Inhibitors of phosphodiesterase IV (PDE IV) increase acid secretion in rabbit isolated gastric glands: correlation between function and interaction with a high-affinity rolipram binding site." J Pharmacol Exp Ther **273**(3): 1396-402.

Basselin, M., M. A. Fox, L. Chang, J. M. Bell, D. Greenstein, M. Chen, D. L. Murphy and S. I. Rapoport (2009). "Imaging elevated brain arachidonic acid signaling in unanesthetized serotonin transporter (5-HTT)-deficient mice." Neuropsychopharmacology **34**(7): 1695-709.

Bauman, A. L. and J. D. Scott (2002). "Kinase- and phosphatase-anchoring proteins: harnessing the dynamic duo." Nat Cell Biol **4**(8): E203-6.

Beanlands, R. S., N. A. Shaikh, W. H. Wen, F. Dawood, A. M. Ugnat, P. R. McLaughlin, R. Carere and P. P. Liu (1994). "Alterations in fatty acid metabolism in adriamycin cardiomyopathy." J Mol Cell Cardiol **26**(1): 109-19.

Beavo, J. A. (1995). "Cyclic nucleotide phosphodiesterases: functional implications of multiple isoforms." Physiological Rev. **75**(4): 725-748.

Beavo, J. A. and L. L. Brunton (2002). "Cyclic nucleotide research -- still expanding after half a century." Nat Rev Mol Cell Biol **3**(9): 710-8.

Bengel, F. M. (2009). "Clinical cardiovascular molecular imaging." J Nucl Med **50**(6): 837-40.

Bengel, F. M. (2010). "Dissecting myocardial signal transduction cascades: Sharp new insights from multi-tracer molecular imaging." J Nucl Cardiol **17**(2): 175-6.

Benjamin, I. J., J. E. Jalil, L. B. Tan, K. Cho, K. T. Weber and W. A. Clark (1989). "Isoproterenol-induced myocardial fibrosis in relation to myocyte necrosis." Circ Res **65**(3): 657-70.

Berridge, M. J. (1987). "Inositol trisphosphate and diacylglycerol: two interacting second messengers." Annu Rev Biochem **56**: 159-93.

Bertolino, A., D. Crippa, S. di Dio, K. Fichte, G. Musmeci, V. Porro, V. Rapisarda, M. Sastre-y-Hernandez and M. Schratzer (1988). "Rolipram versus imipramine in inpatients with major, "minor" or atypical depressive disorder: a double-blind double-dummy study aimed at testing a novel therapeutic approach." Int Clin Psychopharmacol **3**(3): 245-53.

Bester, A. J., E. Bajusz and A. Lochner (1972). "Effect of ischaemia and infarction on the metabolism and function of the isolated, perfused rat heart." Cardiovasc Res **6**(3): 284-94.

Bian, H., J. Zhang, P. Wu, L. A. Varty, Y. Jia, T. Mayhood, J. A. Hey and P. Wang (2004). "Differential type 4 cAMP-specific phosphodiesterase (PDE4) expression and functional sensitivity to PDE4 inhibitors among rats, monkeys and humans." Biochem Pharmacol **68**(11): 2229-36.

Billett, E. E. (2004). "Monoamine oxidase (MAO) in human peripheral tissues." Neurotoxicology **25**(1-2): 139-48.

Bloom, T. J. (2002). "Cyclic nucleotide phosphodiesterase isozymes expressed in mouse skeletal muscle." Can J Physiol Pharmacol **80**(12): 1132-5.

Bloom, T. J. and J. A. Beavo (1996). "Identification and tissue-specific expression of PDE7 phosphodiesterase splice variants." Proc Natl Acad Sci U S A **93**(24): 14188-92.

Bohm, M. (1995). "Alterations of beta-adrenoceptor-G-protein-regulated adenylyl cyclase in heart failure." Mol Cell Biochem **147**(1-2): 147-60.

Bohm, M., K. La Rosee, R. H. Schwinger and E. Erdmann (1995). "Evidence for reduction of norepinephrine uptake sites in the failing human heart." J Am Coll Cardiol **25**(1): 146-53.

Bohm, S. K., E. F. Grady and N. W. Bunnett (1997). "Regulatory mechanisms that modulate signalling by G-protein-coupled receptors." Biochem J **322 ( Pt 1)**: 1-18.

Bolger, G. B., S. Erdogan, R. E. Jones, K. Loughney, G. Scotland, R. Hoffmann, I. Wilkinson, C. Farrell and M. D. Houslay (1997). "Characterization of five different proteins produced by alternatively spliced mRNAs from the human cAMP-specific phosphodiesterase PDE4D gene." Biochem J **328**(Pt 2): 539-48.

Bolger, G. B., A. McCahill, E. Huston, Y. F. Cheung, T. McSorley, G. S. Baillie and M. D. Houslay (2003). "The unique amino-terminal region of the PDE4D5 cAMP phosphodiesterase isoform confers preferential interaction with beta-arrestins." J Biol Chem **278**(49): 49230-8.

Bolger, G. B., L. Rodgers and M. Riggs (1994). "Differential CNS expression of alternative mRNA isoforms of the mammalian genes encoding cAMP-specific phosphodiesterases." Gene **149**(2): 237-44.

Borisy, F. F., P. N. Hwang, G. V. Ronnett and S. H. Snyder (1993). "High-affinity cAMP phosphodiesterase and adenosine localized in sensory organs." Brain Research **610**: 199-207.

Botelho, L. H., L. C. Webster, J. D. Rothermel, J. Baraniak and W. J. Stec (1988). "Inhibition of cAMP-dependent protein kinase by adenosine cyclic 3'-, 5'-phosphorodithioate, a second cAMP antagonist." J Biol Chem **263**(11): 5301-5.

Boudreau, G., F. Peronnet, J. De Champlain and R. Nadeau (1993). "Presynaptic effects of epinephrine on norepinephrine release from cardiac sympathetic nerves in dogs." Am J Physiol **265**(1 Pt 2): H205-11.

Bouvier, M., W. P. Hausdorff, A. De Blasi, B. F. O'Dowd, B. K. Kobilka, M. G. Caron and R. J. Lefkowitz (1988). "Removal of phosphorylation sites from the beta 2-adrenergic receptor delays onset of agonist-promoted desensitization." Nature **333**(6171): 370-3.

Brattelid, T., E. Qvigstad, J. A. Lynham, P. Molenaar, H. Aass, O. Geiran, T. Skomedal, J. B. Osnes, F. O. Levy and A. J. Kaumann (2004). "Functional serotonin 5-HT$_4$ receptors in porcine and human ventricular myocardium with increased 5-HT$_4$ mRNA in heart failure." Naunyn-Schmiedeberg's Archives of Pharmacology **370**(3): 157-66.

Bristow, M. R. (1993). "Changes in myocardial and vascular receptors in heart failure." J Am Coll Cardiol **22**(4 Suppl A): 61A-71A.

Bristow, M. R. (2000). "beta-adrenergic receptor blockade in chronic heart failure." Circulation **101**(5): 558-69.

Bristow, M. R., F. L. Anderson, J. D. Port, L. Skerl, R. E. Hershberger, P. Larrabee, J. B. O'Connell, D. G. Renlund, K. Volkman, J. Murray and et al. (1991). "Differences in beta-adrenergic neuroeffector mechanisms in ischemic versus idiopathic dilated cardiomyopathy." Circulation **84**(3): 1024-39.

Bristow, M. R., R. Ginsburg, W. Minobe, R. S. Cubicciotti, W. S. Sageman, K. Lurie, M. E. Billingham, D. C. Harrison and E. B. Stinson (1982). "Decreased catecholamine sensitivity and beta-adrenergic-receptor density in failing human hearts." N Engl J Med **307**(4): 205-11.

Bristow, M. R., R. E. Hershberger, J. D. Port, W. Minobe and R. Rasmussen (1989). "Beta 1- and beta 2-adrenergic receptor-mediated adenylate cyclase stimulation in nonfailing and failing human ventricular myocardium." Mol Pharmacol **35**(3): 295-303.

Bristow, M. R., J. W. Mason, M. E. Billingham and J. R. Daniels (1981). "Dose-effect and structure-function relationships in doxorubicin cardiomyopathy." Am Heart J **102**(4): 709-18.

Brocks, D. R. (2006). "Drug disposition in three dimensions: an update on stereoselectivity in pharmacokinetics." Biopharm Drug Dispos **27**(8): 387-406.

Brodde, O. E. (1993). "Beta-adrenoceptors in cardiac disease." Pharmacol Ther **60**(3): 405-30.

Brodde, O. E., H. Bruck, K. Leineweber and T. Seyfarth (2001). "Presence, distribution and physiological function of adrenergic and muscarinic receptor subtypes in the human heart." Basic Res Cardiol **96**(6): 528-38.

Bronnikov, G., T. Bengtsson, L. Kramarova, V. Golozoubova, B. Cannon and J. Nedergaard (1999). "beta1 to beta3 switch in control of cyclic adenosine

monophosphate during brown adipocyte development explains distinct beta-adrenoceptor subtype mediation of proliferation and differentiation." Endocrinology **140**(9): 4185-97.

Brouri, F., N. Hanoun, O. Mediani, F. Saurini, M. Hamon, P. M. Vanhoutte and P. Lechat (2004). "Blockade of beta 1- and desensitization of beta 2-adrenoceptors reduce isoprenaline-induced cardiac fibrosis." Eur J Pharmacol **485**(1-3): 227-34.

Brunken, R., J. Tillisch, M. Schwaiger, J. S. Child, R. Marshall, M. Mandelkern, M. E. Phelps and H. R. Schelbert (1986). "Regional perfusion, glucose metabolism, and wall motion in patients with chronic electrocardiographic Q wave infarctions: evidence for persistence of viable tissue in some infarct regions by positron emission tomography." Circulation **73**(5): 951-63.

Budygin, E. A., M. R. Kilpatrick, R. R. Gainetdinov and R. M. Wightman (Lett 2000 Mar 3). "Correlation between behavior and extracellular dopamine levels in rat striatum: comparison of microdialysis and fast-scan cyclic voltammetry [In Process Citation]." Neurosci **281**(1): 9-12.

Calderone, A., J. de Champlain and J. L. Rouleau (1991). "Adriamycin-induced changes to the myocardial beta-adrenergic system in the rabbit." J Mol Cell Cardiol **23**(3): 333-42.

Caldwell, J. H., J. M. Link, W. C. Levy, J. E. Poole and J. R. Stratton (2008). "Evidence for pre- to postsynaptic mismatch of the cardiac sympathetic nervous system in ischemic congestive heart failure." J Nucl Med **49**(2): 234-41.

Campos-Toimil, M., T. Keravis, F. Orallo, K. Takeda and C. Lugnier (2008). "Short-term or long-term treatments with a phosphodiesterase-4 (PDE4) inhibitor result in opposing agonist-induced Ca(2+) responses in endothelial cells." Br J Pharmacol **154**(1): 82-92.

Castellano, M. and M. Bohm (1997). "The cardiac beta-adrenoceptor-mediated signaling pathway and its alterations in hypertensive heart disease." Hypertension **29**(3): 715-22.

Chandrasekaran, A., K. Y. Toh, S. H. Low, S. K. Tay, S. Brenner and D. L. Goh (2008). "Identification and characterization of novel mouse PDE4D isoforms: molecular cloning, subcellular distribution and detection of isoform-specific intracellular localization signals." Cell Signal **20**(1): 139-53.

Chang, H. Y., R. M. Klein and G. Kunos (1982). "Selective desensitization of cardiac beta adrenoceptors by prolonged in vivo infusion of catecholamines in rats." J Pharmacol Exp Ther **221**(3): 784-9.

Chang, J.-Y., S. F. Sawyer, J. M. Paris, A. Kirillov and D. J. Woodward (1997). "Single Neuronal Responses in Medial Prefrontal Cortex During Cocaine Self-Administration in Freely Moving Rats." Synapse **26**: 22-35.

Chang, Y.-H., M. Conti, Y.-C. Lee, H.-L. Lai, Y.-H. Ching and Y. Chern (1997). "Activation of phosphodiesterase IV during densensitization of the $A_{2A}$ adenosine receptor-mediated cyclic AMP response in rat pheochromocytoma (PC12) cells." J. Neurochem. **69**: 1300-1309.

Charkoudian, N. and J. A. Rabbitts (2009). "Sympathetic neural mechanisms in human cardiovascular health and disease." Mayo Clin Proc **84**(9): 822-30.

Chen, G. P., R. Tabibiazar, K. R. Branch, J. M. Link and J. H. Caldwell (2005). "Cardiac receptor physiology and imaging: an update." J Nucl Cardiol **12**(6): 714-30.

Cherin, E., R. Williams, A. Needles, G. Liu, C. White, A. S. Brown, Y. Q. Zhou and F. S. Foster (2006). "Ultrahigh frame rate retrospective ultrasound microimaging and blood flow visualization in mice in vivo." Ultrasound Med Biol **32**(5): 683-91.

Cheung, Y. F., Z. Kan, P. Garrett-Engele, I. Gall, H. Murdoch, G. S. Baillie, L. M. Camargo, J. M. Johnson, M. D. Houslay and J. C. Castle (2007). "PDE4B5, a novel, super-short, brain-specific cAMP phosphodiesterase-4 variant whose isoform-specifying N-terminal region is identical to that of cAMP phosphodiesterase-4D6 (PDE4D6)." J Pharmacol Exp Ther **322**(2): 600-9.

Chida, M., Y. Kagaya, Y. Imahori, S. Namiuchi, R. Fujii, M. Fukuchi, C. Takahashi, F. Tezuka, T. Ido and K. Shirato (2000). "Visualization of myocardial phosphoinositide turnover with 1-[1-(11)C]-butyryl-2-palmitoyl-rac-glycerol in rats with myocardial infarction." J Nucl Med **41**(12): 2063-8.

Chidiac, P. (1998). "Rethinking receptor-G protein-effector interactions." Biochem Pharmacol **55**(5): 549-56.

Choi, D. J., W. J. Koch, J. J. Hunter and H. A. Rockman (1997). "Mechanism of beta-adrenergic receptor desensitization in cardiac hypertrophy is increased beta-adrenergic receptor kinase." J Biol Chem **272**(27): 17223-9.

Chuang, T. T., L. Iacovelli, M. Sallese and A. De Blasi (1996). "G protein-coupled receptors: heterologous regulation of homologous desensitization and its implications." Trends Pharmacol Sci **17**(11): 416-21.

Chun, H. J., J. Narula, L. Hofstra and J. C. Wu (2008). "Intracellular and extracellular targets of molecular imaging in the myocardium." Nat Clin Pract Cardiovasc Med **5 Suppl 2**: S33-41.

Cleator, J. H., N. D. Mehta, D. T. Kurtz and J. D. Hildebrandt (1999). "The N54 mutant of Galphas has a conditional dominant negative phenotype which suppresses hormone-stimulated but not basal cAMP levels." FEBS Lett **443**(2): 205-8.

Cohn, J. N., T. B. Levine, M. T. Olivari, V. Garberg, D. Lura, G. S. Francis, A. B. Simon and T. Rector (1984). "Plasma norepinephrine as a guide to prognosis in patients with chronic congestive heart failure." N Engl J Med **311**(13): 819-23.

Collins, S. and R. S. Surwit (2001). "The beta-adrenergic receptors and the control of adipose tissue metabolism and thermogenesis." Recent Prog Horm Res **56**: 309-28.

Communal, C., K. Singh, D. R. Pimentel and W. S. Colucci (1998). "Norepinephrine stimulates apoptosis in adult rat ventricular myocytes by activation of the beta-adrenergic pathway." Circulation **98**(13): 1329-34.

Communal, C., K. Singh, D. B. Sawyer and W. S. Colucci (1999). "Opposing effects of beta(1)- and beta(2)-adrenergic receptors on cardiac myocyte apoptosis : role of a pertussis toxin-sensitive G protein." Circulation **100**(22): 2210-2.

Conti, M. and J. Beavo (2007). "Biochemistry and physiology of cyclic nucleotide phosphodiesterases: essential components in cyclic nucleotide signaling." Annu Rev Biochem **76**: 481-511.

Conti, M. and S. L. Jin (1999). "The molecular biology of cyclic nucleotide phosphodiesterases." Prog Nucleic Acid Res Mol Biol **63**: 1-38.

Cote, R. H. (2004). "Characteristics of photoreceptor PDE (PDE6): similarities and differences to PDE5." Int J Impot Res **16 Suppl 1**: S28-33.

Cotts, W. G. and R. M. Oren (1997). "Function of the transplanted heart: unique physiology and therapeutic implications." Am J Med Sci **314**(3): 164-72.

Coudray, C., C. Charon, N. Komas, G. Mory, F. Diot-Dupuy, V. Manganiello, P. Ferre and R. Bazin (1999). "Evidence for the presence of several phosphodiesterase isoforms in brown adipose tissue of Zucker rats: modulation of PDE2 by the fa gene expression." FEBS Lett **456**(1): 207-10.

Crick S.J., S. M. N., Anderson R.H. (2000). Neural supply of the heart. The nervous system and the heart. T. H. G.J., Humana Press Inc: 3-54.

Cui, H. and R. D. Green (2003). "Regulation of the cAMP-elevating effects of isoproterenol and forskolin in cardiac myocytes by treatments that cause increases in cAMP." Biochem Biophys Res Commun **307**(1): 119-26.

D'Sa, C., A. J. Eisch, G. B. Bolger and R. S. Duman (2005). "Differential expression and regulation of the cAMP-selective phosphodiesterase type 4A splice variants in rat brain by chronic antidepressant administration." Eur J Neurosci **22**(6): 1463-75.

Daaka, Y., L. M. Luttrell and R. J. Lefkowitz (1997). "Switching of the coupling of the beta2-adrenergic receptor to different G proteins by protein kinase A." Nature **390**(6655): 88-91.

Dasi, F. J., J. L. Ortiz, J. Cortijo and E. J. Morcillo (2000). "Histamine up-regulates phosphodiesterase 4 activity and reduces prostaglandin E2-inhibitory effects in human neutrophils." Inflamm Res **49**(11): 600-9.

DaSilva, J. N., C. M. Lourenco, J. H. Meyer, D. Hussey, W. Z. Potter and S. Houle (2002). "Imaging cAMP-specific phosphodiesterase-4 in human brain with (*R*)-[$^{11}$C]rolipram and positron emission tomography." Eur J Nucl Med Mol Imaging **29**(12): 1680-3.

DaSilva, J. N., C. M. Lourenco, J. H. Meyer, D. Hussey, W. Z. Potter and S. Houle (2002). "Imaging cAMP-specific phosphodiesterase-4 in human brain with R-[$^{11}$C]rolipram and positron emission tomography." Eur J Nuc Med Mol Imaging **29**(12): 1680-1683.

DaSilva, J. N., C. M. Lourenco, A. A. Wilson and S. Houle (2001). "Syntheses of the phosphodiesterase-4 inhibitors [$^{11}$C]Ro 20-1724, *R*-, *R/S*- and *S*-[$^{11}$C]rolipram." J Label Compd Radiopharm **44**(5): 373-384.

DaSilva, J. N., C. M. Valente, A. A. Wilson, J. J. Warsh and S. Houle (1997). "Carbon-11 labeling of the selective inhibitors of phosphodiesterase-IV Ro 20-1724 and rolipram." J Label Compd Radiopharm **40**: 678-680.

Davis, C. W. and J. W. Daly (1979). "A simple direct assay of 3',5'-cyclic nucleotide phosphodiesterase activity based on the use of polyacrylamide-boronate affinity gel chromatography." J. Cycl. Nucleotide Res. **5**(1): 65-74.

Davis, R. L., H. Takayasu, M. Eberwine and J. Myres (1989). "Cloning and characterization of mammalian homologs of the *Drosophila* dunce$^{+}$ gene." Proc. Natl. Acad. Sci. USA **86**: 3604-3608.

de Jong, R. M., P. K. Blanksma, A. van Waarde and D. J. van Veldhuisen (2002). "Measurement of myocardial beta-adrenoceptor density in clinical studies: a role for positron emission tomography?" Eur J Nucl Med **29**(1): 88-97.

de Jong, R. M., A. T. Willemsen, R. H. Slart, P. K. Blanksma, A. van Waarde, J. H. Cornel, W. Vaalburg, D. J. van Veldhuisen and P. H. Elsinga (2005). "Myocardial beta-adrenoceptor downregulation in idiopathic dilated cardiomyopathy measured

in vivo with PET using the new radioligand (S)-[11C]CGP12388." Eur J Nucl Med Mol Imaging **32**(4): 443-7.

de Wit, R. J., D. Hekstra, B. Jastorff, W. J. Stec, J. Baraniak, R. Van Driel and P. J. Van Haastert (1984). "Inhibitory action of certain cyclophosphate derivatives of cAMP on cAMP-dependent protein kinases." Eur J Biochem **142**(2): 255-60.

deGrado, T. R., G. Hutchins, T. SA, W. DM and S. M (1993). "Myocardial Kinetics of Carbon-11-Meta-Hydroxyephedrine: Retention Mechanisms and Effects of Norepinephrine." J Nucl Med **34**(8): 1287-1293.

Degrado, T. R., M. R. Zalutsky and G. Vaidyanathan (1995). "Uptake mechanisms of meta-[123I]iodobenzylguanidine in isolated rat heart." Nucl Med Biol **22**(1): 1-12.

Delforge, J., D. Mesangeau, F. Dolle, P. Merlet, C. Loc'h, M. Bottlaender, R. Trebossen and A. Syrota (2002). "In vivo quantification and parametric images of the cardiac beta-adrenergic receptor density." J Nucl Med **43**(2): 215-26.

Delgado, M., J. A. Fuentes and M. S. Fernandez-Alfonso (2003). "Histamine up-regulates phosphodiesterase IV activity in U-937 cells through $H_2$ receptor stimulation and cAMP increase." Med Sci Monit **9**(6): BR252-59.

Dent, G., S. R. White, H. Tenor, K. Bodtke, C. Schudt, A. R. Leff, H. Magnussen and K. F. Rabe (1998). "Cyclic nucleotide phosphodiesterase in human bronchial epithelial cells: characterization of isoenzymes and functional effects of PDE inhibitors." Pulm Pharmacol Ther **11**(1): 47-56.

Di Carli, M. F. and S. Dorbala (2006). "Integrated PET/CT for cardiac imaging." Q J Nucl Med Mol Imaging **50**(1): 44-52.

Dinter, H., J. Onuffer, D. Faulds and H. D. Perez (1997). "Phosphodiesterase type IV inhibitors in the treatment of multiple sclerosis." J Mol Med **75**: 95-102.

Dlaboga, D., H. Hajjhussein and J. M. O'Donnell (2008). "Chronic haloperidol and clozapine produce different patterns of effects on phosphodiesterase-1B, -4B, and -10A expression in rat striatum." Neuropharmacology **54**(4): 745-54.

Dobrucki, L. W. and A. J. Sinusas (2010). "PET and SPECT in cardiovascular molecular imaging." Nat Rev Cardiol **7**(1): 38-47.

Dodge, K. L., S. Khouangsathiene, M. S. Kapiloff, R. Mouton, E. V. Hill, M. D. Houslay, L. K. Langeberg and J. D. Scott (2001). "mAKAP assembles a protein kinase A/PDE4 phosphodiesterase cAMP signaling module." Embo J **20**(8): 1921-30.

Drake, M. T., S. K. Shenoy and R. J. Lefkowitz (2006). "Trafficking of G protein-coupled receptors." Circ Res **99**(6): 570-82.

Dranitsaris, G., D. Rayson, M. Vincent, J. Chang, K. Gelmon, D. Sandor and G. Reardon (2008). "The development of a predictive model to estimate cardiotoxic risk for patients with metastatic breast cancer receiving anthracyclines." Breast Cancer Res Treat **107**(3): 443-50.

Dulloo, A. G. (2002). "Biomedicine. A sympathetic defense against obesity." Science **297**(5582): 780-1.

Duman, R. S., G. R. Heninger and E. J. Nestler (1997). "A molecular and cellular theory of depression." Arch Gen Psychiatry **54**: 597-606.

Dupre, D. J., A. Baragli, R. V. Rebois, N. Ethier and T. E. Hebert (2007). "Signalling complexes associated with adenylyl cyclase II are assembled during their biosynthesis." Cell Signal **19**(3): 481-9.

Dzimiri, N. (1999). "Regulation of beta-adrenoceptor signaling in cardiac function and disease." Pharmacol Rev **51**(3): 465-501.

Eckhart, A. D. and W. J. Koch (2002). "Expression of a beta-adrenergic receptor kinase inhibitor reverses dysfunction in failing cardiomyocytes." Mol Ther **5**(1): 74-9.

Eisenhofer, G., P. Friberg, B. Rundqvist, A. A. Quyyumi, G. Lambert, D. M. Kaye, I. J. Kopin, D. S. Goldstein and M. D. Esler (1996). "Cardiac sympathetic nerve function in congestive heart failure." Circulation **93**(9): 1667-76.

El-Armouche, A., T. Rau, O. Zolk, D. Ditz, T. Pamminger, W. H. Zimmermann, E. Jackel, S. E. Harding, P. Boknik, J. Neumann and T. Eschenhagen (2003). "Evidence for protein phosphatase inhibitor-1 playing an amplifier role in beta-adrenergic signaling in cardiac myocytes." Faseb J **17**(3): 437-9.

Engelhardt, S., L. Hein, F. Wiesmann and M. J. Lohse (1999). "Progressive hypertrophy and heart failure in beta1-adrenergic receptor transgenic mice." Proc Natl Acad Sci U S A **96**(12): 7059-64.

Engels, P., S. Abdel'Al, P. Hulley and H. Lübbert (1995). "Brain distribution of four rat homologues of the Drosophila *dunce* cAMP phosphodiesterase." J. Neurosci. Res. **41**: 169-178.

Engels, P., K. Fichtel and H. Lübbert (1994). "Expression and regulation of human and rat phosphodiesterase type IV isogenes." The FEBS Letters **350**: 291-295.

Engels, P., M. Sullivan, T. Müller and H. Lübbert (1995). "Molecular cloning and functional expression in yeast of a human cAMP-specific phosphodiesterase subtype (PDE IV-C)." FEBS Letters **358**: 305-310.

Enoksson, S., E. Degerman, E. Hagstrom-Toft, V. Large and P. Arner (1998). "Various phosphodiesterase subtypes mediate the in vivo antilipolytic effect of insulin on adipose tissue and skeletal muscle in man." Diabetologia **41**(5): 560-8.

Erdogan, S. and M. D. Houslay (1997). "Challenge of human jurkat T-cells with the adenylate cyclase activator forskolin elicits major changes in cAMP phosphodiesterase (PDE) expression by up-regulating PDE3 and inducing PDE4D1 and PDE4D2 splice variants as well as down-regulating a novel PDE4A splice variant." Biochem. J. **321**: 165-175.

Esler, M. D., G. L. Jennings, J. Johns, F. Burke, P. J. Little and P. Leonard (1984). "Estimation of 'total' renal, cardiac and splanchnic sympathetic nervous tone in essential hypertension from measurements of noradrenaline release." J Hypertens Suppl **2**(3): S123-5.

Esposito, G., G. Giovacchini, M. Der, J. S. Liow, A. K. Bhattacharjee, K. Ma, P. Herscovitch, M. Channing, W. C. Eckelman, M. Hallett, R. E. Carson and S. I. Rapoport (2007). "Imaging signal transduction via arachidonic acid in the human brain during visual stimulation, by means of positron emission tomography." Neuroimage **34**(4): 1342-51.

Esposito, K., G. W. Reierson, H. R. Luo, G. S. Wu, J. Licinio and M. L. Wong (2009). "Phosphodiesterase genes and antidepressant treatment response: a review." Ann Med **41**(3): 177-85.

Farooqui, S. M., K. Zhang, M. Makhay, K. Jackson, S. Q. Farooqui, J. A. Cherry and J. M. O'Donnell (2000). "Noradrenergic lesions differentially alter the expression of two subtypes of low Km cAMP-sensitive phosphodiesterase type 4 (PDE4A and PDE4B) in rat brain." Brain Res **867**(1-2): 52-61.

Feldman, A. M. (1993). "Modulation of adrenergic receptors and G-transduction proteins in failing human ventricular myocardium." Circulation **87**(5 Suppl): IV27-34.

Feldman, A. M., A. E. Cates, M. R. Bristow and C. Van Dop (1989). "Altered expression of alpha-subunits of G proteins in failing human hearts." J Mol Cell Cardiol **21**(4): 359-65.

Feldman, A. M., A. E. Cates, W. B. Veazey, R. E. Hershberger, M. R. Bristow, K. L. Baughman, W. A. Baumgartner and C. Van Dop (1988). "Increase of the 40,000-mol wt pertussis toxin substrate (G protein) in the failing human heart." J Clin Invest **82**(1): 189-97.

Feldman, M. D., L. Copelas, J. K. Gwathmey, P. Phillips, S. E. Warren, F. J. Schoen, W. Grossman and J. P. Morgan (1987). "Deficient production of cyclic AMP: pharmacologic evidence of an important cause of contractile dysfunction in patients with end-stage heart failure." Circulation **75**(2): 331-9.

Floras, J. S. (2003). "Sympathetic activation in human heart failure: diverse mechanisms, therapeutic opportunities." Acta Physiol Scand **177**(3): 391-8.

Fowler, M. B., J. A. Laser, G. L. Hopkins, W. Minobe and M. R. Bristow (1986). "Assessment of the beta-adrenergic receptor pathway in the intact failing human heart: progressive receptor down-regulation and subsensitivity to agonist response." Circulation **74**(6): 1290-302.

Freedman, N. J., S. B. Liggett, D. E. Drachman, G. Pei, M. G. Caron and R. J. Lefkowitz (1995). "Phosphorylation and desensitization of the human beta 1-adrenergic receptor. Involvement of G protein-coupled receptor kinases and cAMP-dependent protein kinase." J Biol Chem **270**(30): 17953-61.

Frishman, W. H. (2008). "beta-Adrenergic blockers: a 50-year historical perspective." Am J Ther **15**(6): 565-76.

Fu, M., M. Matoba, Q. M. Liang, K. G. Sjogren and A. Hjalmarson (1994). "Properties of G-protein modulated receptor-adenylyl cyclase system in myocardium of spontaneously hypertensive rats treated with adriamycin." Int J Cardiol **44**(1): 9-18.

Fujita, M., M. Imaizumi, C. D'Sa, S. S. Zoghbi, M. S. Crescenzo, J. Hong, J. L. Musachio, A. D. Gee, J. Seidel, M. V. Green, V. W. Pike, R. S. Duman and R. B. Innis (2007). "In vivo and in vitro measurement of brain phosphodiesterase 4 in rats after antidepressant administration." Synapse **61**(2): 78-86.

Fujita, M. and R. B. Innis (2000). "Nuclear psychiatry: specialty for the twenty-first century?" Eur J Nucl Med **27**(1 Suppl): S39-42.

Fujita, M., S. S. Zoghbi, M. S. Crescenzo, J. Hong, J. L. Musachio, J. Q. Lu, J. S. Liow, N. Seneca, D. N. Tipre, V. L. Cropley, M. Imaizumi, A. D. Gee, J. Seidel, M. V. Green, V. W. Pike and R. B. Innis (2005). "Quantification of brain phosphodiesterase 4 in rat with (R)-[(11)C]Rolipram-PET." Neuroimage **26**(4): 1201-10.

Garcia-Sevilla, J. A. and J. K. Zubieta (1986). "Activation and desensitization of presynaptic alpha 2-adrenoceptors after inhibition of neuronal uptake by antidepressant drugs in the rat vas deferens." Br J Pharmacol **89**(4): 673-83.

Gardner, C., N. Robas, D. Cawkill and M. Fidock (2000). "Cloning and characterization of the human and mouse PDE7B, a novel cAMP-specific cyclic nucleotide phosphodiesterase." Biochem Biophys Res Commun **272**(1): 186-92.

Gee, A., C. Parker, J. Matthews, J. Passchier, D. Smith, D. Bender, S. Knibb, A. Gjedde and J. Brown (2002). "Evidence to support the use of S(+)-[11C]Rolipram in estimating the non-specific binding component of R(-)-[11C]Rolipram to PDE4 *in vivo* using PET." NeuroImage **16**(3): S34.

Gee, A., D. Smith, L. Ostergaard, D. Bender, P. Hoest Poulsen, C. Simonsen, K. Roelsgaard and A. Gjedde (1998). "Mapping second messenger activations in the brain." Neuroimage **7**(4): A38.

Gilman, A. G. (1987). "G proteins: Transducers of receptor-generated signals." Ann. Rev. Biochem. **56**: 615-649.

Giordano, D., M. E. De Stefano, G. Citro, A. Modica and M. Giorgi (2001). "Expression of cGMP-binding cGMP-specific phosphodiesterase (PDE5) in mouse tissues and cell lines using an antibody against the enzyme amino-terminal domain." Biochim Biophys Acta **1539**(1-2): 16-27.

Giralt, M. T. and J. A. Garcia-Sevilla (1989). "Acute and long-term regulation of brain alpha 2-adrenoceptors after manipulation of noradrenergic transmission in the rat." Eur J Pharmacol **164**(3): 455-66.

Gomez-Ramirez, J., J. Ortiz and I. Blanco (2002). "Presynaptic $H_3$ autoreceptors modulate histamine synthesis through cAMP pathway." Molec. Pharmacol. **61**(1): 239-45.

Gosselin, H., X. Qi and J. L. Rouleau (1998). "Correlation between cardiac remodelling, function, and myocardial contractility in rat hearts 5 weeks after myocardial infarction." Can J Physiol Pharmacol **76**(1): 53-62.

Greene, M., J. T. Thackeray, M. Kenk, S. L. Thorn, L. Bevilacqua, M.-E. Harper, R. S. Beanlands and J. N. DaSilva (2009). "Reduced *In Vivo* Phosphodiesterase-4 Response to Norepinephrine Challenge in Diet-Induced Obese Rats." Can J Physiol Pharmacol **87**: 196-202.

Gretarsdottir, S., S. Sveinbjornsdottir, H. H. Jonsson, F. Jakobsson, E. Einarsdottir, U. Agnarsson, D. Shkolny, G. Einarsson, H. M. Gudjonsdottir, E. M. Valdimarsson, O. B. Einarsson, G. Thorgeirsson, R. Hadzic, S. Jonsdottir, S. T. Reynisdottir, S. M. Bjarnadottir, T. Gudmundsdottir, G. J. Gudlaugsdottir, R. Gill, K. Lindpaintner, J. Sainz, H. H. Hannesson, G. T. Sigurdsson, M. L. Frigge, A. Kong, V. Gudnason, K. Stefansson and J. R. Gulcher (2002). "Localization of a susceptibility gene for common forms of stroke to 5q12." Am J Hum Genet **70**(3): 593-603.

Gretarsdottir, S., G. Thorleifsson, S. T. Reynisdottir, A. Manolescu, S. Jonsdottir, T. Jonsdottir, T. Gudmundsdottir, S. M. Bjarnadottir, O. B. Einarsson, H. M. Gudjonsdottir, M. Hawkins, G. Gudmundsson, H. Gudmundsdottir, H. Andrason, A. S. Gudmundsdottir, M. Sigurdardottir, T. T. Chou, J. Nahmias, S. Goss, S. Sveinbjornsdottir, E. M. Valdimarsson, F. Jakobsson, U. Agnarsson, V. Gudnason, G. Thorgeirsson, J. Fingerle, M. Gurney, D. Gudbjartsson, M. L. Frigge, A. Kong, K. Stefansson and J. R. Gulcher (2003). "The gene encoding phosphodiesterase 4D confers risk of ischemic stroke." Nat Genet **35**(2): 131-8.

Grierson, J. R., K. J. Yagle, J. F. Eary, J. F. Tait, D. F. Gibson, B. Lewellen, J. M. Link and K. A. Krohn (2004). "Production of [F-18]fluoroannexin for imaging apoptosis with PET." Bioconjug Chem **15**(2): 373-9.

Hadcock, J. R. and C. C. Malbon (1988). "Down-regulation of beta-adrenergic receptors: agonist-induced reduction in receptor mRNA levels." Proc Natl Acad Sci U S A **85**(14): 5021-5.

Haft, J. I. (1974). "Cardiovascular injury induced by sympathetic catecholamines." Prog Cardiovasc Dis **17**(1): 73-86.

Hajjar, R. J., R. Liao, J. B. Young, F. Fuleihan, M. G. Glass and J. K. Gwathmey (1993). "Pathophysiological and biochemical characterisation of an avian model of dilated cardiomyopathy: comparison to findings in human dilated cardiomyopathy." Cardiovasc Res **27**(12): 2212-21.

Han, P., X. Zhu and T. Michaeli (1997). "Alternative splicing of the high affinity cAMP-specific phosphodiesterase (PDE7A) mRNA in human skeletal muscle and heart." J Biol Chem **272**(26): 16152-7.

Hanifin, J. M., S. C. Chan, J. B. Cheng, S. J. Tofte, W. R. J. Henderson, D. S. Kirby and E. S. Weiner (1996). "Type 4 phosphodiesterase inhibitors have clinical and *in vitro* anti-inflammatory effects in atopic dermatitis." J Invest Dermatol **107**: 51-56.

Harada, N., S. Nishiyama, H. Ohba, K. Sato, T. Kakiuchi and H. Tsukada (2002). "Age differences in phosphodiesterase type-IV and its functional response to dopamine $D_1$ receptor modulation in the living brain: a PET study in conscious monkeys." Synapse **44**(3): 139-45.

Harden, T. K. (1983). "Agonist-induced desensitization of the beta-adrenergic receptor-linked adenylate cyclase." Pharmacol Rev **35**(1): 5-32.

Hasking, G. J., M. D. Esler, G. L. Jennings, D. Burton, J. A. Johns and P. I. Korner (1986). "Norepinephrine spillover to plasma in patients with congestive heart failure: evidence of increased overall and cardiorenal sympathetic nervous activity." Circulation **73**(4): 615-21.

Heaslip, R. J. and D. Y. Evans (1995). "Emetic, central nervous system and pulmonary activities of rolipram in the dog." European Journal of Pharmacology **286**: 281-190.

Heather, L. C., A. F. Catchpole, D. J. Stuckey, M. A. Cole, C. A. Carr and K. Clarke (2009). "Isoproterenol induces in vivo functional and metabolic abnormalities: similar to those found in the infarcted rat heart." J Physiol Pharmacol **60**(3): 31-9.

Herzer, W. A., N. J. Thomas, J. A. Carcillo, S. P. Tofovic and E. K. Jackson (1998). "Effects of type IV phosphodiesterase inhibition on cardiac function in the presence and absence of catecholamines." J Cardiovasc Pharmacol **32**(5): 769-76.

Higuchi, T., S. G. Nekolla, M. M. Huisman, S. Reder, T. Poethko, M. Yu, H. J. Wester, D. S. Casebier, S. P. Robinson, R. M. Botnar and M. Schwaiger (2008). "A new 18F-labeled myocardial PET tracer: myocardial uptake after permanent and transient coronary occlusion in rats." J Nucl Med **49**(10): 1715-22.

Higuchi, T. and M. Schwaiger (2006). "Imaging cardiac neuronal function and dysfunction." Curr Cardiol Rep **8**(2): 131-8.

Hildreth, V., R. H. Anderson and D. J. Henderson (2009). "Autonomic innervation of the developing heart: origins and function." Clin Anat **22**(1): 36-46.

Hilton, J., F. Yokoi, R. F. Dannals, H. T. Ravert, Z. Szabo and D. F. Wong (2000). "Column-switching HPLC for the analysis of plasma in PET imaging studies." Nucl Med Biol **27**(6): 627-30.

Hoffmann, R., G. S. Baillie, S. J. MacKenzie, S. J. Yarwood and M. D. Houslay (1999). "The MAP kinase ERK2 inhibits the cyclic AMP-specific phosphodiesterase HSPDE4D3 by phosphorylating it at Ser579." EMBO J **18**(4): 893-903.

Hoffmann, R., I. R. Wilkinson, J. F. McCallum, P. Engels and M. D. Houslay (1998). "cAmp-specific phosphodiesterase Hspde4d3 mutants which mimic activation and changes in rolipram inhibition triggered by protein kinase a phosphorylation of Ser-54: generation of a molecular model." Biochem J **333**(Pt 1): 139-49.

Holthues, H. and L. Vollrath (2004). "The phototransduction cascade in the isolated chick pineal gland revisited." Brain Res **999**(2): 175-80.

Horn, E. M. and J. P. Bilezikian (1990). "Mechanisms of abnormal transmembrane signaling of the beta-adrenergic receptor in congestive heart failure." Circulation **82**(2 Suppl): I26-34.

Hotston, M., J. Y. Jeremy, J. Bloor, N. S. Greaves, R. Persad, G. Angelini and N. Shukla (2008). "Homocysteine and copper interact to promote type 5 phosphodiesterase expression in rabbit cavernosal smooth muscle cells." Asian J Androl **10**(6): 905-13.

Hotta, H., H. Ito, F. Kagitani and A. Sato (1998). "Cilostazol, a selective cAMP phosphodiesterase inhibitor, dilates retinal arterioles and increases retinal and choroidal blood flow in rats." Eur J Pharmacol **344**(1): 49-52.

Houser, S. R. and K. B. Margulies (2003). "Is depressed myocyte contractility centrally involved in heart failure?" Circ Res **92**(4): 350-8.

Houslay, M. D. (2001). "PDE4 cAMP-specific phosphodiesterases." Prog Nucleic Acid Res Mol Biol **69**: 249-315.

Houslay, M. D. and D. R. Adams (2003). "PDE4 cAMP phosphodiesterases: modular enzymes that orchestrate signalling cross-talk, desensitization and compartmentalization." Biochem J **370**(Pt 1): 1-18.

Houslay, M. D., G. S. Baillie and D. H. Maurice (2007). "cAMP-Specific phosphodiesterase-4 enzymes in the cardiovascular system: a molecular toolbox for generating compartmentalized cAMP signaling." Circ Res **100**(7): 950-66.

Houslay, M. D. and G. Milligan (1997). "Tailoring cAMP-signalling responses through isoform multiplicity." TIBS **22**: 217-224.

Houslay, M. D., P. Schafer and K. Y. Zhang (2005). "Keynote review: Phosphodiesterase-4 as a therapeutic target." Drug Discov Today **10**(22): 1503-19.

Houslay, M. D., G. Scotland, S. Erdogan, E. Huston, S. Mackenzie, J. F. McCallum, I. McPhee, L. Pooley, G. Rena, A. Ross, M. Beard, A. Peder, F. Begg, I. Wilkinson, S. Yarwood, C. Ackerman, E. S. Houslay, R. Hoffman, P. Engels, M. Sullivan and G. Bolger (1997). "Intracellular targeting, interaction with Src homology 3 (SH3) domains and rolipram-detected conformational switches in cAMP-specific PDE4A phosphodiesterase." Biochem Soc Trans **25**(2): 374-81.

Houslay, M. D., M. Sullivan and G. B. Bolger (1998). "The multienzyme PDE4 cyclic adenosine monophosphate-specific phosphodiesterase family: intracellular targeting, regulation, and selective inhibition by compounds exerting anti-inflammatory and antidepressant actions." Adv Pharmacol **44**: 225-342.

Hu, A., X. Jiao, E. Gao, W. J. Koch, S. Sharifi-Azad, Z. Grunwald, X. L. Ma and J. Z. Sun (2006). "Chronic beta-Adrenergic Receptor Stimulation Induces Cardiac

Apoptosis and Aggravates Myocardial Ischemia/Reperfusion Injury by Provoking Inducible Nitric-Oxide Synthase-Mediated Nitrative Stress." J Pharmacol Exp Ther **318**(2): 469-75.

Hughes, B., R. Owens, M. Perry, G. Warrellow and R. Allen (1997). "PDE4 inhibitors: the use of molecular cloning in the design and development of novel drugs." Drug Discovery Today **2**: 89-101.

Hume, S. P., R. N. Gunn and T. Jones (1998). "Pharmacological constraints associated with positron emission tomographic scanning of small laboratory animals." Eur J Nucl Med **25**(2): 173-6.

Ikegaya, T., A. Kobayashi, R. B. Hong, H. Masuda, M. Kaneko and Y. Noboru (1992). "Stimulatory guanine nucleotide-binding protein and adenylate cyclase activities in Bio 14.6 cardiomyopathic hamsters at the hypertrophic stage." Mol Cell Biochem **110**(1): 83-90.

International commission on radiological protection (ICRP) (2008). "Annex C Biokinetic models and dose tables." Annals of the ICRP **38**(1-2): 51-162.

Iona, S., M. Cuomo, T. Bushnik, F. Naro, C. Sette, M. Hess, E. R. Shelton and M. Conti (1998). "Characterization of the rolipram-sensitive, cyclic AMP-specific phosphodiesterases: identification and differential expression of immunologically distinct forms in the rat brain." Mol Pharmacol **53**(1): 23-32.

Ito, M., M. Nishikawa, M. Fujioka, M. Miyahara, N. Isaka, H. Shiku and T. Nakano (1996). "Characterization of the isoenzymes of cyclic nucleotide phosphodiesterase in human platelets and the effects of E4021." Cell. Signal. **8**: 575-581.

Itoh, T., K. Abe, J. Hong, O. Inoue, V. W. Pike, R. B. Innis and M. Fujita (2010). "Effects of cAMP-dependent protein kinase activator and inhibitor on in vivo rolipram binding to phosphodiesterase 4 in conscious rats." Synapse **64**(2): 172-6.

Itoh, T., K. Abe, M. Tokumura, M. Horiuchi, O. Inoue and N. Ibii (2003). "Different regulation of adenylyl cyclase and rolipram-sensitive phosphodiesterase activity on the frontal cortex and hippocampus in learned helplessness rats." Brain Res **991**(1-2): 142-9.

Itoh, T., K. Abe, S. S. Zoghbi, O. Inoue, J. Hong, M. Imaizumi, V. W. Pike, R. B. Innis and M. Fujita (2009). "PET measurement of the in vivo affinity of 11C-(R)-rolipram and the density of its target, phosphodiesterase-4, in the brains of conscious and anesthetized rats." J Nucl Med **50**(5): 749-56.

Itoh, T., M. Tokumura and K. Abe (2004). "Effects of rolipram, a phosphodiesterase 4 inhibitor, in combination with imipramine on depressive behavior, CRE-binding activity and BDNF level in learned helplessness rats." Eur J Pharmacol **498**(1-3): 135-42.

Iwahashi, Y., T. Furuyama, Y. Tano, I. Ishimoto, Y. Shimomura and S. Inagaki (1996). "Differential distribution of mRNA encoding cAMP-specific phosphodiesterase isoforms in the rat brain." Brain Res Mol Brain Res **38**(1): 14-24.

Jacobitz, S., M. M. McLaughlin, G. P. Livi, M. Burman and T. J. Torphy (1996). "Mapping the functional domains of human recombinant phosphodiesterase 4A: structural requirements for catalytic activity and rolipram binding." Mol Pharmacol **50**(4): 891-9.

Jacobitz, S., M. D. Ryan, M. M. McLaughlin, G. P. Livi, W. E. DeWolf, Jr. and T. J. Torphy (1997). "Role of conserved histidines in catalytic activity and inhibitor binding of human recombinant phosphodiesterase 4A." Mol Pharmacol **51**(6): 999-1006.

Jagoda, E. M., J. J. Vaquero, J. Seidel, M. V. Green and W. C. Eckelman (2004). "Experiment assessment of mass effects in the rat: implications for small animal PET imaging." Nucl Med Biol **31**(6): 771-779.

Jin, S. L., T. Bushnik, L. Lan and M. Conti (1998). "Subcellular localization of rolipram-sensitive, cAMP-specific phosphodiesterases. Differential targeting and activation of the splicing variants derived from the PDE4D gene." J Biol Chem **273**(31): 19672-8.

Johnson, R. W., T. Reisine, S. Spotnitz, N. Wiech, R. Ursillo and H. I. Yamamura (1980). "Effects of desipramine and yohimbine on alpha 2- and beta-adrenoreceptor sensitivity." Eur J Pharmacol **67**(1): 123-7.

Johnston, L. A., S. Erdogan, Y. F. Cheung, M. Sullivan, R. Barber, M. J. Lynch, G. S. Baillie, G. Van Heeke, D. R. Adams, E. Huston and M. D. Houslay (2004). "Expression, intracellular distribution and basis for lack of catalytic activity of the PDE4A7 isoform encoded by the human PDE4A cAMP-specific phosphodiesterase gene." Biochem J **380**(Pt 2): 371-84.

Jurevicius, J. and R. Fischmeister (1996). "cAMP compartmentation is responsible for a local activation of cardiac $Ca^{2+}$ channels by b-adrenergic agonists." Proc. Natl. Acad. Sci. USA **93**: 295-299.

Kajimoto, K., N. Hagiwara, H. Kasanuki and S. Hosoda (1997). "Contribution of phosphodiesterase isozymes to the regulation of the L-type calcium current in human cardiac myocytes." Br J Pharmacol **121**: 1549-1556.

Kant, G. J., J. L. Meyerhoff and R. H. Lenox (1980). "In vivo effects of apomorphine and 4-(3-butoxy-4-methoxybenzyl)-2-imidazolidinone (Ro 20-1724) on cyclic nucleotides in rat brain and pituitary." Biochem. Pharmacol. **29**: 369-373.

Katano, Y. and M. Endoh (1990). "Differential effects of Ro 20-1724 and isobutylmethylxanthine on the basal force of contraction and beta-adrenoceptor-mediated response in the rat ventricular myocardium." Biochem Biophys Res Commun **167**(1): 123-9.

Katano, Y. and M. Endoh (1992). "Effects of a cardiotonic quinolinone derivative Y-20487 on the isoproterenol-induced positive inotropic action and cyclic AMP accumulation if rat ventricular myocardium: comparison with rolipram, Ro 20-1724, milrinone, and isobutylmethylxanthine." J Cardiovasc Pharmacol **20**: 715-722.

Katz, A. M. (1986). "Potential deleterious effects of inotropic agents in the therapy of chronic heart failure." Circulation **73**(3 Pt 2): III184-90.

Katz, A. M. (1989). "Changing strategies in the management of heart failure." J Am Coll Cardiol **13**(3): 513-23.

Kaulen, P., G. Brüning, H. H. Schneider, M. Sarter and H. G. Baumgarten (1989). "Autoradiographic mapping of selective cyclic adenosine monophosphate phosphodiesterase in rat brain with the antidepressant [$^{3}$H] rolipram." Brain Res. **503**: 229-245.

Kaumann, A. J., S. Engelhardt, L. Hein, P. Molenaar and M. Lohse (2001). "Abolition of (-)-CGP 12177-evoked cardiostimulation in double beta1/beta2-adrenoceptor knockout mice. Obligatory role of beta1-adrenoceptors for putative beta4-adrenoceptor pharmacology." Naunyn Schmiedebergs Arch Pharmacol **363**(1): 87-93.

Kawada, T., T. Yamazaki, T. Akiyama, T. Sato, T. Shishido, M. Sugimachi and K. Sunagawa (2000). "Chronic adriamycin treatment impairs myocardial interstitial neuronal release of norepinephrine and epinephrine." J Cardiovasc Pharmacol **36 Suppl 2**: S31-4.

Kebabian, J. W. and D. B. Calne (1979). "Multiple receptors for dopamine." Nature **277**: 93-96.

Kelly, J. J., P. J. Barnes and M. A. Giembycz (1996). "Phosphodiesterase 4 in macrophages: relationship between cAMP accumulation, suppression of cAMP hydrolysis and inhibition of [3H]R-(- )-rolipram binding by selective inhibitors." Biochem. J. **318**(Pt 2): 425-36.

Kenk, M., M. Greene, M. Lortie, R. A. Dekemp, R. S. Beanlands and J. N. Dasilva (2008). "Use of a column-switching high-performance liquid chromatography method to assess the presence of specific binding of (R)- and (S)-[(11)C]rolipram and their labeled metabolites to the phosphodiesterase-4 enzyme in rat plasma and tissues." Nucl Med Biol **35**(4): 515-21.

Kenk, M., M. Greene, J. Thackeray, R. A. Dekemp, M. Lortie, S. Thorn, R. S. Beanlands and J. N. Dasilva (2007). "In vivo selective binding of (R)-[(11)C]rolipram to phosphodiesterase-4 provides the basis for studying intracellular cAMP signaling in the myocardium and other peripheral tissues." Nucl Med Biol **34**(1): 71-7.

Kenk, M., M. Lortie, S. Thorn, D. Davis, D. Birnie, M. Labinaz, A. Tang, R. deKemp, R. Beanlands and J. DaSilva (2006). Imaging Myocardial cAMP-Specific Phosphodiesterase-4 Activity in Canine Models. Canadian Cardiovascular Congress, Vancouver, B.C.

Kenk, M., J. T. Thackeray, S. L. Thorn, K. Dhami, B. J. Chow, K. J. Ascah, J. N. Dasilva and R. S. Beanlands (2010). "Alterations of pre- and postsynaptic noradrenergic signaling in a rat model of adriamycin-induced cardiotoxicity." J Nucl Cardiol **17**(2): 175-176.

Kessler, P. D., A. E. Cates, C. Van Dop and A. M. Feldman (1989). "Decreased bioactivity of the guanine nucleotide-binding protein that stimulates adenylate cyclase in hearts from cardiomyopathic Syrian hamsters." J Clin Invest **84**(1): 244-52.

Kiesewetter, D. O., M. B. Sassaman, J. Robbins, M. J. Elaine, R. E. Carson, N. M. Appel, E. Sutkowski, P. Herscovitch, A. Braun and W. C. Eckelman (2000). "Synthesis and evaluation of an $^{18}$F analog of forskolin for imaging adenylyl cyclase." Journal of Fluorine Chemistry **101**: 297-304.

Kimura, H., A. Miyamoto and H. Ohshika (1993). "Down-regulation of beta-adrenoceptors and loss of Gs alpha subunit levels in ventricular myocardium of rats treated with isoproterenol." Life Sci **53**(10): PL171-6.

Kiuchi, K., R. P. Shannon, K. Komamura, D. J. Cohen, C. Bianchi, C. J. Homcy, S. F. Vatner and D. E. Vatner (1993). "Myocardial beta-adrenergic receptor function

during the development of pacing-induced heart failure." J Clin Invest **91**(3): 907-14.

Kizaki, K., K. Akatsuka, M. Momozaki, Y. Fujimori, T. Uchide, K. Temma and Y. Hara (2004). "Changes in myocardial beta1-adrenergic receptor and stimulatory G-protein gene expression after chronic treatment with doxorubicin in rat." J Vet Med Sci **66**(8): 989-92.

Knuuti, J. and F. M. Bengel (2008). "Positron emission tomography and molecular imaging." Heart **94**(3): 360-7.

Kobayashi, T., M. Gamanuma, T. Sasaki, Y. Yamashita, K. Yuasa, J. Kotera and K. Omori (2003). "Molecular comparison of rat cyclic nucleotide phosphodiesterase 8 family: unique expression of PDE8B in rat brain." Gene **319**: 21-31.

Koch, W. J., J. Inglese, W. C. Stone and R. J. Lefkowitz (1993). "The binding site for the beta gamma subunits of heterotrimeric G proteins on the beta-adrenergic receptor kinase." J Biol Chem **268**(11): 8256-60.

Koch, W. J., R. J. Lefkowitz and H. A. Rockman (2000). "Functional consequences of altering myocardial adrenergic receptor signaling." Annu Rev Physiol **62**: 237-60.

Koch, W. J., H. A. Rockman, P. Samama, R. A. Hamilton, R. A. Bond, C. A. Milano and R. J. Lefkowitz (1995). "Cardiac function in mice overexpressing the beta-adrenergic receptor kinase or a beta ARK inhibitor." Science **268**(5215): 1350-3.

Kostic, M. M., S. Erdogan, G. Rena, G. Borchert, B. Hoch, S. Bartel, G. Scotland, E. Huston, M. D. Houslay and E. G. Krause (1997). "Altered expression of PDE1 and PDE4 cyclic nucleotide phosphodiesterase isoforms in 7-oxo-prostacyclin-preconditioned rat heart." J Mol Cell Cardiol **29**(11): 3135-46.

Kotera, J., K. Fujishige and K. Omori (2000). "Immunohistochemical localization of cGMP-binding cGMP-specific phosphodiesterase (PDE5) in rat tissues." J Histochem Cytochem **48**(5): 685-93.

Koyama, M., N. Seyedi, W. P. Fung-Leung, T. W. Lovenberg and R. Levi (2003). "Norepinephrine release from the ischemic heart is greatly enhanced in mice lacking histamine $H_3$ receptors." Mol Pharmacol **63**(2): 378-82.

Krause, W. and G. Kühne (1988). "Pharmacokinetics of rolipram in the rhesus and cynomolgus monkeys, the rat and the rabbit. Studies on species differences." Xenobiotica **18**(5): 561-571.

Krause, W. and G. Kühne (1992). "High-performance liquid chromatographic procedure for specificity testing of radioimmunoassays: rolipram." Journal of Chromatography **573**: 303-308.

Krause, W. and G. Kühne (1993). "Biotransformation of the antidepressant D,L-rolipram. II. Metabolite patterns in man, rat, rabbit, rehesus and cynomolgus monkey." Xenobiotica **23**(11): 1277-1288.

Krause, W., G. Kuhne, U. Jakobs and G. A. Hoyer (1993). "Biotransformation of the antidepressant DL-rolipram. I. Isolation and identification of metabolites from rat, monkey, and human urine." Drug Metab Dispos **21**(4): 682-9.

Krause, W., G. Kühne and H. Matthes (1989). "Pharmacokinetics of the antidepressant rolipram in healthy volunteers." Xenobiotica **19**(6): 683-692.

Krause, W., G. Kühne and N. Sauerbrey (1990). "Pharmacokinetics of (+)-rolipram and (-)-rolipram in healthy volunteers." European Journal of Clinical Pharmacology**?8 ( 38 or 58 )**: 71-75.

Kudo, T., K. Fukuchi, A. J. Annala, A. F. Chatziioannou, V. Allada, M. Dahlbom, Y. C. Tai, M. Inubushi, S. C. Huang, S. R. Cherry, M. E. Phelps and H. R. Schelbert (2002). "Noninvasive measurement of myocardial activity concentrations and perfusion defect sizes in rats with a new small-animal positron emission tomograph." Circulation **106**(1): 118-23.

Kurz, T., G. Richardt, S. Hagl, M. Seyfarth and A. Schomig (1995). "Two different mechanisms of noradrenaline release during normoxia and simulated ischemia in human cardiac tissue." J Mol Cell Cardiol **27**(5): 1161-72.

L'Ecuyer, T., S. Sanjeev, R. Thomas, R. Novak, L. Das, W. Campbell and R. V. Heide (2006). "DNA damage is an early event in doxorubicin-induced cardiac myocyte death." Am J Physiol Heart Circ Physiol **291**(3): H1273-80.

Laliberte, F., Y. Han, A. Govindarajan, A. Giroux, S. Liu, B. Bobechko, P. Lario, A. Bartlett, E. Gorseth, M. Gresser and Z. Huang (2000). "Conformational difference between PDE4 apoenzyme and holoenzyme." Biochemistry **39**(21): 6449-58.

Laliberte, F., S. Liu, E. Gorseth, B. Bobechko, A. Bartlett, P. Lario, M. J. Gresser and Z. Huang (2002). "In vitro PKA phosphorylation-mediated human PDE4A4 activation." FEBS Lett **512**(1-3): 205-8.

Lamb, T. D. and E. N. Pugh, Jr. (2006). "Phototransduction, dark adaptation, and rhodopsin regeneration the proctor lecture." Invest Ophthalmol Vis Sci **47**(12): 5137-52.

Lamoureux, M., S. L. Thorn, T. Dumouchel, R. Klein, J. Renaud, M. Lortie, R. Beanlands, J. N. DaSilva and R. deKemp (2010 (Submitted)). "Uniformity and Reproducibility of Normal Resting Myocardial Blood Flow in Rats with $^{13}$N-ammonia and small animal PET." Molec Imag Biol.

Landsberg, L. (1986). "Diet, obesity and hypertension: an hypothesis involving insulin, the sympathetic nervous system, and adaptive thermogenesis." Q J Med **61**(236): 1081-90.

Laurent, C. E., R. Cardinal, G. Rousseau, M. Vermeulen, C. Bouchard, M. Wilkinson, J. A. Armour and M. Bouvier (2001). "Functional desensitization to isoproterenol without reducing cAMP production in canine failing cardiocytes." Am J Physiol Regul Integr Comp Physiol **280**(2): R355-64.

Lautamaki, R., D. Tipre and F. M. Bengel (2007). "Cardiac sympathetic neuronal imaging using PET." Eur J Nucl Med Mol Imaging **34 Suppl 1**: S74-85.

Lee, T. M., P. Y. Lai and N. C. Chang (2010). "Effect of N-acetylcysteine on sympathetic hyperinnervation in post-infarcted rat hearts." Cardiovasc Res **85**(1): 137-46.

Lefkowitz, R. J. (1998). "G protein-coupled receptors. III. New roles for receptor kinases and beta-arrestins in receptor signaling and desensitization." J Biol Chem **273**(30): 18677-80.

Lefkowitz, R. J., H. A. Rockman and W. J. Koch (2000). "Catecholamines, cardiac beta-adrenergic receptors, and heart failure." Circulation **101**(14): 1634-7.

Lefrak, E. A., J. Pitha, S. Rosenheim and J. A. Gottlieb (1973). "A clinicopathologic analysis of adriamycin cardiotoxicity." Cancer **32**(2): 302-14.

Lehnart, S. E., X. H. Wehrens, S. Reiken, S. Warrier, A. E. Belevych, R. D. Harvey, W. Richter, S. L. Jin, M. Conti and A. R. Marks (2005). "Phosphodiesterase 4D deficiency in the ryanodine-receptor complex promotes heart failure and arrhythmias." Cell **123**(1): 25-35.

Leimbach, W. N., Jr., B. G. Wallin, R. G. Victor, P. E. Aylward, G. Sundlof and A. L. Mark (1986). "Direct evidence from intraneural recordings for increased central sympathetic outflow in patients with heart failure." Circulation **73**(5): 913-9.

Lemos Legnazzi, B., C. Shayo, F. Monczor, M. E. Martin, N. Fernandez, A. Brodsky, A. Baldi and C. Davio (2000). "Rapid desensitization and slow recovery of the cyclic AMP response mediated by histamine $H_2$ receptors in the U937 cell line." Biochem Pharmacol **60**(2): 159-66.

Leroy, J., A. Abi-Gerges, V. O. Nikolaev, W. Richter, P. Lechene, J. L. Mazet, M. Conti, R. Fischmeister and G. Vandecasteele (2008). "Spatiotemporal dynamics of beta-adrenergic cAMP signals and L-type Ca2+ channel regulation in adult rat ventricular myocytes: role of phosphodiesterases." Circ Res **102**(9): 1091-100.

Levi, R. and N. C. Smith (2000). "Histamine $H_3$-receptors: a new frontier in myocardial ischemia." J Pharmacol Exp Ther **292**(3): 825-30.

Levin, B. E. and A. A. Dunn-Meynell (2000). "Defense of body weight against chronic caloric restriction in obesity-prone and -resistant rats." Am J Physiol Regul Integr Comp Physiol **278**(1): R231-7.

Levin, B. E., A. A. Dunn-Meynell, B. Balkan and R. E. Keesey (1997). "Selective breeding for diet-induced obesity and resistance in Sprague-Dawley rats." Am J Physiol **273**(2 Pt 2): R725-30.

Levin, B. E., J. Triscari and A. C. Sullivan (1983). "Altered sympathetic activity during development of diet-induced obesity in rat." Am J Physiol **244**(3): R347-55.

Levin, M. C., S. Marullo, O. Muntaner, B. Andersson and Y. Magnusson (2002). "The myocardium-protective Gly-49 variant of the beta 1-adrenergic receptor exhibits constitutive activity and increased desensitization and down-regulation." J Biol Chem **277**(34): 30429-35.

Levy, F. O., E. Qvigstad, K. A. Krobert, T. Skomedal and J. B. Osnes (2008). "Effects of serotonin in failing cardiac ventricle: signalling mechanisms and potential therapeutic implications." Neuropharmacology **55**(6): 1066-71.

Levy, F. O., X. Zhu, A. J. Kaumann and L. Birnbaumer (1993). "Efficacy of beta 1-adrenergic receptors is lower than that of beta 2-adrenergic receptors." Proc Natl Acad Sci U S A **90**(22): 10798-802.

Li, L., J. Desantiago, G. Chu, E. G. Kranias and D. M. Bers (2000). "Phosphorylation of phospholamban and troponin I in beta-adrenergic-induced acceleration of cardiac relaxation." Am J Physiol Heart Circ Physiol **278**(3): H769-79.

Li, T., I. Danelisen, A. Bello-Klein and P. K. Singal (2000). "Effects of probucol on changes of antioxidant enzymes in adriamycin-induced cardiomyopathy in rats." Cardiovasc Res **46**(3): 523-30.

Liang, W. and S. E. Mills (2002). "Quantitative analysis of beta-adrenergic receptor subtypes in pig tissues." J Anim Sci **80**(4): 963-70.

Liggett, S. B., N. M. Tepe, J. N. Lorenz, A. M. Canning, T. D. Jantz, S. Mitarai, A. Yatani and G. W. Dorn, 2nd (2000). "Early and delayed consequences of beta(2)-adrenergic receptor overexpression in mouse hearts: critical role for expression level." Circulation **101**(14): 1707-14.

Lin, F. T., K. M. Krueger, H. E. Kendall, Y. Daaka, Z. L. Fredericks, J. A. Pitcher and R. J. Lefkowitz (1997). "Clathrin-mediated endocytosis of the beta-adrenergic

receptor is regulated by phosphorylation/dephosphorylation of beta-arrestin1." J Biol Chem **272**(49): 31051-7.

Link, J. M. and J. H. Caldwell (2008). "Diagnostic and prognostic imaging of the cardiac sympathetic nervous system." Nat Clin Pract Cardiovasc Med **5 Suppl 2**: S79-86.

Link, J. M., J. R. Stratton, W. Levy, J. E. Poole, S. C. Shoner, W. Stuetzle and J. H. Caldwell (2003). "PET measures of pre- and post-synaptic cardiac beta adrenergic function." Nucl Med Biol **30**(8): 795-803.

Liu, H. and D. H. Maurice (1999). "Phosphorylation-mediated activation and translocation of the cyclic AMP-specific phosphodiesterase PDE4D3 by cyclic AMP-dependent protein kinase and mitogen-activated protein kinases. A potential mechanism allowing for the coordinated regulation of PDE4D activity and targeting." J Biol Chem **274**(15): 10557-65.

Liu, H., D. Palmer, S. L. Jimmo, D. G. Tilley, H. A. Dunkerley, S. C. Pang and D. H. Maurice (2000). "Expression of phosphodiesterase 4D (PDE4D) is regulated by both the cyclic AMP-dependent protein kinase and mitogen-activated protein kinase signaling pathways. A potential mechanism allowing for the coordinated regulation of PDE4D activity and expression in cells." J Biol Chem **275**(34): 26615-24.

Liu, P., M. Arnold, I. Belenkie, J. Howlett, V. Huckell, A. Ignazewski, M. H. LeBlanc, R. McKelvie, J. Niznick, J. D. Parker, V. Rao, H. Ross, D. Roy, S. Smith, B. Sussex, K. Teo, R. Tsuyuki, M. White, D. Beanlands, V. Bernstein, R. Davies, D. Issac, D. Johnstone, H. Lee, G. Moe, G. Newton, P. Pflugfelder, S. Roth, J. Rouleau and S. Yusuf (2001). "The 2001 Canadian Cardiovascular Society consensus guideline update for the management and prevention of heart failure." Can J Cardiol **17 Suppl E**: 5E-25E.

Liu, S., F. Laliberte, B. Bobechko, A. Bartlett, P. Lario, E. Gorseth, J. Van Hamme, M. J. Gresser and Z. Huang (2001). "Dissecting the cofactor-dependent and independent bindings of PDE4 inhibitors." Biochemistry **40**(34): 10179-86.

Lloyd-Jones, D., R. J. Adams, T. M. Brown, M. Carnethon, S. Dai, G. De Simone, T. B. Ferguson, E. Ford, K. Furie, C. Gillespie, A. Go, K. Greenlund, N. Haase, S. Hailpern, P. M. Ho, V. Howard, B. Kissela, S. Kittner, D. Lackland, L. Lisabeth, A. Marelli, M. M. McDermott, J. Meigs, D. Mozaffarian, M. Mussolino, G. Nichol, V. L. Roger, W. Rosamond, R. Sacco, P. Sorlie, R. Stafford, T. Thom, S. Wasserthiel-Smoller, N. D. Wong and J. Wylie-Rosett (2010). "Heart disease and stroke statistics--2010 update: a report from the American Heart Association." Circulation **121**(7): e46-e215.

Loffelholz, K. and A. J. Pappano (1985). "The parasympathetic neuroeffector junction of the heart." Pharmacol Rev **37**(1): 1-24.

Longabaugh, J. P., D. E. Vatner, S. F. Vatner and C. J. Homcy (1988). "Decreased stimulatory guanosine triphosphate binding protein in dogs with pressure-overload left ventricular failure." J Clin Invest **81**(2): 420-4.

Lortie, M., J. DaSilva, M. Kenk, S. Thorn, R. Beanlands and R. deKemp (2006). Kinetics of (*R*)-[$^{11}$C]rolipram and (*S*)-[$^{11}$C]rolipram in the Dog Heart: Investigation of Four Compartment Models. IEEE Medical Imaging Conference, San Diego, California.

Lortie, M., J. N. Dasilva, M. Kenk, S. L. Thorn, D. Davis, D. Birnie, R. Beanlands and R. deKemp (2009 (Submitted)). "Quantification of Phosphodiesterase-4 in Canine Myocardium with (*R*)-[$^{11}$C]rolipram and PET." J Nucl Med.

Loughney, K., J. Taylor and V. A. Florio (2005). "3',5'-cyclic nucleotide phosphodiesterase 11A: localization in human tissues." Int J Impot Res **17**(4): 320-5.

Lourenco, C. M., J. N. DaSilva, J. J. Warsh, A. A. Wilson and S. Houle (1999). "Imaging of cAMP-specific phosphodiesterase-IV: comparison of [$^{11}$C]rolipram and [$^{11}$C]Ro 20-1724 in rats." Synapse **31**(1): 41-50.

Lourenco, C. M., S. Houle, A. A. Wilson and J. N. DaSilva (2001). "Characterization of (*R*)-[$^{11}$C]rolipram for PET imaging of phosphodiesterase-4: in vivo binding, metabolism, and dosimetry studies in rats." Nucl Med Biol **28**(4): 347-58.

Lourenco, C. M., M. Kenk, R. S. Beanlands and J. N. DaSilva (2006). "Increasing synaptic noradrenaline, serotonin and histamine enhances in vivo binding of phosphodiesterase-4 inhibitor (R)-[11C]rolipram in rat brain, lung and heart." Life Sci **79**(4): 356-64.

Lu, H. (2007). "Stereoselectivity in drug metabolism." Expert Opin Drug Metab Toxicol **3**(2): 149-58.

Lugnier, C. (2006). "Cyclic nucleotide phosphodiesterase (PDE) superfamily: a new target for the development of specific therapeutic agents." Pharmacol Ther **109**(3): 366-98.

Lugnier, C., T. Keravis, A. Le Bec, O. Pauvert, S. Proteau and E. Rousseau (1999). "Characterization of cyclic nucleotide phosphodiesterase isoforms associated to isolated cardiac nuclei." Biochimica et Biophysica Acta **1472**(3): 431-46.

Lymperopoulos, A., G. Rengo, H. Funakoshi, A. D. Eckhart and W. J. Koch (2007). "Adrenal GRK2 upregulation mediates sympathetic overdrive in heart failure." Nat Med **13**(3): 315-23.

Lynch, M. J., G. S. Baillie, A. Mohamed, X. Li, C. Maisonneuve, E. Klussmann, G. van Heeke and M. D. Houslay (2005). "RNA silencing identifies PDE4D5 as the functionally relevant cAMP phosphodiesterase interacting with beta arrestin to control the protein kinase A/AKAP79-mediated switching of the beta2-adrenergic receptor to activation of ERK in HEK293B2 cells." J Biol Chem **280**(39): 33178-89.

MacKenzie, S. J., G. S. Baillie, I. McPhee, G. B. Bolger and M. D. Houslay (2000). "ERK2 mitogen-activated protein kinase binding, phosphorylation, and regulation of the PDE4D cAMP-specific phosphodiesterases. The involvement of COOH-terminal docking sites and NH2-terminal UCR regions." J Biol Chem **275**(22): 16609-17.

Madelian, V. and E. La Vigne (1996). "Rapid Regulation of a Cyclic AMP-Specific Phosphodiesterase (PDE IV) by Forskolin and Isoproterenol in LRM55 Astroglial Cells." Biochem Pharmacol **51**: 1739 - 1747.

Maisel, A. S., H. J. Motulsky and P. A. Insel (1985). "Externalization of beta-adrenergic receptors promoted by myocardial ischemia." Science **230**(4722): 183-6.

Maisel, A. S., H. J. Motulsky and P. A. Insel (1987). "Life cycles of cardiac alpha 1- and beta-adrenergic receptors." Biochem Pharmacol **36**(1): 1-6.

Makhay, M. M., M. D. Houslay and J. M. O'Donnell (2001). "Discriminative stimulus effects of the type-4 phosphodiesterase inhibitor rolipram in rats." Psychopharmacology (Berl) **158**(3): 297-304.

Makhlouf, A., A. Kshirsagar and C. Niederberger (2006). "Phosphodiesterase 11: a brief review of structure, expression and function." Int J Impot Res **18**(6): 501-9.

Malagie, I., A. C. Trillat, C. Jacquot and A. M. Gardier (1995). "Effects of acute fluoxetine on extracellular serotonin levels in the raphe: an in vivo microdialysis study." Eur J Pharmacol **286**(2): 213-7.

Manning, C. D., M. Burman, S. B. Christensen, L. B. Cieslinski, D. M. Essayan, M. Grous, T. J. Torphy and M. S. Barnette (1999). "Suppression of human inflammatory cell function by subtype-selective PDE4 inhibitors correlates with inhibition of PDE4A and PDE4B." Br J Pharmacol **128**(7): 1393-8.

Manning, C. D., M. M. McLaughlin, G. P. Livi, L. B. Cieslinski, T. J. Torphy and M. S. Barnette (1996). "Prolonged beta adrenoceptor stimulation up-regulates cAMP phosphodiesterase activity in human monocytes by increasing mRNA and protein for phosphodiesterases 4A and 4B." J Pharmacol Exp Ther **276**(2): 810-818.

Marchandise, B., E. Schroeder, A. Bosly, C. Doyen, P. Weynants, R. Kremer and H. Pouleur (1989). "Early detection of doxorubicin cardiotoxicity: interest of Doppler echocardiographic analysis of left ventricular filling dynamics." Am Heart J **118**(1): 92-8.

Martins, T. J., M. C. Mumby and J. A. Beavo (1982). "Purification and characterization of a cyclic GMP-stimulated cyclic nucleotide phosphodiesterase from bovine tissues." J Biol Chem **257**(4): 1973-9.

Mason, D. A., J. D. Moore, S. A. Green and S. B. Liggett (1999). "A gain-of-function polymorphism in a G-protein coupling domain of the human beta1-adrenergic receptor." J Biol Chem **274**(18): 12670-4.

Maurice, D. H., D. Palmer, D. G. Tilley, H. A. Dunkerley, S. J. Netherton, D. R. Raymond, H. S. Elbatarny and S. L. Jimmo (2003). "Cyclic nucleotide phosphodiesterase activity, expression, and targeting in cells of the cardiovascular system." Mol Pharmacol **64**(3): 533-46.

McDonald, K. M., T. Rector, P. F. Carlyle, G. S. Francis and J. N. Cohn (1994). "Angiotensin-converting enzyme inhibition and beta-adrenoceptor blockade regress established ventricular remodeling in a canine model of discrete myocardial damage." J Am Coll Cardiol **24**(7): 1762-8.

McLaughlin, M. M., L. B. Cieslinski, M. Burman, T. J. Torphy and G. P. Livi (1993). "A low-$K_m$, rolipram-sensitive, cAMP-specific phosphodiesterase from human brain." J. Biol. Chem. **268**(9): 6470-6476.

Merlet, P., J. Delforge, A. Syrota, E. Angevin, B. Maziere, C. Crouzel, H. Valette, D. Loisance, A. Castaigne and J. L. Rande (1993). "Positron emission tomography with 11C CGP-12177 to assess beta-adrenergic receptor concentration in idiopathic dilated cardiomyopathy." Circulation **87**(4): 1169-78.

Michaeli, T., T. J. Bloom, T. Martins, K. Loughney, K. Ferguson, M. Riggs, L. Rodgers, B. J. A. and M. Wigler (1993). "Isolation and characterization of a previously undetected human cAMP phosphodiesterase by complementation of cAMP phosphodiesterase-deficient *Saccharomyces cerevisiae*." Journal of Biological Chemistry **268**(17): 12925-12932.

Mills, S. E. (2002). "Implications of feedback regulation of beta-adrenergic signaling." J Anim Sci **80**: E30-E35.

Minotti, G., P. Menna, E. Salvatorelli, G. Cairo and L. Gianni (2004). "Anthracyclines: molecular advances and pharmacologic developments in antitumor activity and cardiotoxicity." Pharmacol Rev **56**(2): 185-229.

Miro, X., S. Perez-Torres, F. Artigas, P. Puigdomenech, J. M. Palacios and G. Mengod (2002). "Regulation of cAMP phosphodiesterase mRNAs expression in rat brain by acute and chronic fluoxetine treatment. An in situ hybridization study." Neuropharmacology **43**(7): 1148-57.

Mongillo, M., T. McSorley, S. Evellin, A. Sood, V. Lissandron, A. Terrin, E. Huston, A. Hannawacker, M. J. Lohse, T. Pozzan, M. D. Houslay and M. Zaccolo (2004). "Fluorescence resonance energy transfer-based analysis of cAMP dynamics in live neonatal rat cardiac myocytes reveals distinct functions of compartmentalized phosphodiesterases." Circ Res **95**(1): 67-75.

Mongillo, M., C. G. Tocchetti, A. Terrin, V. Lissandron, Y. F. Cheung, W. R. Dostmann, T. Pozzan, D. A. Kass, N. Paolocci, M. D. Houslay and M. Zaccolo (2006). "Compartmentalized phosphodiesterase-2 activity blunts beta-adrenergic cardiac inotropy via an NO/cGMP-dependent pathway." Circ Res **98**(2): 226-34.

Monti, B., C. Berteotti and A. Contestabile (2006). "Subchronic rolipram delivery activates hippocampal CREB and arc, enhances retention and slows down extinction of conditioned fear." Neuropsychopharmacology **31**(2): 278-86.

Moreland, R. B., I. Goldstein and A. Traish (1998). "Sildenafil, a novel inhibitor of phosphodiesterase type 5 in human corpus cavernosum smooth muscle cells." Life Sci **62**(20): PL 309-18.

Morin, F., C. Lugnier, J. Kameni and P. Voisin (2001). "Expression and role of phosphodiesterase 6 in the chicken pineal gland." J Neurochem **78**(1): 88-99.

Movsesian, M., J. Stehlik, F. Vandeput and M. R. Bristow (2009). "Phosphodiesterase inhibition in heart failure." Heart Fail Rev **14**(4): 255-63.

Movsesian, M. A. (1998). "cAMP-mediated signal transduction and sarcoplasmic reticulum function in heart failure." Ann N Y Acad Sci **853**: 231-9.

Müller, B., C. Lugnier and J.-C. Stoclet (1990). "Involvement of rolipram-sensitive cyclic AMP phosphodiesterase in the regulation of cardiac contraction." J Cardiovasc Pharmacol **16**: 796-803.

Murthy, K. S., H. Zhou and G. M. Makhlouf (2002). "PKA-dependent activation of PDE3A and PDE4 and inhibition of adenylyl cyclase V/VI in smooth muscle." Am J Physiol Cell Physiol **282**(3): C508-17.

Muzik, O., R. Beanlands, E. Wolfe, G. Hutchins and Schwaiger M. (1993). "Automated Region Definition for Cardiac Nitrogen-13-Ammonia PET Imaging." J Nucl Med **34**(2): 336-344.

Myslivecek, J. and S. Trojan (2003). "Regulation of adrenoceptors and muscarinic receptors in the heart." Gen Physiol Biophys **22**(1): 3-14.

Nagaoka, T., T. Shirakawa, T. W. Balon, J. C. Russell and Y. Fujita-Yamaguchi (1998). "Cyclic nucleotide phosphodiesterase 3 expression in vivo: evidence for tissue-specific expression of phosphodiesterase 3A or 3B mRNA and activity in the aorta and adipose tissue of atherosclerosis-prone insulin-resistant rats." Diabetes **47**(7): 1135-44.

Newton, G. E. and J. D. Parker (1996). "Acute effects of beta 1-selective and nonselective beta-adrenergic receptor blockade on cardiac sympathetic activity in congestive heart failure." Circulation **94**(3): 353-8.

Ng, S. S. and C. C. Pang (1998). "Zaprinast, a type V phosphodiesterase inhibitor, dilates capacitance vessels in anaesthetised rats." Eur J Pharmacol **351**(3): 323-8.

Nikolaev, V. O., M. Bunemann, E. Schmitteckert, M. J. Lohse and S. Engelhardt (2006). "Cyclic AMP imaging in adult cardiac myocytes reveals far-reaching beta1-adrenergic but locally confined beta2-adrenergic receptor-mediated signaling." Circ Res **99**(10): 1084-91.

Nikulina, E., J. L. Tidwell, H. N. Dai, B. S. Bregman and M. T. Filbin (2004). "The phosphodiesterase inhibitor rolipram delivered after a spinal cord lesion promotes axonal regeneration and functional recovery." Proc Natl Acad Sci U S A **101**(23): 8786-90.

Nony, P., J. P. Boissel, M. Lievre, A. Leizorovicz, M. C. Haugh, S. Fareh and B. de Breyne (1994). "Evaluation of the effect of phosphodiesterase inhibitors on mortality in chronic heart failure patients. A meta-analysis." Eur J Clin Pharmacol **46**(3): 191-6.

O'Connolly, M., D. Dierdorf, W. H. Greb, M.-E. R. Mayer and D. Wolf (1988). "Efficacy of denbufylline in patients with multi-infarct dementia." Drug Dev Res **14**: 195-198.

O'Donnell, J. M. and H. T. Zhang (2004). "Antidepressant effects of inhibitors of cAMP phosphodiesterase (PDE4)." Trends Pharmacol Sci **25**(3): 158-63.

Ohkura, K., J. D. Lee, H. Shimizu, A. Nakano, H. Uzui, M. Horikoshi, Y. Fujibayashi, Y. Yonekura and T. Ueda (2003). "Mitochondrials complex I activity is reduced in latent adriamycin-induced cardiomyopathy of rat." Mol Cell Biochem **248**(1-2): 203-8.

Ohmori, Y., Y. Imahori, S. Ueda, R. Fujii, T. Ido, K. Wakita and H. Nakahashi (1993). "Protein kinase C imaging using carbon-11-labeled phorbol esters: 12-deoxyphorbol 13-isobutyrate-20-[1-11C]butyrate as the potential ligand for positron emission tomography." J Nucl Med **34**(3): 431-9.

Oishi, R., Y. Itoh, M. Nishibori and K. Saeki (1989). "Effects of the histamine H3-agonist (R)-alpha-methylhistamine and the antagonist thioperamide on histamine metabolism in the mouse and rat brain." J Neurochem **52**(5): 1388-92.

Omori, K. and J. Kotera (2007). "Overview of PDEs and their regulation." Circ Res **100**(3): 309-27.

Osadchii, O., G. Norton, D. Deftereos and A. Woodiwiss (2007). "Rat strain-related differences in myocardial adrenergic tone and the impact on cardiac fibrosis, adrenergic responsiveness and myocardial structure and function." Pharmacol Res **55**(4): 287-94.

Osadchii, O., G. Norton and A. Woodiwiss (2005). "Inotropic responses to phosphodiesterase inhibitors in cardiac hypertrophy in rats." Eur J Pharmacol **514**(2-3): 201-8.

Osadchii, O. E. (2007). "Myocardial phosphodiesterases and regulation of cardiac contractility in health and cardiac disease." Cardiovasc Drugs Ther **21**(3): 171-94.

Osadchii, O. E., A. J. Woodiwiss, D. Deftereos and G. R. Norton (2007). "Temporal changes in myocardial adrenergic regulation with the progression to pump

dysfunction after chronic beta-adrenoreceptor activation in rats." Pflugers Arch **455**(2): 251-60.

Otani, H., Y. Kagaya, Y. Imahori, S. Yasuda, R. Fujii, M. Chida, S. Namiuchi, M. Takeda, M. Sakuma, J. Watanabe, T. Ido, H. Nonogi and K. Shirato (2005). "Myocardial 11C-diacylglycerol accumulation and left ventricular remodeling in patients after myocardial infarction." J Nucl Med **46**(4): 553-9.

Owens, R. J., S. Lumb, K. Rees-Milton, A. Russell, D. Baldock, V. Lang, T. Crabbe, M. Ballesteros and M. J. Perry (1997). "Molecular cloning and expression of a human phosphodiesterase 4C." Cell Signal **9**(8): 575-85.

Packer, M., M. R. Bristow, J. N. Cohn, W. S. Colucci, M. B. Fowler, E. M. Gilbert and N. H. Shusterman (1996). "The effect of carvedilol on morbidity and mortality in patients with chronic heart failure. U.S. Carvedilol Heart Failure Study Group." N Engl J Med **334**(21): 1349-55.

Pages, L., A. Gavalda and M. D. Lehner (2009). "PDE4 inhibitors: a review of current developments (2005 - 2009)." Expert Opin Ther Pat **19**(11): 1501-19.

Panjrath, G. S. and D. Jain (2006). "Monitoring chemotherapy-induced cardiotoxicity: role of cardiac nuclear imaging." J Nucl Cardiol **13**(3): 415-26.

Parker, C. A., J. C. Matthews, R. N. Gunn, L. Martarello, V. J. Cunningham, D. Dommett, S. T. Knibb, D. Bender, S. Jakobsen, J. Brown and A. D. Gee (2005). "Behaviour of [(11)C]R(-)- and [(11)C]S(+)-rolipram in vitro and in vivo, and their use as PET radiotracers for the quantificative assay of PDE4." Synapse **55**(4): 270-9.

Parker, J. D., G. E. Newton, J. S. Landzberg, J. S. Floras and W. S. Colucci (1995). "Functional significance of presynaptic alpha-adrenergic receptors in failing and nonfailing human left ventricle." Circulation **92**(7): 1793-800.

Parmley, W. W. (1989). "Pathophysiology and current therapy of congestive heart failure." J Am Coll Cardiol **13**(4): 771-85.

Pavoine, C. and N. Defer (2005). "The cardiac beta2-adrenergic signalling a new role for the cPLA2." Cell Signal **17**(2): 141-52.

Pearse, B. M. and M. S. Robinson (1990). "Clathrin, adaptors, and sorting." Annu Rev Cell Biol **6**: 151-71.

Perez-Torres, S., R. Cortes, M. Tolnay, A. Probst, J. M. Palacios and G. Mengod (2003). "Alterations on phosphodiesterase type 7 and 8 isozyme mRNA expression in Alzheimer's disease brains examined by in situ hybridization." Exp Neurol **182**(2): 322-34.

Perry, S. J., G. S. Baillie, T. A. Kohout, I. McPhee, M. M. Magiera, K. L. Ang, W. E. Miller, A. J. McLean, M. Conti, M. D. Houslay and R. J. Lefkowitz (2002). "Targeting of cyclic AMP degradation to beta 2-adrenergic receptors by beta-arrestins." Science **298**(5594): 834-6.

Pfeffer, M., J. Pfeffer, C. Fishbein, P. Fletcher, J. Spadaro, R. Kloner and E. Braunwald (1979). "Myocardial infarct size and ventricular function in rats." Circ Res **44**(4): 503-12.

Pietila, M., K. Malminiemi, H. Ukkonen, M. Saraste, K. Nagren, P. Lehikoinen and L. M. Voipio-Pulkki (2001). "Reduced myocardial carbon-11 hydroxyephedrine retention is associated with poor prognosis in chronic heart failure." Eur J Nucl Med **28**(3): 373-6.

Pike, V. W. (2009). "PET radiotracers: crossing the blood-brain barrier and surviving metabolism." Trends Pharmacol Sci **30**(8): 431-40.

Pike, V. W., M. P. Law, S. Osman, R. J. Davenport, O. Rimoldi, D. Giardina and P. G. Camici (2000). "Selection, design and evaluation of new radioligands for PET studies of cardiac adrenoceptors." Pharm Acta Helv **74**(2-3): 191-200.

Ping, P., T. Anzai, M. Gao and H. K. Hammond (1997). "Adenylyl cyclase and G protein receptor kinase expression during development of heart failure." Am J Physiol **273**(2 Pt 2): H707-17.

Pitcher, J., M. J. Lohse, J. Codina, M. G. Caron and R. J. Lefkowitz (1992). "Desensitization of the isolated beta 2-adrenergic receptor by beta-adrenergic receptor kinase, cAMP-dependent protein kinase, and protein kinase C occurs via distinct molecular mechanisms." Biochemistry **31**(12): 3193-7.

Pyne, N. J. and B. L. Furman (2003). "Cyclic nucleotide phosphodiesterases in pancreatic islets." Diabetologia **46**(9): 1179-89.

Raffel, D. and D. Wieland (2001). "Assessment of cardiac sympathetic nerve integrity with positron emission tomography." Nucl Med Biol **28**: 541-559.

Ramani, G. V., P. A. Uber and M. R. Mehra (2010). "Chronic heart failure: contemporary diagnosis and management." Mayo Clin Proc **85**(2): 180-95.

Rao, Y. J. and L. Xi (2009). "Pivotal effects of phosphodiesterase inhibitors on myocyte contractility and viability in normal and ischemic hearts." Acta Pharmacol Sin **30**(1): 1-24.

Reinhardt, R. R., E. Chin, J. Zhou, M. Taira, T. Murata, V. C. Manganiello and C. A. Bondy (1995). "Distinctive anatomical patterns of gene expression for cGMP-inhibited cyclic nucleotide phosphodiesterases." J Clin Invest **95**(4): 1528-38.

Rena, G., F. Begg, A. Ross, C. MacKenzie, I. McPhee, L. Campbell, E. Huston, M. Sullivan and M. D. Houslay (2001). "Molecular cloning, genomic positioning, promoter identification, and characterization of the novel cyclic amp-specific phosphodiesterase PDE4A10." Mol Pharmacol **59**(5): 996-1011.

Reneerkens, O. A., K. Rutten, H. W. Steinbusch, A. Blokland and J. Prickaerts (2009). "Selective phosphodiesterase inhibitors: a promising target for cognition enhancement." Psychopharmacology (Berl) **202**(1-3): 419-43.

Renstrom, E., L. Eliasson and P. Rorsman (1997). "Protein kinase A-dependent and -independent stimulation of exocytosis by cAMP in mouse pancreatic B-cells." J Physiol **502 ( Pt 1)**: 105-18.

Reyes-Irisarri, E., M. Markerink-Van Ittersum, G. Mengod and J. de Vente (2007). "Expression of the cGMP-specific phosphodiesterases 2 and 9 in normal and Alzheimer's disease human brains." Eur J Neurosci **25**(11): 3332-8.

Richter, W., S. L. Jin and M. Conti (2005). "Splice variants of the cyclic nucleotide phosphodiesterase PDE4D are differentially expressed and regulated in rat tissue." Biochem J **388**(Pt 3): 803-11.

Riemann, B., K. P. Schafers, O. Schober and M. Schafers (2008). "Small animal PET in preclinical studies: opportunities and challenges." Q J Nucl Med Mol Imaging **52**(3): 215-21.

Riemann, B., M. Schafers, M. P. Law, T. Wichter and O. Schober (2003). "Radioligands for imaging myocardial alpha- and beta-adrenoceptors." Nuklearmedizin **42**(1): 4-9.

Robidoux, J., T. L. Martin and S. Collins (2004). "Beta-Adrenergic Receptors and Regulation of Energy Expenditure: A Family Affair." Annu Rev Pharmacol Toxicol **44**: 297-323.

Rockman, H. A., W. J. Koch and R. J. Lefkowitz (2002). "Seven-transmembrane-spanning receptors and heart function." Nature **415**(6868): 206-12.

Rodriguez-Porcel, M., W. Cai, O. Gheysens, J. K. Willmann, K. Chen, H. Wang, I. Y. Chen, L. He, J. C. Wu, Z. B. Li, K. A. Mohamedali, S. Kim, M. G. Rosenblum, X. Chen and S. S. Gambhir (2008). "Imaging of VEGF receptor in a rat myocardial infarction model using PET." J Nucl Med **49**(4): 667-73.

Rose, R. J., H. Liu, D. Palmer and D. H. Maurice (1997). "Cyclic AMP-mediated regulation of vascular smooth muscle cell cyclic AMP phosphodiesterase activity." Br J Pharmacol **122**(2): 233-40.

Rosenspire, K. C., M. S. Haka, M. E. Van Dort, D. M. Jewett, D. L. Gildersleeve, M. Schwaiger and D. M. Wieland (1990). "Synthesis and preliminary Evaluation of Carbon-11-Meta-Hydroxyephedrine: A False Transmitter Agent for Heart Neuronal Imaging." J. Nucl. Med. **31**(8): 1328-1334.

Rosskopf, D. and M. C. Michel (2008). "Pharmacogenomics of G protein-coupled receptor ligands in cardiovascular medicine." Pharmacol Rev **60**(4): 513-35.

Ruat, M., E. Traiffort, J. M. Arrang, J. Tardivel-Lacombe, J. Diaz, R. Leurs and J. C. Schwartz (1993). "A novel rat serotonin (5-HT$_6$) receptor: molecular cloning, localization and stimulation of cAMP accumulation." Biochem Biophys Res Commun **193**(1): 268-76.

Ruat, M., E. Traiffort, R. Leurs, J. Tardivel-Lacombe, J. Diaz, J. M. Arrang and J. C. Schwartz (1993). "Molecular cloning, characterization, and localization of a high-affinity serotonin receptor (5-HT$_7$) activating cAMP formation." Proc Natl Acad Sci USA **90**(18): 8547-51.

Rudin, M., P. Allegrini, N. Beckmann, H. U. Gremlich, R. Kneuer, D. Laurent, M. Rausch and M. Stoeckli (2004). "Noninvasive imaging in drug discovery and development." Ernst Schering Res Found Workshop(48): 47-75.

Saletu, B., P. Anderer, P. K. Fischhof, H. Lorenz, R. Barousch and F. Böhmer (1992). "EEG mapping and psychopharmacological studies with denbufylline in SDAT and MID." Biol Psychiatry **32**: 668-681.

Sanbe, A. and S. Takeo (1995). "Effects of NKH477, a water-soluble forskolin derivative, on cardiac function in rats with chronic heart failure after myocardial infarction." J Pharmacol Exp Ther **274**(1): 120-6.

Sanbe, A., K. Tanonaka, Y. Hanaoka, T. Katoh and S. Takeo (1993). "Regional energy metabolism of failing hearts following myocardial infarction." J Mol Cell Cardiol **25**(9): 995-1013.

Sasaki, T., A. Enta, T. Nozaki, S. Ishii and M. Senda (1993). "Carbon-11-forskolin: a ligand for visualization of the adenylate cyclase-related second messenger system." J Nucl Med **34**(11): 1944-8.

Sasaki, T., S.-I. Ishii, M. Senda, S. Akinaga and C. Murakata (1996). "Synthesis of [7ß-methoxy $^{11}$C]methoxy staurosporine for imaging protein kinase C localization in the brain." Appl. Radiat. Isot. **47**(1): 67-69.

Sasaki, T., J. Kotera and K. Omori (2002). "Novel alternative splice variants of rat phosphodiesterase 7B showing unique tissue-specific expression and phosphorylation." Biochem J **361**(Pt 2): 211-20.

Sasano, T., M. R. Abraham, K. C. Chang, H. Ashikaga, K. J. Mills, D. P. Holt, J. Hilton, S. G. Nekolla, J. Dong, A. C. Lardo, H. Halperin, R. F. Dannals, E. Marban and F. M. Bengel (2008). "Abnormal sympathetic innervation of viable myocardium and the substrate of ventricular tachycardia after myocardial infarction." J Am Coll Cardiol **51**(23): 2266-75.

Satwani, S., G. W. Dec and J. Narula (2004). "Beta-adrenergic blockers in heart failure: review of mechanisms of action and clinical outcomes." J Cardiovasc Pharmacol Ther **9**(4): 243-55.

Sauer, D., R. Rischke, T. Beck, C. RoBberg, H.-D. Mennel, G. W. Bielenberg and J. Krieglstein (1988). "Vinpocetine prevents ischemic cell damage in rat hippocampus." Life Sci. **43**: 1733-1739.

Schmiechen, R., H. H. Schneider and H. Wachtel (1990). "Close correlation between behavioural response and binding in vivo for inhibitors of the rolipram-sensitive phosphodiesterase." Psychopharmacology **102**: 17-20.

Schneider, H. H., R. Schmiechen, M. Brezinski and J. Seidler (1986). "Stereospecific binding of the antidepressant rolipram to brain protein structures." Eur J Pharmacol **127**: 105-115.

Seeger, T. F., B. Bartlett, T. M. Coskran, J. S. Culp, L. C. James, D. L. Krull, J. Lanfear, A. M. Ryan, C. J. Schmidt, C. A. Strick, A. H. Varghese, R. D. Williams, P. G. Wylie and F. S. Menniti (2003). "Immunohistochemical localization of PDE10A in the rat brain." Brain Res **985**(2): 113-26.

Sethi, R., N. Bector, N. Takeda, M. Nagano, G. Jasmin and N. S. Dhalla (1994). "Alterations in G-proteins in congestive heart failure in cardiomyopathic (UM-X7.1) hamsters." Mol Cell Biochem **140**(2): 163-70.

Sethi, R., K. S. Dhalla, R. E. Beamish and N. S. Dhalla (1997). "Differential changes in left and right ventricular adenylyl cyclase activities in congestive heart failure." Am J Physiol **272**(2 Pt 2): H884-93.

Sethi, R., V. Elimban, D. Chapman, I. M. Dixon and N. S. Dhalla (1998). "Differential alterations in left and right ventricular G-proteins in congestive heart failure due to myocardial infarction." J Mol Cell Cardiol **30**(11): 2153-63.

Sette, C. and M. Conti (1996). "Phosphorylation and activation of a cAMP-specific phosphodiesterase by the cAMP-dependent protein kinase." J. Biol. Chem. **271**: 16526-16534.

Sette, C., S. Iona and M. Conti (1994). "The short-term activation of a rolipram-sensitive, cAMP-specific phosphodiesterase by thyroid-stimulating hormone in thyroid FRTL-5 cells is mediated by a cAMP-dependent phosphorylation." J Biol Chem **269**(12): 9245-9252.

Shahid, M. and C. D. Nicholson (1990). "Comparison of cyclic nucleotide phosphodiesterase isoenzymes in rat and rabbit ventricular mycardium: positive inotropic and phosphodiesterase inhibitory effects of Org 30029, milrinone and rolipram." Naunyn-Schmiedeberg's Arch. Pharmacol. **342**: 698-705.

Shakur, Y., M. Wilson, L. Pooley, M. Lobban, S. L. Griffiths, A. M. Campbell, J. Beattie, C. Daly and M. D. Houslay (1995). "Identification and characterization of the

type-ivA cyclic AMP-specific phosphodiesterase RD1 as a membrane-bound protein expressed in cerebellum." Biochem. J. **306**: 801-809.

Shepherd, J. T. and P. M. Vanhoutte (1981). "George E. Brown memorial lecture. Local modulation of adrenergic neurotransmission." Circulation **64**(4): 655-66.

Shepherd, M., T. McSorley, A. E. Olsen, L. A. Johnston, N. C. Thomson, G. S. Baillie, M. D. Houslay and G. B. Bolger (2003). "Molecular cloning and subcellular distribution of the novel PDE4B4 cAMP-specific phosphodiesterase isoform." Biochem J **370**(Pt 2): 429-38.

Shirani, J. and V. Dilsizian (2008). "Imaging left ventricular remodeling: targeting the neurohumoral axis." Nat Clin Pract Cardiovasc Med **5 Suppl 2**: S57-62.

Shirani, J. and V. Dilsizian (2009). "Molecular imaging targets of cardiac remodeling." Curr Cardiol Rep **11**(2): 148-54.

Shizukuda, Y. and P. M. Buttrick (2002). "Subtype specific roles of beta-adrenergic receptors in apoptosis of adult rat ventricular myocytes." J Mol Cell Cardiol **34**(7): 823-31.

Shusterman, V., C. F. McTiernan, A. Goldberg, S. Saba, G. Salama and B. London (2009). "Adrenergic stimulation promotes T-wave alternans and arrhythmia inducibility in a TNF-{alpha} genetic mouse model of congestive heart failure." Am J Physiol Heart Circ Physiol.

Sibley, D. R. and R. J. Lefkowitz (1985). "Molecular mechanisms of receptor desensitization using the beta-adrenergic receptor-coupled adenylate cyclase system as a model." Nature **317**(6033): 124-9.

Singal, P. K., C. M. Deally and L. E. Weinberg (1987). "Subcellular effects of adriamycin in the heart: a concise review." J Mol Cell Cardiol **19**(8): 817-28.

Smith, S. J., L. B. Cieslinski, R. Newton, L. E. Donnelly, P. S. Fenwick, A. G. Nicholson, P. J. Barnes, M. S. Barnette and M. A. Giembycz (2004). "Discovery of BRL 50481 [3-(N,N-dimethylsulfonamido)-4-methyl-nitrobenzene], a selective inhibitor of phosphodiesterase 7: in vitro studies in human monocytes, lung macrophages, and CD8+ T-lymphocytes." Mol Pharmacol **66**(6): 1679-89.

Soderling, S. H., S. J. Bayuga and J. A. Beavo (1999). "Isolation and characterization of a dual-substrate phosphodiesterase gene family: PDE10A." Proc Natl Acad Sci U S A **96**(12): 7071-6.

Sonnenburg, W. K., S. D. Rybalkin, K. E. Bornfeldt, K. S. Kwak, I. G. Rybalkina and J. A. Beavo (1998). "Identification, quantitation, and cellular localization of PDE1 calmodulin-stimulated cyclic nucleotide phosphodiesterases." Methods **14**(1): 3-19.

Souness, J. E. and S. Rao (1997). "Proposal for pharmacologically distinct conformers of PDE4 cyclic AMP phosphodiesterases." Cell. Signal. **9**: 227-236.

Spann, J. F., Jr., E. H. Sonnenblick, T. Cooper, C. A. Chidsey, V. L. Willman and E. Braunwald (1966). "Cardiac norepinephrine stores and the contractile state of heart muscle." Circ Res **19**(2): 317-25.

Sprague, D. R., M. Fujita, Y. H. Ryu, J. S. Liow, V. W. Pike and R. B. Innis (2008). "Whole-body biodistribution and radiation dosimetry in monkeys and humans of the phosphodiesterase 4 radioligand [(11)C](R)-rolipram: comparison of two-dimensional planar, bisected and quadrisected image analyses." Nucl Med Biol **35**(4): 493-500.

Steinberg, S. F. and L. L. Brunton (2001). "Compartmentation of G protein-coupled signaling pathways in cardiac myocytes." Annu Rev Pharmacol Toxicol **41**: 751-73.

Strome, E. M., S. Jivan and D. J. Doudet (2005). "Quantitative in vitro phosphor imaging using [3H] and [18F] radioligands: the effects of chronic desipramine treatment on serotonin 5-HT2 receptors." J Neurosci Methods **141**(1): 143-54.

Sturton, G. and M. Fitzgerald (2002). "Phosphodiesterase 4 inhibitors for the treatment of COPD." Chest **121**(5 Suppl): 192S-196S.

Summers, R. J., L. R. McMartin, A. Kompa, X. Gu and P. Molenaar (1995). "Signalling pathways in cardiac failure." Clin Exp Pharmacol Physiol **22**(11): 874-6.

Sunahara, R. K., C. W. Dessauer and A. G. Gilman (1996). "Complexity and diversity of mammalian adenylyl cyclases." Annu Rev Pharmacol Toxicol **36**: 461-80.

Sutton, M. G. and N. Sharpe (2000). "Left ventricular remodeling after myocardial infarction: pathophysiology and therapy." Circulation **101**(25): 2981-8.

Suuronen, E. J., J. Price, J. P. Veinot, K. Ascah, V. Kapila, X. W. Guo, S. Wong, T. G. Mesana and M. Ruel (2007). "Comparative effects of mesenchymal progenitor cells, endothelial progenitor cells, or their combination on myocardial infarct regeneration and cardiac function." J Thorac Cardiovasc Surg **134**(5): 1249-58.

Swain, S. M., F. S. Whaley and M. S. Ewer (2003). "Congestive heart failure in patients treated with doxorubicin: a retrospective analysis of three trials." Cancer **97**(11): 2869-79.

Swaney, J. S., H. H. Patel, U. Yokoyama, N. C. Lai, M. Spellman, P. A. Insel and D. M. Roth (2007). "Adenylyl cyclase activity and function are decreased in rat cardiac fibroblasts after myocardial infarction." Am J Physiol Heart Circ Physiol **293**(5): H3216-20.

Swedberg, K., C. Viquerat, J. L. Rouleau, M. Roizen, B. Atherton, W. W. Parmley and K. Chatterjee (1984). "Comparison of myocardial catecholamine balance in chronic congestive heart failure and in angina pectoris without failure." Am J Cardiol **54**(7): 783-6.

Takahashi, K., T. Osanai, T. Nakano, M. Wakui and K. Okumura (2002). "Enhanced activities and gene expression of phosphodiesterase types 3 and 4 in pressure-induced congestive heart failure." Heart Vessels **16**(6): 249-56.

Takahashi, M., R. Terwilliger, C. Lane, P. S. Mezes, M. Conti and R. S. Duman (1999). "Chronic antidepressant administration increases the expression of cAMP-specific phosphodiesterase 4A and 4B isoforms." J Neurosci **19**: 610-618.

Takahashi, T., T. Tang, N. C. Lai, D. M. Roth, B. Rebolledo, M. Saito, W. Y. Lew, P. Clopton and H. K. Hammond (2006). "Increased cardiac adenylyl cyclase expression is associated with increased survival after myocardial infarction." Circulation **114**(5): 388-96.

Tardito, D., J. Perez, E. Tiraboschi, L. Musazzi, G. Racagni and M. Popoli (2006). "Signaling pathways regulating gene expression, neuroplasticity, and neurotrophic mechanisms in the action of antidepressants: a critical overview." Pharmacol Rev **58**(1): 115-34.

Taylor, S. S., J. A. Buechler and W. Yonemoto (1990). "cAMP-dependent protein kinase: framework for a diverse family of regulatory enzymes." Annu Rev Biochem **59**: 971-1005.

Tenor, H., A. Hatzelmann, M. K. Church, C. Schudt and J. K. Shute (1996). "Effects of theophylline and rolipram on leukotriene C4 (LTC4) synthesis and chemotaxis of human eosinophils from normal and atopic subjects." Br. J. Pharmacol. **118**: 1727-1735.

Tenor, H. and C. Schudt (1996). Analysis of PDE isoenzyme profiles in cells and tissues by pharmacological methods. Phosphodiesterase inhibitors. C. Schudt, G. Dent and K. F. Rabe. San Diego, Academic Press: 21-40.

Terry, R., Y. F. Cheung, M. Praestegaard, G. S. Baillie, E. Huston, I. Gall, D. R. Adams and M. D. Houslay (2003). "Occupancy of the catalytic site of the PDE4A4 cyclic AMP phosphodiesterase by rolipram triggers the dynamic redistribution of this specific isoform in living cells through a cyclic AMP independent process." Cell Signal **15**(10): 955-71.

Thackeray, J. T., R. S. Beanlands and J. N. Dasilva (2007). "Presence of Specific 11C-meta-Hydroxyephedrine Retention in Heart, Lung, Pancreas, and Brown Adipose Tissue." J Nucl Med **48**(10): 1733-1740.

Thomas, A. J., J. M. Renaud, M. Lortie, M. Kenk, R. S. Beanlands, J. N. DaSilva and R. A. deKemp (2010). "In vivo characterization of (R)-[11C]Rolipram PDE4-specific binding in rat heart using small animal PET." J Nucl Med (Submitted).

Thomas, D., H. Bal, J. Arkles, J. Horowitz, L. Araujo, P. D. Acton and V. A. Ferrari (2008). "Noninvasive assessment of myocardial viability in a small animal model: comparison of MRI, SPECT, and PET." Magn Reson Med **59**(2): 252-9.

Thomas, J. A. and B. H. Marks (1978). "Plasma norepinephrine in congestive heart failure." Am J Cardiol **41**(2): 233-43.

Thomas, L., S. Bellmont, M. O. Christen, B. La Roche and L. Monassier (2004). "Cardiovascular and survival effects of sympatho-inhibitors in adriamycin-induced cardiomyopathy in rats." Fundam Clin Pharmacol **18**(6): 649-55.

Thome, J., N. Sakai, K. Shin, C. Steffen, Y. Zhang, S. Impey, D. Storm and R. S. Duman (2000). "cAmp response element-mediated gene transcription is upregulated by chronic antidepressant treatment [In Process Citation]." J Neurosci **20**(11): 4030-6.

Thompson, W. J. and M. M. Appleman (1971). "Multiple cyclic nucleotide phosphodiesterase activities from rat brain." Biochemistry **10**(2): 311-6.

Tilley, D. G. and D. H. Maurice (2002). "Vascular smooth muscle cell phosphodiesterase (PDE) 3 and PDE4 activities and levels are regulated by cyclic AMP in vivo." Mol Pharmacol **62**(3): 497-506.

Tipre, D. N., J. J. Fox, D. P. Holt, G. Green, J. Yu, M. Pomper, R. F. Dannals and F. M. Bengel (2008). "In vivo PET imaging of cardiac presynaptic sympathoneuronal mechanisms in the rat." J Nucl Med **49**(7): 1189-95.

Tokarska-Schlattner, M., T. Wallimann and U. Schlattner (2006). "Alterations in myocardial energy metabolism induced by the anti-cancer drug doxorubicin." C R Biol **329**(9): 657-68.

Tong, J., P. K. Ganguly and P. K. Singal (1991). "Myocardial adrenergic changes at two stages of heart failure due to adriamycin treatment in rats." Am J Physiol **260**(3 Pt 2): H909-16.

Torphy, T. J. (1998). "Phosphodiesterase isozymes: molecular targets for novel antiasthma agents." Am J Respir Crit Care Med **157**(2): 351-70.

Torphy, T. J., J. M. Stadel, M. Burman, L. B. Cieslinski, M. M. McLaughlin, J. R. White and G. P. Livi (1992). "Coexpression of human cAMP-specific phosphodiesterase activity and high affinity rolipram binding in yeast." J. Biol. Chem. **267**(3): 1798-1804.

Torphy, T. J., H.-L. Zhou and L. B. Cieslinski (1992). "Stimulation of *beta* adrenoceptors in a human monocyte cell line (U937) up-regulates cyclic AMP-specific phosphodiesterase activity." J Pharmacol Exp Ther **263**(3): 1195-1205.

Torres, G. E., Y. Chaput and R. Andrade (1995). "Cyclic AMP and protein kinase A mediate 5-hydroxytryptamine type 4 receptor regulation of calcium-activated potassium current in adult hippocampal neurons." Mol Pharmacol **47**(1): 191-7.

Toyoshima, H., Y. Nasa, Y. Kohsaka, Y. Isayama, F. Yamaguchi, A. Sanbe and S. Takeo (1998). "The effect of chronic treatment with trandolapril on cyclic AMP-and cyclic GMP-dependent relaxations in aortic segments of rats with chronic heart failure." Br J Pharmacol **123**(2): 344-52.

Triposkiadis, F., G. Karayannis, G. Giamouzis, J. Skoularigis, G. Louridas and J. Butler (2009). "The sympathetic nervous system in heart failure physiology, pathophysiology, and clinical implications." J Am Coll Cardiol **54**(19): 1747-62.

Tse, J., N. L. Brackett and J. F. Kuo (1978). "Alterations in activities of cyclic nucleotide systems and in beta-adrenergic receptor-mediated activation of cyclic AMP-dependent protein kinase during progression and regression of isoproterenol-induced cardiac hypertrophy." Biochim Biophys Acta **542**(3): 399-411.

Tse, J., M. W. Huang, R. J. Leone, H. R. Weiss, Y. Q. He and P. M. Scholz (2000). "Down regulation of myocardial beta1-adrenoceptor signal transduction system in pacing-induced failure in dogs with aortic stenosis-induced left ventricular hypertrophy." Mol Cell Biochem **205**(1-2): 67-73.

Tsukada, H., D. Fukumoto, S. Nishiyama, K. Sato and T. Kakiuchi (2004). "Transient focal ischemia affects the cAMP second messenger system and coupled dopamine D1 and 5-HT1A receptors in the living monkey brain: a positron emission tomography study using microdialysis." J Cereb Blood Flow Metab **24**(8): 898-906.

Tsukada, H., N. Harada, H. Ohba, S. Nishiyama and T. Kakiuchi (2001). "Facilitation of dopaminergic neural transmission does not affect [(11)C]SCH23390 binding to the striatal D(1) dopamine receptors, but the facilitation enhances phosphodiesterase type-IV activity through D(1) receptors: PET studies in the conscious monkey brain." Synapse **42**(4): 258-65.

Tsukada, H., T. Kakiuchi, S. Nishiyama, H. Ohba and N. Harada (2001). "Effects of aging on 5-HT(1A) receptors and their functional response to 5-HT(1a) agonist in the living brain: PET study with [carbonyl-(11)C]WAY-100635 in conscious monkeys." Synapse **42**(4): 242-51.

Ungerer, M., M. Bohm, J. S. Elce, E. Erdmann and M. J. Lohse (1993). "Altered expression of beta-adrenergic receptor kinase and beta 1-adrenergic receptors in the failing human heart." Circulation **87**(2): 454-63.

Ungerer, M., H. J. Weig, S. Kubert, M. Overbeck, F. Bengel, A. Schomig and M. Schwaiger (2000). "Regional pre- and postsynaptic sympathetic system in the failing human heart--regulation of beta ARK-1." Eur J Heart Fail **2**(1): 23-31.

Vallbo, A. B., K. E. Hagbarth and B. G. Wallin (2004). "Microneurography: how the technique developed and its role in the investigation of the sympathetic nervous system." J Appl Physiol **96**(4): 1262-9.

van Staveren, W. C., J. Glick, M. Markerink-van Ittersum, M. Shimizu, J. A. Beavo, H. W. Steinbusch and J. de Vente (2002). "Cloning and localization of the cGMP-specific phosphodiesterase type 9 in the rat brain." J Neurocytol **31**(8-9): 729-41.

Van Waarde, A., P. H. Elsinga, O.-E. Brodde, G. M. Visser and W. Vaalburg (1995). "Myocardial and pulmonary uptake of *S*-1'[$^{18}$F]fluorocarazolol in intact rats reflects radioligand binding to ß-adrenoceptors." European Journal of Pharmacology **272**: 159-168.

van Waarde, A., J. G. Meeder, P. K. Blanksma, J. Bouwer, G. M. Visser, P. H. Elsinga, A. M. Paans, W. Vaalburg and K. I. Lie (1992). "Suitability of CGP-12177 and CGP-26505 for quantitative imaging of beta-adrenoceptors." Int J Rad Appl Instrum B **19**(7): 711-8.

Vasdev, N., F. J. LaRonde, J. R. Woodgett, A. Garcia, E. A. Rubie, J. H. Meyer, S. Houle and A. A. Wilson (2008). "Rationally designed PKA inhibitors for positron emission tomography: Synthesis and cerebral biodistribution of N-(2-(4-bromocinnamylamino)ethyl)-N-[11C]methyl-isoquinoline-5-sulfonamide." Bioorg Med Chem **16**(9): 5277-84.

Vecsey, C. G., G. S. Baillie, D. Jaganath, R. Havekes, A. Daniels, M. Wimmer, T. Huang, K. M. Brown, X. Y. Li, G. Descalzi, S. S. Kim, T. Chen, Y. Z. Shang, M. Zhuo, M. D. Houslay and T. Abel (2009). "Sleep deprivation impairs cAMP signalling in the hippocampus." Nature **461**(7267): 1122-5.

Verghese, M. W., R. T. McConnell, J. M. Lenhard, L. Hamacher and S.-L. C. Jin (1995). "Regulation of distinct cyclic AMP-specific phosphodiesterase (phosphodiesterase type 4) isozymes in human monocytic cells." Mol Pharmacol **47**: 1164-1171.

Violin, J. D., L. M. DiPilato, N. Yildirim, T. C. Elston, J. Zhang and R. J. Lefkowitz (2008). "beta2-adrenergic receptor signaling and desensitization elucidated by quantitative modeling of real time cAMP dynamics." J Biol Chem **283**(5): 2949-61.

Vogel, J. H. and C. A. Chidsey (1969). "Cardiac adrenergic activity in experimental heart failure assessed with beta receptor blockade." Am J Cardiol **24**(2): 198-208.

Wachtel, H. (1982). "Characteristic behavioral alterations in rats induced by rolipram and other selective adenosine cyclic 3',5' -monophosphate phosphodiesterase inhibitors." Psychopharmacology **77**: 309-316.

Wachtel, H. (1983). "Neurotropic effects of the optical isomers of the selective adenosine cyclic 3',5'-monophosphate phosphodiesterase inhibitor rolipram in rats in-vivo." J. Pharm. Pharmacol. **35**: 440-444.

Wachtel, H. (1983). "Potential antidepressant activity of rolipram and other selective cyclic adenosine 3',5'-monophosphate phosphodiesterase inhibitors." Neuropharmacology **22**(3A): 267-272.

Wachtel, H. (1988). Defective Second-messenger Function in the Etiology of Endogenous Depression: Novel Therapeutic Approaches. New Concepts in Depression. M. a. G. F. Briley. Basingstoke, MacMillan Press. **2:** 277-293.

Wachtel, H. (1990). "The second-messenger dysbalance hypothesis of affective disorders." Pharmacopsychiatry **23**: 27-32.

Wachtel, H. and H. H. Schneider (1986). "Rolipram, a novel antidepressant drug, reverses the hypothermia and hypokinesia of monoamine-depleted mice by an action beyond postsynaptic monoamine receptors." Neuropharmacology **25**(no.10): 1119-1126.

Wakasugi, S., A. Wada, Y. Hasegawa, S. Nakano and N. Shibata (1992). "Detection of abnormal cardiac adrenergic neuron activity in adriamycin-induced cardiomyopathy with iodine-125-metaiodobenzylguanidine." J Nucl Med **33**(2): 208-14.

Wallukat, G. (2002). "The beta-adrenergic receptors." Herz **27**(7): 683-90.

Wang, P., P. Wu, R. W. Egan and M. M. Billah (2001). "Human phosphodiesterase 8A splice variants: cloning, gene organization, and tissue distribution." Gene **280**(1-2): 183-94.

Weinberg, L. E. and P. K. Singal (1987). "Refractory heart failure and age-related differences in adriamycin-induced myocardial changes in rats." Can J Physiol Pharmacol **65**(9): 1957-65.

Weishaar, R. E., M. H. Cain and J. A. Bristol (1985). "A new generation of phosphodiesterase inhibitors: multiple molecular forms of phosphodiesterase and the potential for drug selectivity." J. Med. Chem. **28**(5): 537-545.

Wells, J. N. and G. L. Kramer (1981). "Phosphodiesterase inhibitors as tools in cyclic nucleotide research: a precautionary comment." Mol Cell Endocrinol **23**(1): 1-9.

Whalin, M. E., R. L. Garrett Jr., W. J. Thompson and S. J. Strada (1989). "Correlation of cell-free brain cyclic nucleotide phosphodiesterse activities to cyclic AMP decay in intact brain slices." Second Messengers Phosphoproteins **12**(5 & 6): 311-325.

Witte, K., K. Hu, J. Swiatek, C. Mussig, G. Ertl and B. Lemmer (2000). "Experimental heart failure in rats: effects on cardiovascular circadian rhythms and on myocardial beta-adrenergic signaling." Cardiovasc Res **47**(2): 350-8.

Wong, M. L., F. Whelan, P. Deloukas, P. Whittaker, M. Delgado, R. M. Cantor, S. M. McCann and J. Licinio (2006). "Phosphodiesterase genes are associated with susceptibility to major depression and antidepressant treatment response." Proc Natl Acad Sci U S A **103**(41): 15124-9.

Wu, J. C., I. Y. Chen, Y. Wang, J. R. Tseng, A. Chhabra, M. Salek, J. J. Min, M. C. Fishbein, R. Crystal and S. S. Gambhir (2004). "Molecular imaging of the kinetics of vascular endothelial growth factor gene expression in ischemic myocardium." Circulation **110**(6): 685-91.

Xiang, Y. and B. K. Kobilka (2003). "Myocyte adrenoceptor signaling pathways." Science **300**(5625): 1530-2.

Xiang, Y., F. Naro, M. Zoudilova, S. L. Jin, M. Conti and B. Kobilka (2005). "Phosphodiesterase 4D is required for beta2 adrenoceptor subtype-specific signaling in cardiac myocytes." Proc Natl Acad Sci USA **102**(3): 909-14.

Xiao, R. P., P. Avdonin, Y. Y. Zhou, H. Cheng, S. A. Akhter, T. Eschenhagen, R. J. Lefkowitz, W. J. Koch and E. G. Lakatta (1999). "Coupling of beta2-adrenoceptor to Gi proteins and its physiological relevance in murine cardiac myocytes." Circ Res **84**(1): 43-52.

Xiao, R. P., H. Cheng, Y. Y. Zhou, M. Kuschel and E. G. Lakatta (1999). "Recent advances in cardiac beta(2)-adrenergic signal transduction." Circ Res **85**(11): 1092-100.

Xiao, R. P., S. J. Zhang, K. Chakir, P. Avdonin, W. Zhu, R. A. Bond, C. W. Balke, E. G. Lakatta and H. Cheng (2003). "Enhanced G(i) signaling selectively negates beta2-adrenergic receptor (AR)--but not beta1-AR-mediated positive inotropic effect in myocytes from failing rat hearts." Circulation **108**(13): 1633-9.

Xu, R. X., A. M. Hassell, D. Vanderwall, M. H. Lambert, W. D. Holmes, M. A. Luther, W. J. Rocque, M. V. Milburn, Y. Zhao, H. Ke and R. T. Nolte (2000). "Atomic structure of PDE4: insights into phosphodiesterase mechanism and specificity." Science **288**(5472): 1822-5.

Yamamoto, T., M. Yano, X. Xu, H. Uchinoumi, H. Tateishi, M. Mochizuki, T. Oda, S. Kobayashi, N. Ikemoto and M. Matsuzaki (2008). "Identification of target domains of the cardiac ryanodine receptor to correct channel disorder in failing hearts." Circulation **117**(6): 762-72.

Yan, C., J. K. Bentley, W. K. Sonnenburg and J. A. Beavo (1994). "Differential expression of the 61 kDa and 63 kDa calmodulin-dependent phosphodiesterases in the mouse brain." J Neurosci **14**(3 Pt 1): 973-84.

Yanaka, N., J. Kotera, A. Ohtsuka, H. Akatsuka, Y. Imai, H. Michibata, K. Fujishige, E. Kawai, S. Takebayashi, K. Okumura and K. Omori (1998). "Expression, structure and chromosomal localization of the human cGMP-binding cGMP-specific phosphodiesterase PDE5A gene." Eur J Biochem **255**(2): 391-9.

Yasui, K. and A. Komiyama (2001). "New clinical applications of xanthine derivatives: modulatory actions on leukocyte survival and function." Int J Hematol **73**(1): 87-92.

Ye, J., L. Yang, R. Sethi, J. Copps, B. Ramjiawan, R. Summers and R. Deslauriers (1997). "A new technique of coronary artery ligation: experimental myocardial infarction in rats in vivo with reduced mortality." Mol Cell Biochem **176**(1-2): 227-33.

Ye, Y., M. Conti, M. D. Houslay, S. M. Farooqui, M. Chen and J. M. O'Donnell (1997). "Noradrenergic activity differentially regulates the expression of rolipram-sensitive, high-affinity cyclic AMP phosphodiesterase (PDE4) in rat brain." J Neurochem **69**(6): 2397-404.

Ye, Y., K. Jackson and J. M. O'Donnell (2000). "Effects of repeated antidepressant treatment of type 4A phosphodiesterase (PDE4A) in rat brain." J Neurochem **74**(3): 1257-62.

Ye, Y. and J. M. O'Donnell (1996). "Diminished noradrenergic stimulation reduces the activity of rolipram-sensitive, high-affinity cyclic AMP phosphodiesterase in rat cerebral cortex." J Neurochem **66**: 1894-1902.

Yoshida, H., K. Tanonaka, Y. Miyamoto, T. Abe, M. Takahashi, M. B. Anand-Srivastava and S. Takeo (2001). "Characterization of cardiac myocyte and tissue beta-adrenergic signal transduction in rats with heart failure." Cardiovasc Res **50**(1): 34-45.

Yoshikawa, T., S. Handa, M. Suzuki and K. Nagami (1994). "Abnormalities in sympathoneuronal regulation are localized to failing myocardium in rabbit heart." J Am Coll Cardiol **24**(1): 210-5.

Zaccolo, M. and T. Pozzan (2002). "Discrete microdomains with high concentration of cAMP in stimulated rat neonatal cardiac myocytes." Science **295**(5560): 1711-5.

Zahniser, N. R., G. A. Larson and G. A. Gerhardt (1999). "In vivo dopamine clearance rate in rat striatum: regulation by extracellular dopamine concentration and dopamine transporter inhibitors." J Pharmacol Exp Ther **289**(1): 266-77.

Zaugg, M., W. Xu, E. Lucchinetti, S. A. Shafiq, N. Z. Jamali and M. A. Siddiqui (2000). "Beta-adrenergic receptor subtypes differentially affect apoptosis in adult rat ventricular myocytes." Circulation **102**(3): 344-50.

Zeller, E., H.-J. Stief, B. Pflug and M. Sastre-y-Hernández (1984). "Results of a phase II study of the antidepressant effect of rolipram." Pharmacopsychiatry **17**: 188-190.

Zhang, H. T. (2009). "Cyclic AMP-specific phosphodiesterase-4 as a target for the development of antidepressant drugs." Curr Pharm Des **15**(14): 1688-98.

Zhang, K., S. M. Farooqui and O. D. JM (1999). "Ontogeny of rolipram-sensitive, low-K(m), cyclic AMP-specific phosphodiesterase in rat brain [In Process Citation]." Brain Res Dev Brain Res **112**(1): 11-9.

Zhao, Y., H. T. Zhang and J. M. O'Donnell (2003). "Antidepressant-induced increase in high-affinity rolipram binding sites in rat brain: dependence on noradrenergic and serotonergic function." J Pharmacol Exp Ther **307**(1): 246-53.

Zhao, Y., H. T. Zhang and J. M. O'Donnell (2003). "Inhibitor binding to type 4 phosphodiesterase (PDE4) assessed using [3H]piclamilast and [3H]rolipram." J Pharmacol Exp Ther **305**(2): 565-72.